

Three new species of *Iodosphaeria* (Xylariomycetidae): *I. chiayiensis*, *I. jinghongensis* and *I. thailandica*

Lakmali S. Dissanayake¹, Diana S. Marasinghe^{2,6}, Milan C. Samarakoon²,
Sajeewa S.N. Maharachchikumbura³, Peter E. Mortimer⁴, Kevin D. Hyde^{2,5},
Chang-Hsin Kuo⁶, Ji-Chuan Kang¹

1 Engineering and Research Center for Southwest Bio-Pharmaceutical Resources of National Education Ministry of China, Guizhou University, Guiyang 550025, China **2** Center of Excellence in Fungal Research, Mae Fah Luang University, Chiang Rai 57100, Thailand **3** School of Life Science and Technology, University of Electronic Science and Technology of China, Chengdu 611731, China **4** Centre for Mountain Futures (CMF), Kunming Institute of Botany, Honghe County 654400, Yunnan, China **5** Innovative Institute for Plant Health, Zhongkai University of Agriculture and Engineering, Guangzhou 510225, China **6** Department of Plant Medicine, National Chiayi University, 300 Syuefu Road, Chiayi City 60004, Taiwan

Corresponding author: Ji-Chuan Kang (jkang@gzu.edu.cn)

Academic editor: Andrew Miller | Received 27 September 2021 | Accepted 15 December 2021 | Published 7 January 2022

Citation: Dissanayake LS, Marasinghe DS, Samarakoon MC, Maharachchikumbura SSN, Mortimer PE, Hyde KD, Kuo C-H, Kang J-C (2022) Three new species of *Iodosphaeria* (Xylariomycetidae): *I. chiayiensis*, *I. jinghongensis* and *I. thailandica*. MycoKeys 86: 1–17. <https://doi.org/10.3897/mycokeys.86.75801>

Abstract

Three fungal specimens (two sexual and one asexual) were collected during fieldwork conducted in China, Taiwan and Thailand. Both sexual morphs share superficial, black ascomata surrounded by flexuous setae; 8-spored, unitunicate, cylindrical asci, with J+, apical ring, and ellipsoidal to allantoid, aseptate, guttulate ascospores. The asexual morph has ceratosporium-like conidia arising from aerial hyphae with a single arm and are usually attached or with 2–3 arms, brown, often with a subglobose to conical cell at the point of attachment. Morphological examinations and phylogenetic analyses of a combined LSU-ITS dataset *via* maximum likelihood and Bayesian analyses indicated that these three collections were new species. *Iodosphaeria chiayiensis* (sexual morph), *I. thailandica* (sexual morph) and *I. jinghongensis* (asexual morph) are therefore introduced as new species in this study. *Iodosphaeria chiayiensis* has small, hyaline and ellipsoidal to allantoid ascospores, while *I. thailandica* has large ascomata, cylindrical to allantoid asci and hyaline to pale brown ascospores.

Keywords

Ceratosporium-like asexual morph, Sordariomycetes, taxonomy, three new taxa

Introduction

Iodosphaeria was introduced by Samuels et al. (1987) with its type *I. phyllophila* on a rachis of *Cyathea* sp., from Brazil. Only five of the nine *Iodosphaeria* species have been sequenced (Li et al. 2015; Marasinghe et al. 2019; Miller and Réblová 2021) and several species of them lack DNA-based sequence data. The sexual morph of *Iodosphaeria* is characterized by superficial, black, apapillate ascomata with unbranched, brown radial flexuous hairs, a two layered peridium composed of a pigmented outer layer and a hyaline inner layer; unitunicate, amyloid or non-amyloid, cylindrical to narrowly clavate, 8-spored asci; and mostly allantoid to ellipsoidal, aseptate, hyaline ascospores with or without a gelatinous sheath (Miller and Réblová 2021). The asexual morphs of *Iodosphaeria* are considered selenosporella-like or ceratosporium-like (Samuels et al. 1987; Li et al. 2015; Miller and Réblová 2021). Members of *Iodosphaeria* are regarded as cosmopolitan species (Li et al. 2015). These species are usually saprobic on dead branches, twigs, stems, and petioles of economically important plants, such as *Alnus* sp., *Archontophoenix alexandrae*, *Arundinaria* sp., *Corylus* sp., *Cyathea dealbata*, *Podocarpus parlatoresi*, *Polygonum chinense* and *Ripogonum scandens* (Samuels et al. 1987; Barr 1993; Hyde 1995; Candoussau et al. 1996; Hsieh et al. 1997; Taylor and Hyde 1999; Catania and Romero 2012; Li et al. 2015; Miller and Réblová 2021), but have never been reported as pathogens (Hyde et al. 2020a).

Samuels et al. (1987) accepted *Iodosphaeria* in Amphisphaeriaceae, and later, various authors placed it in Lasiosphaeriaceae and Trichosphaeriaceae (Barr 1990, 1994; Kang et al. 1998; Hilber and Hilber 2002; Jeewon et al. 2003). Again, Eriksson et al. (2001) placed *Iodosphaeria* in Amphisphaeriaceae. Later, Hilber and Hilber (2002) accommodated *Iodosphaeria* in the newly introduced family Iodosphaeriaceae. Maharachchikumbura et al. (2016) and Samarakoon et al. (2016) provided multigene phylogenies and accepted Iodosphaeriaceae in Xylariales. Hongsanan et al. (2017) treated it as Xylariomycetidae family *incertae sedis*, while Hyde et al. (2020a) and Wijayawardene et al. (2020) accepted Iodosphaeriaceae in Amphisphaeriales. In the most recent study of Miller and Réblová (2021), Iodosphaeriaceae is accounted as a family in Xylariales.

This study introduces three novel *Iodosphaeria* species from China, Taiwan, and Thailand. Detailed morphological descriptions, illustrations and a key are provided, and phylogenetic affinities of the new taxa are discussed.

Materials and methods

Morphological observations

Dead leaves were collected from Dahu Forest (Chiayi City, Taiwan) during autumn (September 2019), from dead twigs in Jinghong City (Yunnan Province, China) during winter (December 2019) and from dead leaves at MRC (Mushroom Research Centre, Chiang Mai, Thailand) during the rainy season (September 2020). Specimens

were treated following the methods outlined in Senanayake et al. (2020). A Motic SMZ 168 Series microscope was used to examine fruiting structures. Hand sections of the fruiting structures were mounted in water and 5% KOH for microscopic studies and microphotography. Indian ink was used to stain any gelatinous sheath around the ascospores and Melzer's reagent for ascus apical ring reaction. The micro-morphologies were examined using a Nikon ECLIPSE 80i compound microscope and photographed using a Canon 750D digital camera fitted to the microscope. Tarosoft (R) Image Frame Work program (IFW 0.97 version) and Adobe Photoshop CS6 software (Adobe Systems, USA) were used for image processing and measurements. The type specimens were deposited in the Mae Fah Luang University Herbarium (MFLU), Chiang Rai, Thailand and the Cryptogamic Herbarium, Kunming Institute of Botany Academia Sinica (HKAS), Chinese Academy of Sciences, Kunming, China. The new taxa were linked with Facesoffungi (Jayasiri et al. 2015) and Index Fungorum (<http://www.indexfungorum.org>).

DNA extraction, PCR amplification and sequencing

DNA extraction, PCR amplification and sequencing were carried out following the methods described in Dissanayake et al. (2020). Direct DNA extraction was done using a Biospin Fungus Genomic DNA Extraction Kit-BSC14S1 (BioFlux, P.R. China) with 15–20 fruiting bodies of the fungus as described in Wanasinghe et al. (2018). PCR amplification was done using LSU and ITS DNA regions with LR0R/LR5 (Vilgalys and Hester 1990) and ITS5/ITS4 (White et al. 1990) primer pairs, respectively. The thermal cycling program was followed by Wanasinghe et al. (2020). Purified PCR products were sent to a commercial sequencing provider, Beijing Biomed Gene Technology Co., Ltd., Shijingshan District, TsingKe Biological Technology Co., Beijing, China.

Phylogenetic analyses

Newly generated sequences were assembled and subjected to the standard BLAST search to identify the closest matches in GenBank. The accession numbers of taxa used in our analyses are shown in Table 1. Single datasets (LSU and ITS) were aligned using MAFFT v. 6.864b (<http://mafft.cbrc.jp/alignment/server/index.html>, Katoh and Standley 2013; Katoh et al. 2019), combined and manually improved using BioEdit v. 7.0.5.2 (Hall 1999). Maximum likelihood analysis and Bayesian inference (BI) were performed using RAxML-HPC2 on the XSEDE v. 8.2.10 tool and MrBayes 3.2.2 on the XSEDE tool in the CIPRES Science Gateway portal (Miller et al. 2012; Ronquist et al. 2012; Stamatakis 2014). The optimal ML tree was obtained with 1,000 separate runs under the GTR+GAMMA substitution model resulting from model tests using MrModeltest v. 2.3 (Nylander 2004) under the AIC (Akaike Information Criterion) implemented in PAUP v. 4.0b10. Maximum Likelihood bootstrap values (ML) equal or greater than 60% and Bayesian posterior probabilities (BYPP) equal or greater than 0.95 are presented above each node (Figure 1). All trees were visualized with FigTree v1.4.0 (Rambaut 2012), and

Table 1. Taxa used in the phylogenetic analyses and corresponding GenBank accession numbers.

Taxon	Specimen/Strain	GenBank accession numbers		References
		ITS	LSU	
<i>Delonicicola siamense</i>	MFLUCC 15-0670 T	MF167586	MF158345	Perera et al. (2017)
<i>Furfurella luteostiolata</i>	CBS 143620 T	MK527842	MK527842	Voglmayr et al. (2019)
<i>Iodosphaeria chiayiensis</i>	MFLU 21-0042 T	MZ918994	MZ918992	This study
<i>I. foliicola</i>	NBM-F-07096 T	MZ509148	MZ509160	Miller and Réblová (2021)
<i>I. honghensis</i>	MFLU 19-0719 T	MK737501	MK722172	Marasinghe et al. (2019)
<i>I. jingbongensis</i>	HKAS 115761 T	MZ918989	MZ923776	This study
<i>I. phyllophila</i>	PDD 56626	MZ509149	MZ509149	Miller and Réblová (2021)
<i>I. phyllophila</i>	FC 5099-2d	MZ509150	N/A	Miller and Réblová (2021)
<i>I. phyllophila</i>	ILLS00121493 T	MZ509151	N/A	Miller and Réblová (2021)
<i>I. ripogoni</i>	PDD 103350	MZ509152	MZ509152	Miller and Réblová (2021)
<i>I. thailandica</i>	MFLU 21-0041 T	MZ923759	MZ923758	This study
<i>I. tongrenensis</i>	MFLU 15-0393 T	KR095282	KR095283	Li et al. (2015)
<i>Ocydothis metroxylicola</i>	MFLUCC 15-0281 T	KY206776	KY206765	Konta et al. (2016)
<i>O. palmicola</i>	MFLUCC 15-0806 T	KY206774	KY206763	Konta et al. (2016)
<i>O. phoenicis</i>	MFLUCC 18-0270 T	MK088066	MK088062	Hyde et al. (2020a)
<i>Pseudosporidesmium knawiae</i>	CBS 123529 T	FJ349609	FJ349610	Vu et al. (2019)
<i>P. lambertiae</i>	CBS 143169 T	MG386034	MG386087	Crous et al. (2017)
<i>Vialaea insculpta</i>	DAOM 240257	KC181926	KC181924	McTaggart et al. (2013)
<i>V. mangiferae</i>	MFLUCC 12-0808 T	KF724974	KF724975	Senanayake et al. (2014)
<i>V. minutella</i>	BRIP 56959	JX139726	JX139726	Shoemaker et al. (2013)

Types strains are indicated with (T). Newly generated sequences are indicated in bold. “N/A” sequences are unavailable.

Abbreviations: **BRIP**: Queensland Plant Pathology Herbarium, Australia; **CBS**: Centraalbureau voor Schimmelcultures, Utrecht, The Netherlands; **DAOM**: Plant Research Institute, Department of Agriculture (Mycology), Ottawa, Canada; **HKAS**: Chinese Academy of Sciences, Kunming, China. **KUMCC**: Kunming Institute of Botany Culture Collection, Chinese Academy of Science, Kunming, China; **MFLUCC**: Mae Fah Luang University Culture Collection, Chiang Rai, Thailand; **MFLU**: Mae Fah Luang University Herbarium, Chiang Rai, Thailand; **Others**: information not available.

the final layout was done with Microsoft PowerPoint (2016). The finalized alignment and tree were registered in TreeBASE (submission ID TB2: S29095). Reviewer access URL: <http://purl.org/phylo/treebase/phylovs/study/TB2:S29095?x-access-code=43fac9fe7622929c65c2bd4120a2c10a&format=html>

Results

Phylogenetic analyses

The combined LSU and ITS comprise 20 taxa including the outgroup taxa. The best scoring RAxML tree is shown in Figure with a final ML optimization likelihood value of -7278.703992. The matrix had 575 distinct alignment patterns, with 19.44% undetermined characters or gaps. Estimated base frequencies were: A = 0.245534,

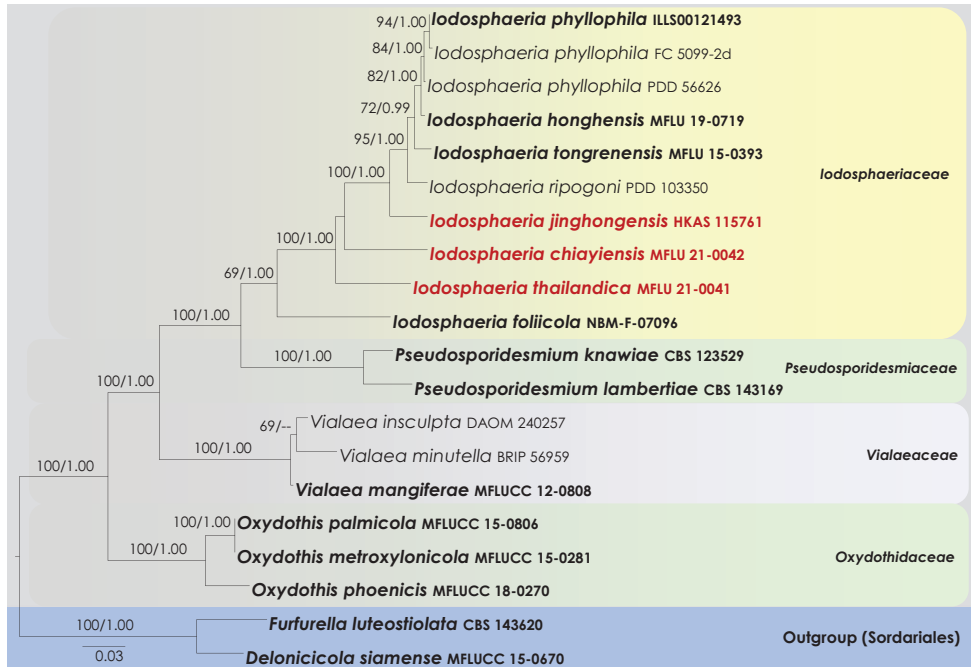


Figure 1. RAxML tree based on a combined dataset of partial LSU and ITS sequence analyses. The tree is rooted to *Delonicicola siamense* (MFLUCC 15-0670) and *Furfurella luteostiolata* (CBS 143620). Type strains are in bold, and the newly generated strains are in red.

C = 0.244177, G = 0.286855, T = 0.223434 substitution rates AC = 1.190714, AG = 2.269637, AT = 1.889784, CG = 1.069908, CT = 5.997198, GT = 1.000000; proportion of invariable sites I = 0.39717; gamma distribution shape parameters $\alpha = 0.578305$. Both trees (ML and BYPP) were similar in topology and did not differ in species relationships, which is in agreement with multi-gene phylogenies of previous studies (Marasinghe et al. 2019; Miller and Réblová 2021).

In the combined multi-gene phylogenetic analysis, Iodosphaeriaceae received 100% ML and 1.00 BYPP support values (Figure 1). Three strains of *Iodosphaeria phyllophila* grouped as a monophyletic clade with 82% ML and 1.00 BYPP support. *Iodosphaeria honghensis* (MFLU 19-0719) nested as a sister clade to *I. phyllophila* with 82% ML and 1.00 BYPP support. Within the *Iodosphaeria* clade, our new collections viz. HKAS 115761 (*I. jinghongensis*), MFLU 21-0042 (*I. chiayiensis*) and MFLU 21-0041 (*I. thailandica*) grouped as distinct lineages (Figure 1). *Iodosphaeria jinghongensis* was distinct from *I. ripogoni* by 100% ML and 1.00 BYPP support values. *Iodosphaeria chiayiensis* nested between *I. thailandica* and *I. jinghongensis*. However, this relationship is statistically not supported. *Iodosphaeria thailandica* received 100% ML and 1.00 BYPP support values. *Iodosphaeria foliicola* (NBM-F-07096) is grouped as the basal taxon in the Iodosphaeriaceae.

Taxonomy

Iodosphaeria chiayiensis Marasinghe, C.H. Kuo & K.D. Hyde, sp. nov.

IndexFungorum number: IF558412

Facesoffungi Number No: FoF09711

Figure 2

Etymology. The specific epithet *chiayiensis* refers to the city name where the fungus was collected.

Holotype. MFLU 21-0042.

Description. *Saprobic* on dead leaves of an unidentified host. **Sexual morph:** *Ascomata* 150–190 × 160–200 µm (\bar{x} = 170 × 180 µm, n = 10), globose to subglobose, superficial, black, solitary to gregarious, consisting of numerous long, flexuous setae. *Setae* 3–5 µm wide, arising from cells at the peridium surface, brown, unbranched, septate, apex flattened. *Ostiole* periphysate, apapillate. *Peridium* 50–55 µm wide (\bar{x} = 53.4 µm, n = 10), comprises two layers of *textura angularis* cells, outer layer of dark brown to black thick-walled cells, and an inner layer of flattened, light brown. *Paraphyses* 2–4 µm wide, shorter than asci, hyaline, embedded in a gelatinous matrix. *Asci* 60–90 × 8–10 µm (\bar{x} = 72.9 × 9.2 µm, n = 30), 8-spored, unitunicate, cylindrical, shortly pedicellate, apex rounded, with a J+ apical ring. *Ascospores* 15–20 × 4–6 µm (\bar{x} = 17.2 × 5.2 µm, n = 30), overlapping uni-seriate, ellipsoidal to allantoid, aseptate, hyaline, guttulate. **Asexual morph:** Undetermined

Material examined. Taiwan, Chiayi, Fanlu Township area, on dead leaves of an undetermined species, 10 September 2019, D.S Marasinghe, DTF018 (MFLU 21-0042, *holotype*).

Notes. *Iodosphaeria chiayiensis* resembles *I. polygoni* which has globose to sub globose, superficial, solitary to gregarious ascomata, cylindrical, short pedicellate asci with J+, apical rings and ellipsoidal to allantoid, aseptate, guttulate ascospores. However, *I. chiayiensis* differs from *I. polygoni* in having smaller ascomata (150–190 × 160–200 µm *vs.* 270–475 × 250–500 µm) and shorter asci (60–90 × 8–10 µm *vs.* 150–180 × 10–13 µm) (Hsieh et al. 1997). In the multi-gene phylogenetic analyses (Figure 1), our collection (*Iodosphaeria chiayiensis*, MFLU 21-0042) has close affinity to *I. thailandica*. However, it was not possible to compare *I. chiayiensis* and *I. jinghongensis* as they occur as different morphs.

Iodosphaeria jinghongensis L.S. Dissan., J.C. Kang & K.D. Hyde, sp. nov.

IndexFungorum number: IF558800

Facesoffungi Number No: FoF09712

Figure 3

Etymology. The specific epithet *jinghongensis* refers to the city name where the fungus was collected.

Holotype. HKAS 115761.

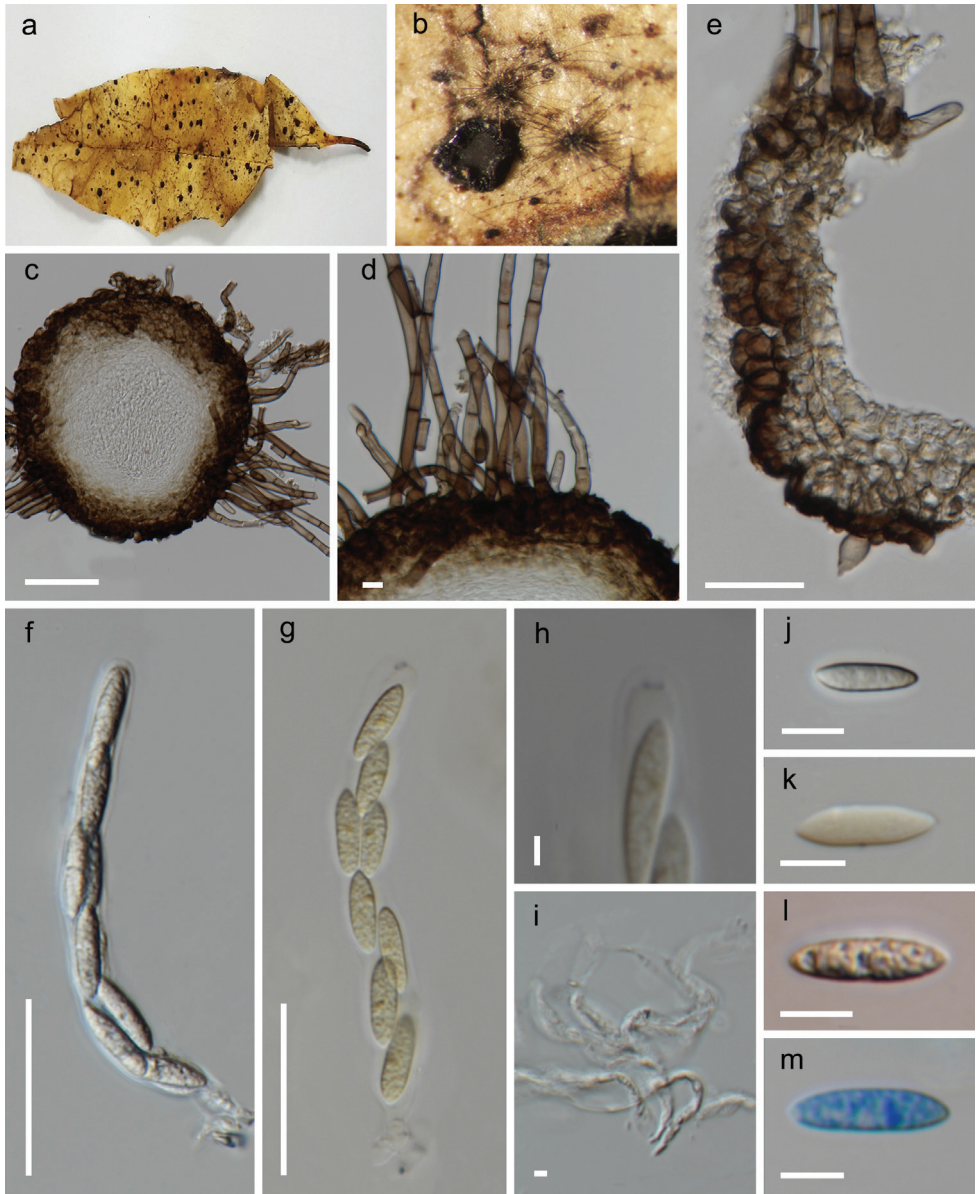


Figure 2. *Iodosphaeria chiayiensis* (MFLU 21-0042, holotype) **a** substrate **b** ascomata on the host surface **c** section of ascoma **d** appearance of setae on peridium **e** peridium **f, g** asci **h** J+ apical ring (in Melzer's reagent) **i** paraphyses **j-m** ascospores (**m** stained in lactophenol cotton blue). Scale bars: 50 μm (**c, e**); 5 μm (**d**); 20 μm (**f-g**); 5 μm (**h, i**); 10 μm (**j-m**).

Description. *Saprobic* on dead twigs of an unidentified host. **Sexual morph:** Undetermined. **Asexual morph:** Colonies on natural substrate effuse, punctiform, scattered, blackish brown, mycelium mostly superficial, non-branched, hyaline,

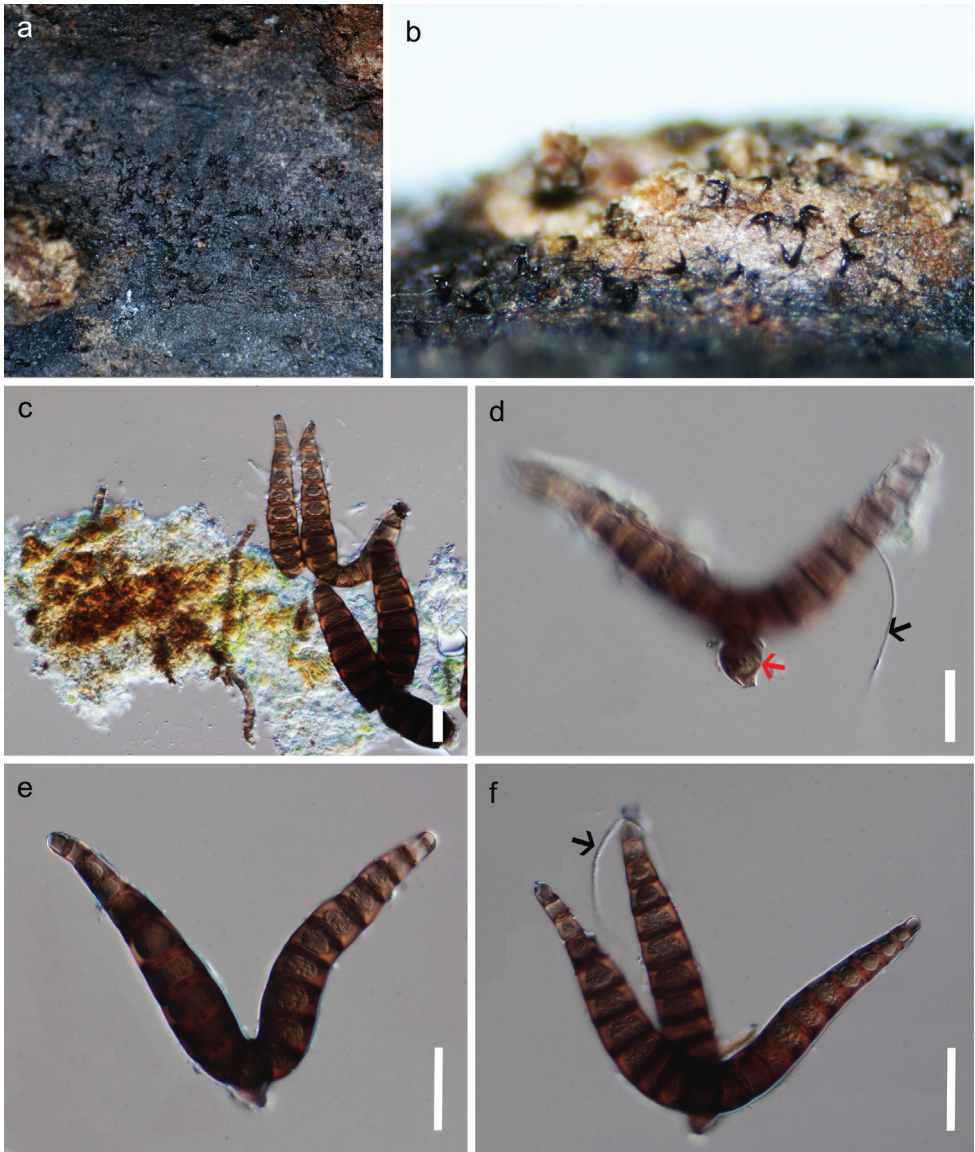


Figure 3. *Iodosphaeria jinghongensis* (HKAS 115761, holotype) **a, b** colonies on the host surface **c–f** conidia, conidiogenous cells and conidiophores (black arrow shows hyphae, red arrow shows conidiophore). Scale bars: 20 μm (**c–f**).

smooth hyphae. *Conidiophores* micronematous, smooth, flexuous, pale brown. *Conidia* ceratosporium-like, arising from aerial hyphae, solitary, dry, composed of a central cell and 2–3 arms. *Arms* 70–93 \times 9–14 μm (\bar{x} = 79.8 \times 12.1 μm , n = 20), wide at the tip 5–8 μm (\bar{x} = 6.9 μm), radiating from the centrally located attachment

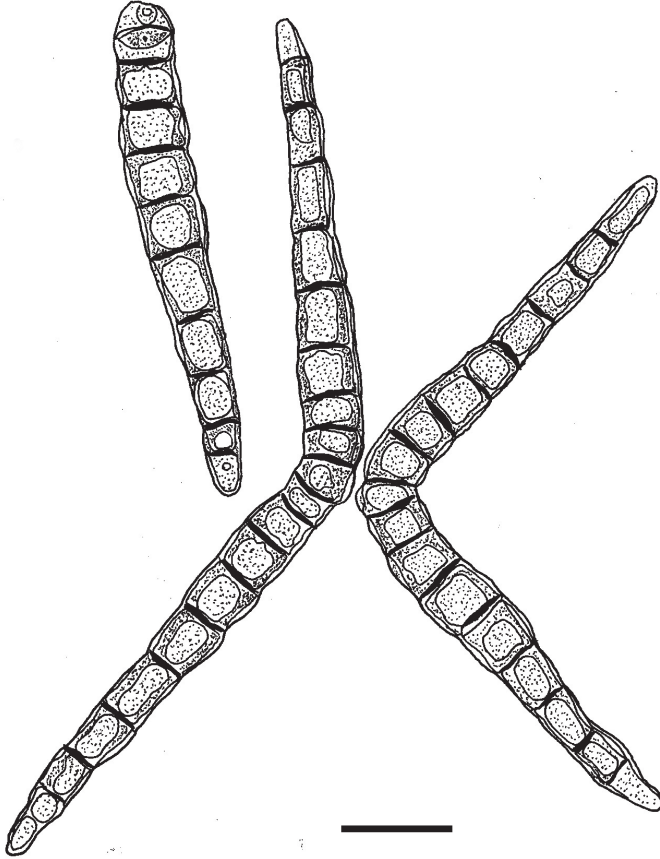


Figure 4. Asexual morph of *Iodosphaeria ripogoni* (ceratosporium-like conidia). Redrawn from: Samuels et al. (1987). Scale bar: 20 μm .

point, multi-septate (9–10), each septum with a central pore, brown, often with a sub-globose to conical cell at the point of attachment, dehiscence scar circular 3–4 μm diam. (\bar{x} = 3.5 μm).

Material examined. China, Yunnan Province, Xishuangbanna Dai Autonomous Prefecture, Jinghong City, Jinghaxiang (21°78'0617"N, 101°05'6122"E), on a dead twig of undetermined species, 19 December 2019, D.N. Wanasinghe, DW060 (HKAS 115761, *holotype*).

Notes. *Iodosphaeria jinghongensis* is similar to *I. ripogoni* in having septate, brown, subglobose to conical conidia with 2–3 arms (Figure 4; Samuels et al. 1987). However, *I. jinghongensis* differs from *I. ripogoni* in having smaller arms (70–93 \times 9–14 μm vs 95–120 \times 14–16 μm). *Iodosphaeria ripogoni* was collected from the stem of *Ripogonum scandens* from New Zealand, and *I. jinghongensis* was collected from twigs of undetermined species from China.

***Iodosphaeria thailandica* L.S. Dissan., Marasinghe, & K.D. Hyde, sp. nov.**

IndexFungorum number: IF558411

Facesoffungi number No: FoF09710

Figure 5

Etymology. The specific epithet *thailandica* refers to the country where the fungus was collected.

Holotype. MFLU 21-0041

Description. *Saprobic* on dead leaves of unidentified host. **Sexual morph:** *Ascomata* 250–285 × 250–295 μm (\bar{x} = 267.3 × 272 μm, n = 10), globose to subglobose, superficial, black, solitary to gregarious, consisting of numerous long, flexuous setae. *Setae* 4.5 μm wide, arising from cells at the peridium surface, dark brown to brown, unbranched, septate. *Ostiole* periphysate, apicillate. *Peridium* 40–50 μm wide (\bar{x} = 44.6 μm, n = 10), comprising two layers of cells of *textura angularis*, outer layer of dark brown to black thick-walled cells and an inner layer of flattened, hyaline cells. *Paraphyses* 5–8 μm wide, length as longer than asci, septate, hyaline, branched, embedded in a gelatinous matrix. *Asci* 65–100 × 8–10 μm (\bar{x} = 84.3 × 8.9 μm, n = 30), 8-spored, unitunicate, cylindrical, short pedicellate, apex rounded, with a J+ apical ring. *Ascospores* 20–35 × 2–4 μm (\bar{x} = 29.1 × 3.2 μm, n = 30), overlapping uni-seriate, cylindrical to allantoid, aseptate, hyaline to pale brown, guttulate, slightly curved. **Asexual morph:** Undetermined.

Material examined. Thailand, Chiang Mai, Mushroom Research Centre, on dead leaves of an undetermined species, 11 September 2020, D.S Marasinghe, DMRC011 (MFLU 21-0041, **holotype**)

Notes. *Iodosphaeria thailandica* shares similar characteristics with *I. honghensis* in having globose to subglobose, superficial, solitary to gregarious ascomata, cylindrical, short pedicellate, J+, apical ring and cylindrical to allantoid asci with aseptate, guttulate ascospores (Marasinghe et al. 2019). However, *I. thailandica* differs from *I. honghensis* in having long, narrow (20–35 × 2–4 μm) and hyaline to pale brown ascospores versus short, broad (18.5–22.5 × 4.5–6.5 μm) and hyaline ascospores. In the phylogenetic analyses, *I. thailandica* is distinct from other species in the genus by 100 % ML and 1.00BYPP and sister to the *I. chiayiensis*. *Iodosphaeria thailandica* has larger ascomata (250–285 × 250–295 μm), cylindrical to allantoid asci and hyaline to pale brown ascospores, while the ascomata of *I. chiayiensis* are smaller (150–190 × 160–200 μm) and ascospores are hyaline and ellipsoidal to allantoid. *Iodosphaeria thailandica* is the first report of *Iodosphaeria* from Thailand.

Key to the accepted *Iodosphaeria* species based on known sexual morph

- | | | |
|---|---|------------------------|
| 1 | Asci with a distinct apical ring | 2 |
| – | Asci lacking a distinct apical ring | 10 |
| 2 | Apical ring not staining blue in Melzer's reagent | <i>I. arundinariae</i> |
| – | Apical ring staining blue in Melzer's reagent..... | 3 |

3	Ascomata immersed to erumpent.....	<i>I. aquatica</i>
–	Ascomata superficial	4
4	Ascospores guttulate	5
–	Ascospores eguttulate.....	8
5	Ascospores ellipsoidal.....	6
–	Ascospores cylindrical	7
6	Ascomata 270–475 × 250–500 µm.....	<i>I. polygoni</i>
–	Ascomata 150–190 × 160–200 µm.....	<i>I. chiayiensis</i>
7	Ascospores 18.5–22.5 × 4.5–6.5 µm, hyaline.....	<i>I. honghensis</i>
–	Ascospores 20–35 × 2–4 µm, hyaline to pale brown.....	<i>I. thailandica</i>
8	Asci shorter than 150 µm.....	9
–	Asci longer than 150 µm.....	<i>I. tongrenensis</i>
9	Ascospores allantoid.....	11
–	Ascospores ellipsoidal.....	<i>I. podocarp</i>
10	Ascospores with a mucilaginous sheath	<i>I. ripogoni</i>
–	Ascospores without a mucilaginous sheath	<i>I. hongkongensis</i>
11	Paraphyses of similar length to asci	<i>I. foliicola</i>
–	Paraphyses longer than asci	<i>I. phyllophila</i>

Discussion

Iodosphaeria is seldom collected. In 15 years of studying fungi in Hong Kong, only a single collection was found despite intensive collection efforts (Taylor and Hyde 1999). *Iodosphaeria* is widely distributed in temperate and tropical regions, e.g., China (Guizhou, Yunnan), Europe (Belgium, Germany), Great Britain, Canada, Hong Kong, New Zealand, South America (Brazil, Argentina, French Guiana), Taiwan and USA (Louisiana) (Samuels et al. 1987; Barr 1993; Hyde 1995; Candoussau et al. 1996; Hsieh et al. 1997; Taylor and Hyde 1999; Catania and Romero 2012; Li et al. 2015; Marasinghe et al. 2019; Miller and Réblová 2021). This genus is saprobic on dead plant substrates in terrestrial grassland habitats (Barr 1993), on fern rachides (Samuels et al. 1987), on dead petioles of palms (Taylor and Hyde 1999), and on submerged wood in freshwater (Hyde 1995) but has never been reported as pathogenic on hosts. They are likely endophytes that become saprobes during leaf senescence (Hyde et al. 2020a). *Iodosphaeria* species may not be host-specific due to their wide distribution range (Miller and Réblová 2021). The genus may be much more diverse than presently known, as is true for many other microfungi genera (Hyde et al. 2020b).

The asexual morphs of this genus were recorded as selenosporella- or ceratosporium-like (Samuels et al. 1987; Li et al. 2015; Marasinghe et al. 2019). *Iodosphaeria phyllophila*, *I. polygoni* and *I. ripogoni* (Figure 4) were introduced with both sexual and asexual morphs (Hsieh et al. 1997; Samuels et al. 1987). *Iodosphaeria honghensis* and *I. tongrenensis* were observed to have ceratosporium-like conidia on their host surface

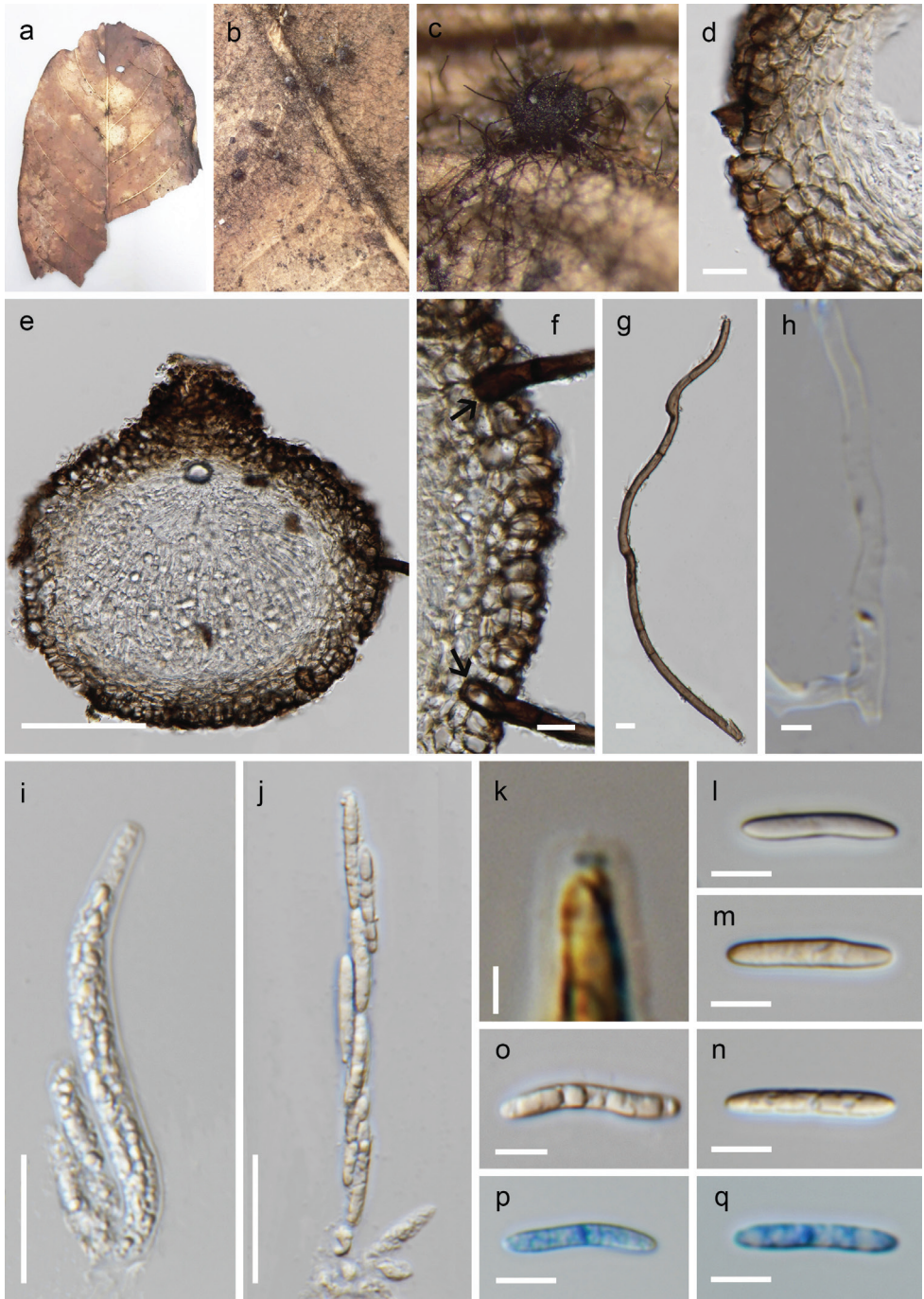


Figure 5. *Iodosphaeria thailandica* (MFLU 21-0041, holotype) **a** substrate **b, c** ascomata on the host surface **d** peridium **e** section of ascomata **f** appearance of setae (black arrow) on peridium **g** setae **h** paraphyses **i, j** asci **k** J+ apical ring (in Melzer's reagent) **l–q** ascospores (**p, q** stained in Lactophenol Cotton Blue). Scale bars: 10 µm (**d**); 100 µm (**e**); 5 µm (**f–h**); 20 µm (**i, j**); 10 µm (**k–q**).

(Li et al. 2015; Marasinghe et al. 2019). Samuels et al. (1987) observed another asexual morph of selenosporella-like conidia that was different from ceratosporium-like conidia. In present study, we establish ceratosporium-like conidia as an asexual morph of *Iodosphaeria*.

Acknowledgements

Ji-Chuan Kang thanks the National Natural Science Foundation of China (NSFC Grants Nos. 31670027 & 31460011) and the Open Fund Program of Engineering Research Center of Southwest Bio-Pharmaceutical Resources, Ministry of Education, Guizhou University (No. GZUKEY 20160705). Shaun Pennycook is thanked for the nomenclatural advice. Dhanushka Wanasinghe is thanked for the specimen collections and for providing sequence data. Peter Mortimer thanks the National Science Foundation of China (grant no. 41761144055) and High-End Foreign Experts” in the High-Level Talent Recruitment Plan of Yunnan Province (2021). Austin G. Smith at World Agroforestry (ICRAF), Kunming Institute of Botany, China, is thanked for English editing.

References

- Barr ME (1990) Prodrum to non-lichenized pyrenomycetous members of the class Hymenoascomycetes. *Mycotaxon* 39: 43–184.
- Barr ME (1993) Redisposition of some taxa described by J. B. Ellis. *Mycotaxon* 46: 45–76.
- Barr ME (1994) Notes on the Amphisphaeriaceae and related families. *Mycotaxon* 51: 191–224.
- Candoussau F, Magni JF, Petrini LE, Barr ME, Petrini O (1996) Bambusicolous fungi collected in Southwestern France: an annotated list. *Mycologia Helvetica* 8: 11–20.
- Catania MV, Romero AI (2012) *Crassoascus monocaudatus* and *Iodosphaeria podocarpi*, two new species on *Podocarpus parlatorei* from “Las Yungas”, Argentina. *Mycosphere* 3: 37–44. <https://doi.org/10.5943/mycosphere/3/1/4>
- Crous PW, Wingfield MJ, Burgess TI, Carnegie AJ, Hardy GESTJ, Smith D, Summerell BA, Cano-Lira JF, Guarro J, Houbraeken J, Lombard L, Martín MP, Sandoval-Denis M, Alexandrova AV, Barnes CW, Baseia IG, Bezerra JDP, Guarnaccia V, May TW, Hernández-Restrepo M, Stchigel AM, Miller AN, Ordoñez ME, Abreu VP, Accioly T, Agnello C, Agustin Colmán A, Albuquerque CC, Alfredo DS, Alvarado P, Araújo-Magalhães GR, Arauzo S, Atkinson T, Barili A, Barreto RW, Bezerra JL, Cabral TS, Camello Rodríguez F, Cruz RHSE, Daniëls PP, da Silva BDB, de Almeida DAC, de Carvalho Júnior AA, Decock CA, Delgat L, Denman S, Dimitrov RA, Edwards J, Fedosova AG, Ferreira RJ, Firmino AL, Flores JA, García D, Gené J, Góis JS, Gomes AAM, Gonçalves CM, Gouliamova DE, Groenewald M, Guéorguiev BV, Guevara-Suarez M, Gusmão LFP, Hosaka K, Hubka V, Huhndorf SM, Jadan M, Jurjević Ž, Kraak B, Kučera V, Kumar TKA, Kušan I, Lacerda SR, Lamlertthong S, Lisboa WS, Loizides M, Luangsa-ard JJ, Lysková P, Mac

- Cormack WP, Macedo DM, Machado AR, Malysheva EF, Marinho P, Matočec N, Meijer M, Mešić A, Mongkolsamrit S, Moreira KA, Morozova OV, Nair KU, Nakamura N, Noisripoom W, Olariaga I, Oliveira RJV, Paiva LM, Pawar P, Pereira OL, Peterson SW, Prieto M, Rodríguez-Andrade E, Rojo De Blas C, Roy M, Santos ES, Sharma R, Silva GA, Souza-Motta CM, Takeuchi-Kaneko Y, Tanaka C, Thakur A, Smith MT, Tkalčec Z, Valenzuela-Lopez N, Van der Kleij P, Verbeken A, Viana MG, Wang XW, Groenewald JZ (2017) Fungal Planet description sheets: 625–715. *Persoonia* 39: 270–467. <https://doi.org/10.3767/persoonia.2017.39.11>
- Dissanayake AJ, Bhunjun CS, Maharachchikumbura SSN, Liu JK (2020) Applied aspects of methods to infer phylogenetic relationships amongst fungi. *Mycosphere* 11: 2652–2676. <https://doi.org/10.5943/mycosphere/11/1/18>
- Eriksson OE, Baral HO, Currah RS, Hansen K, Kurtzman CP, Rambold G, Laessøe T (2001) Outline of Ascomycota-2001. *Myconet* 7: 1–88. <https://doi.org/10.1038/npg.els.0000346>
- Hall TA (1999) BioEdit: A user-friendly biological sequence alignment editor and analysis program for Windows 95/98/NT. *Nucleic Acids Symposium, Series* 41: 95–98.
- Hilber R, Hilber O (2002) The genus *Lasiosphaeria* and allied taxa. *Publ* 9. Germany, 1–18.
- Hongsanan S, Maharachchikumbura SSN, Hyde KD, Samarakoon MC, Jeewon R, Zhao Q, Al-Sadi AM, Bahkali AH (2017) An updated phylogeny of Sordariomycetes based on phylogenetic and molecular clock evidence. *Fungal Diversity* 84: 25–41. <https://doi.org/10.1007/s13225-017-0384-2>
- Hsieh WH, Chen CY, Sivanesan A (1997) *Iodosphaeria polygoni* sp. nov. a new pyrenomycete from Taiwan. *Mycological Research* 101: 841–842. <https://doi.org/10.1017/S095375629600319X>
- Hyde KD (1995) Tropical Australian freshwater fungi. VII. New genera and species of ascomycetes. *Nova Hedwigia* 61: 119–140.
- Hyde KD, Norphanphoun C, Maharachchikumbura SSN, Bhat DJ, Jones EBG, Bundhun D, Chen YJ, Bao DF, Boonmee S, Calabon MS, Chaiwan N, Chethana KWT, Dai DQ, Dayarathne MC, Devadatha B, Dissanayake AJ, Dissanayake LS, Doilom M, Dong W, Fan XL, Goonasekara ID, Hongsanan S, Huang SK, Jayawardena RS, Jeewon R, Karunarathna A, Konta S, Kumar V, Lin CG, Liu JK, Liu NG, Luangsa-ard J, Lumyong S, Luo ZL, Marasinghe DS, McKenzie EHC, Niego AGT, Niranjana M, Perera RH, Phukhamsakda C, Rathnayaka AR, Samarakoon MC, Samarakoon SMBC, Sarma VV, Senanayake IC, Shang QJ, Stadler M, Tibpromma S, Wanasinghe DN, Wei DP, Wijayawardene NN, Xiao YP, Yang J, Zeng XY, Zhang SN, Xiang MM (2020a) Refined families of Sordariomycetes. *Mycosphere* 11: 305–1059. <https://doi.org/10.5943/mycosphere/11/1/7>
- Hyde KD, Jeewon R, Chen YJ, Bhunjun CS, Calabon MS, Jiang HB, Lin CG, Norphanphoun C, Sysouphanthong P, Pem D, Tibpromma S, Zhang Q, Doilom M, Jayawardena RS, Liu JK, Maharachchikumbura SSN, Phukhamsakda C, Phookamsak R, Al-Sadi AM, Naritsada Thongklang N, Wang Y, Gafforov Y, Jones EBG, Lumyong S (2020b) The numbers of fungi: is the descriptive curve flattening?. *Fungal Diversity* 103: 219–271. <https://doi.org/10.1007/s13225-020-00458-2>
- Jayasiri SC, Hyde KD, Ariyawansa HA, Bhat J, Buyck B, Cai L, Dai YC, Abd-Elsalam KA, Ertz D, Hidayat I, Jeewon R, Jones EBG, Bahkali AH, Karunarathna SC, Liu JK, Luangsa-ard

- JJ, Lumbsch HT, Maharachchikumbura SSN, McKenzie EHC, Moncalvo JM, Ghobad-Nejhad M, Nilsson H, Pang K, Pereira OL, Phillips AJL, Raspé O, Rollins AW, Romero AI, Etayo J, Selçuk F, Stephenson SL, Suetrong S, Taylor JE, Tsui CKM, Vizzini A, Abdel-Wahab MA, Wen TC, Boonmee S, Dai DQ, Daranagama DA, Dissanayake AJ, Ekanayaka AH, Fryar SC, Hongsanan S, Jayawardena RS, Li WJ, Perera RH, Phookamsak R, De Silva NI, Thambugala KM, Tian Q, Wijayawardene NN, Zhao RL, Zhao Q, Kang JC, Promputtha I (2015) The Faces of Fungi database: fungal names linked with morphology, phylogeny and human impacts. *Fungal Diversity* 74: 3–18. <https://doi.org/10.1007/s13225-015-0351-8>
- Jeewon R, Liew ECY, Hyde KD (2003) Molecular systematics of the Amphisphaeriaceae based on cladistic analyses of partial LSU rDNA gene sequences. *Mycological Research* 107: 1392–1402. <https://doi.org/10.1017/S095375620300875X>
- Kang JC, Kong RYC, Hyde KD (1998) Studies on the Amphisphaeriales 1. Amphisphaeriaceae (*sensu stricto*) and its phylogenetic relationships inferred from 5.8S rDNA and ITS2 sequences. *Fungal Diversity* 1: 147–157.
- Katoh K, Rozewicki J, Yamada KD (2019) MAFFT online service: multiple sequence alignment, interactive sequence choice and visualization. *Briefings in Bioinformatics* 20: 1160–1166. <https://doi.org/10.1093/bib/bbx108>
- Katoh K, Standley DM (2013) MAFFT Multiple Sequence Alignment Software Version 7: Improvements in Performance and Usability. *Molecular Biology and Evolution* 30: 772–780. <https://doi.org/10.1093/molbev/mst010>
- Konta S, Hongsanan S, Tibpromma S, Thongbai B, Maharachchikumbura SSN, Bahkali AH, Hyde KD, Boonmee S (2016) An advance in the endophyte story: Oxydothidaceae fam. nov. with six new species of *Oxydothis*. *Mycosphere* 9: 1425–1446. <https://doi.org/10.5943/mycosphere/7/9/15>
- Li Q, Kang JC, Hyde KD (2015) A multiple gene genealogy reveals the phylogenetic placement of *Iodosphaeria tongrenensis* sp. nov. in Iodosphaeriaceae (Xylariales). *Phytotaxa* 234: 121–132. <http://dx.doi.org/10.11646/phytotaxa.234.2.2>
- Maharachchikumbura SSN, Hyde KD, Jones EBG, McKenzie EHC, Bhat JD, Dayarathne MC, Huang SK, Norphanphoun C, Senanayake IC, Perera RH, Shang QJ, Xiao Y, D'souza MJ, Hongsanan S, Jayawardena RS, Daranagama DA, Konta S, Goonasekara ID, Zhuang WY, Jeewon R, Phillips AJL, Abdel-Wahab MA, Al-Sadi AM, Bahkali AH, Boonmee S, Boonyuen N, Cheewangkoon R, Dissanayake AJ, Kang J, Li QR, Liu JK, Liu XZ, Liu ZY, Luangsa-ard JJ, Pang KL, Phookamsak R, Promputtha I, Suetrong S, Stadler M, Wen T, Wijayawardene NN (2016) Families of Sordariomycetes. *Fungal Diversity* 79: 1–317. <https://doi.org/10.1007/s13225-016-0369-6>
- McTaggart AR, Grice KR, Shivas RG (2013) First report of *Vialaea minutella* in Australia, its association with mango branch dieback and systematic placement of *Vialaea* in the Xylariales. *Australasian Plant Disease Notes* 8: 63–66. <https://doi.org/10.1007/s13314-013-0096-8>
- Miller AN, Réblová M (2021) Phylogenetic placement of Iodosphaeriaceae (Xylariales, Ascomycota), designation of an epitype for the type species of *Iodosphaeria*, *I. phyllophila*, and description of *I. foliicola* sp. nov. *Fungal Systematics and Evolution* 8: 49–64. <https://doi.org/10.3114/fuse.2021.08.05>

- Miller MA, Pfeiffer W, Schwartz T (2012) Creating the CIPRES Science Gateway for inference of large phylogenetic trees. In: Gateway Computing Environments Workshop 2010 (GCE). Ieee, 1–8. <https://doi.org/10.1109/GCE.2010.5676129> [Accessed on 20 September 2021]
- Nylander JA (2004) MrModeltest v2. Program distributed by the author. Evolutionary Biology Centre, Uppsala University, Uppsala, Sweden, 1–3.
- Perera RH, Maharachchikumbura SSN, Jones EBG, Bahkali AH, Elgorban AM, Liu JK, Liu ZY, Hyde KD (2017) *Delonicicola siamense* gen. & sp. nov. (*Delonicicolaceae* fam. nov., *Delonicicolales* ord. nov.), a saprobic species from *Delonix regia* seed pods. *Cryptogamie, Mycologie* 38: 321–340. <https://doi.org/10.7872/crym/v38.iss3.2017.321>
- Rambaut A (2012) FigTree v. 1.4. Molecular evolution, phylogenetics and epidemiology. Edinburgh, UK: University of Edinburgh, Institute of Evolutionary Biology. <http://tree.bio.ed.ac.uk/software/figtree/> [Accessed on 20 September 2021]
- Ronquist F, Teslenko M, Van Der Mark P, Ayres DL, Darling A, Höhna S, Huelsenbeck JP (2012) MrBayes 3.2: efficient Bayesian phylogenetic inference and model choice across a large model space. *Systematic Biology* 61: 539–542. <https://doi.org/10.1093/sysbio/sys029>
- Samarakoon MC, Hyde KD, Promputtha I, Hongsanan S, Ariyawansa HA, Maharachchikumbura SSN, Daranagama DA, Stadler M, Mapook A (2016) Evolution of Xylariomycetidae (Ascomycota: Sordariomycetes). *Mycosphere* 7: 1746–1761. <https://doi.org/10.5943/mycosphere/7/11/9>
- Samuels GJ, Müller E, Petrini O (1987) Studies in the Amphisphaeriaceae (*sensu lato*) 3. New species of *Monographella* and *Pestalotphaeria* and two new genera. *Mycotaxon* 28: 473–499.
- Senanayake IC, Maharachchikumbura SSN, Mortimer PE, Xu J, Bhat JD, Hyde KD (2014) Phylogenetic studies on Vialaeaceae reveals a novel species, *Vialaea mangiferae*. *Sydowia* 66: 203–216. [https://doi.org/10.12905/0380.sydowia66\(2\)2014-0203](https://doi.org/10.12905/0380.sydowia66(2)2014-0203)
- Senanayake IC, Rathnayaka AR, Marasinghe DS, Calabon MS, Gentekaki E, Wanasinghe DN, Lee HB, Hurdeal VG, Pem D, Dissanayake LS, Wijesinghe SN, Bundhun D, Nguyen TT, Goonasekara ID, Abeywickrama PD, Bhunjun CS, Chomnunti P, Boonmee S, Jayawardena RS, Wijayawardene NN, Doilom M, Jeewon R, Bhat JD, Zhang HX, Xie N (2020) Morphological approaches in studying fungi: collection, examination, isolation, sporulation and preservation. *Mycosphere* 11: 2678–2754. <https://doi.org/10.5943/mycosphere/11/1/20>
- Shoemaker RA, Hambleton S, Liu M (2013) *Vialaea insculpta* revisited. *North American Fungi* 8: 1–13. <https://doi:http://dx.doi.org/10.2509/naf2013.008.010>
- Stamatakis A (2014) RAxML version 8: A tool for phylogenetic analysis and post-analysis of large phylogenies. *Bioinformatics* 30: 1312–1313. <https://doi.org/10.1093/bioinformatics/btu033>
- Taylor JE, Hyde KD (1999) Fungi from palms. XL. *Iodosphaeria*. *Sydowia* 51: 127–132.
- Vilgalys R, Hester M (1990) Rapid genetic identification and mapping of enzymatically amplified ribosomal DNA from several *Cryptococcus* species. *Journal of Bacteriology* 172: 4238–4246. <https://doi.org/10.1128/JB.172.8.4238-4246.1990>
- Vu D, Groenewald M, de Vries M, Gehrman T, Stielow B, Eberhardt U, Al-Hatmi A, Groenewald JZ, Cardinali G, Houbraken J, Boekhout T, Crous PW, Robert V, Verkley GJM (2019) Large-scale generation and analysis of filamentous fungal DNA barcodes

- boosts coverage for kingdom fungi and reveals thresholds for fungal species and higher taxon delimitation. *Studies in Mycology* 92: 135–154. <https://doi.org/10.1016/j.simyco.2018.05.001>
- Wanasinghe DN, Phukhamsakda C, Hyde KD, Jeewon R, Lee HB, Jones EBG, Tibpromma S, Tennakoon DS, Dissanayake AJ, Jayasiri SC, Gafforov Y, Camporesi E, Bulgakov TS, Ekanayake AH, Perera RH, Samarakoon MC, Goonasekara ID, Mapook A, Li WJ, Senanayake IC, Li JF, Norphanphoun C, Doilom M, Bahkali AH, Xu JC, Mortimer PE, Tibell L, Savic ST, Karunarathna SC (2018) Fungal Diversity notes 709–839: taxonomic and phylogenetic contributions to fungal taxa with an emphasis on fungi on Rosaceae. *Fungal Diversity* 89: 1–236. <https://doi.org/10.1007/s13225-018-0395-7>
- Wanasinghe DN, Wijayawardene NN, Xu J, Cheewangkoon R, Mortimer PE (2020) Taxonomic novelties in *Magnolia*-associated pleosporalean fungi in the Kunming Botanical Gardens (Yunnan, China). *PLoS ONE* 15(7): e0235855. <https://doi.org/10.1371/journal.pone.0235855>
- Wijayawardene NN, Hyde KD, Al-Ani LKT, Tedersoo L, Haelewaters D, Rajeshkumar KC, Zhao RL, Aptroot A, Leontyev DV, Saxena RK, Tokarev YS, Dai DQ, Letcher PM, Stephenson SL, Ertz D, Lumbsch HT, Kukwa M, Issi IV, Madrid H, Phillips AJL, Selbmann L, Pfliegler WP, Horváth E, Bensch K, Kirk P, Kolaříková Z, Raja HA, Radek R, Papp V, Dima B, Ma J, Malosso E, Takamatsu S, Rambold G, Gannibal PB, Triebel D, Gautam AK, Avasthi S, Suetrong S, Timdal E, Fryar SC, Delgado G, Réblová M, Doilom M, Dolatabadi S, Pawłowska J, Humber RA, Kodsueb R, SánchezCastro I, Goto BT, Silva DKA, De Souza FA, Oehl F, Da Silva GA, Silva IR, Błaszczkowski J, Jobim K, Maia LC, Barbosa FR, Fiuza PO, Divakar PK, Shenoy BD, Castañeda-Ruiz RF, Somrithipol S, Karunarathna SC, Tibpromma S, Mortimer PE, Wanasinghe DN, Phookamsak R, Xu J, Wang Y, Fenghua T, Alvarado P, Li DW, Kušan I, Matočec N, Maharachchikumbura SSN, Papizadeh M, Heredia G, Wartchow F, Bakhshi M, Boehm E, Youssef N, Hustad VP, Lawrey JD, Santiago ALCMA, Bezerra JDP, Souza-Motta CM, Firmino AL, Tian Q, Houbraken J, Hongsanan S, Tanaka K, Dissanayake AJ, Monteiro JS, Grossart HP, Suija A, Weerakoon G, Etayo J, Tsurukau A, Kuhnert E, Vázquez V, Mungai P, Damm U, Li QR, Zhang H, Boonmee S, Lu YZ, Becerra AG, Kendrick B, Brearley FQ, Motiejūnaitė J, Sharma B, Khare R, Gaikwad S, Wijesundara DSA, Tang LZ, He MQ, Flakus A, Rodriguez-Flakus P, Zhurbenko MP, McKenzie EHC, Stadler M, Bhat DJ, Liu JK, Raza M, Jeewon R, Nasonova ES, Prieto M, Jayalal RGU, Yurkov A, Schnittler M, Shchepin ON, Novozhilov YK, Liu P, Cavender JC, Kang Y, Mohammad S, Zhang LF, Xu RF, Li YM, Dayarathne MC, Ekanayaka AH, Wen TC, Deng CY, Lateef AA, Pereira OL, Navathe S, Hawksworth DL, Fan XL, Dissanayake LS, Erdođdu M (2020) Outline of Fungi and fungus-like taxa. *Mycosphere* 11: 1060–1456. <https://doi.org/10.5943/mycosphere/11/1/8>
- White TJ, Bruns T, Lee S, Taylor JW (1990) Amplification and direct sequencing of fungal ribosomal RNA genes for phylogenetics. In: Innis MA, Gelfand DH, Sninsky JJ, White TJ (Eds) *PCR protocols: a guide to methods and applications*. Academic Press, 315–322. <https://doi.org/10.1016/B978-0-12-372180-8.50042-1>

Species diversity, molecular phylogeny and ecological habits of *Cyanosporus* (Polyporales, Basidiomycota) with an emphasis on Chinese collections

Shun Liu¹, Tai-Min Xu¹, Chang-Ge Song¹,
Chang-Lin Zhao², Dong-Mei Wu³, Bao-Kai Cui¹

1 Institute of Microbiology, School of Ecology and Nature Conservation, Beijing Forestry University, Beijing 100083, China **2** College of Biodiversity Conservation, Southwest Forestry University, Kunming 650224, China **3** Biotechnology Research Institute, Xinjiang Academy of Agricultural and Reclamation Sciences / Xinjiang Production and Construction Group Key Laboratory of Crop Germplasm Enhancement and Gene Resources Utilization, Shihezi, Xinjiang 832000, China

Corresponding authors: Bao-Kai Cui (cuibakai@bjfu.edu.cn), Dong-Mei Wu (wdm0999123@sina.com)

Academic editor: María P. Martín | Received 23 November 2021 | Accepted 28 December 2021 | Published 11 January 2022

Citation: Liu S, Xu T-M, Song C-G, Zhao C-L, Wu D-M, Cui B-K (2022) Species diversity, molecular phylogeny and ecological habits of *Cyanosporus* (Polyporales, Basidiomycota) with an emphasis on Chinese collections. MycoKeys 86: 19–46. <https://doi.org/10.3897/mycokeys.86.78305>

Abstract

Cyanosporus is a genus widely distributed in Asia, Europe, North America, South America and Oceania. It grows on different angiosperm and gymnosperm trees and can cause brown rot of wood. Blue-tinted basidiomata of *Cyanosporus* makes it easy to distinguish from other genera, but the similar morphological characters make it difficult to identify species within the genus. Phylogeny and taxonomy of *Cyanosporus* were carried out based on worldwide samples with an emphasis on Chinese collections, and the species diversity of the genus is updated. Four new species, *C. flavus*, *C. rigidus*, *C. subungulatus* and *C. tenuicontextus*, are described based on the evidence of morphological characters, distribution areas, host trees and molecular phylogenetic analyses inferred from the internal transcribed spacer (ITS) regions, the large subunit of nuclear ribosomal RNA gene (nLSU), the small subunit of nuclear ribosomal RNA gene (nSSU), the small subunit of mitochondrial rRNA gene (mtSSU), the largest subunit of RNA polymerase II (RPB1), the second largest subunit of RNA polymerase II (RPB2), and the translation elongation factor 1- α gene (TEF). Our study expanded the number of *Cyanosporus* species to 35 around the world including 23 species from China. Detailed descriptions of the four new species and the geographical locations of the *Cyanosporus* species in China are provided.

Keywords

brown-rot fungi, distribution areas, host trees, multi-gene phylogeny, new species

Introduction

Cyanosporus was proposed as a monotypic genus for *Polyporus caesius* (Schrad.) Fr. based on its cyanophilous basidiospores (McGinty 1909). However, *Tyromyces caesius* (Schrad.) Murrill and *Postia caesia* (Schrad.) P. Karst. were frequently used instead of *Cyanosporus caesius* (Schrad.) McGinty in subsequent studies (Donk 1960; Jahn 1963; Lowe 1975). Later, four species in the *Postia caesia* complex were described from Europe, viz., *P. luteocaesia* (A. David) Jülich, *P. subcaesia* (A. David) Jülich, *P. alni* Niemelä & Vampola and *P. mediterraneocaesia* M. Pieri & B. Rivoire (David 1974, 1980; Jahn 1979; Pieri and Rivoire 2005). Then, the subgenus *Cyanosporus* (McGinty) V. Papp was proposed for the species of *P. caesia* complex (Papp 2014). Miettinen et al. (2018) revised the species concept of the *P. caesia* complex based on morphology and two gene markers (ITS and TEF) and raised the species number of the complex to 24, including six species from China.

Previously, species identification of the *P. caesia* complex was only based on morphological characters and host trees in China, and only two species were recorded from China before Dai (2012), viz., *P. alni* and *P. caesia*. Recently, taxonomic studies of *P. caesia* complex in China have been carried out, and some new species have been described based on both morphological characteristics and molecular data. Shen et al. (2019) carried out a comprehensive study on *Postia* and related genera, in which *Cyanosporus* was supported as an independent genus with 12 species were accepted in this genus. Liu et al. (2021a) studied the species diversity and molecular phylogeny of *Cyanosporus* and the number of *Cyanosporus* species was expanded to 31 around the world, including 19 species from China. These studies have greatly enriched the species of *Cyanosporus* in China. Currently, the morphological characteristics of the genus are as follows: basidiomata annual, pileate or resupinate to effused-reflexed, soft corky, corky to fragile. Pileal surface white to cream to greyish brown, usually with blue tint. Pore surface white to cream, frequently bluish; pores round to angular. Context white to cream, corky. Tubes cream, fragile. Hyphal system monomitic; generative hyphae clamped, IKI–, CB–. Cystidia usually absent, cystidioles occasionally present. Basidiospores narrow, allantoid to cylindrical, hyaline, usually slightly thick-walled, smooth, IKI–, weakly CB+.

Cyanosporus species usually have blue-tinted basidiomata, which makes it easy to recognize. Some specimens with blue-tinted basidiomata were collected during investigations into the diversity of polypores in China, and four undescribed species of *Cyanosporus* were discovered. To confirm the affinity of the undescribed species to *Cyanosporus*, phylogenetic analyses were carried out based on the combined datasets of ITS+TEF and ITS+nLSU+nSSU+mtSSU+RPB1+RPB2+TEF sequences. During the investigation and study of *Cyanosporus*, the information of host trees and distribution areas of species in the genus from China were also obtained (Table 1). Four new species are described and illustrated in the current study, and the geographical locations of the *Cyanosporus* species distributed in China are indicated on the map (Fig. 1).

Table 1. The main ecological habits of *Cyanosporus* with an emphasis on distribution areas and host trees. New species are shown in bold.

Species	Distribution in the world	Distribution in China	Climate zone	Host	Reference
<i>C. alni</i> (Niemiälä & Vampola) B.K. Cui, L.L. Shen & Y.C. Dai	Europe (Czech Republic, Denmark, Finland, Germany, Norway, Poland, Russia, Slovakia), East Asia (China)	Guizhou, Hebei	Temperate	Angiosperm (<i>Alnus</i> , <i>Betula</i> , <i>Corylus</i> , <i>Fagus</i> , <i>Populus</i> , <i>Quercus</i>)	Miettinen et al. 2018; present study
<i>C. arbuti</i> (Spirin) B.K. Cui & Shun Liu	North America (USA)		Temperate	Angiosperm (<i>Arbutus</i>)	Miettinen et al. 2018
<i>C. auricomus</i> (Spirin & Niemiälä) B.K. Cui & Shun Liu	Europe (Finland, Poland, Russia), East Asia (China)	Inner Mongolia	Temperate to boreal	Gymnosperm (<i>Pinus</i> , <i>Picea</i>)	Miettinen et al. 2018; Liu et al. 2021a
<i>C. bifarius</i> (Spirin) B.K. Cui & Shun Liu	Europe (Russia), East Asia (China, Japan)	Jilin, Sichuan, Yunnan	Cold temperate	Gymnosperm (<i>Picea</i> , <i>Pinus</i> , <i>Larix</i>)	Miettinen et al. 2018; present study
<i>C. bubalinus</i> B.K. Cui & Shun Liu	East Asia (China)	Yunnan	Temperate	Gymnosperm (<i>Pinus</i>)	Liu et al. 2021a
<i>C. caesiostimulans</i> (G.F. Atk.) B.K. Cui & Shun Liu	Europe (Finland, Russia), North America (USA)		Temperate	Angiosperm (<i>Corylus</i> , <i>Fagus</i> , <i>Populus</i>) and gymnosperm (<i>Abies</i> , <i>Picea</i>)	Miettinen et al. 2018
<i>C. caesius</i> (Schrad.) McGinty	Europe (Czech Republic, Denmark, Finland, France, Germany, Russia, Slovakia, Spain, UK)		Common in temperate, rare in south boreal zone	Angiosperm (<i>Betula</i> , <i>Fagus</i> , <i>Salix</i>) and gymnosperm (<i>Abies</i> , <i>Picea</i>)	Miettinen et al. 2018
<i>C. coerulevivrens</i> (Corner) B.K. Cui, Shun Liu & Y.C. Dai	Asia (China, Indonesia), Europe (Russia)	Hunan, Jilin, Zhejiang	Warm temperate	Angiosperm (<i>Tilia</i> , <i>Ulmus</i>)	Miettinen et al. 2018; present study
<i>C. comatus</i> (Miettinen) B.K. Cui & Shun Liu	North America (USA), East Asia (China)	Sichuan, Xizang	Temperate	Angiosperm (<i>Acer</i>) and gymnosperm (<i>Abies</i> , <i>Picea</i> , <i>Tsuga</i>)	Miettinen et al. 2018; present study
<i>C. cyanescens</i> (Miettinen) B.K. Cui & Shun Liu	Europe (Estonia, Finland, France, Poland, Russia, Spain, Sweden)		Temperate to Mediterranean mountains	Gymnosperm (<i>Abies</i> , <i>Picea</i> , <i>Pinus</i>)	Miettinen et al. 2018
<i>C. flavus</i> B.K. Cui & Shun Liu	East Asia (China)	Sichuan	Plateau humid climate	Gymnosperm (<i>Abies</i>, <i>Picea</i>)	Present study
<i>C. fusiformis</i> B.K. Cui, L.L. Shen & Y.C. Dai	East Asia (China)	Guizhou, Sichuan	North temperate to subtropical	Angiosperm (<i>Rhododendron</i>)	Shen et al. 2019
<i>C. glauca</i> (Spirin & Miettinen) B.K. Cui & Shun Liu	East Asia (China), Europe (Russia)	Jilin	Cold temperate mountains	Gymnosperm (<i>Abies</i> , <i>Picea</i>)	Miettinen et al. 2018
<i>C. gossypinus</i> (Moug. & Lév.) B.K. Cui & Shun Liu	Europe (France)		Temperate	Gymnosperm (<i>Cedrus</i>)	Miettinen et al. 2018
<i>C. hirsutus</i> B.K. Cui & Shun Liu	East Asia (China)	Qinghai, Sichuan, Yunnan	Temperate to plateau continental climate	Gymnosperm (<i>Abies</i> , <i>Picea</i>)	Liu et al. 2021a; present study
<i>C. livens</i> (Miettinen & Vlasák) B.K. Cui & Shun Liu	North America (Canada, USA)		Temperate	Angiosperm (<i>Acer</i> , <i>Betula</i> , <i>Fagus</i>) and gymnosperm (<i>Abies</i> , <i>Larix</i> , <i>Picea</i> , <i>Tsuga</i>)	Miettinen et al. 2018
<i>C. luteocaesius</i> (A. David) B.K. Cui, L.L. Shen & Y.C. Dai	Europe (France)		Mediterranean	Gymnosperm (<i>Pinus</i>)	Miettinen et al. 2018
<i>C. magnus</i> (Miettinen) B.K. Cui & Shun Liu	East Asia (China)	Chongqin, Jilin, Hainan, Yunnan	Temperate	Angiosperm (<i>Populus</i>) and gymnosperm (<i>Cunninghamia</i>)	Miettinen et al. 2018; present study
<i>C. mediterraneaesius</i> (M. Pieri & B. Rivoire) B.K. Cui, L.L. Shen & Y.C. Dai	Europe (France, Spain)		Warm temperate to Mediterranean	Angiosperm (<i>Buxus</i> , <i>Erica</i> , <i>Populus</i> , <i>Quercus</i>) and gymnosperm (<i>Cedrus</i> , <i>Juniperus</i> , <i>Pinus</i>)	Miettinen et al. 2018
<i>C. microporus</i> B.K. Cui, L.L. Shen & Y.C. Dai	East Asia (China)	Yunnan	subtropical	Angiosperm (undetermined)	Shen et al. 2019
<i>C. nothofagicola</i> B.K. Cui, Shun Liu & Y.C. Dai	Oceania (Australia), South America (Argentina)		Temperate marine climate	Angiosperm (<i>Nothofagus</i>)	Liu et al. 2021a

Species	Distribution in the world	Distribution in China	Climate zone	Host	Reference
<i>C. picicola</i> B.K. Cui, L.L. Shen & Y.C. Dai	East Asia (China)	Sichuan, Xizang, Yunnan	Warm temperate to subtropical	Gymnosperm (<i>Picea</i>)	Shen et al. 2019
<i>C. populi</i> (Miettinen) B.K. Cui & Shun Liu	East Asia (China), Europe (Finland, Norway, Poland, Russia), North America (USA)	Qinghai, Jilin, Sichuan, Yunnan	Boreal to temperate	Angiosperm (<i>Acer</i> , <i>Alnus</i> , <i>Betula</i> , <i>Populus</i> , <i>Salix</i>) and gymnosperm (<i>Picea</i>)	Miettinen et al. 2018; Liu et al. 2021a; present study
<i>C. rigidus</i> B.K. Cui & Shun	East Asia (China)	Yunnan	Warm temperate	Gymnosperm (<i>Picea</i>)	Present study
<i>C. simulans</i> (P. Karst.) B.K. Cui & Shun Liu	East Asia (China), Europe (Estonia, Finland, France, Germany, Norway, Russia), North America (Canada, USA)	Jilin	Warm temperate to boreal	Angiosperm (<i>Corylus</i> , <i>Fagus</i> , <i>Populus</i> , <i>Sorbus</i> , <i>Ulmus</i>) and gymnosperm (<i>Abies</i> , <i>Cedrus</i> , <i>Juniperus</i> , <i>Picea</i> , <i>Pinus</i> , <i>Thuja</i> , <i>Tsuga</i>)	Miettinen et al. 2018
<i>C. subcaesius</i> (A. David) B.K. Cui, L.L. Shen & Y.C. Dai	Europe (Czech Republic, Finland, France, Russia, UK)		Temperate	Angiosperm (<i>Alnus</i> , <i>Carpinus</i> , <i>Crataegus</i> , <i>Corylus</i> , <i>Fagus</i> , <i>Fraxinus</i> , <i>Malus</i> , <i>Populus</i> , <i>Prunus</i> , <i>Quercus</i> , <i>Salix</i> , <i>Ulmus</i>)	Miettinen et al. 2018
<i>C. subhirsutus</i> B.K. Cui, L.L. Shen & Y.C. Dai	East Asia (China)	Guizhou, Fujian, Yunnan	Warm temperate to subtropical	Angiosperm (<i>Pterocarya</i>)	Shen et al. 2019
<i>C. submicroporus</i> B.K. Cui & Shun Liu	East Asia (China)	Sichuan, Yunnan, Zhejiang	Alpine plateau to subtropical	Angiosperm (<i>Alnus</i> , <i>Cyclobalanopsis</i>)	Liu et al. 2021a; present study
<i>C. subungulatus</i> B.K. Cui & Shun Liu	East Asia (China)	Yunnan	Subtropical	Angiosperm (undetermined) and gymnosperm (<i>Pinus</i>)	Present study
<i>C. subviridis</i> (Ryvarden & Guzmán) B.K. Cui & Shun Liu	Europe (Finland), North America (Mexico, USA)		Temperate to boreal	Gymnosperm (<i>Abies</i> , <i>Picea</i> , <i>Pinus</i>)	Miettinen et al. 2018
<i>C. tenuicontextus</i> B.K. Cui & Shun Liu	East Asia (China)	Yunnan	Subtropical	Angiosperm (undetermined) and gymnosperm (<i>Pinus</i>)	Present study
<i>C. tenuis</i> B.K. Cui, Shun Liu & Y.C. Dai	East Asia (China)	Sichuan	Subtropical monsoon to Alpine plateau	Gymnosperm (<i>Picea</i>)	Liu et al. 2021a
<i>C. tricolor</i> B.K. Cui, L.L. Shen & Y.C. Dai	East Asia (China)	Sichuan, Xizang	Alpine plateau	Gymnosperm (<i>Abies</i> , <i>Picea</i>)	Shen et al. 2019
<i>C. unguilatus</i> B.K. Cui, L.L. Shen & Y.C. Dai	East Asia (China)	Sichuan	Subtropical monsoon to Alpine plateau	Angiosperm (<i>Castanopsis</i>) and gymnosperm (<i>Abies</i>)	Shen et al. 2019
<i>C. yanae</i> (Miettinen & Kotir.) B.K. Cui & Shun Liu	Europe (Russia)		Temperate continental climate	Gymnosperm (<i>Larix</i> , <i>Pinus</i>)	Miettinen et al. 2018

Materials and methods

Morphological studies

The examined specimens were deposited in the herbarium of the Institute of microbiology, Beijing Forestry University (BJFC), and some duplicates were deposited at the Institute of Applied Ecology, Chinese Academy of Sciences, China (IFP) and Southwest Forestry University (SWFC). Macro-morphological descriptions were based on the field notes and measurements of herbarium specimens. Special colour terms followed Petersen (1996). Micro-morphological data were obtained from the dried specimens and observed under a light microscope following Cui et al. (2019) and Liu et al. (2021b). Sections were studied at a magnification up to $\times 1000$ using a Nikon Eclipse 80i microscope and phase contrast

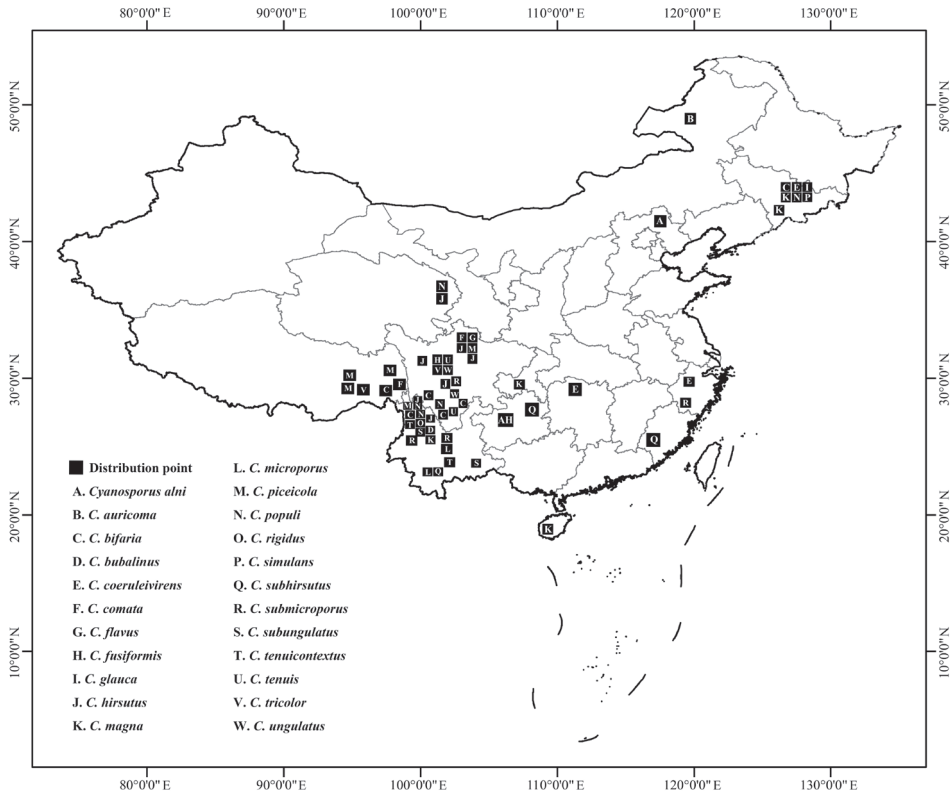


Figure 1. The geographical locations of the *Cyanosporus* species distributed in China.

illumination (Nikon, Tokyo, Japan). Drawings were made with the aid of a drawing tube. Microscopic features, measurements and drawings were made from slide preparations stained with Cotton Blue and Melzer's reagent. Spores were measured from sections cut from the tubes. To present variation in the size of basidiospores, 5% of measurements were excluded from each end of the range and extreme values are given in parentheses.

In the text the following abbreviations were used: IKI = Melzer's reagent, IKI- = neither amyloid nor dextrinoid, KOH = 5% potassium hydroxide, CB = Cotton Blue, CB + = cyanophilous, CB - = acyanophilous, L = mean spore length (arithmetic average of all spores), W = mean spore width (arithmetic average of all spores), Q = variation in the L/W ratios between the specimens studied, n (a/b) = number of spores (a) measured from given number (b) of specimens.

Molecular studies and phylogenetic analysis

A cetyl trimethylammonium bromide (CTAB) rapid plant genome extraction kit-DN14 (Aidlab Biotechnologies Co., Ltd, Beijing, China) was used to extract total genomic DNA from dried specimens, and performed the polymerase chain reaction

(PCR) according to the manufacturer's instructions with some modifications as described by Shen et al. (2019) and Liu et al. (2021a). The ITS regions were amplified with primer pairs ITS5 and ITS4 (White et al. 1990). The nLSU regions were amplified with primer pairs LR0R and LR7 (<http://www.biology.duke.edu/fungi/mycolab/primers.htm>). The nSSU regions were amplified with primer pairs NS1 and NS4 (White et al. 1990). The mtSSU regions were amplified with primer pairs MS1 and MS2 (White et al. 1990). RPB1 was amplified with primer pairs RPB1-Af and RPB1-Cr (Matheny et al. 2002). RPB2 was amplified with primer pairs fRPB2-f5F and bRPB2-7.1R (Matheny 2005). Part of TEF was amplified with primer pairs EF1-983 F and EF1-1567R (Rehner 2001).

The PCR cycling schedule for ITS, mtSSU and TEF included an initial denaturation at 95 °C for 3 min, followed by 35 cycles at 94 °C for 40 s, 54 °C for ITS and mtSSU, 54–55 °C for TEF for 45 s, 72 °C for 1 min, and a final extension at 72 °C for 10 min. The PCR cycling schedule for nLSU and nSSU included an initial denaturation at 94 °C for 1 min, followed by 35 cycles at 94 °C for 30 s, 50 °C for nLSU and 52 °C for nSSU for 1 min, 72 °C for 1.5 min, and a final extension at 72 °C for 10 min. The PCR procedure for RPB1 and RPB2 follow Justo and Hibbett (2011) with slight modifications: initial denaturation at 94 °C for 2 min, followed by 10 cycles at 94 °C for 40 s, 60 °C for 40 s and 72 °C for 2 min, then followed by 37 cycles at 94 °C for 45 s, 55 °C for 1.5 min and 72 °C for 2 min, and a final extension of 72 °C for 10 min. The PCR products were purified and sequenced at Beijing Genomics Institute (BGI), China, with the same primers. All newly generated sequences were deposited at GenBank (Table 1).

Additional sequences were downloaded from GenBank (Table 1). All sequences of ITS, nLSU, nSSU, mtSSU, RPB1, RPB2 and TEF were respectively aligned in MAFFT 7 (Kato and Standley 2013; <http://mafft.cbrc.jp/alignment/server/>) and manually adjusted in BioEdit (Hall 1999). Alignments were spliced in Mesquite (Maddison and Maddison 2017). The missing sequences were coded as “N”. Ambiguous nucleotides were coded as “N”. The final concatenated sequence alignment was deposited at Tree-Base (<http://purl.org/phylo/treebase>; submission ID: 29010).

Most parsimonious phylogenies were inferred from the combined 2-gene dataset (ITS+TEF) and 7-gene dataset (ITS+nLSU+nSSU+mtSSU+RPB1+RPB2+TEF), and their congruences were evaluated with the incongruence length difference (ILD) test (Farris et al. 1994) implemented in PAUP* 4.0b10 (Swofford 2002), under heuristic search and 1000 homogeneity replicates. Phylogenetic analyses approaches followed Liu et al. (2019) and Sun et al. (2020). In phylogenetic reconstruction, the sequences of *Antrodia serpens* (Fr.) Donk and *A. tanakae* (Murrill) Spirin & Miettinen obtained from GenBank were used as outgroups. Maximum parsimony analysis was applied to the combined multiple genes datasets, and the tree construction procedure was performed in PAUP* version 4.0b10. All characters were equally weighted and gaps were treated as missing data. Trees were inferred using the heuristic search option with TBR branch swapping and 1000 random sequence additions. Max-trees were set to 5000, branches of zero length were collapsed and all parsimonious trees were saved. Clade robustness was assessed using a bootstrap (BT) analysis with 1000 replicates

(Felsenstein 1985). Descriptive tree statistics tree length (TL), consistency index (CI), retention index (RI), rescaled consistency index (RC), and homoplasy index (HI) were calculated for each most Parsimonious Tree (MPT) generated. RAxML v.7.2.8 was used to construct a maximum likelihood (ML) tree with a GTR+G+I model of site substitution including estimation of Gamma-distributed rate heterogeneity and a proportion of invariant sites (Stamatakis 2006). The branch support was evaluated with a bootstrapping method of 1000 replicates (Hillis and Bull 1993). The phylogenetic tree was visualized using FigTree v1.4.2 (<http://tree.bio.ed.ac.uk/software/figtree/>).

MrModeltest 2.3 (Posada and Crandall 1998; Nylander 2004) was used to determine the best-fit evolution model for the combined multi-gene dataset for Bayesian inference (BI). Bayesian inference was calculated with MrBayes 3.1.2 with a general time reversible (GTR) model of DNA substitution and a gamma distribution rate variation across sites (Ronquist and Huelsenbeck 2003). Four Markov chains were run for 2 runs from random starting trees for 1.8 million generations (ITS+TEF), for 3.5 million generations (ITS+nLSU+nSSU+mtSSU+RPB1+RPB2+TEF) and trees were sampled every 100 generations. The first one-fourth generations were discarded as burn-in. A majority rule consensus tree of all remaining trees was calculated. Branches that received bootstrap support for maximum parsimony (MP), maximum likelihood (ML) and Bayesian posterior probabilities (BPP) greater than or equal to 75% (MP and ML) and 0.95 (BPP) were considered as significantly supported, respectively.

Results

Phylogeny

The combined 2-gene (ITS+TEF) sequences dataset had an aligned length of 1015 characters, of which 502 characters were constant, 62 were variable and parsimony-uninformative, and 451 were parsimony-informative. MP analysis yielded 10 equally parsimonious trees (TL = 2396, CI = 0.379, RI = 0.735, RC = 0.279, HI = 0.621). The best model for the concatenate sequence dataset estimated and applied in the Bayesian inference was GTR+I+G with equal frequency of nucleotides. ML analysis resulted in a similar topology as MP and Bayesian analyses, and only the ML topology is shown in Fig. 2.

The combined 7-gene (ITS+nLSU+nSSU+mtSSU+RPB1+RPB2+TEF) sequences dataset had an aligned length of 5634 characters, of which 3843 characters were constant, 247 were variable and parsimony-uninformative, and 1544 were parsimony-informative. MP analysis yielded 23 equally parsimonious trees (TL = 5756, CI = 0.468, RI = 0.752, RC = 0.352, HI = 0.532). The best model for the concatenate sequence dataset estimated and applied in the Bayesian inference was GTR+I+G with equal frequency of nucleotides. ML analysis resulted in a similar topology as MP and Bayesian analyses, and only the ML topology is shown in Fig. 3.

The phylogenetic trees inferred from ITS+TEF and ITS+nLSU+nSSU+mtSSU+RPB1+RPB2+TEF gene sequences were all obtained from 106 fungal samples represent-

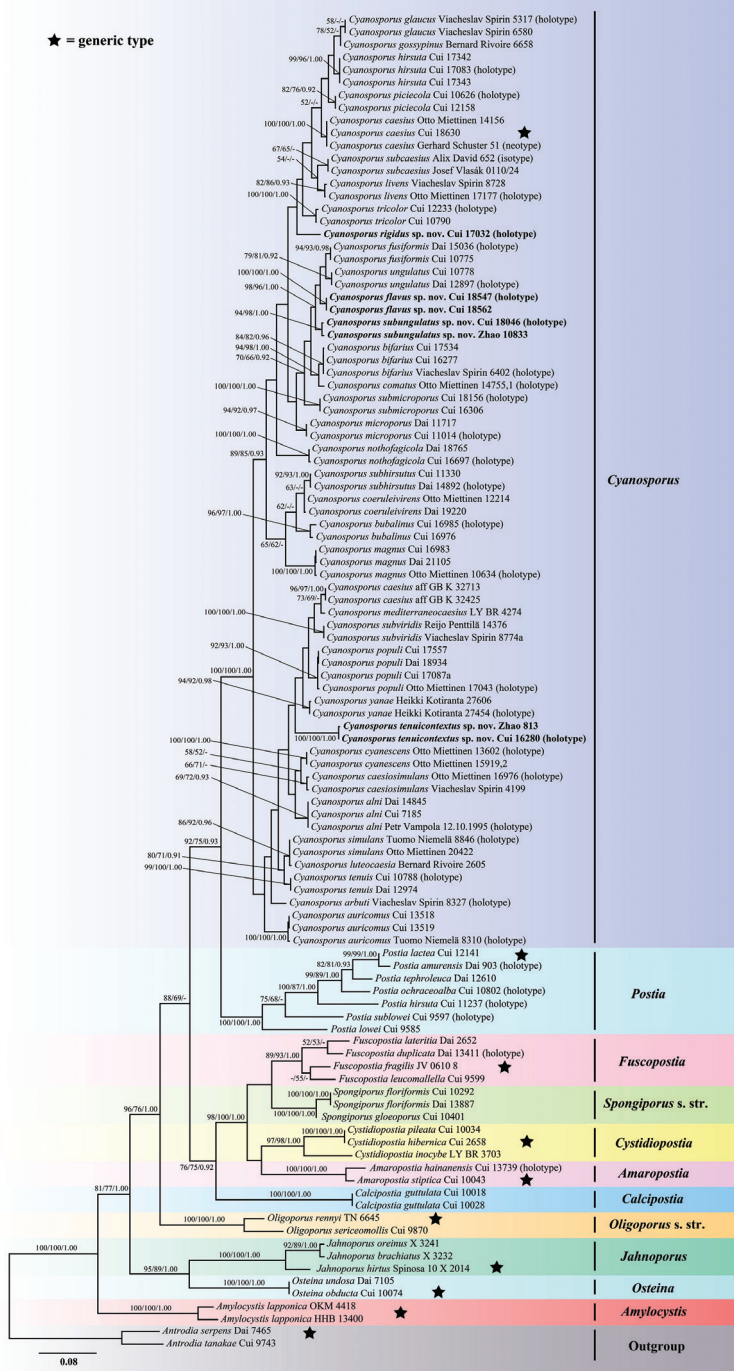


Figure 2. Maximum likelihood tree illustrating the phylogeny of *Cyanosporus* and its related genera in the antrodia clade based on the combined sequences dataset of ITS+TEF. Branches are labelled with maximum likelihood bootstrap higher than 50%, parsimony bootstrap proportions higher than 50% and Bayesian posterior probabilities more than 0.90 respectively. Bold names = New species.

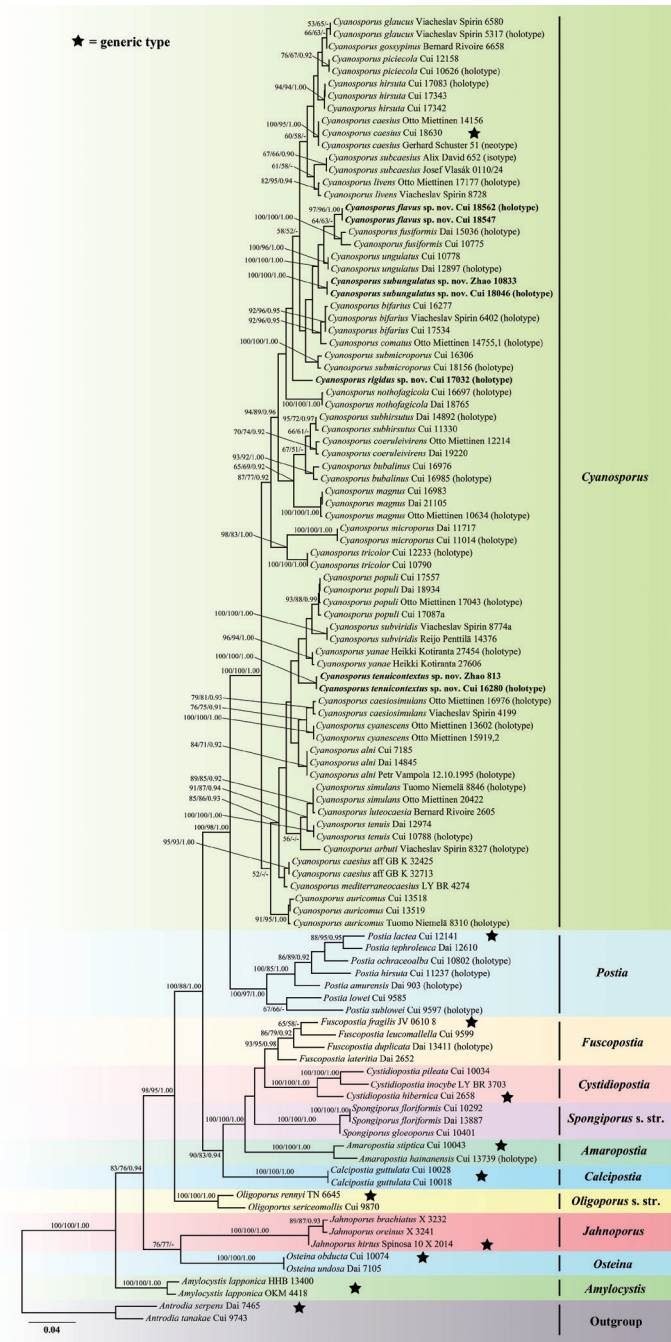


Figure 3. Maximum likelihood tree illustrating the phylogeny of *Cyanosporus* and its related genera in the antrodia clade based on the combined sequences dataset of ITS+nLSU+nSSU+mtSSU+RPB1+RPB2 +TEF. Branches are labelled with maximum likelihood bootstrap higher than 50%, parsimony bootstrap proportions higher than 50% and Bayesian posterior probabilities more than 0.90 respectively. Bold names = New species.

ing 65 taxa of *Cyanosporus* and its related genera within the antrodia clade. 74 samples representing 35 taxa of *Cyanosporus* clustered together and separated from species of *Postia* and other related genera. As for *Cyanosporus*, the sequences used in phylogenetic analyses include 28 holotype specimen sequences, one isotype specimen sequence and one neotype specimen sequence (Table 1).

Taxonomy

Cyanosporus flavus B.K. Cui & Shun Liu, sp. nov.

MycoBank No: 842319

Figs 4, 5

Diagnosis. *Cyanosporus flavus* is characterised by flabelliform to semicircular and hirsute pileus with ash grey to light vinaceous grey pileal surface when fresh, buff to lemon-chrome pore surface when dry, and allantoid and slightly curved basidiospores ($4.6\text{--}5.2 \times 0.8\text{--}1.3 \mu\text{m}$).

Holotype. China. Sichuan Province, Jiuzhaigou County, on stump of *Picea* sp., 19.IX.2020, Cui 18547 (BJFC 035408).

Etymology. *Flavus* (Lat.): referring to its lemon-chrome pore surface when dry.

Fruiting body. Basidiomata annual, pileate, soft and watery, without odour or taste when fresh, becoming corky to fragile and light in weight upon drying. Pileus flabelliform to semicircular, projecting up to 3.2 cm, 5.7 cm wide and 0.9 cm thick at base. Pileal surface ash-grey to light vinaceous grey when fresh, becoming pale mouse-grey to mouse-grey when dry, hirsute; margin acute to slightly obtuse, white with a little blue tint when fresh, olivaceous buff to greyish brown when dry. Pore surface white to cream when fresh, becoming buff to lemon-chrome when dry; sterile margin narrow to almost lacking; pores angular, 5–7 per mm; dissepiments thin, entire to lacerate. Context white to cream, soft corky, up to 6 mm thick. Tubes pale mouse-grey to ash-grey, fragile, up to 4 mm long.

Hyphal structure. Hyphal system monomitic; generative hyphae with clamp connections, IKI–, CB–; hyphae unchanged in KOH.

Context. Generative hyphae hyaline, thin- to slightly thick-walled with a wide lumen, occasionally branched, loosely interwoven, $2.7\text{--}6.5 \mu\text{m}$ in diam.

Tubes. Generative hyphae hyaline, thin- to slightly thick-walled with a wide lumen, rarely branched, interwoven, $2.2\text{--}4.7 \mu\text{m}$ in diam. Cystidia absent; cystidioles present, fusoid, thin-walled, $12.3\text{--}17.8 \times 2.2\text{--}3.5 \mu\text{m}$. Basidia clavate, bearing four sterigmata and a basal clamp connection, $13.2\text{--}16.5 \times 3.2\text{--}5.5 \mu\text{m}$; basidioles dominant, in shape similar to basidia, but smaller, $12.6\text{--}15.7 \times 2.9\text{--}5.2 \mu\text{m}$.

Spores. Basidiospores slim allantoid, slightly curved, hyaline, thin- to slightly thick-walled, smooth, IKI–, CB–, $4.6\text{--}5.2 \times 0.8\text{--}1.3 \mu\text{m}$, $L = 5 \mu\text{m}$, $W = 0.99 \mu\text{m}$, $Q = 4.96\text{--}5.25$ ($n = 60/2$).

Type of rot. Brown rot.

Additional specimen (paratype) examined. China. Sichuan Province, Jiuzhaigou County, Jiuzhaigou Nature Reserve, on fallen trunk of *Abies* sp., 20.IX.2020, Cui 18562 (BJFC 035423).



Figure 4. Basidiomata of *Cyanosporus flavus* (Holotype, Cui 18547). Scale bar: 1 cm. The upper figure is the upper surface and the lower figure is the lower surface of the basidiomata.

***Cyanosporus rigidus* B.K. Cui & Shun Liu, sp. nov.**

Mycobank No: 842320

Figs 6, 7

Diagnosis. *Cyanosporus rigidus* is characterised by corky, hard corky to rigid basidiomata with a buff yellow to clay-buff and tomentose pileal surface when fresh, becom-

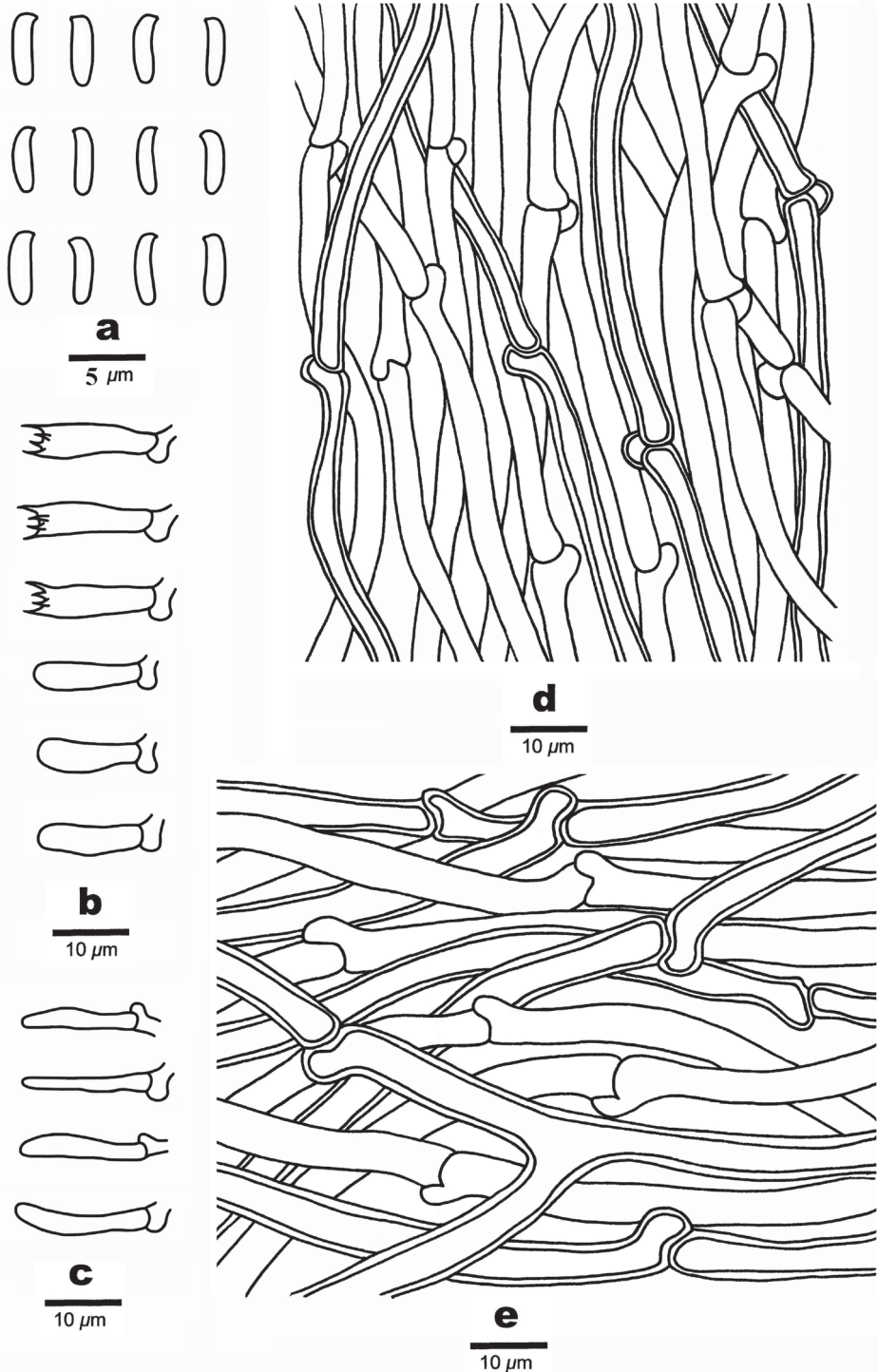


Figure 5. Microscopic structures of *Cyanosporus flavus* (Holotype, Cui 18547) **a** basidiospores **b** basidia and basidioles **c** cystidioles **d** hyphae from trama **e** hyphae from context. Drawings by: Shun Liu.



Figure 6. Basidiomata of *Cyanosporus rigidus* (Holotype, Cui 17032). Scale bar: 1.5 cm. The upper figure is the upper surface and the lower figure is the lower surface of the basidiomata.

ing olivaceous buff to greyish brown when dry, smaller and cylindrical to allantoid basidiospores ($3.7\text{--}4.2 \times 0.9\text{--}1.3 \mu\text{m}$).

Holotype. China. Yunnan Province, Yulong County, Laojun Mountain, Jiushijiu Longtan, on fallen trunk of *Abies* sp., 15.IX.2018, Cui 17032 (BJFC 030331).

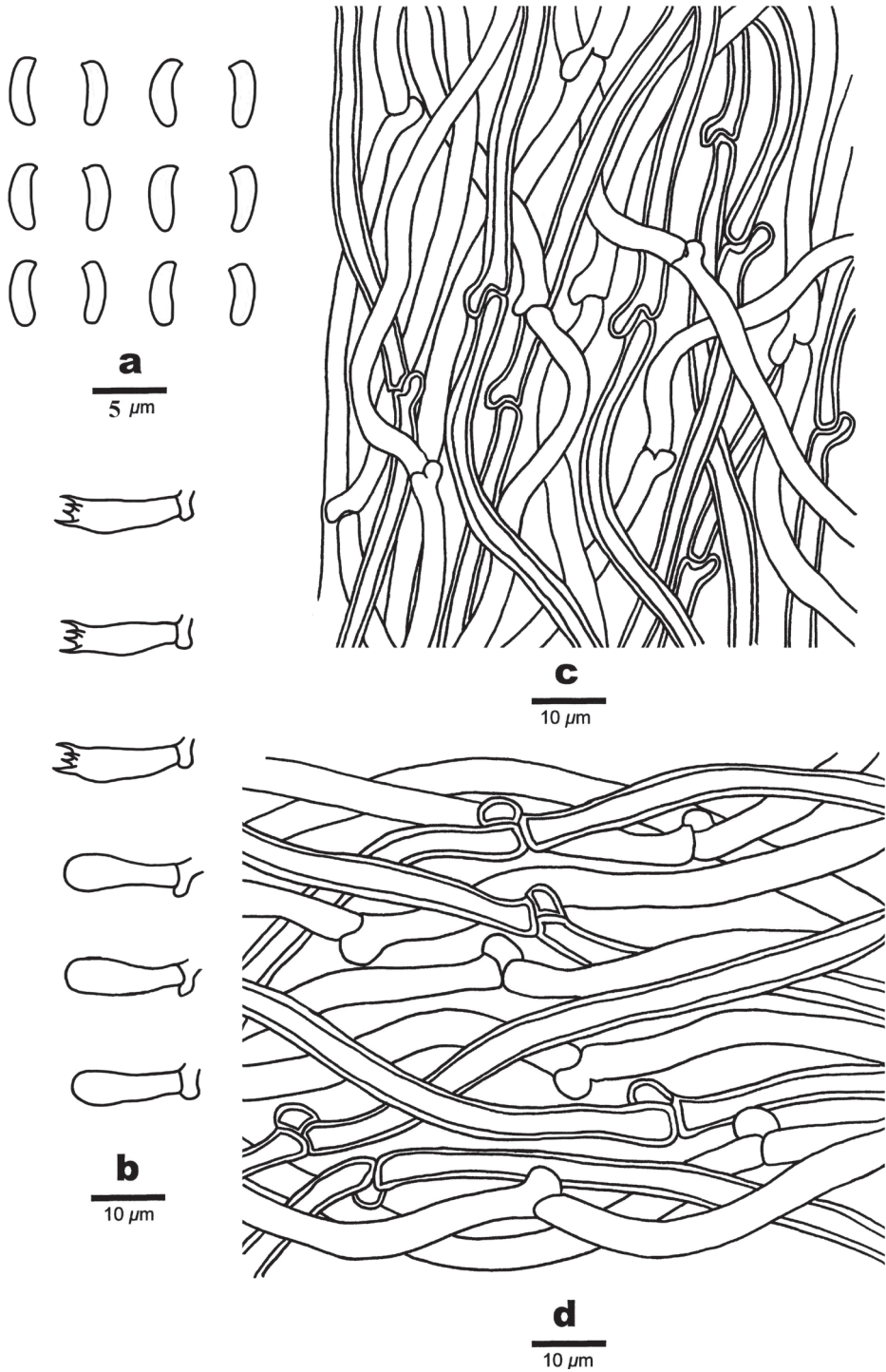


Figure 7. Microscopic structures of *Cyanosporus rigidus* (Holotype, Cui 17032) **a** basidiospores **b** basidia and basidioles **c** hyphae from trama **d** hyphae from context. Drawings by: Shun Liu.

Etymology. *Rigidus* (Lat.): referring to the rigid basidiomata.

Fruiting body. Basidiomata annual, pileate, corky, without odour or taste when fresh, becoming hard corky to rigid upon drying. Pileus flabelliform, projecting up to 1.6 cm, 3.8 cm wide and 0.6 cm thick at base. Pileal surface tomentose, buff yellow to clay-buff, when fresh, becoming smooth, rugose, olivaceous buff to greyish brown when dry; margin obtuse. Pore surface white to cream when fresh, becoming buff-yellow to pinkish buff when dry; sterile margin narrow to almost lacking; pores angular, 5–8 per mm; dissepiments thin, entire to lacerate. Context cream to buff, hard corky, up to 4 mm thick. Tubes cream to pinkish buff, brittle, up to 5 mm long.

Hyphal structure. Hyphal system monomitic; generative hyphae with clamp connections, IKI–, CB–; hyphae unchanged in KOH.

Context. Generative hyphae hyaline, thin- to slightly thick-walled with a wide lumen, rarely branched, loosely interwoven, 2.2–5 µm in diam.

Tubes. Generative hyphae hyaline, thin- to slightly thick-walled with a wide lumen, occasionally branched, interwoven, 2–4 µm in diam. Cystidia and cystidioles absent. Basidia clavate, bearing four sterigmata and a basal clamp connection, 12.4–14.8 × 3–4.2 µm; basidioles dominant, in shape similar to basidia, but smaller, 11.8–13.9 × 2.6–4 µm.

Spores. Basidiospores allantoid to cylindrical, slightly curved, hyaline, thin- to slightly thick-walled, smooth, IKI–, CB–, (3.5–)3.7–4.2 × (0.8–)0.9–1.3(–1.4) µm, L = 3.94 µm, W = 1.09 µm, Q = 3.66 (n = 60/1).

Type of rot. Brown rot.

***Cyanosporus subungulatus* B.K. Cui & Shun Liu, sp. nov.**

Mycobank No: 842321

Figs 8, 9

Diagnosis. *Cyanosporus subungulatus* is characterised by shell-shaped pileus with a pale mouse-grey to ash-grey pileal surface when fresh, dark-grey to mouse-grey when dry, allantoid to cylindrical and slightly curved basidiospores (4.5–5.2 × 1.1–1.4 µm).

Holotype. China. Yunnan Province, Yangbi County, Shimenguan Nature Reserve, on fallen trunk of *Pinus* sp., 6.IX.2019, Cui 18046 (BJFC 034905).

Etymology. *Subungulatus* (Lat.): referring to the species resembling *Cyanosporus unguatus* in morphology.

Fruiting body. Basidiomata annual, pileate, soft corky, without odour or taste when fresh, becoming corky to fragile and light in weight upon drying. Pileus shell-shaped, projecting up to 1.7 cm, 2.8 cm wide and 1.2 cm thick at base. Pileal surface velutinate, pale mouse-grey to ash-grey when fresh, becoming smooth, rugose, dark-grey to mouse-grey when dry; margin obtuse. Pore surface white to cream when fresh, becoming cream to pinkish buff when dry; sterile margin narrow to almost lacking; pores round, 4–6 per mm; dissepiments thin, entire to lacerate. Context white to cream, soft corky, up to 5 mm thick. Tubes pale mouse-grey to ash-grey, fragile, up to 6 mm long.



Figure 8. Basidiomata of *Cyanosporus subungulatus* (Holotype, Cui 18046). Scale bar: 10 mm. The upper figure is the upper surface and the lower figure is the lower surface of the basidiomata.

Hyphal structure. Hyphal system monomitic; generative hyphae with clamp connections, IKI–, CB–; hyphae unchanged in KOH.

Context. Generative hyphae hyaline, slightly thick-walled with a wide lumen, rarely branched, loosely interwoven, 2.5–6.4 μm in diam.

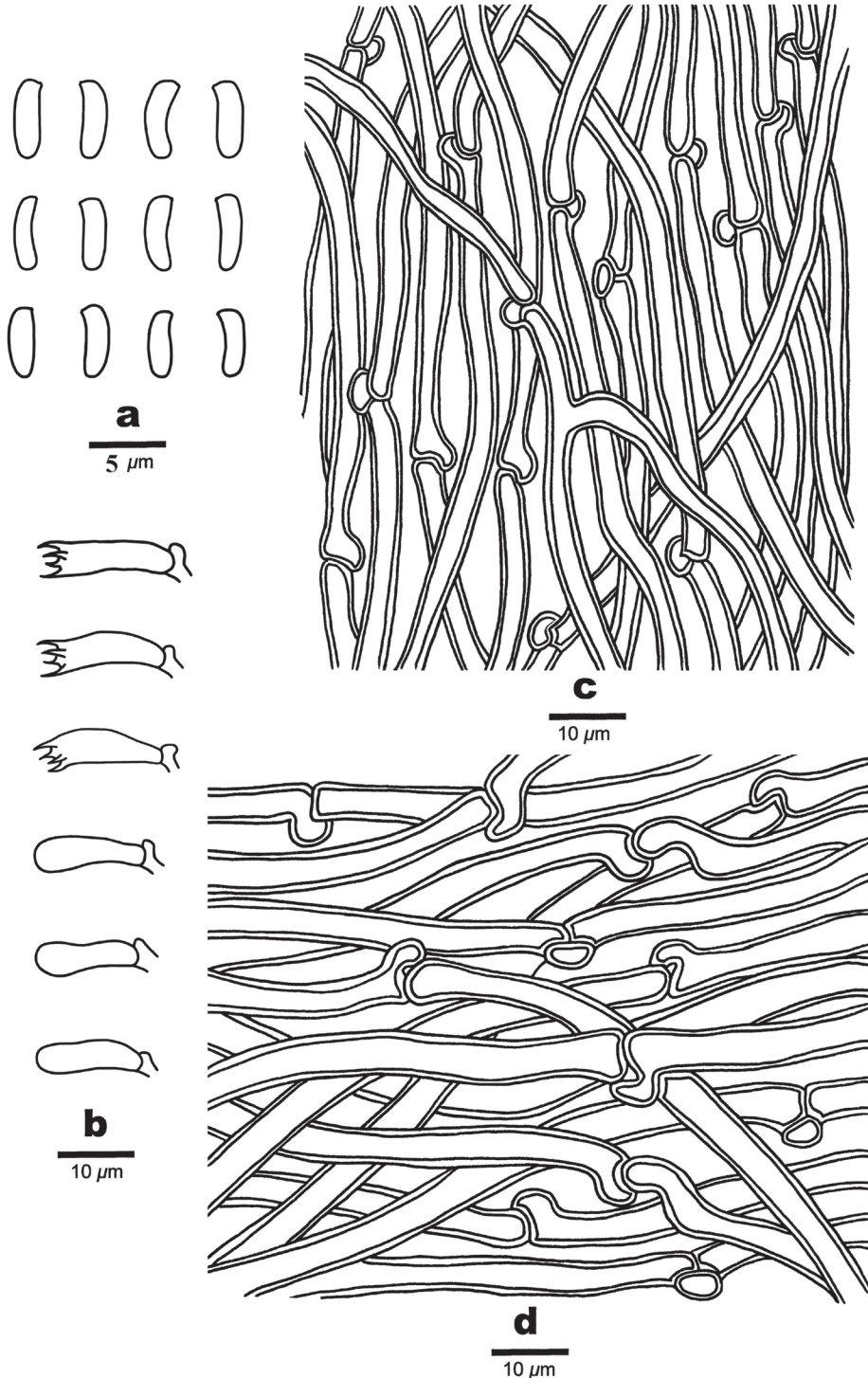


Figure 9. Microscopic structures of *Cyanosporus subungulatus* (Holotype, Cui 18046) **a** basidiospores **b** basidia and basidioles **c** hyphae from trama **d** hyphae from context. Drawings by: Shun Liu.

Tubes. Generative hyphae hyaline, slightly thick-walled with a wide lumen, occasionally branched, interwoven, 2–4.2 μm in diam. Cystidia and cystidioles absent. Basidia clavate, bearing four sterigmata and a basal clamp connection, 13.6–17.8 \times 3–5.5 μm ; basidioles dominant, in shape similar to basidia, but smaller, 12.8–17.2 \times 2.4–5.2 μm .

Spores. Basidiospores allantoid to cylindrical, slightly curved, hyaline, thin- to slightly thick-walled, smooth, IKI–, CB–, (4.3–)4.5–5.2 \times 1.1–1.4 μm , L = 4.73 μm , W = 1.22 μm , Q = 3.48–3.66 (n = 60/2).

Type of rot. Brown rot.

Additional specimen (paratype) examined. China, Yunnan Province, Xichou County, Xiaoqiaogou Nature Reserve, on fallen angiosperm trunk, 14.I.2019, Zhao 10833 (SWFC 010833).

***Cyanosporus tenuicontextus* B.K. Cui & Shun Liu, sp. nov.**

MycoBank No: 842323

Figs 10, 11

Diagnosis. *Cyanosporus tenuicontextus* is characterised by flabelliform pileus with a velutinate, cream to pinkish buff with a little blue tint pileal surface when fresh, becoming glabrous, light vinaceous grey to pale mouse-grey when dry, small and round pores (6–8 per mm), thin context (up to 0.8 mm) and allantoid basidiospores (3.8–4.3 \times 0.8–1.2 μm).

Holotype. China. Yunnan Province, Lanping County, Tongdian Town, Luoguing, on fallen trunk of *Pinus* sp., 19.IX.2017, Cui 16280 (BJFC 029579).

Etymology. *Tenuicontextus* (Lat.): referring to the species having thin context.

Fruiting body. Basidiomata annual, pileate, soft corky, without odour or taste when fresh, becoming corky to fragile and light in weight upon drying. Pileus flabelliform, projecting up to 1.3 cm, 3.2 cm wide and 0.5 cm thick at base. Pileal surface velutinate, cream to pinkish buff with a little blue tint when fresh, becoming glabrous, light vinaceous grey to pale mouse-grey when dry; margin acute. Pore surface white to cream when fresh, becoming pinkish buff to buff when dry; sterile margin narrow to almost lacking; pores round, 6–8 per mm; dissepiments thin, entire to lacerate. Context cream to buff, soft corky, up to 0.8 mm thick. Tubes pale mouse-grey to buff, fragile, up to 4.3 mm long.

Hyphal structure. Hyphal system monomitic; generative hyphae with clamp connections, IKI–, CB–; hyphae unchanged in KOH.

Context. Generative hyphae hyaline, thin- to slightly thick-walled with a wide lumen, occasionally branched, loosely interwoven, 2.3–5.5 μm in diam.

Tubes. Generative hyphae hyaline, thin- to slightly thick-walled with a wide lumen, occasionally branched, interwoven, 2–4 μm in diam. Cystidia absent; cystidioles present, fusoid, thin-walled, 9.5–14.6 \times 2.8–3.4 μm . Basidia clavate, bearing four sterigmata and a basal clamp connection, 11.7–16.8 \times 3.4–4.3 μm ; basidioles dominant, in shape similar to basidia, but smaller, 10.6–14.7 \times 2.9–3.6 μm .



Figure 10. Basidiomata of *Cyanosporus tenuicontextus* (Holotype, Cui 16280). Scale bar: 1 cm. The upper figure is the upper surface and the lower figure is the lower surface of the basidiomata.

Spores. Basidiospores allantoid, slightly curved, hyaline, thin- to slightly thick-walled, smooth, IKI-, CB-, $(3.7\text{--})3.8\text{--}4.3 \times 0.8\text{--}1.2 \mu\text{m}$, $L = 3.97 \mu\text{m}$, $W = 1.02 \mu\text{m}$, $Q = 3.78\text{--}4.26$ ($n = 60/2$).

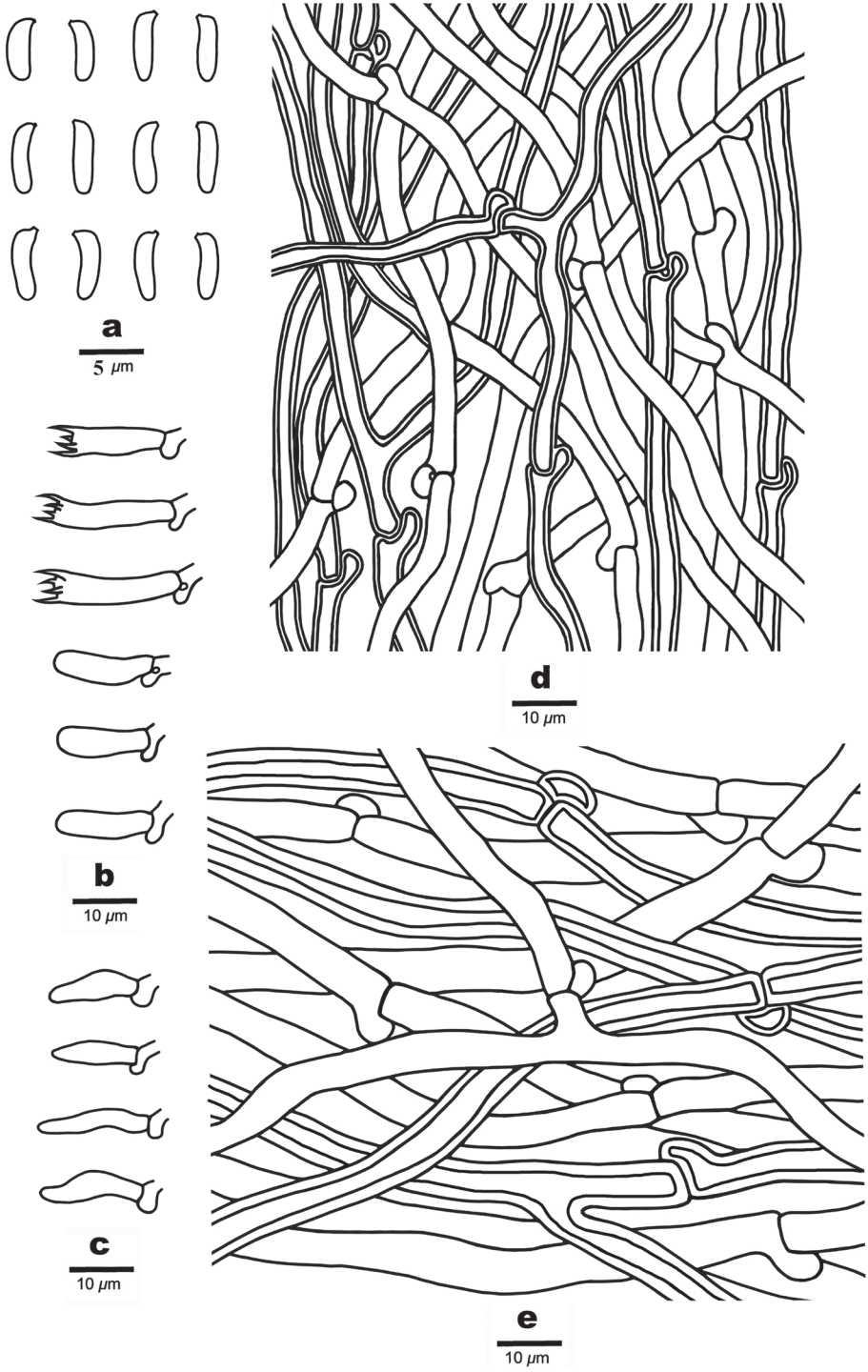


Figure 11. Microscopic structures of *Cyanosporus tenuicontextus* (Holotype, Cui 16280) **a** basidiospores **b** basidia and basidioles. **c** cystidioles **d** hyphae from trama **e** hyphae from context. Drawings by: Shun Liu.

Type of rot. Brown rot.

Additional specimen (paratype) examined. China. Yunnan Province, Yuxi, Xiping County, Mopanshan National Forest Park, on angiosperm stump, 16.I.2017, Zhao 813 (SWFC 000813).

Discussion

In the current phylogenetic analyses based on the combined datasets of ITS+TEF and ITS+nLSU+mtSSU+nSSU+RPB1+RPB2+TEF sequences, species of *Cyanosporus* formed a highly supported lineage, distant from *Postia* and other brown-rot fungal genera (Figs 2, 3) and consistent with previous studies (Shen et al. 2019; Liu et al. 2021a). Based on morphological characters and phylogenetic analyses, 35 species are accepted in *Cyanosporus* around the world, including four new species from China, viz., *C. flavus*, *C. rigidus*, *C. subungulatus* and *C. tenuicontextus*. The main ecological habits of the species in *Cyanosporus* with an emphasis on distribution areas and host trees are provided in Table 2.

In the phylogenetic trees, *Cyanosporus flavus* grouped together with *C. fusiformis*, *C. subungulatus* and *C. unguulatus* (Figs 2, 3). *Cyanosporus fusiformis* differs from *C. flavus* by having white to cream pileal surface when fresh, clay-buff pore surface when dry and larger pores (4–5 per mm) and by growing on angiosperm woods (Shen et al. 2019); *C. subungulatus* differs from *C. flavus* in its glabrous pileal surface, cream to pinkish buff pore surface when dry and wider basidiospores ($4.5\text{--}5.2 \times 1.1\text{--}1.4 \mu\text{m}$); *C. unguulatus* differs from *C. flavus* by having unguulate basidiomata, sulcate pileal surface with olivaceous buff, pinkish buff, cream to ash-grey and white zones when fresh (Shen et al. 2019). *Cyanosporus hirsutus* and *C. subhirsutus* have pileate basidiomata with hirsute, blue tint to the pileal surface and slightly thick-walled basidiospores like *C. flavus*, but *C. hirsutus* differs by having wider basidiospores ($4\text{--}4.7 \times 1.2\text{--}1.5 \mu\text{m}$; Liu et al. 2021a), while *C. subhirsutus* has larger pores (2–3 per mm; Shen et al. 2019). Besides, *C. hirsutus* and *C. subhirsutus* are distant from *C. flavus* in the phylogenetic analyses (Figs 2, 3). *Cyanosporus subungulatus* and *C. unguulatus* share similar pores and basidiospores; however, *C. unguulatus* differs by having unguulate basidiomata, glabrous and sulcate pileal surface, narrower context hyphae and tramal hyphae (Shen et al. 2019).

Phylogenetically, *Cyanosporus rigidus* form a separate lineage different from other species in the genus. Morphologically, *C. submicroporus* share similar pores and basidiospores with *C. rigidus*, but *C. submicroporus* differs by having cream to pinkish buff pileal surface and white to smoke grey pore surface when fresh, buff to buff-yellow pileal surface and buff to olivaceous buff pore surface when dry. *Cyanosporus auricomus* and *C. luteocaesius* resemble *C. rigidus* in morphology by producing yellow-colored basidiomata, but *C. auricomus* differs from *C. rigidus* by having a hirsute pileal surface and larger basidiospores ($4.4\text{--}5.6 \times 1.5\text{--}1.8 \mu\text{m}$; Miettinen et al. 2018); *C. luteocaesius* differs from *C. rigidus* by having larger pores (3–5 per mm) and basidiospores ($4.3\text{--}6.1 \times 1.5\text{--}1.9 \mu\text{m}$; Miettinen et al. 2018).

Table 2. A list of species, specimens, and GenBank accession number of sequences used for phylogenetic analyses in this study.

Species	Sample no.	Locality	GenBank accessions						References
			ITS	nLSU	mtSSU	nSSU	RPB1	RPB2	
<i>Amaropositia hainanensis</i>	Cui 13739 (holotype)	China	KX900909	KX900979	KX901053	KX901123	KX901171	KX901223	Shen et al. 2019
<i>A. stipica</i>	Cui 10043	China	KX900906	KX900976	KX901046	KX901119	KX901167	KX901219	Shen et al. 2019
<i>Amyloclystis lapponica</i>	FHB-13400	United States	KC585237	KC585059					Oritz-Santana et al. 2013
<i>Aloponia</i>	OKM-4418	United States	KC585238	KC585060					Oritz-Santana et al. 2013
<i>Anurodia serpens</i>	Dai 7465	Luxembourg	KR605813	KR605752	KR606013	KR605913		KR610832	Han et al. 2016
<i>A. tanakae</i>	Cui 9743	China	KR605814	KR605753	KR606014	KR605914		KR610743	Han et al. 2016
<i>Calosporia guttulata</i>	Cui 10018	China	KJ727432	KJ684978	KX901065	KX901138	KX901181	KX901236	Shen et al. 2019
<i>C. guttulata</i>	Cui 10028	China	KJ727433	KJ684979	KX901066	KX901139	KX901182	KX901237	Shen et al. 2019
<i>Cyanoagaricus albi</i>	Petr Vampola 12.10.1995 (holotype)	Slovakia	MG137026						Miettinen et al. 2018
<i>C. albi</i>	Cui 7185	China	KX900879	KX900949	KX901017	KX901092	KX901155	KX901202	Shen et al. 2019
<i>C. albi</i>	Dai 14845	Poland	KX900880	KX900950	KX901018	KX901093	KX901156	KX901203	Shen et al. 2019
<i>C. arbusti</i>	Viacheslav Spirin 8327 (holotype)	United States	MG137039					MG137132	Miettinen et al. 2018
<i>C. auricomus</i>	Cui 13518	China	KX900887	KX900957	KX901025	KX901100		KX901209	Shen et al. 2019
<i>C. auricomus</i>	Cui 13519	China	KX900888	KX900958	KX901026	KX901101			Shen et al. 2019
<i>C. auricomus</i>	Tuomo Niemelä 8310 (holotype)	Finland	MG137040					MG137133	Miettinen et al. 2018
<i>C. bifarius</i>	Viacheslav Spirin 6402 (holotype)	Russia	MG137043						Miettinen et al. 2018
<i>C. bifarius</i>	Cui 17534	China	OL423598*	OL437195*	OL423608*	OL423620*	OL444985*	OL444994*	Present study
<i>C. bifarius</i>	Cui 16277	China	OL423599*	OL437196*	OL423609*	OL423621*	OL444986*	OL444995*	Present study
<i>C. bubalinus</i>	Cui 16976	China	MW182172	MW182225	MW182208	MW182189	MW191547	MW191530	Liu et al. 2021a
<i>C. bubalinus</i>	Cui 16985 (holotype)	China	MW182173	MW182226	MW182209	MW182190	MW191548	MW191551	Liu et al. 2021a
<i>C. caesioidulans</i>	Viacheslav Spirin 4199	Russia	MG137061					MG137140	Miettinen et al. 2018
<i>C. caesioidulans</i>	Otto Miettinen 16976 (holotype)	United States	MG137054					MG137137	Miettinen et al. 2018
<i>C. caesioidulans</i>	Gerhard Schuster 51 (neotype)	Germany	MG137045					MG137134	Miettinen et al. 2018
<i>C. caesioidulans</i>	Otto Miettinen 14156	Finland	MG137048					MG137134	Miettinen et al. 2018
<i>C. caesioidulans</i>	Cui 18630	France	OL423600*	OL423610*	OL437197*	OL423622*		OL444996*	Present study
<i>C. caesioidulans</i>	K 32713	United Kingdom	AY599576						Miettinen et al. 2018
<i>C. caesioidulans</i>	K 32425	United Kingdom	AY599575						Miettinen et al. 2018
<i>C. caesioidulans</i>	Otto Miettinen 12214	Indonesia	MG137063						Miettinen et al. 2018
<i>C. caesioidulans</i>	Dai 19220	China	MW182174	MW182227	MW182210	MW182191	MW191549	MW191552	Liu et al. 2021a
<i>C. cyaneus</i>	Otto Miettinen 14755;1 (holotype)	United States	MG137066						Miettinen et al. 2018
<i>C. cyaneus</i>	Otto Miettinen 13602 (holotype)	Finland	MG137067					MG137142	Miettinen et al. 2018
<i>C. cyaneus</i>	Otto Miettinen 15919,2	Spain	MG137071					MG137144	Miettinen et al. 2018
<i>C. flavus</i>	Cui 18547	China	MW448564*	MW448561*			MW452596*	MW452601	Present study
<i>C. flavus</i>	Cui 18562 (holotype)	China	MW448565*	MW448562*			MW452597*	MW452602	Present study
<i>C. fusiformis</i>	Cui 10775	China	KX900868	KX900938	KX901006	KX901081		KX901245	Shen et al. 2019

Species	Sample no.	Locality	ITS	nLSU	mtSSU	nSSU	RPBI	RPB2	TEF	References
<i>C. fastiformis</i>	Dai 15036 (holotype)	China	KX900867	KX900937	KX901005	KX901080		KX901190	KX901244	Shen et al. 2019
<i>C. glaucus</i>	Viacheslav Spirin 5317	Russia	MG137078							Miettinen et al. 2018
<i>C. glaucus</i>	Viacheslav Spirin 6580 (holotype)	Russia	MG137081							Miettinen et al. 2018
<i>C. gossypinus</i>	Bernard Rivoire 6658	France								Miettinen et al. 2018
<i>C. hirsutus</i>	Cui 17083 (holotype)	China	MW182179	MW182233	MW182214	MW182197	MW191554	MW191568	MW191538	Liu et al. 2021a
<i>C. hirsutus</i>	Cui 17343	China	OL423601*	OL423611*	OL437198*	OL423623*	OL444987*	OL447001*	OL444997*	Present study
<i>C. hirsutus</i>	Cui 17342	China	OL423602*	OL423612*	OL437199*	OL423624*	OL444988*	OL447002*	OL444998*	Present study
<i>C. livens</i>	Viacheslav Spirin 8728	United States	MG137090							Miettinen et al. 2018
<i>C. livens</i>	Otto Miettinen 17177 (holotype)	United States	MG137082							Miettinen et al. 2018
<i>C. lutocacia</i>	Bernard Rivoire 2605	France	MG137091							Miettinen et al. 2018
<i>C. magnus</i>	Dai 21105	China	OL423603*	OL423613*	OL437200*	OL423625*	OL444989*	OL447003*	OL444999*	Present study
<i>C. magnus</i>	Cui 16983	China	MW182180	MW182234	MW182215	MW182198	MW191555	MW191569	MW191539	Liu et al. 2021a
<i>C. magnus</i>	Otto Miettinen 10634 (holotype)	China	KC595944							Miettinen et al. 2018
<i>C. mediterraneocaeus</i>	LY BR 4274	France	KX900886		KX901024	KX901099				Shen et al. 2019
<i>C. microporus</i>	Cui 11014 (holotype)	China	KX900878	KX900948	KX901016	KX901091		KX901201		Shen et al. 2019
<i>C. microporus</i>	Dai 11717	China	KX900877	KX900947	KX901015	KX901090		KX901200		Shen et al. 2019
<i>C. nothofagicala</i>	Cui 16697 (holotype)	Australia	MW182181	MW182235	MW182216	MW182199	MW191556	MW191570	MW191540	Liu et al. 2021a
<i>C. nothofagicala</i>	Cui 16765	Australia	MW182182	MW182236	MW182217	MW182200	MW191557		MW191541	Liu et al. 2021a
<i>C. picicola</i>	Cui 10626 (holotype)	China	KX900862	KX900932	KX901001	KX901075		KX901185		Shen et al. 2019
<i>C. picicola</i>	Cui 12158	China	KX900866	KX900936	KX901004	KX901079	KX901153	KX901189	KX901243	Shen et al. 2019
<i>C. populi</i>	Otto Miettinen 17043 (holotype)	United States	MG137092							Miettinen et al. 2018
<i>C. populi</i>	Cui 17087a	China	MW182183	MW182237	MW182218	MW182201	MW191558	MW191571	MW191542	Liu et al. 2021a
<i>C. populi</i>	Dai 18934	China	OL423604*	OL423614*	OL437201*	OL423626*	OL444990*	OL447004*	OL445000*	Present study
<i>C. populi</i>	Cui 17557	China	OL423605*	OL423615*	OL437202*	OL423627*	OL444991*	OL447005*	OL445001*	Present study
<i>C. rigidus</i>	Cui 17032 (holotype)	China	OL423606*	OL423617*	OL437204*	OL423629*	OL444993*		OL445003*	Present study
<i>C. simulans</i>	Otto Miettinen 20422	Finland	MG137110							Miettinen et al. 2018
<i>C. simulans</i>	Tuomo Niemelä 8846 (holotype)	Finland	MG137103							Miettinen et al. 2018
<i>C. subcaesus</i>	Josef Vlasak 0110/24	Czech Republic	MG137117							Miettinen et al. 2018
<i>C. subcaesus</i>	Alix David 652 (isotype)	France	MG137116							Miettinen et al. 2018
<i>C. subcaesus</i>	Cui 11330	China	KX900873	KX900943	KX901011	KX901086		KX901196	KX901250	Shen et al. 2019
<i>C. subhirsutus</i>	Dai 14892 (holotype)	China	KX900871	KX900941	KX901009	KX901084		KX901194	KX901248	Shen et al. 2019
<i>C. submicroporus</i>	Cui 16306	China	MW182184	MW182239	MW182220	MW182203	MW191560	MW191573	MW191544	Liu et al. 2021a
<i>C. submicroporus</i>	Cui 18156 (holotype)	China	MW182186	MW182241	MW182222	MW182205		MW191574		Liu et al. 2021a
<i>C. submicroporus</i>	Cui 18046 (holotype)	China	MW448566*	MW448563*	MW448560*	MW448559*	MW452598*		MW452603	Present study
<i>C. subungulatus</i>	Zhao 10833	China	MW742586*	OL423616*	OL437203*	OL423628*	OL444992*		OL445002*	Present study
<i>C. subnitidus</i>	Viacheslav Spirin 8774a	United States	MG137120							Miettinen et al. 2018
<i>C. subnitidus</i>	Reijo Penttilä 14376	Finland								Miettinen et al. 2018

Species	Sample no.	Locality	GenBank accessions						References
			ITS	nLSU	mtSSU	nSSU	RPBI	RPB2	
<i>C. tenuiscontectus</i>	Cui 16280 (holotype)	China	OL423607*	OL423618*	OL437205*	OL423630*		OL445004*	Present study
<i>C. tenuiscontectus</i>	Zhao 813	China	MG231802*	OL437206*	OL437206*	OL423631*		OL445005*	Present study
<i>C. tenuis</i>	Cui 10788 (holotype)	China	KX900885	KX900955	KX901023	KX901098	KX901161	KX901208	Shen et al. 2019
<i>C. tenuis</i>	Dai 12974	China	KX900884	KX900954	KX901022	KX901097	KX901160	KX901207	Shen et al. 2019
<i>C. tricolor</i>	Cui 12233 (holotype)	China	KX900876	KX900946	KX901014	KX901089	KX901199	KX901253	Shen et al. 2019
<i>C. triolor</i>	Cui 10790	China	KX900875	KX900945	KX901013	KX901088	KX901198	KX901252	Shen et al. 2019
<i>C. rugulatus</i>	Cui 10778	China	KX900870	KX900940	KX901008	KX901083	KX901193	KX901247	Shen et al. 2019
<i>C. rugulatus</i>	Dai 12897 (holotype)	China	KX900869	KX900939	KX901007	KX901082	KX901154	KX901246	Shen et al. 2019
<i>C. yanae</i>	Heikki Kotiranta 27/606	Russia	MG137122					MG137168	Miettinen et al. 2018
<i>C. yanae</i>	Heikki Kotiranta 27/454 (holotype)	Russia	MG137121					MG137167	Miettinen et al. 2018
<i>Cystodopostia hibernica</i>	Heikki Kotiranta 27/454 (holotype)	Russia	MG137121					MG137167	Miettinen et al. 2018
<i>C. inocybe</i>	Cui 2658	China	KX900905	KX900975	KX901045	KX901118	KX901218		Shen et al. 2019
<i>C. pilata</i>	LY BR 3703	France	KX900903	KX900973	KX901044	KX901116	KX901267		Shen et al. 2019
<i>C. pilata</i>	Cui 10034	China	KX900908	KX900956	KX901050	KX901122	KX901170	KX901222	Shen et al. 2019
<i>Fuscopostia dupliatae</i>	Dai 13411 (holotype)	China	KF69125	KJ684976	KR606027	KR605928	KX901174	KR610845	Han et al. 2016
<i>F. fragilis</i>	JV 0610-8	Czech	JF930573						Vampola et al. 2014
<i>F. lateritia</i>	Dai 2652	China	KX900913	KX900983					Shen et al. 2019
<i>F. leucomallella</i>	Cui 9599	China	KF69123	KJ684983	KX901056	KX901129	KX901176	KX901228	Shen et al. 2019
<i>Johnoporus brachiatus</i>	X 3232	Russia	KU165781						Spirin et al. 2015
<i>J. birrus</i>	Spinosa 10 X 2014	United States	KU165784				KY949044		Spirin et al. 2015
<i>J. oreinus</i>	X 3241	Russia	KU165785						Spirin et al. 2015
<i>Oligoporus renniji</i>	TN-6645	Finland	KC595929	KC595929	KX901068	KX901141	KX901184		Ortiz-Santana et al. 2013
<i>O. sericeomollis</i>	Cui 9870	China	KX900920	KX900990	KX901071	KX901144		KX901240	Shen et al. 2019
<i>Osteina obducta</i>	Cui 10074	China	KX900924	KX900994	KX901069	KX901142		KX901238	Shen et al. 2019
<i>O. undosa</i>	Dai 7105	China	KX900921	KX900991	KX901042				Shen et al. 2019
<i>Postia amurensis</i>	Dai 903 (holotype)	China	KX900901	KX900971	KX901038	KX901113		KX901266	Shen et al. 2019
<i>P. birsuta</i>	Cui 11237 (holotype)	China	KJ684970	KJ684984	KX901038	KX901104	KX901163	KX901211	Shen et al. 2019
<i>P. lactea</i>	Cui 12141	China	KX900892	KX900962	KX901029	KX901104		KX901260	Shen et al. 2019
<i>P. loiwei</i>	Cui 9585	China	KX900898	KX900968	KX901035	KX901110			Shen et al. 2019
<i>P. ochraceoalba</i>	Cui 10802 (holotype)	China	KM107903	KM107908	KX901041	KX901115		KX901216	Shen et al. 2015
<i>P. sublovei</i>	Cui 9597 (holotype)	China	KX900900	KX900970	KX901037	KX901112		KX901265	Shen et al. 2019
<i>P. tephaloeca</i>	Dai 12610	Finland	KX900897	KX900967	KX901034	KX901109	KX901166	KX901263	Shen et al. 2019
<i>Spongiosa gloeoporus</i>	Cui 10401	China	KX900915	KX900985	KX901060	KX901133		KX901232	Shen et al. 2019
<i>S. floriformis</i>	Cui 10292	China	KM107899	KM107904	KX901058	KX901131	KX901178	KX901230	Shen et al. 2019
<i>S. floriformis</i>	Dai 13887	China	KX900914	KX900984	KX901057	KX901130	KX901177	KX901229	Shen et al. 2019

*Newly generated sequences for this study. New species are shown in bold.

Phylogenetically, *C. tenuicontextus* is closely related to *C. caesiosimulans*, *C. cyanescens*, *C. populi*, *C. subviridis* and *C. yanae* (Figs 2, 3). Morphologically, they share similar pores; but *C. caesiosimulans* differs by having larger basidiospores ($4.2\text{--}5.5 \times 1.1\text{--}1.4 \mu\text{m}$), and a wide distribution area (Europe and North America; Miettinen et al. 2018); *C. cyanescens* differs in having light bluish-greyish tint in older and dry specimens and larger basidiospores ($4.7\text{--}6.1 \times 1.1\text{--}1.6 \mu\text{m}$; Miettinen et al. 2018); *C. populi* differs in its larger basidiospores ($4.2\text{--}5.6 \times 1\text{--}1.3 \mu\text{m}$), and a wide distribution area (East Asia, Europe and North America; Miettinen et al. 2018; Liu et al. 2021a); *C. subviridis* differs in its conchate basidiomata, distributed in Europe and North America and grows only on gymnosperms (*Abies* sp., *Picea* sp. and *Pinus* sp.; Miettinen et al. 2018); *C. yanae* differs by having narrower generative hyphae ($3\text{--}4 \mu\text{m}$ in context, $2.2\text{--}2.9 \mu\text{m}$ in tubes), larger basidiospores ($4.3\text{--}5.8 \times 1.2\text{--}1.6 \mu\text{m}$), distributed in Europe and grows only on gymnosperm (*Larix* sp., *Pinus* sp.; Miettinen et al. 2018). *Cyanosporus bifarius* is also distributed in Lanping County, Yunnan Province of China, they share similar pores and basidiospores, but *C. bifarius* grows only on gymnosperm trees (*Picea* sp., *Pinus* sp., *Larix* sp.; Miettinen et al. 2018), and *C. bifarius* is distant from *C. tenuicontextus* in the phylogenetic analyses (Figs 2, 3).

The natural distribution of plant-associated fungi across broad geographic ranges is determined by a combination of the distributions of suitable hosts and environmental conditions (Lodge 1997; Brandle and Brandl 2006; Gilbert et al. 2007, 2008). Species in *Cyanosporus* have a wide distribution range (Asia, Europe, North America, South America and Oceania; Table 2) and variable host type (angiosperms and gymnosperms). As for distribution ranges, 23 species of *Cyanosporus* are distributed in Asia, 16 species in Europe, seven species in North America, one species in South America and one species in Oceania. As for host trees, nine species of *Cyanosporus* grow only on angiosperm trees, 15 species only on gymnosperm trees, and eleven species both on angiosperm and gymnosperm trees (Table 1). In some cases, some *Cyanosporus* species have host specificity, at least regionally, such as in Europe, *C. auricomus* only growth on *Pinus sylvestris*, *C. cyanescens* only growth on *Picea abies*, *C. populi* prefers *Populus tremula*, and *C. luteocaesia* have been recorded only from *Pinus* sp. (Miettinen et al. 2018).

In the current study, 77 samples of *Cyanosporus* throughout China and 11 samples outside of China have been morphologically examined in detail. The specimens collected from China representing 21 species were sequenced here and referred to in our phylogeny, viz., *C. alni*, *C. auricomus*, *C. bifarius*, *C. bubalinus*, *C. coeruleivirens*, *C. comatus*, *C. flavus*, *C. fusiformis*, *C. hirsutus*, *C. magnus*, *C. microporus*, *C. piceicola*, *C. populi*, *C. rigidus*, *C. subhirsutus*, *C. submicroporus*, *C. subungulatus*, *C. tenuicontextus*, *C. tenuis*, *C. tricolor* and *C. unguulatus*. Another two species reported in a previous study, viz., *C. glauca* (= *Postia glauca* Spirin & Miettinen) and *C. simulans* (= *Postia simulans* (P. Karst.) Spirin & Rivoire; Miettinen et al. 2018) were also found from China. Among these *Cyanosporus* species, 15 are endemic to China so far, viz., *C. bubalinus*, *C. flavus*, *C. fusiformis*, *C. hirsutus*, *C. microporus*, *C. piceicola*, *C. rigidus*, *C. subhirsutus*, *C. submicroporus*, *C. subungulatus*, *C. tenuicontextus*, *C. tenuis*, *C. tricolor* and *C. unguulatus*. The *Cyanosporus* species formed a distribution center in Southwest China. This may be due

to the complex and diverse ecological environment and diverse host trees in this region, which provide a rich substrate for the growth of *Cyanosporus* species. The geographical locations of the *Cyanosporus* species distributed in China are indicated on the map (Fig. 1).

In summary, we performed a comprehensive study on the species diversity and phylogeny of *Cyanosporus* with an emphasis on Chinese collections. So far, 35 species are accepted in the *Cyanosporus* around the world, including 23 species from China. Currently, *Cyanosporus* is characterized by an annual growth habit, resupinate to effused-reflexed or pileate, soft corky, corky, fragile to hard corky basidiomata, velutinate to hirsute or glabrous pileal surface with blue-tinted, white to cream or yellow-colored, white to cream pore surface with round to angular pores, a monomitic hyphal system with clamped generative hyphae, and hyaline, thin- to slightly thick-walled, smooth, narrow, allantoid to cylindrical basidiospores that are usually weakly cyanophilous; it grows on different angiosperm and gymnosperm trees, causes a brown rot of wood and has a distribution in Asia, Europe, North America, Argentina in South America and Australia in Oceania (McGinty 1909; Shen et al. 2019; Liu et al. 2021a).

Acknowledgements

We express our gratitude to the curators of herbaria of IFP and SWFC for their loan of specimens. Ms. Yi-Fei Sun (China), Xing Ji (China) and Yan Wang (China) are grateful for help during field collections and molecular studies. Drs. Jun-Zhi Qiu (China), Shi-Liang Liu (China) and Long-Fei Fan (China) are thanked for their companionship during field collections. The research is supported by the National Natural Science Foundation of China (Nos. U2003211, 31750001), the Scientific and Technological Tackling Plan for the Key Fields of Xinjiang Production and Construction Corps (No. 2021AB004), and Beijing Forestry University Outstanding Young Talent Cultivation Project (No. 2019JQ03016).

References

- Brandle M, Brandl R (2006) Is the composition of phytophagous insects and parasitic fungi among trees predictable? *Oikos* 113: 296–304. <https://doi.org/10.1111/j.2006.0030-1299.14418.x>
- Cui BK, Li HJ, Ji X, Zhou JL, Song J, Si J, Yang ZL, Dai YC (2019) Species diversity, taxonomy and phylogeny of Polyporaceae (Basidiomycota) in China. *Fungal Diversity* 97: 137–392. <https://doi.org/10.1007/s13225-019-00427-4>
- Dai YC (2012) Polypore diversity in China with an annotated checklist of Chinese polypores. *Mycoscience* 53: 49–80. <https://doi.org/10.1007/s10267-011-0134-3>
- David A (1974) Une nouvelle espèce de Polyporaceae: *Tyromyces subcaesius*. *Bulletin Mensuel de la Société Linnéenne de Lyon* 43: 119–126
- David A (1980) Étude du genre *Tyromyces* sensu lato: répartition dans les genres *Leptoporus*, *Spongiporus* et *Tyromyces* sensu stricto. *Bulletin Mensuel de la Société Linnéenne de Lyon* 49: 6–56. <https://doi.org/10.3406/linly.1980.10404>

- Donk MA (1960) The generic names proposed for Polyporaceae. *Persoonia* 1: 173–302.
- Farris JS, Källersjö M, Kluge AG, Kluge AG, Bult C (1994) Testing significance of incongruence. *Cladistics* 10: 315–319. <https://doi.org/10.1111/j.1096-0031.1994.tb00181.x>
- Felsenstein J (1985) Confidence intervals on phylogenies: an approach using the bootstrap. *Evolution* 39: 783–791. <https://doi.org/10.1111/j.1558-5646.1985.tb00420.x>
- Hall TA (1999) Bioedit: A user-friendly biological sequence alignment editor and analysis program for Windows 95/98/NT. *Nucleic Acids Symposium Series* 41: 95–98.
- Han ML, Chen YY, Shen LL, Song J, Vlasák J, Dai YC, Cui BK (2016) Taxonomy and phylogeny of the brown-rot fungi: *Fomitopsis* and its related genera. *Fungal Diversity* 80: 343–373. <https://doi.org/10.1007/s13225-016-0364-y>
- Hillis DM, Bull JJ (1993) An empirical test of bootstrapping as a method for assessing confidence in phylogenetic analysis. *Systematics and Biodiversity* 42: 182–192. <https://doi.org/10.1093/sysbio/42.2.182>
- Jahn H (1963) Mitteleuropäische Porlinge (Polyporaceae s. lato) und ihr Vorkommen in Westfalen. *Westfälische Pilzbriefe* 4: 1–143.
- Jahn H (1979) *Pilze die an Holz Wachsen*. Herford: Busse.
- Justo A, Hibbett DS (2011) Phylogenetic classification of *Trametes* (Basidiomycota, Polyporales) based on a five-marker dataset. *Taxon* 60: 1567–1583. <https://doi.org/10.1002/tax.606003>
- Katoh K, Standley DM (2013) MAFFT Multiple sequence alignment software version 7: improvements in performance and usability. *Molecular Biology and Evolution* 30: 772–780. <https://doi.org/10.1093/molbev/mst010>
- Liu S, Shen LL, Wang Y, Xu TM, Gates G, Cui BK (2021a) Species diversity and molecular phylogeny of *Cyanosporus* (Polyporales, Basidiomycota). *Frontiers in Microbiology* 12: e631166. <https://doi.org/10.3389/fmicb.2021.631166>
- Liu S, Han ML, Xu TM, Wang Y, Wu DM, Cui BK (2021b) Taxonomy and phylogeny of the *Fomitopsis pinicola* complex with descriptions of six new species from east Asia. *Frontiers in Microbiology* 12: e644979. <https://doi.org/10.3389/fmicb.2021.644979>
- Liu S, Song CG, Cui BK (2019) Morphological characters and molecular data reveal three new species of *Fomitopsis* (Basidiomycota). *Mycological Progress* 18: 1317–1327. <https://doi.org/10.1007/s11557-019-01527-w>
- Lodge DJ (1997) Factors related to diversity of decomposer fungi in tropical forests. *Biodiversity and Conservation* 6: 681–688. <https://doi.org/10.1023/A:1018314219111>
- Lowe JL (1975) Polyporaceae of North America. The genus *Tyromyces*. *Mycotaxon* 2: 1–82.
- Maddison WP, Maddison DR (2017) *Mesquite: a modular system for evolutionary analysis*, Version 3.2. <http://mesquiteproject.org>
- Matheny PB (2005) Improving phylogenetic inference of mushrooms with RPB1 and RPB2 nucleotide sequences (Inocybe, Agaricales). *Molecular Phylogenetics and Evolution* 35: 1–20. <https://doi.org/10.1016/j.ympev.2004.11.014>
- Matheny PB, Liu YJ, Ammirati JF, Hall BD (2002) Using RPB1 sequences to improve phylogenetic inference among mushrooms (Inocybe, Agaricales). *American Journal of Botany* 89: 688–698. <https://doi.org/10.3732/ajb.89.4.688>
- McGinty NJ (1909) A new genus, *Cyanosporus*. *Mycological Notes* 33: e436.

- Miettinen O, Vlasák J, Rivoire B, Spirin V (2018) *Postia caesia* complex (Polyporales, Basidiomycota) in temperate Northern Hemisphere. *Fungal Systematics and Evolution* 1: 101–129. <https://doi.org/10.3114/fuse.2018.01.05>
- Nylander JAA (2004) MrModeltest v2. Evolutionary Biology Centre, Uppsala University, Program distributed by the author.
- Ortiz-Santana B, Lindner DL, Miettinen O, Justo A, Hibbett DS (2013) A phylogenetic overview of the antrodia clade (Basidiomycota, Polyporales). *Mycologia* 105: 1391–1411. <https://doi.org/10.3852/13-051>
- Papp V (2014) Nomenclatural novelties in the *Postia caesia* complex. *Mycotaxon* 129: 407–413. <https://doi.org/10.5248/129.407>
- Petersen JH (1996) Farvekort. The Danish Mycological Society's colour-chart. Foreningen til Svampekundskabens Fremme, Greve.
- Pieri M, Rivoire B (2005) *Postia mediterraneocaesia*, une nouvelle espèce de polypore découverte dans le sud de l'Europe. *Bulletin Semestriel de la Fédération des Associations Mycologiques Méditerranéennes* 28: 33–38.
- Posada D, Crandall KA (1998) Modeltest: testing the model of DNA substitution. *Bioinformatics* 14: 817–818. <https://doi.org/10.1093/bioinformatics/14.9.817>
- Rehner S (2001) Primers for Elongation Factor 1-a (EF1-a). <http://ocid.nacse.org/research/deephyphae/EF1primer.pdf>
- Ronquist F, Huelsenbeck JP (2003) MRBAYES 3: Bayesian phylogenetic inference under mixed models. *Bioinformatics* 19: 1572–1574. <https://doi.org/10.1093/bioinformatics/btg180>
- Shen LL, Wang M, Zhou JL, Xing JH, Cui BK, Dai YC (2019) Taxonomy and phylogeny of *Postia*. Multi-gene phylogeny and taxonomy of the brown-rot fungi: *Postia* (Polyporales, Basidiomycota) and related genera. *Persoonia* 42: 101–126. <https://doi.org/10.3767/persoonia.2019.42.05>
- Spirin V, Vlasák J, Milakovsky B, Miettinen O (2015) Searching for indicator species of old-growth spruce forests: studies in the genus *Jahnoporus* (Polyporales, Basidiomycota). *Cryptogamie Mycologie* 36: 409–418. <https://doi.org/10.7872/crym/v36.iss4.2015.409>
- Sun YF, Costa-Rezende DH, Xing JH, Zhou JL, Zhang B, Gibertoni TB, Gates G, Glen M, Dai YC, Cui BK (2020) Multi-gene phylogeny and taxonomy of *Amauroderma* s. lat. (Ganodermataceae). *Persoonia* 44: 206–239. <https://doi.org/10.3767/persoonia.2020.44.08>
- Swofford DL (2002) PAUP*: phylogenetic analysis using parsimony (*and other methods). Version 4.0b10. Sinauer Associates, Sunderland.
- Stamatakis A (2006) RAxML-VI-HPC: maximum likelihood-based phylogenetic analysis with thousands of taxa and mixed models. *Bioinformatics* 22: 2688–2690. <https://doi.org/10.1093/bioinformatics/btl446>
- Vampola P, Ordynets A, Vlasak J (2014) The identity of *Postia lowei* (Basidiomycota, Polyporales) and notes on related or similar species. *Czech Mycology* 66: 39–52. <https://doi.org/10.33585/cmy.66102>
- White TJ, Bruns T, Lee S, Taylor J (1990) Amplification and direct sequencing of fungal ribosomal RNA genes for phylogenetics. In: Innis MA, Gefand DH, Sninsky JJ, White, JT (Eds) *PCR Protocols: A Guide to Methods and Applications*. Academic Press, San Diego, 315–322. <https://doi.org/10.1016/B978-0-12-372180-8.50042-1>

Three new *Xylaria* species (Xylariaceae, Xylariales) on fallen leaves from Hainan Tropical Rainforest National Park

Xiao-Yan Pan^{1,2}, Zi-Kun Song^{2,3}, Zhi Qu², Tie-Dong Liu¹, Hai-Xia Ma^{2,4}

1 College of Forestry, Hainan University, Haikou 570228, China **2** Institute of Tropical Bioscience and Biotechnology, Chinese Academy of Tropical Agricultural Sciences, Haikou 571101, China **3** College of Plant Protection, Jilin Agricultural University, Jilin 130000, China **4** Hainan Institute for Tropical Agricultural Resources, Chinese Academy of Tropical Agricultural Sciences, Haikou 571101, China

Corresponding authors: Hai-Xia Ma (mahaixia@itbb.org.cn), Tie-Dong Liu (liu@hainanu.edu.cn)

Academic editor: Thorsten Lumbsch | Received 15 July 2021 | Accepted 21 December 2021 | Published 12 January 2022

Citation: Pan X-Y, Song Z-K, Qu Z, Liu T-D, Ma H-X (2022) Three new *Xylaria* species (Xylariaceae, Xylariales) on fallen leaves from Hainan Tropical Rainforest National Park. MycoKeys 86: 47–63. <https://doi.org/10.3897/mycokeys.86.71623>

Abstract

Three new species of *Xylaria* on fallen leaves in Hainan Province of China are described and illustrated, based on morphological and molecular evidence. *Xylaria hedyosmicola* is found on fallen leaves of *Hedyosmum orientale* and featured by thread-like stromata with a long sterile filiform apex. Phylogenetically, *X. hedyosmicola* is closely related to an undescribed *Xylaria* sp. from Hawaii Island, USA and morphologically similar to *X. vagans*. *Xylaria lindericola* is found on fallen leaves of *Lindera robusta* and characterised by its subglobose stromata and a long filiform stipe. It is phylogenetically closely related to *X. sicula* f. *major*. *Xylaria polysporicola* is found on fallen leaves of *Polyspora hainanensis*, it is distinguished by upright or prostrate stromata and ascospores sometimes with a slimy sheath or non-cellular appendages. *Xylaria polysporicola* is phylogenetically closely related to *X. amphithele* and *X. ficicola*. An identification key to the ten species on fallen leaves in China is given.

Keywords

Follicolous fungi, Phylogeny, Pyrenomycetes, Taxonomy

Introduction

Species of *Xylaria* Hill ex Schrank are commonly found throughout the temperate, subtropical and tropical regions of the world, associated with wood, fallen fruits or seeds, fallen leaves or petioles and termite nests (Dennis 1956; Rogers 1986; Rogers and Samuels 1986; San Martin and Rogers 1989; Ju and Rogers 1999; Ju and Hsieh 2007; Fournier 2014). Previous studies on *Xylaria* have dealt primarily with species growing on wood and termite nests (Rogers et al. 2005; Ju and Hsieh 2007; Fournier et al. 2020), but the species diversity and distribution of the genus on other substrates, such as fallen fruits or seeds and fallen leaves or petioles, are still poorly studied (Hsieh et al. 2010; Ju et al. 2018). Especially, the study of *Xylaria* species growing on fallen leaves or petioles is far behind those mentioned taxa associated with other substrates and only seven species have been reported on those substrates in China (Dennis 1956; Rogers et al. 1988; Zhu and Guo 2011; Huang et al. 2014, 2015; Ma and Li 2018).

Hainan Province (20°01.04'N, 110°20.95'E) is located in southern China and enjoys a tropical monsoon climate. More than 6036 plant species, 1895 genera and 243 families have been reported in the province (Yang 2015). Different kinds of tropical vegetations (e.g. Moraceae, Euphorbiaceae and Areaceae) and rainforests are distributed over the vast territory of the province, in which abundant fungi occur (Dai et al. 2009; Dai 2012; Gao and Yang 2016; Cui et al. 2019). Two intensive surveys of xylariaceous fungi were carried out in Hainan province in 2019 and 2020 and about 400 specimens of Xylariaceae were collected. These materials have been carefully studied through both morphological and phylogenetic methods and three new species on fallen leaves were identified. The new taxa are described and illustrated, and an identification key is provided for the 10 known species of *Xylaria* on fallen leaves in China.

Materials and methods

Morphological studies

Voucher specimens are deposited in the Fungarium of the Institute of Tropical Bioscience and Biotechnology, Chinese Academy of Tropical Agricultural Sciences (FCATAS), Hainan Province, China. Samples for microscopic examination were mounted in distilled water, Melzer's reagent, India ink or 1% SDS. Microscopic features observation, measurements and photographing were performed by using a Zeiss Axio Imager A2 microscope (Göttingen, Germany) by differential interference contrast microscopy (DIG) and brightfield microscopy (BF). The photographs of stromata, perithecia and ostioles were taken with a VHX-600E stereomicroscope Keyence Corporation (Osaka Japan). The methods of collecting, preservation and identification of the specimens follow Ma and Li (2018).

DNA extraction and sequencing

A modified cetyltrimethylammonium bromide (CTAB) extraction kit (Aidlab Biotechnologies, Beijing, China) was employed for total DNA extraction from dried specimens. The ITS region was amplified with the primer pair ITS4 and ITS5 (White et al. 1990) using the following procedure: initial denaturation at 95 °C for 3 min, followed by 30 cycles of 94 °C for 40 s, 55.8 °C for 45 s and 72 °C for 1 min and a final extension of 72 °C for 10 min. The TUB and RPB2 gene region were amplified with primers T1/T22 (O'Donnell and Cigelnik 1997) and fRPB2-5F/fRPB2-7CR (Liu et al. 1999), respectively, using the following procedure: initial denaturation at 95 °C for 3 min, followed by 35 °C cycles of 94 °C for 1 min, 52 °C for 1 min and 72 °C for 1.5 min and a final extension of 72 °C for 10 min (Hsieh et al. 2005). DNA sequencing was performed at BGI tech (Guangzhou, China) and sequences were deposited in GenBank (Table 1).

Table 1. Species, specimens and GenBank accession number of sequences used in this study. New species and sequences are set in bold.

Taxon	Substrate / Origin	Specimen No.	GenBank No.			Reference
			ITS	TUB	RPB2	
<i>Xylaria</i>	termite nests / China Taiwan	HAST 623	EU178738	GQ502711	GQ853028	Hsieh et al. (2010)
<i>acuminatolongissima</i>						
<i>X. adscendens</i>	wood / Guadeloupe	HAST 570	GU300101	GQ487708	GQ844817	Hsieh et al. (2010)
<i>X. allantoidea</i>	trunk / China Taiwan	HAST 94042903	GU324743	GQ502692	GQ848356	Hsieh et al. (2010)
<i>X. amphithele</i>	dead leaves / Guadeloupe	HAST 529	GU300083	GQ478218	GQ844796	Hsieh et al. (2010)
<i>X. apoda</i>	bark / China Taiwan	HAST 90080804	GU322437	GQ495930	GQ844823	Hsieh et al. (2010)
<i>X. arbuscula</i>	bark / China Taiwan	HAST 89041211	GU300090	GQ478226	GQ844805	Hsieh et al. (2010)
<i>X. arbuscula</i> var. <i>plenofissura</i> .	wood / China Taiwan	HAST 93082814	GU339495	GQ478225	GQ844804	Hsieh et al. (2010)
<i>X. atrodivaricata</i>	termite nests / China Taiwan	HAST 95052001	EU178739	GQ502713	GQ853030	Hsieh et al. (2010)
<i>X. badia</i>	bamboo culm / China Taiwan	HAST 95070101	GU322446	GQ495939	GQ844833	Hsieh et al. (2010)
<i>X. bambusicola</i>	bamboo culm / Thailand	JDR 162	GU300088	GQ478223	GQ844801	Hsieh et al. (2010)
<i>X. berterii</i>	bark / USA	JDR 256	GU324750	GQ502698	GQ848363	Hsieh et al. (2010)
<i>X. berterii</i>	bark / China Taiwan	HAST 90112623	GU324749	AY951763	GQ848362	Hsieh et al. (2010)
<i>X. betulicola</i>	leaves of <i>Betula</i> / China	FCATAS 750	MF774332	–	–	Ma and Li (2018)
<i>X. brunneovinosa</i>	termite nests / China Taiwan	HAST 720	EU179862	GQ502706	GQ853023	Hsieh et al. (2010)
<i>X. castorea</i>	wood / New Zealand	PDD 600	GU324751	GQ502703	GQ853018	Hsieh et al. (2010)
<i>X. cirrata</i>	termite nests / China Taiwan	HAST 664	EU179863	GQ502707	GQ853024	Hsieh et al. (2010)
<i>X. cocophora</i>	wood / French	HAST 786	GU300093	GQ487701	GQ844809	Hsieh et al. (2010)
<i>X. crinalis</i>	wood / China	FCATAS 751	MF774330	–	–	Ma and Li (2018)
<i>X. crozonensis</i>	bark / France	HAST 398	GU324748	GQ502697	GQ848361	Hsieh et al. (2010)
<i>X. cubensis</i>	log / Russian Far East	HAST 477	–	GQ502699	GQ848364	Hsieh et al. (2010)
<i>X. culleniae</i>	pod / Thailand	JDR 189	GU322442	GQ495935	GQ844829	Hsieh et al. (2010)
<i>X. escharoidea</i>	termite nests / China Taiwan	HAST 658	EU179864	GQ502709	GQ853026	Hsieh et al. (2010)
<i>X. feejeensis</i>	bark / China Taiwan	HAST 92092013	GU322454	GQ495947	GQ848336	Hsieh et al. (2010)
<i>X. ficicola</i>	fallen leaves and petioles of <i>Ficus auriculata</i> / China	HMJAU 22818	MZ351258	–	–	This study
<i>X. filiformis</i>	herbaceous stem / Iran	GUM 1052	KP218907	–	–	Hashemi et al. (2015)
<i>X. fimbriata</i>	termite nests / French West Indies	HAST 491	GU324753	GQ502705	GQ853022	Hsieh et al. (2010)
<i>X. cf. glebulosa</i>	fruit / French West Indies	HAST 431	GU322462	GQ495956	GQ848345	Hsieh et al. (2010)

Taxon	Substrate / Origin	Specimen No.	GenBank No.			Reference
			ITS	TUB	RPB2	
<i>X. grammica</i>	wood / China Taiwan	HAST 479	GU300097	GQ487704	GQ844813	Hsieh et al. (2010)
<i>X. griseosepiacea</i>	termite nests / China Taiwan	HAST 641	EU179865	GQ502714	GQ853031	Hsieh et al. (2010)
<i>X. hedyosmicola</i>	fallen leaves of <i>Hedyosmum orientale</i> / China Hainan	FCATAS 856	MZ227121	MZ221183	MZ683407	This study
<i>X. hedyosmicola</i>	fallen leaves of <i>Hedyosmum orientale</i> / China Hainan	FCATAS 857	MZ227023	MZ221184	MZ851780	This study
<i>X. hypoxylon</i>	wood / Belgium	HAST 152	GU300096	GQ260187	GQ844812	Hsieh et al. (2010)
<i>X. hypoxylon</i>	wood / China Taiwan	HAST 95082001	GU300095	GQ487703	GQ844811	Hsieh et al. (2010)
<i>X. hypoxylon</i>	leaf debris / Sweden	CBS 122617	AM993146	–	–	Persoh et al. (2009)
<i>X. ianthinovelutina</i>	fruit of <i>Swietenia</i> / Martinique	HAST 553	GU322441	GQ495934	GQ844828	Hsieh et al. (2010)
<i>X. intraflava</i>	termite nests / China Taiwan	HAST 725	EU179866	GQ502718	GQ853035	Hsieh et al. (2010)
<i>X. juruensis</i>	<i>Arenga engleri</i> / China Taiwan	HAST 92042501	GU322439	GQ495932	GQ844825	Hsieh et al. (2010)
<i>X. laevis</i>	wood / Martinique	HAST 419	GU324746	GQ502695	GQ848359	Hsieh et al. (2010)
<i>X. leavis</i>	bark / China Taiwan	HAST 95072910	GU324747	GQ502696	GQ848360	Hsieh et al. (2010)
<i>X. lindericola</i>	fallen leaves of <i>Lindera robusta</i> / China Hainan	FCATAS 852	MZ005635	MZ031978	MZ031982	This study
<i>X. lindericola</i>	fallen leaves of <i>Lindera robusta</i> / China Hainan	FCATAS 853	MZ005636	MZ031979	MZ048749	This study
<i>X. liquidambar</i>	fruits of <i>Liquidambar formosana</i> / China Taiwan	HAST 93090701	GU300094	GQ487702	GQ844810	Hsieh et al. (2010)
<i>X. longissima</i>	wood / China	FCATAS 749	MF774331	–	–	Ma and Li (2018)
<i>X. longissima</i>	wood / Iran	IRAN 16582 F	KP218906	–	–	Hashemi et al. (2015)
<i>X. meliacearum</i>	petioles and infructescence of <i>Guarea guidonia</i> / Puerto Rico	JDR 148	GU300084	GQ478219	GQ844797	Hsieh et al. (2010)
<i>X. multiplex</i>	wood / USA	JDR 259	GU300099	GQ487706	GQ844815	Hsieh et al. (2010)
<i>X. muscula</i>	dead branch / French West	HAST 520	GU300087	GQ478222	GQ844800	Hsieh et al. (2010)
<i>X. nigripes</i>	termite nests / China Taiwan	HAST 653	GU324755	GQ502710	GQ853027	Hsieh et al. (2010)
<i>X. oxyacanthae</i>	fallen seeds / USA	JDR 859	GU322434	GQ495927	GQ844820	Hsieh et al. (2010)
<i>X. oxyacanthae</i>	fruits / Germany	LZ 2010-502	HQ414587	–	–	Roensch et al. (2010)
<i>X. palmicola</i>	fruits / New Zealand	PDD 604	GU322436	GQ495929	GQ844822	Hsieh et al. (2010)
<i>X. phyllocharis</i>	dead leaves / French West	HAST 528	GU322445	GQ495938	GQ844832	Hsieh et al. (2010)
<i>X. plebeja</i>	trunk / China Taiwan	HAST 91122401	GU324740	GQ502689	GQ848353	Hsieh et al. (2010)
<i>X. polymorpha</i>	wood / USA	JDR 1012	GU322460	GQ495954	GQ848343	Hsieh et al. (2010)
<i>X. polymorpha</i>	Stump / Germany	M:M-0125909	FM164944	–	–	Persoh et al. (2009)
<i>X. polysporicola</i>	fallen leaves of <i>Polyspora hainanensis</i> / China Hainan	FCATAS 848	MZ005592	MZ031976	MZ031980	This study
<i>X. polysporicola</i>	fallen leaves of <i>Polyspora hainanensis</i> / China Hainan	FCATAS 849	MZ005591	MZ031977	MZ031981	This study
<i>X. regalis</i>	log of <i>Ficus racemosa</i> / India	HAST 920	GU324745	GQ502694	GQ848358	Hsieh et al. (2010)
<i>X. schweinitzii</i>	bark / China Taiwan	HAST 92092023	GU322463	GQ495957	GQ848346	Hsieh et al. (2010)
<i>X. sicula</i> f. <i>major</i>	fallen leaves / China Taiwan	HAST 90071613	GU300081	GQ478216	GQ844794	Hsieh et al. (2010)
<i>Xylaria</i> sp. 6	fallen leaves of <i>Tibouchina semidecandra</i> / USA	JDR 258	GU300082	GQ478217	GQ844795	Hsieh et al. (2010)
<i>X. striata</i>	branch / China	HAST 304	GU300089	GQ478224	GQ844803	Hsieh et al. (2010)
<i>X. tentaculata</i>	leaf litter or wood / Korea	KA12-0530	KM077162	–	–	Kim et al. (2016)
<i>X. tentaculata</i>	leaf litter or wood / Korea	KA13-1324	KM077163	–	–	Kim et al. (2016)
<i>X. tentaculata</i>	leaf litter or wood / Korea	KA13-1325	KM077164	–	–	Kim et al. (2016)
<i>X. venosula</i>	twigs / USA	HAST 94080508	EF026149	EF025617	GQ844806	Hsieh et al. (2010)
<i>X. venustula</i>	bark / China Taiwan	HAST 88113002	GU300091	GQ487699	GQ844807	Hsieh et al. (2010)
<i>X. xylarioides</i>	wood / Iran	GUM 1151	KP218909	–	–	Hashemi et al. (2015)
<i>Hypoxylon fragiforme</i>	bark / France	HAST 383	JN979420	AY951720	–	Hsieh et al. (2005)
<i>Camillea obularia</i>	– / Puerto Rico	ATCC 28093	KY610384	KX271243	–	Wendt et al. (2018)

Phylogenetic analyses

The molecular phylogeny was inferred from a combined dataset of ITS, TUB and RPB2 sequences. The sequences retrieved from open databases originated from Hsieh et al. (2005), Persoh et al. (2009), Hsieh et al. (2010), Roensch et al. (2010), Hashemi et al. (2015), Kim et al. (2016), Ma and Li (2018) and Wendt et al. (2018) (Table 1). *Hypoxylon fragiforme* (Pers.) J. Kickx f. and *Camillea obularia* (Fr.) Læssøe, J.D. Rogers & Lodge were selected as outgroup taxa. Sequences were aligned using the MAFFT online (<http://mafft.cbrc.jp/alignment/server/>). Alignments were optimised manually in BioEdit 7.0.5.3 (Hall 1999).

A combined matrix of ITS-RPB2-TUB and ITS-exons of TUB and RPB2 were used to construct phylogenetic analysis by two methods including maximum likelihood (ML) and Bayesian Inference (BI) analysis, respectively. ML tree generation and bootstrap analyses were performed via the programme RAxML7.2.6 (Stamatakis 2006) running 1000 replicates combined with a ML search. Bayesian analysis was performed with MrBayes 3.1 (Huelsenbeck and Ronquist 2005) implementing the Markov Chain Monte Carlo (MCMC) technique and parameters predetermined by MrModeltest 2.3 (Nylander 2004).

Results

Molecular phylogeny

This study used genetic sequences of 57 species, including 69 ITS sequences, 57 TUB sequences and 54 RPB2 sequences. We applied two tree construction methods to improve the reliability of the results.

After the alignment sequence was adjusted using MAFFT, the ITS alignment, shown in BioEdit 7.0.5, consisted of 778 character positions, 2219 in the TUB alignment and 1241 in the RPB2 alignment. After curing, the constructed multigene alignment (MGA) consisted of 3138 characters (523 of which were derived from the ITS alignment, 1550 from TUB alignment, 1065 from RPB2 alignment). Of the MGA, 1354 characters were considered parsimony-informative.

The analysis results show that the phylogenetic tree, generated by ML in RAxML7.2.6, is basically the same as that generated by BI in MrBayes 3.1. Topology of the phylogenetic analyses, based on ITS-RPB2-TUB and ITS-exons of TUB and RPB2, have no significant conflicts. Only the BI tree is shown in Figure 1 with Bayesian posterior probabilities ≥ 0.95 and ML bootstrap values $\geq 50\%$ labelled along the branches. The phylogenetic tree showed that *X. hedyosmicola* is clustered with *Xylaria* sp. 6, *X. polysporicola* is clustered with *X. amphithele* F. San Martín & J.D. Rogers and *X. ficicola* Hai X. Ma, Lar.N. Vassiljeva & Yu Li, *X. lindericola* is clustered with *X. sicula* Pass. & Beltr. f. *major* Ciccarone, but were separated from other species, as well as from each other.

Taxonomy

Xylaria hedyosmicola Hai X. Ma & X.Y. Pan, sp. nov.

Mycobank No: 839780

GenBank No: MZ227121, MZ221183, MZ683407

Figure 2

Diagnosis. Differs from *X. vagans* by its stromata without a black rhizomorphoid mycelium connecting dead leaves, larger ascospores and tubular to slightly urn-shaped apical apparatus. Differs from *X. betulicola* by its smaller stromata and larger ascospores.

Typification. CHINA. Hainan Province, Lingshui County, Diaoluoshan Natural Reserve, on fallen leaves of *Hedyosmum orientale* (Chloranthaceae), 31 December 2020, Haixia Ma (holotype, FCATAS 856).

Etymology. “*hedyosmicola*” refers to the growth on leaves of *Hedyosmum orientale*.

Teleomorph. *Stromata* upright, solitary to cespitose, thread-like, unbranched or occasionally branched once at top, 2–5.5 cm total length; with a long sterile filiform apex up to 0.5–3 cm long; fertile part 3–17 mm long × 0.5–1 mm diam., usually consisting of closely packed or scattered perithecia; stipe 8–18 mm long × 0.1–0.5 mm diam., glabrous, finely longitudinally striate, the base slightly swollen; surface roughened, with half-exposed to fully exposed perithecial contours and wrinkles. Externally black, interior white. Texture soft. *Perithecia* subglobose, 200–470 µm diam. *Ostioles* papillate, 11–22 µm diam. *Asci* with eight ascospores arranged in uniseriate manner, cylindrical, 105–160 µm total length, the spore-bearing parts 70–100 µm long × 8–12 µm broad, the stipes 25–70 µm long, with apical apparatus bluing in Melzer’s reagent, tubular to slightly urn-shaped, 2.5–4.8 µm high × 2.5–3.5 µm broad. *Ascospores* brown, unicellular, ellipsoid-inequilateral, with narrowly rounded ends, smooth, (12–)13–15(–16.7) × (6–) 6.5–7.5 (–8.5) µm ($M = 14 \times 7 \mu\text{m}$, $n = 60$), straight to slightly sigmoid germ slit spore-length or almost spore-length, with a slimy sheath on ventral side swollen at both ends to form rounded non-cellular appendages visible in Indian ink.

Additional specimen examined. CHINA. Hainan Province, Lingshui County, Diaoluoshan Natural Reserve, on fallen leaves of *Hedyosmum orientale*, 31 December 2020, Haixia Ma (FCATAS 857).

Remarks. *Xylaria hedyosmicola* closely resembles *X. vagans* Petch by sharing thread-like or long hair-like stromata bearing closely packed or scattered perithecia with a long sterile filiform apex. *Xylaria vagans* was originally described and illustrated by Petch (1915) from Sri Lanka. However, based on comparisons of the descriptions and illustrations, there were some differences between the two species. *Xylaria hedyosmicola* has larger sporiferous part of asci (70–100 µm × 8–12 µm) with tubular to slightly urn-shaped apical apparatus bluing in Melzer’s reagent, brown and larger ascospores with straight (Fig. 2n and p) to slightly sigmoid germ slit (Fig. 2o), with narrowly rounded ends and a slimy sheath on ventral side swollen at both ends to form rounded non-cellular appendages, while *X. vagans* has a black rhizomorphoid mycelium connecting dead leaves, smaller sporiferous part 68–72 µm × 6 µm and black-brown, cymbiform,

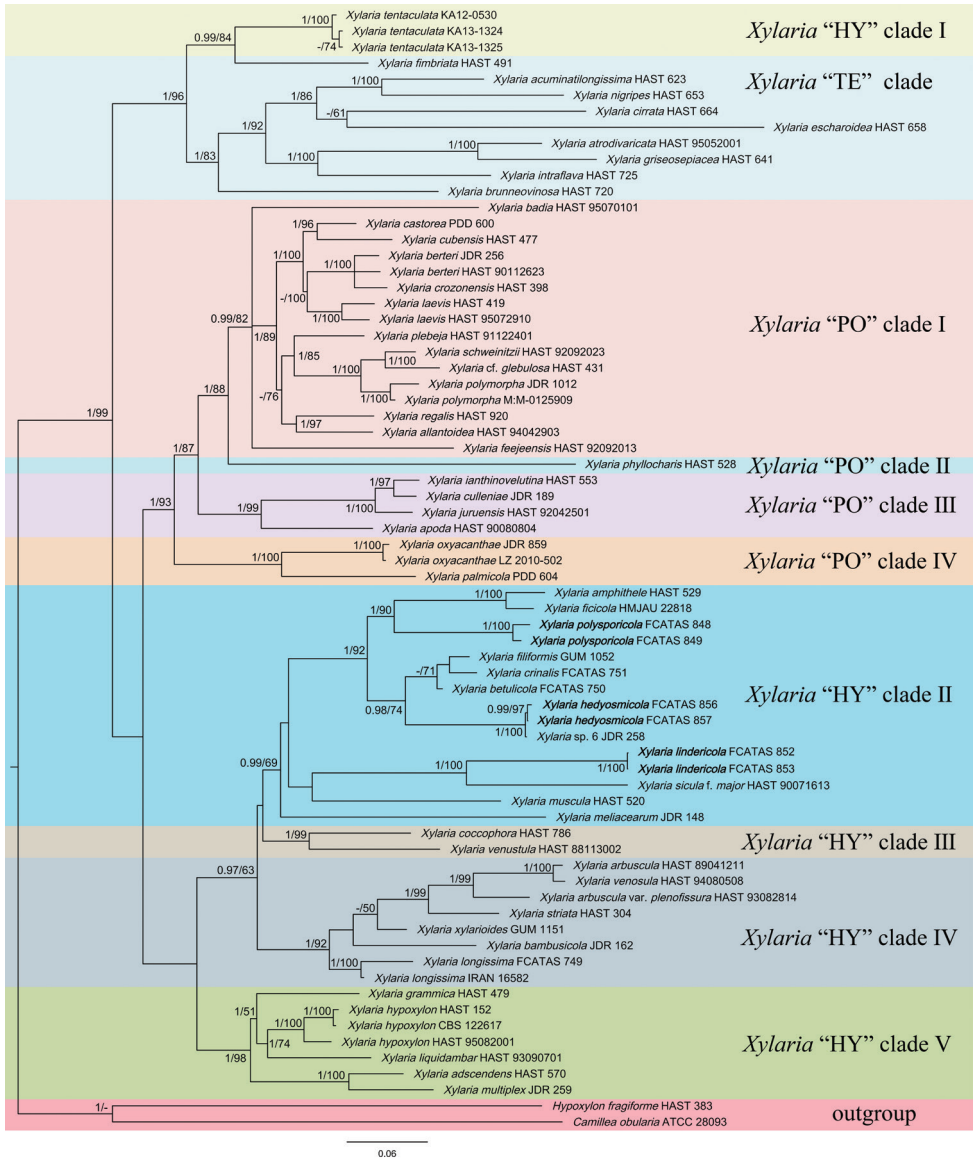


Figure 1. Phylogenetic tree of *Xylaria* based on multigene alignment of ITS-TUB-RPB2 in the Bayesian analysis. Bayesian posterior probabilities (≥ 0.95 , before the slash markers) and RaxML bootstrap values (≥ 50 , after the slash markers) are shown. Different clades are indicated as coloured blocks.

smaller ascospores $9\text{--}12 \times 5\text{--}6 \mu\text{m}$, with broadly rounded ends and is without apical apparatus, germ slit and sheath or appendages (Petch 1915). Unfortunately, the molecular sequences of *X. vagans* from Sri Lanka were not available.

Xylaria betulicola Hai X. Ma, Lar.N. Vassiljeva & Yu Li is similar to *X. hedyosmicola* in stromatal morphology, but differs in having larger stromata $3\text{--}7 \text{ cm}$, slightly smaller

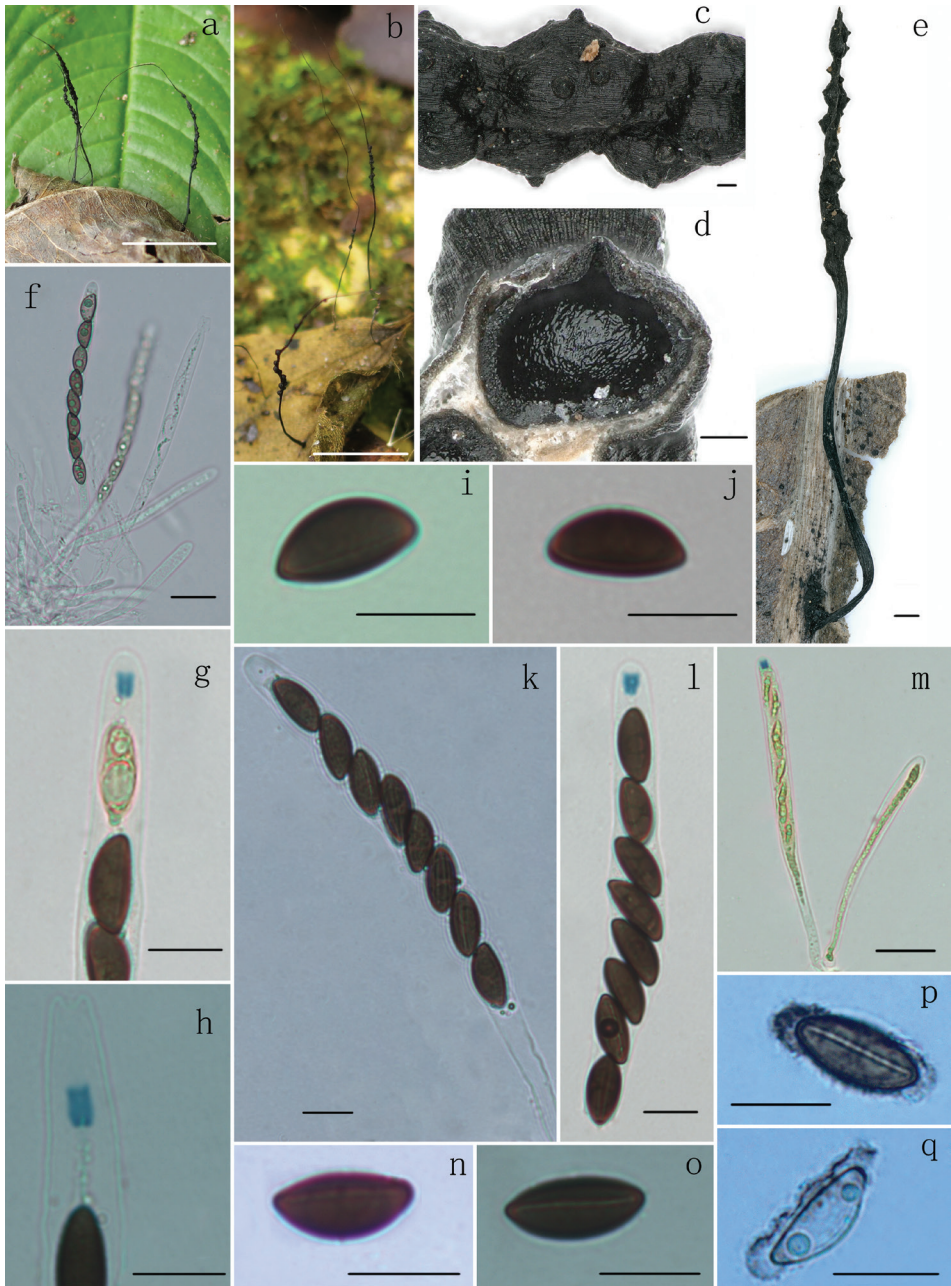


Figure 2. *Xylaria hedyosmicola* (FCATAS 856, holotype) **a, b, e** stromata on leaves (b, FCATAS 857) **c** stromatal surface **d** section through stroma, showing a perithecium **f** immature asci in water **g, h** ascial apical ring in Melzer's reagent **i, j** ascospores in Melzer's reagent **k** ascus in 1% SDS **l, m** asci and ascial apical ring in Melzer's reagent **n** ascospore in Melzer's reagent showing straight germ slit **o** ascospore in Melzer's reagent showing slightly sigmoid germ slit **p, q** ascospore showing a slimy sheath and non-cellular appendages in India ink. Scale bars: 1 cm (**a, b**); 0.1 mm (**c, d**); 0.5 mm (**e**); 20 μ m (**f, m**); 10 μ m (**g-l, n-q**).

ascospores (11.5)12–14(15) × 5–6 µm, without sheath or appendages (Ma and Li 2018). In the phylogenetic tree, *X. hedyosmicola* formed a fully supported clade with *Xylaria* sp. 6 from Hawaiian Islands, USA (Hsieh et al. 2010). Although there are no descriptions on *Xylaria* sp. 6 in the study of Hsieh et al. (2010), we suspected that it is conspecific with *X. hedyosmicola*. The sequences comparison showed that there are 98.7%, 99% and 99.9% maximal percentage identities, respectively in ITS, TUB and RPB2 between *X. hedyosmicola* (FCATAS 856) and *Xylaria* sp. 6 from USA (JDR 258).

***Xylaria lindericola* Hai X. Ma & X.Y. Pan, sp. nov.**

Mycobank No: 839554

GenBank No: MZ005635, MZ031978, MZ031982

Figure 3

Diagnosis. Differs from *X. sicula* f. *major* by its subglobose stromata without a long sterile apex, larger ascospores and host plant. Differs from *X. hypsipoda* by its black stromata, glabrous stipes and smaller apical apparatus.

Typification. CHINA. Hainan Province, Lingshui County, Diaoluoshan Natural Reserve, on fallen leaves of *Lindera robusta* (Lauraceae), 31 December 2020, Haixia Ma (holotype, FCATAS 852).

Etymology. “*lindericola*” refers to the growth on leaves of *Lindera robusta*.

Teleomorph. *Stromata* upright or prostrate, solitary to cespitose, unbranched or branched once or more at stipe, 3–26 cm total length; fertile part subglobose on long filiform stipes, 0.1–0.4 cm diam., the stipe 3–25 cm long × 0.1–1 mm diam., glabrous, finely longitudinally striate, the base slightly swollen; surface roughened by wrinkles and barely exposes perithecial contours. External black, interior white. Texture soft. *Perithecia* subglobose, 300–550 µm diam. *Ostioles* black, papillate. *Asci* with eight ascospores in uniseriate manner, cylindrical, 105–165 µm total length, the spore-bearing parts 65–115 µm long × 7.5–10.5 µm broad, the stipes 25–65 µm long, with apical apparatus bluing in Melzer’s reagent, tubular to urn-shaped, 3.9–5.5 µm high × 3–5 µm broad. *Ascospores* brown, unicellular, ellipsoid-inequilateral, with slightly narrowly rounded ends, aberrant ascospores with strongly pinched or beaked ends, smooth, (12.5–)13.5–15.5(–18) × (7–) 7.5–8.5 (–9.5) µm (M = 14.8 × 8 µm, n=60), with straight germ slit spore-length, without sheath or appendages visible in India ink.

Additional specimen examined. CHINA. Hainan Province, Lingshui County, Diaoluoshan Natural Reserve, on fallen leaves of *Lindera robusta*, 31 December 2020, Haixia Ma (FCATAS 853).

Remarks. *Xylaria lindericola* is distinguished by its subglobose fertile part of stroma on a long filiform stipe and growing on fallen leaves of *Lindera robusta*. The species is somewhat similar to *X. sicula* f. *major* in morphology of stromatal fertile part. However, *X. sicula* f. *major* has stromata with long sterile apex, slightly smaller ascospores 9–13(–15) × (3–) 4.5–6 (–7) µm and grows on dead *Olea* leaves (Ciccarone 1947;

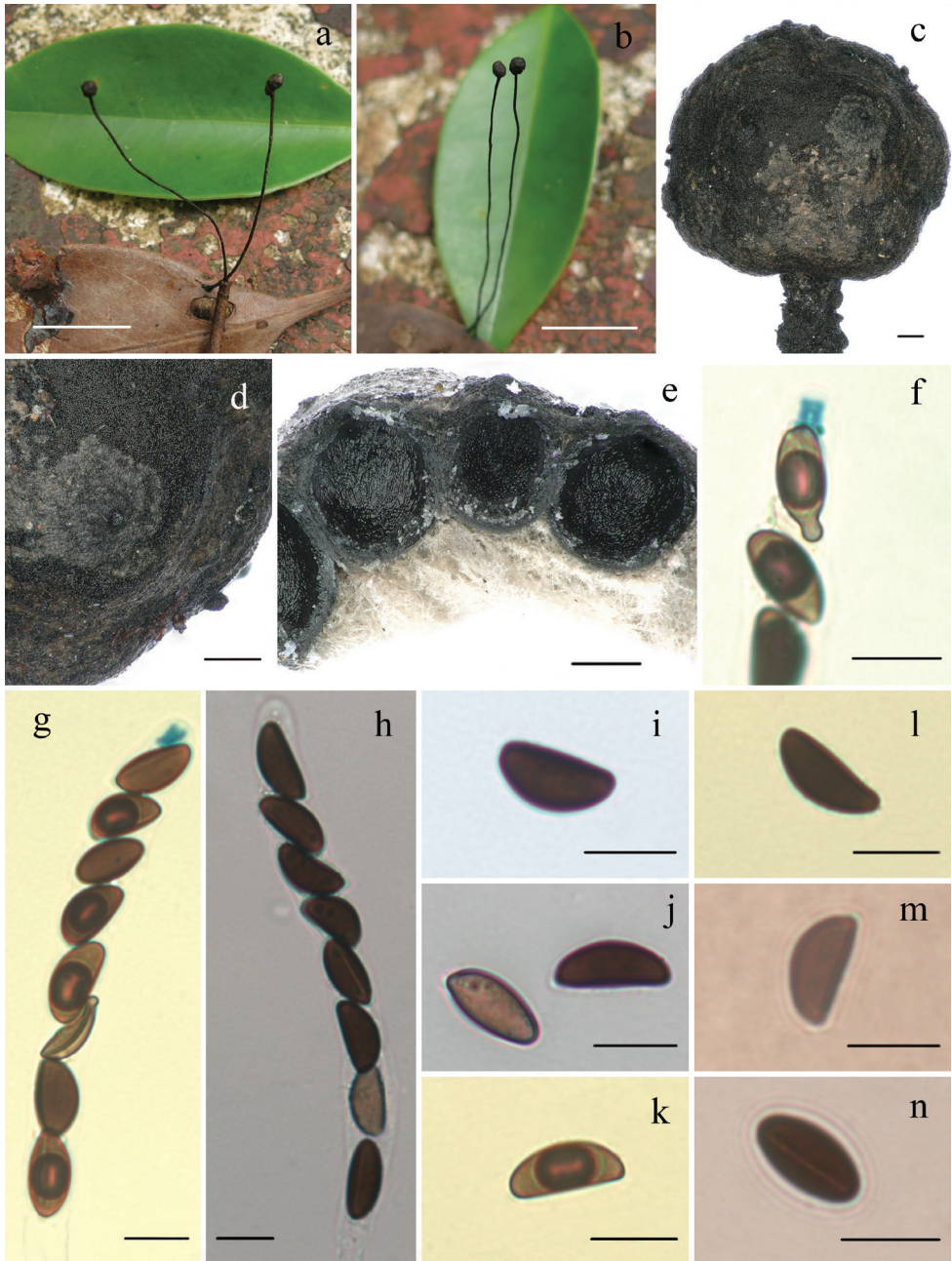


Figure 3. *Xylaria lindericola* (FCATAS 852, holotype) **a, b** stromata on leaves **c** fertile part of stroma **d** stromatal surface **e** section through stroma, showing perithecia **f** ascus apical ring and ascospores with beaked ends in Melzer's reagent **g** ascus and ascus apical ring in Melzer's reagent **h** ascus in water **i, j** ascospores in water **k, l** ascospore in Melzer's reagent **m** ascospore in India ink **n** ascospore in 1% SDS showing germ slit. Scale bars: 1.5 cm (**a, b**); 0.2 mm (**c–e**); 10 μ m (**f–n**).

Graniti 1959; Fournier 2014). In the phylogenetic tree, *X. lindericola* formed a fully supported clade with *X. sicula* f. *major* (Figure 1).

Xylaria hypsipoda Masee is similar to *X. lindericola* by sharing globose stromata and ascospores dimensions, but differs in having stromata with whitish scales, hairy stipes and urn-shaped, slightly larger apical apparatus 5–8 μm high \times 2.9–5 μm broad (Rogers et al. 1987).

Xylaria ficicola resembles *X. lindericola* in stromatal morphology, but differs in having strongly exposed perithecial mounds of stromatal surface, larger ascospores (16–) 17.5–21(–22.7) \times 6.5–8.5 μm with conspicuous hyaline noncellular appendage and grows on fallen leaves and petioles of *Ficus auriculata* (Ma et al. 2011). *Xylaria beloidea* Penz. & Sacc. from Indonesia is somewhat similar to *X. lindericola* in stromatal morphology, but the former has obconical, convex stromatal top, larger ascospores (14.5–) 15.5–18(–19) \times (5–)5.5–6.5(–7) μm (16.7 \times 6.1 μm), with a hyaline sheath swelling at both ends to form non-cellular appendages and grows on fallen fruits, twigs, petioles, and leaves of various plants (Ju et al. 2018).

Xylaria comosa (Mont.) Fr. and *X. clusiae* K.F. Rodrigues, J.D. Rogers & Samuels are also somewhat similar to *X. lindericola* in stromatal morphology. However, *X. comosa* has larger ascospores (21)–26–40 \times 7–11 μm and larger apical ring 10.5 μm high \times 7.5 μm broad (Dennis 1956) and *X. clusiae* has smaller stromata 1–3.5 cm, ascospores broadly ovoidal to nearly globose (11.6–)12.8–16.7(–18) \times 8–15 μm , with colorless appendage at one end (Samuels and Rogerson 1990).

***Xylaria polysporicola* Hai X. Ma & X.Y. Pan, sp. nov.**

Mycobank No: 839552

GenBank No: MZ005592, MZ031976, MZ031980

Figure 4

Diagnosis. Differs from *X. phyllocharis* by its half-exposed to fully exposed perithecial contours, the fertile part cylindrical and larger perithecia. Differs from *X. phyllophila* by its smaller ascospores. Differs from *X. amphithele* by its cylindrical stromata.

Typification. CHINA. Hainan Province, Lingshui County, Diaoluoshan Natural Reserve, on fallen leaves of *Polyspora hainanensis* (Theaceae), 31 December 2020, Haixia Ma (holotype, FCATAS 848).

Etymology. “*polysporicola*” refers to the growth on leaves of *Polyspora hainanensis*.

Teleomorph. *Stromata* solitary, upright or prostrate, cylindrical, unbranched or occasionally branched, 1–4 cm total length, with acute sterile apex up to 2 mm long; fertile part 2–15 mm long \times 0.5–1.6 mm diam., usually consists of closely packed perithecia and occasionally with scattered perithecia; the stipe 5–30 mm long \times 0.3–1 mm diam., glabrous, finely longitudinally striate, the base slightly swollen; surface roughened, with half-exposed to fully exposed perithecial contours and wrinkles. Externally black, interior white. Texture soft. *Perithecia* subglobose, 0.4–0.6 mm diam.

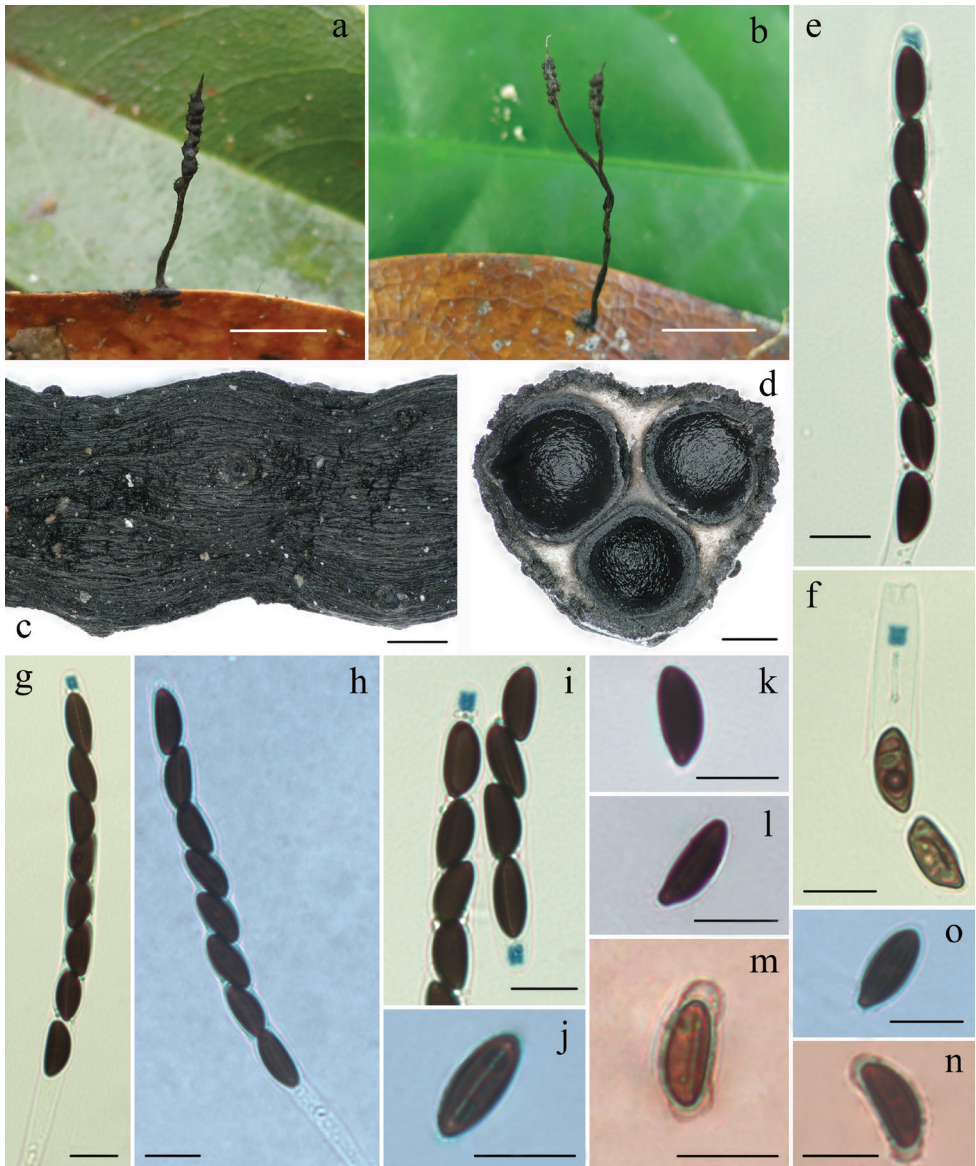


Figure 4. *Xylaria polysporicola* (FCATAS 848, holotype) **a, b** stromata on leaves (b, FCATAS 851) **c** stromatal surface **d** section through stroma, showing perithecia **e, g** asci and ascial apical ring in Melzer's reagent **f, i** ascial apical ring in Melzer's reagent **h** asci in black India ink **j** ascospore with germ slit in 1% SDS **k, l** ascospore in water **m, n** ascospore showing a slimy sheath and non-cellular appendages in India ink (FCATAS 850) **o** Ascospore in 1% SDS. Scale bars: 1 cm (**a, b**); 0.2 mm (**c, d**); 10 μ m (**e–o**).

Ostioles papillate. *Asci* with eight ascospores arranged in uniseriate manner, cylindrical, 115–185 μ m total length, the spore-bearing parts 75–100 μ m long \times 6.5–9 μ m broad, the stipes 30–90 μ m long, with apical apparatus bluing in Melzer's reagent, inverted hat-shaped or urn-shaped, 2.5–4.5 μ m high \times 2–3.2 μ m broad. *Ascospores* brown to

dark-brown, unicellular, ellipsoidal-inequilateral, with broadly rounded ends, one end slightly pinched sometimes, smooth, $(11.5\text{--}12.5\text{--}14.5\text{--}15) \times 5.5\text{--}8 \mu\text{m}$ ($M = 13.2 \times 6.4 \mu\text{m}$, $n=60$), with straight germ slit slightly less than spore-length, a slimy sheath or non-cellular appendages visible occasionally in Indian ink.

Additional specimens examined. CHINA. Hainan Province, Lingshui County, Diaoluoshan Natural Reserve, on fallen leaves of *Polyspora hainanensis*, 31 December 2020, Haixia Ma (FCATAS 849); 5 July 2019, Haixia Ma (FCATAS 850 & 851).

Remarks. *Xylaria polysporicola* is morphologically similar to *X. phyllocharis* Mont. However, *X. phyllocharis* has fully immersed perithecia, the fertile part with peg-like structures and smaller perithecia 0.2–0.3 mm diam (San Martín and Rogers 1989; Fournier et al. 2020). *Xylaria polysporicola* is similar to *Xylaria* sp. (80082005) from Taiwan in stromatal morphology, but the latter has slightly smaller stroma (11–14 mm total length \times 1 mm diam. vs. 10–40 mm total length \times 0.5–1.6 mm diam.), hard texture, slightly larger ascospores $13.5\text{--}16.5 \times 5\text{--}6 \mu\text{m}$, with narrowly rounded ends (Ju and Rogers 1999). *Xylaria phyllophila* Ces. somewhat resembles *X. polysporicola* in stromatal morphology, but the former has larger ascospores $20 \times 10 \mu\text{m}$ (Cooke 1883).

Xylaria polysporicola is somewhat similar to *X. amphithele* F. San Martín & J.D. Rogers in shape and size of apical apparatus and ascospores. However, *X. amphithele* has globose to conical stromata with 3–4 to 20 naked perithecia (San Martín and Rogers 1989). In the phylogenetic tree, *X. polysporicola* formed a lineage close to *X. amphithele* and *X. ficicola*, but is distant from *X. phyllocharis*.

Discussion

We included ten *Xylaria* species on fallen leaves in the phylogenetic analyses of the present study. Except for *X. phyllocharis*, the other nine studied species formed a monophyletic clade with two wood-inhabiting species, *X. muscula* Lloyd and *X. crinalis* Hai X. Ma, Lar. N. Vassiljeva & Yu Li, in our phylogenetic tree (Figure 1). In China, only three species have been previously reported with molecular evidence: *X. ficicola* from tropical Yunnan, *X. sicula* f. *major* from tropical Taiwan and *X. betulicola* from temperate Jilin (Ma and Li 2018). Within the clade, *X. meliacearum*, associated with petioles and infructescence of *Guarea guidonia*, formed a separate branch from other *Xylaria* species on other leaves. In Hsieh et al. (2010), *X. phyllocharis* grouped with the wood-inhabiting *Xylaria* species, which did not reveal any contradictions in our tree. Three species, *X. polysporicola*, *X. amphithele* and *X. ficicola* formed a highly supported clade. Morphologically, these species have some similar features, such as ascospores with slimy sheath or non-cellular appendages, inverted hat-shaped or urn-shaped apical apparatus (San Martín and Rogers 1989; Ma et al. 2020). As *Xylaria hedyosmicola* formed a fully supported clade with *Xylaria* sp. 6, the two species should be the same, based on the ITS-TUB-RPB2 (Hsieh et al. 2010). *Xylaria lindericola*, on leaves of *Lindera robusta* formed a sister lineage to *X. sicula* f. *major* on unknown fallen leaves with high bootstrap value 100%. *Xylaria muscula*, growing on dead branches, formed a weakly supported branch with *X. lindericola* and *X. sicula* f. *major* associated

with fallen leaves in our tree. This may be because our phylogenetic analysis did not include more taxa related to *X. muscula*.

Until now, ten taxa, *X. betulicola*, *X. diminuta* F. San Martín & J.D. Rogers, *X. ficicola*, *X. foliicola* G. Huang & L. Guo, *X. hainanensis* Y.F. Zhu & L. Guo, *X. hedyosmicola*, *X. jiangsuensis* G. Huang & L. Guo, *X. lindericola*, *X. polysporicola* and *X. sicula* f. *major* have been found on fallen leaves in China (Hsieh et al. 2010; Ma et al. 2011; Zhu and Guo 2011; Huang et al. 2014, 2015; Ma and Li 2018). Amongst these species, *X. diminuta*, originally reported from Mexico, was found in Yunnan province of China in 2013 (Huang et al. 2014). *Xylaria sicula* f. *major* was first described from Sicily in 1878 and then found in Spain, Kenya, Sardinia, and Taiwan province of China (Hsieh et al. 2010; Fournier 2014). Unfortunately, except for the three species in this study, the molecular data of the other *Xylaria* species from China were not available. We anticipate that additional species of *Xylaria* on fallen leaves will be discovered as more studies are conducted.

Key to species of *Xylaria* on fallen leaves in China

- 1 Stromata with rounded fertile apices 2
- Stromata with acute sterile apices 3
- 2 Stromata associated with leaves and petioles of *Ficus auriculata* (Moraceae), ascospores (16–)17.5–21(–22.7) × 6.5–8.5 µm ***X. ficicola***
- Stromata associated with leaves of *Lindera robusta* (Lauraceae), ascospores (12.5–)13.5–15.5(–18) × (7–)7.5–8.5(–9.5) µm ***X. lindericola***
- 3 Stipes tomentose ***X. hainanensis***
- Stipes glabrous 4
- 4 Fertile part subglobose ***X. sicula* f. *major***
- Fertile part not subglobose 5
- 5 Stromata cylindrical 6
- Stromata filiform 8
- 6 Ascospores (5.5–)6–8 × 3–3.5(–4) µm ***X. diminuta***
- Ascospores length > 8.5 µm 7
- 7 Stromata with conspicuous perithecial contours, ascospores (11.5–)12.5–14.5(–15) × 5.5–8 µm ***X. polysporicola***
- Stromata with inconspicuous perithecial contours, ascospores (8.5–)9–11 × 4–6 µm ***X. foliicola***
- 8 Ascospores 16.5–20(–21.5) × 4–5(–6) µm ***X. jiangsuensis***
- Ascospores length < 16.5 µm 9
- 9 Stromata associated with leaves of *Betula* (Betulaceae), ascospores (11.5)12–14(15) × 5–6 µm, with a straight germ slit, without appendages visible in India ink ***X. betulicola***
- Stromata associated with leaves of *Hedyosmum orientale* (Chloranthaceae), ascospores (12–)13–15(–16.7) × (6–)6.5–7.5(–8.5) µm, with straight to slightly sigmoid germ slit, with appendages visible in Indian ink ***X. hedyosmicola***

Acknowledgements

The authors thank Prof. Yu-Ming Ju (Institute of Plant and Microbial Biology, Academia Sinica, Taiwan, China) for suggestions on the manuscript. This study was supported by the National Natural Science Foundation of China (no. 31770023, 31972848, U1803232). We are also grateful to the Key Research and Development Program of Hainan (ZDYF2020062) and Hainan Basic and Applied Research Project for Cultivating High-Level Talents (2019RC305).

References

- Ciccarone (1947) Alcune osservazioni su una forma de *Xylaria sicula* Pass. e Beltr. Nuovo Giornale Botanico Italiano 53(1946): 356–358.
- Cooke MC (1883) On *Xylaria* and its allies. Grevillea 11: 81–94.
- Cui BK, Li HJ, Ji X, Zhou JL, Song J, Si J, Yang ZL, Dai YC (2019) Species diversity, taxonomy and phylogeny of Polyporaceae (Basidiomycota) in China. Fungal Diversity 97: 137–392. <https://doi.org/10.1007/s13225-019-00427-4>
- Dai YC (2012) Polypore diversity in China with an annotated checklist of Chinese polypores. Mycoscience 53: 49–80. <https://doi.org/10.1007/s10267-011-0134-3>
- Dai YC, Yang ZL, Cui BK, Yu CJ, Zhou LW (2009) Species diversity and utilization of medicinal mushrooms and fungi in China. International Journal of Medicinal Mushrooms 11: 287–302. <https://doi.org/10.1615/IntJMedMushr.v11.i3.80>
- Dennis RWG (1956) Some *Xylarias* of tropical America. Kew Bulletin 11: 401–444. <https://doi.org/10.2307/4109126>
- Fournier J (2014) Update on European species of *Xylaria*, 120 pp.
- Fournier J, Lechat C, Courtecuisse R (2020) The genus *Xylaria* sensu lato (Xylariaceae) in Guadeloupe and Martinique (French West Indies) III. Taxa with slender upright stromata. Ascomycete.org 12(3): 81–164. <https://doi.org/10.1128/jb.172.8.4238-4246.1990>
- Gao Q, Yang ZL (2016) Diversity and distribution patterns of root-associated fungi on herbaceous plants in alpine meadows of southwestern China. Mycologia 108: 281–291. <https://doi.org/10.3852/14-324>
- Graniti (1959) Presenza di *Xylaria sicula* Pass. Et Beltr. su frutti e foglie di olivo e considerazioni sulla specie e sulle sue forme. Nuovo Giornale Botanico Italiano 66: 364–376.
- Hall TA (1999) BioEdit: a user-friendly biological sequence alignment editor and analysis program for Windows 95/98/NT. NucleicAcids Symposium Series 41: 95–98. <https://doi.org/10.1021/bk-1999-0734.ch008>
- Hashemi SA, Zare R, Khodaparast SA, Elahinia SA (2015) A new *Xylaria* species from Iran. Mycologia Iranica 2: 1–10.
- Hsieh HM, Ju YM, Rogers JD (2005) Molecular phylogeny of *Hypoxylon* and related genera. Mycologia 97(4): 844–865. <https://doi.org/10.1080/15572536.2006.11832776>
- Hsieh HM, Lin CR, Fang MJ, Rogers JD, Fournier J, Lechat C, Ju YM (2010) P-hylogenetic status of *Xylaria* subgen. *Pseudoxylaria* among taxa of the subfamily Xylarioideae

- (Xylariaceae) and phylogeny of the taxa involved in the s-ubfamily. *Molecular Phylogenetics and Evolution* 54: 957–969. <https://doi.org/10.1016/j.ympev.2009.12.015>
- Huang G, Guo L, Liu N (2014) Two new species of *Xylaria* and *X. diminuta* new to China. *Mycotaxon* 129(1): 149–152. <https://doi.org/10.5248/129.149>
- Huang G, Wang RS, Guo L, Liu N (2015) Three new species of *Xylaria* from China. *Mycotaxon* 130: 299–304. <https://doi.org/10.5248/130.299>
- Huelsenbeck JP, Ronquist F (2005) Bayesian analysis of molecular evolution using MrBayes. In: Nielsen R (Ed.) *Statistical methods in molecular evolution*. Springer, New York, 183–226. https://doi.org/10.1007/0-387-27733-1_7
- Ju YM, Rogers JD (1999) The Xylariaceae of Taiwan (excluding *Anthostomella*). *Mycotaxon* 73: 343–440.
- Ju YM, Hsieh HM (2007) *Xylaria* species associated with nests of *Odontotermes formosanus* in Taiwan. *Mycologia* 99: 936–957. <https://doi.org/10.1080/15572536.2007.11832525>
- Ju YM, Rogers JD, Hsieh HM (2018) *Xylaria* species associated with fallen fruits and seeds. *Mycologia* 110(4): 726–749. <https://doi.org/10.1080/00275514.2018.1469879>
- Kim CS, Jo GW, Kwag YN, Oh SO, Lee SG, Sung GH, Oh G, Shrestha B, Ki-m SY, Shin CH, Han SK (2016) New Records of *Xylaria* Species in Korea: *X. ripicola* sp. nov. and *X. tentaculata*. *Mycobiology* 44(1): 21–28. <https://doi.org/10.5941/MYCO.2016.44.1.21>
- Laessle T, Lodge DJ (1994) Three host-specific *Xylaria* species. *Mycologia* 86(3): 436–446. <https://doi.org/10.1080/00275514.1994.12026431>
- Liu YJ, Whelen S, Hall BD (1999) Phylogenetic relationships among ascomycetes: evidence from an RNA polymerase II subunit. *Molecular Biology And Evolution* 16: 1799–1808. <https://doi.org/10.1093/oxfordjournals.molbev.a026092>
- Ma HX, Li Y (2018) *Xylaria crinalis* and *X. betulicola* from China – two new species with thread-like stromata. *Sydowia* 70: 37–49. <https://doi.org/10.12905/0380.sydowia70-2018-0037>
- Ma HX, Vasilyeva L, Li Y (2011) A new species of *Xylaria* from China. *Mycotaxon* 116: 151–155. <https://doi.org/10.5248/116.151>
- Ma HX, Qu Z, Peng MK, Li Y (2020) Two penzigoid *Xylaria* species described from China based on morphological and molecular characters. *Phytotaxa* 436(1): 036–044. <https://doi.org/10.11646/phytotaxa.436.1.3>
- Nylander JAA (2004) *MrModeltest 2.3*. Program distributed by the author. Evolutionary Biology Center, Uppsala University.
- O'Donnell K, Cigelnik E (1997) Two Divergent Intragenomic rDNA ITS2 Types within a Monophyletic Lineage of the Fungus. *Molecular Phylogenetics and Evolution* 7(1): 103–116. <https://doi.org/10.1006/mpev.1996.0376>
- Persoh D, Melcher M, Graf K, Fournier J, Stadler M, Rambold G (2009) Molecular and morphological evidence for the delimitation of *Xylaria hypoxylon*. *Mycologia* 101(2): 256–268. <https://doi.org/10.3852/08-108>
- Petch (1915) *Annals of the Royal Botanical Gardens, Peradeniya* 6(1): e68.
- Roensch P, Roensch S, Reiher A, Otto P (2010) Investigations on the fructicolous *Xylaria delitschii* and *Xylaria oxyacanthae*. *Boletus* 32 (2): 106–122.
- Rogers JD (1986) Provisional keys to *Xylaria* species in continental United States. *Mycotaxon* 26: 85–97.

- Rogers JD, Samuels GJ (1986) Ascomycetes of New Zealand 8. *Xylaria*. New Zealand Journal of Botany 24(4): 615–650. <https://doi.org/10.1080/0028825X.1986.10409947>
- Rogers DJ, Callan BE, Samuels GJ (1987) The Xylariaceae of the rain forests of North Sulawesi (Indonesia). Mycotaxon 31: 113–172.
- Rogers JD, Ju YM, Lehmann J (2005) Some *Xylaria* species on termite nests. Mycologia 97(4): 914–923. <http://dx.doi.org/10.1080/15572536.2006.11832783>
- Rogers JD, Callan BE, Rossman AY, Samuels GJ (1988) *Xylaria* (Sphaeriales, Xylariaceae) from Cerro de la Neblina, Venezuela. Mycotaxon 31: 103–153. <https://doi.org/10.1007/BF00455669>
- Samuels GJ, Rogerson CT (1990) New Ascomycetes from the Guayana Highland. Memoirs of the New York Botanical Garden 64: 165–183.
- San Martin GF, Rogers JD (1989) A preliminary account of *Xylaria* of Mexico. Mycotaxon 34: 283–373.
- Stamatakis A (2006) RAxML-VI-HPC: maximum likelihood-based phylogenetic analyses with thousands of taxa and mixed models. Bioinformatics 22: 2688–2690. <https://doi.org/10.1093/bioinformatics/btl446>
- Wendt LC, Sir EB, Kuhnert E, Heitkaemper S, Lambert C, Hladki AI, Romero A-I, Luangsard JJ, Srikritikulchai P, Persoh D, Stadler M (2018) Resurrection and emendation of the Hypoxylaceae, recognised from multigene phylogeny of the Xylariales. Mycological Progress 17: 115–154. <https://doi.org/10.1007/s11557-017-1311-3>.
- White TJ, Burns T, Lee S, Taylor J (1990) Amplification and direct sequencing of fungal ribosomal RNA genes for phylogenetics. In: Innis MA, Gelfand DH, Sninsky JJ, White TJ (Eds) PCR protocols, a guide to methods and applications. Academic, San Diego, 315–322. <https://doi.org/10.1016/B978-0-12-372180-8.50042-1>
- Yang XB (2015) The colored illustrated flora of Hainan Province. Science Press, Beijing. [in Chinese]
- Zhu YF, Guo L (2011) *Xylaria hainanensis* sp. nov. (Xylariaceae) from China. Mycosystema 30(4): 526–528. <https://doi.org/10.13346/j.mycosystema.2011.04.014>

Taxonomy and phylogeny of the novel rhytidhysterion-like collections in the Greater Mekong Subregion

Guang-Cong Ren^{1,2,3}, Dhanushka N. Wanasinghe^{5,6},
Rajesh Jeewon⁷, Jutamart Monkai¹, Peter E. Mortimer^{4,5},
Kevin D. Hyde^{1,2}, Jian-Chu Xu^{4,5}, Heng Gui^{4,5}

1 Center of Excellence in Fungal Research, Mae Fah Luang University, Chiang Rai 57100, Thailand **2** School of Science, Mae Fah Luang University, Chiang Rai 57100, Thailand **3** Guiyang Nursing Vocational College, Guiyang 550081, Guizhou, China **4** Department of Economic Plants and Biotechnology, Yunnan Key Laboratory for Wild Plant Resources, Kunming Institute of Botany, Chinese Academy of Sciences, Kunming 650201, China **5** Center for Mountain futures, Kunming Institute of Botany, Chinese Academy of Sciences, Honghe County 654400, Yunnan, China **6** World Agroforestry Centre, East and Central Asia, Kunming 650201, Yunnan, China **7** Department of Health Sciences, Faculty of Medicine and Health Sciences, University of Mauritius, Reduit, Mauritius

Corresponding authors: Dhanushka N. Wanasinghe (dnadeeshan@gmail.com), Heng Gui (guiheng@mail.kib.ac.cn)

Academic editor: Thorsten Lumbsch | Received 25 June 2021 | Accepted 26 December 2021 | Published 12 January 2022

Citation: Ren G-C, Wanasinghe DN, Jeewon R, Monkai J, Mortimer PE, Hyde KD, Xu J-C, Gui H (2022) Taxonomy and phylogeny of the novel rhytidhysterion-like collections in the Greater Mekong Subregion. MycoKeys 86: 65–85. <https://doi.org/10.3897/mycokeys.86.70668>

Abstract

During our survey into the diversity of woody litter fungi across the Greater Mekong Subregion, three rhytidhysterion-like taxa were collected from dead woody twigs in China and Thailand. These were further investigated based on morphological observations and multi-gene phylogenetic analyses of a combined DNA data matrix containing SSU, LSU, ITS, and *tefl*- α sequence data. A new species of *Rhytidhysterion*, *R. xiaokongense* sp. nov. is introduced with its asexual morph, and it is characterized by semi-immersed, subglobose to ampulliform conidiomata, dark brown, oblong to ellipsoidal, 1-septate, conidia, which are granular in appearance when mature. In addition to the new species, two new records from Thailand are reported viz. *Rhytidhysterion tectonae* on woody litter of *Betula* sp. (Betulaceae) and *Fabaceae* sp. and *Rhytidhysterion neorufulum* on woody litter of *Tectona grandis* (Lamiaceae). Morphological descriptions, illustrations, taxonomic notes and phylogenetic analyses are provided for all entries.

Keywords

Ascomycota, one new taxon, phylogeny, saprobic, taxonomy, Yunnan

Introduction

Hysteriaceae was introduced by Chevallier (1826) with *Hysterium* as the type genus, which was characterized by hysterothecial or apothecioid, carbonaceous ascomata with a pronounced, longitudinal slit running the length of the long axis, 8-spored, clavate to cylindrical asci with an ocular chamber as well as obovoid, clavate, ellipsoid or fusoid, hyaline to light- or dark brown, one to multi-septate or muriform, smooth-walled ascospores with or without a sheath (Boehm et al. 2009b; Hongsanan et al. 2020; Hyde et al. 2020a). In recent outlines of Dothideomycetes (Hongsanan et al. 2020; Pem et al. 2020; Wijayawardene et al. 2020), 14 genera have been accepted in Hysteriaceae.

Rhytidhysteron was introduced by Spegazzini (1881) to accommodate two species: *Rhytidhysteron brasiliense* (type species) and *R. viride* in Patellariaceae (Clements and Shear 1931; Kutorga and Hawksworth 1997). Boehm et al. (2009a, b) transferred *Rhytidhysteron* from Patellariaceae to Hysteriaceae based on molecular data. Subsequent studies introduced more taxa and records in *Rhytidhysteron* with both morphological and molecular evidence (Thambugala et al. 2016; Doilom et al. 2017; Cobos-Villagrán et al. 2020; Dayarathne et al. 2020; de Silva et al. 2020; Hyde et al. 2020a, b; Mapook et al. 2020; Wanasinghe et al. 2021). Currently, 24 species are recognized in *Rhytidhysteron* (Species Fungorum 2021; Wanasinghe et al. 2021).

Rhytidhysteron species have been documented from a wide range of hosts in various countries such as Australia, Bermuda, Bolivia, Brazil, China, Colombia, Cuba, France, Hawaii, India, New Zealand, Thailand, Ukraine, USA, and Venezuela (Kutorga and Hawksworth 1997; de Silva et al. 2020). Most *Rhytidhysteron* species are identified as saprobes on woody-based substrates in terrestrial habitats as well as from mangrove wood in marine habitats (Thambugala et al. 2016; Kumar et al. 2019; Hyde et al. 2020a, b; Wanasinghe et al. 2021). However, they have also been reported as endophytes or weak pathogens on woody plants and seldom as human pathogens (Soto and Lucking 2017; de Silva et al. 2020). From a biotechnological perspective, *Rhytidhysteron* species have great potential for their commercial applications and in industry. In particular, interest in secondary metabolites has rekindled in recent years, for instance with the discovery of palmarumycins. The latter is a potential inhibitor of thioredoxin–thioredoxin reductase cellular redox systems, with potential antimicrobial and antifungal properties (Murillo et al. 2009). Other *Rhytidhysteron* species discovered from the Southeast Asian region, such as *R. bruguierae* (MFLUCC 17-1515) and *R. chromolaenae* (MFLUCC 17-1516) also showed antimicrobial activity against *Mucor plumbeus* (Mapook et al. 2020) and hence this demonstrates a potential biotechnological application.

The Greater Mekong Subregion (GMS) is regarded as a global biodiversity hotspot due to its widely varying environmental conditions. Accordingly, the GMS harbors a diverse array of numerous floras, fauna and microorganisms (Li et al. 2018). Woody litter microfungi is an overlooked group of fungi in GMS and based on previous fungal estimates, there is undoubtedly a large number of new species yet to be described from this region. Our ongoing studies into the diversity of microfungi of the GMS are actively contributing towards filling in the knowledge gap in fungal taxonomy, phylogeny, host

association and ecological distribution of *Rhytidhysteron* species in this region (Luo et al. 2018; Bao et al. 2019; Dong et al. 2020; Hyde et al. 2020b; Monkai et al. 2020, 2021; Wanasinghe et al. 2020, 2021; Yasanthika et al. 2020). Our specific objectives of this study are as follows: 1) to describe a novel species of *Rhytidhysteron* with evidence from morphology and DNA sequence data; 2) to characterize (based on morphology and phylogeny) additional new records of *Rhytidhysteron*; 3) to investigate the phylogenetic relationships of our *Rhytidhysteron* samples based on DNA sequence analyses from rDNA and protein coding genes and update the taxonomy of *Rhytidhysteron*.

Materials and methods

Samples collection and morphological analyses

Woody litter samples were collected from China (Kunming, Yunnan Province) during the wet season (August 2019) and during the dry season (December 2019) collections were done in Thailand (Chiang Rai and Tak Provinces). Samples were brought to the laboratory in plastic Ziploc bags. Fungal specimens were then examined using a stereomicroscope (Olympus SZ61, China). Pure cultures were obtained via single spore isolation on potato dextrose agar (PDA) following the methods described in Senanayake et al. (2020). Cultures were incubated at 25 °C for one week in the dark. Digital images of the fruiting structures were captured with a Canon (EOS 600D) digital camera fitted to a Nikon ECLIPSE Ni compound microscope. Squash mount preparations were prepared to determine micro-morphology and free hand sections of sporocarps made to observe the shapes of ascomata/conidiomata and peridium structures. Measurements of morphological structures were taken from the widest part of each structure. When possible, more than 30 measurements were made. Measurements were taken using the Tarosoft (R) Image Frame Work program. Figures were processed using Adobe Photoshop CS6. Field data are presented in 'Material examined'. Other details pertaining to good practices of morphological examinations were done following guidelines by Senanayake et al. (2020). New species are established based on recommendations proposed by Jeewon and Hyde (2016). Type specimens were deposited in the herbarium of the Cryptogams Kunming Institute of Botany Academia Sinica (KUN-HKAS). Ex-type living cultures were deposited at the Culture Collection of Mae Fah Luang University (MFLUCC) and Kunming Institute of Botany Culture Collection (KUMCC).

DNA extraction, amplification and sequencing

Genomic DNA was extracted from the mycelium grown on PDA at 25–30 °C for one week using a Biospin Fungus Genomic DNA Extraction Kit (BioFlux Hangzhou, P. R. China). Three partial rDNA genes and a protein coding gene were processed in our study, including the small ribosomal subunit RNA (SSU) using the primer pair NS1/

NS4 (White et al. 1990), internal transcribed spacer region (ITS) using the primer pair ITS5/ITS4 (White et al. 1990), large nuclear ribosomal subunit (LSU) using primer pair LR0R/LR5 (Vilgalys and Hester 1990), translation elongation factor 1-alpha gene (*tefl- α*) using primer pair 983F/2218R (Rehner and Buckley 2005). Amplification reactions were performed in a total volume of 25 μ L of PCR mixtures containing 8.5 μ L ddH₂O, 12.5 μ L 2X PCR MasterMix (TIANGEN Co., China), 2 μ L DNA template and 1 μ L of each primer. PCR thermal cycle program for SSU, LSU, ITS, and *tefl- α* were set as described in Wanasinghe et al. (2020). The PCR products were sent to the Qingke Company, Kunming City, Yunnan Province, China, for sequencing. Sequences were deposited in GenBank (Table 1).

Table 1. GenBank accession numbers of sequences used for the phylogenetic analyses.

Taxon	Strain number	GenBank accession numbers				Reference
		SSU	LSU	ITS	<i>tefl-α</i>	
<i>Gloniopsis calami</i>	MFLUCC 15-0739	KX669034	NG_059715	KX669036	KX671965	Hyde et al. (2016)
<i>Gloniopsis praelonga</i>	CBS 112415	FJ161134	FJ161173	NA	FJ161090	Boehm et al. (2009a)
<i>Rhytidhysterion bruguierae</i>	MFLUCC 18-0398 ^T	MN017901	MN017833	NA	MN077056	Dayarathne et al. (2020)
<i>Rhytidhysterion bruguierae</i>	MFLUCC 17-1515	MN632463	MN632452	MN632457	MN635661	Mapook et al. (2020)
<i>Rhytidhysterion bruguierae</i>	MFLUCC 17-1511	MN632465	MN632454	MN632459	NA	Mapook et al. (2020)
<i>Rhytidhysterion bruguierae</i>	MFLUCC 17-1502	MN632464	MN632453	MN632458	MN635662	Mapook et al. (2020)
<i>Rhytidhysterion bruguierae</i>	MFLUCC 17-1509	MN632466	MN632455	MN632460	NA	Mapook et al. (2020)
<i>Rhytidhysterion camporesii</i>	HKAS 104277 ^T	NA	MN429072	MN429069	MN442087	Hyde et al. (2020a)
<i>Rhytidhysterion chromolaenae</i>	MFLUCC 17-1516 ^T	MN632467	MN632456	MN632461	MN635663	Mapook et al. (2020)
<i>Rhytidhysterion erioi</i>	MFLU 16-0584 ^T	NA	MN429071	MN429068	MN442086	Hyde et al. (2020a)
<i>Rhytidhysterion hongbeense</i>	KUMCC 20-0222 ^T	MW264224	MW264194	MW264215	MW256816	Wanasinghe et al. (2021)
<i>Rhytidhysterion hongbeense</i>	HKAS112348	MW541831	MW541820	MW54182	MW556132	Wanasinghe et al. (2021)
<i>Rhytidhysterion hongbeense</i>	HKAS112349	MW541832	MW541821	MW541825	MW556133	Wanasinghe et al. (2021)
<i>Rhytidhysterion hysterinum</i>	EB 0351	NA	GU397350	NA	GU397340	Boehm et al. (2009b)
<i>Rhytidhysterion magnoliae</i>	MFLUCC 18-0719 ^T	MN989382	MN989384	MN989383	MN997309	de Silva et al. (2020)
<i>Rhytidhysterion mangrovei</i>	MFLUCC 18-1113 ^T	NA	MK357777	MK425188	MK450030	Kumar et al. (2019)
<i>Rhytidhysterion neurufulum</i>	MFLUCC 13-0216 ^T	KU377571	KU377566	KU377561	KU510400	Thambugala et al. (2016)
<i>Rhytidhysterion neurufulum</i>	GKM 361A	GU296192	GQ221893	NA	NA	Thambugala et al. (2016)
<i>Rhytidhysterion neurufulum</i>	HUEFS 192194	NA	KF914915	NA	NA	Thambugala et al. (2016)
<i>Rhytidhysterion neurufulum</i>	MFLUCC 12-0528	KJ418119	KJ418117	KJ418118	NA	Thambugala et al. (2016)
<i>Rhytidhysterion neurufulum</i>	CBS 306.38	AF164375	FJ469672	NA	GU349031	Thambugala et al. (2016)
<i>Rhytidhysterion neurufulum</i>	MFLUCC 12-0011	KJ418110	KJ418109	KJ206287	NA	Thambugala et al. (2016)
<i>Rhytidhysterion neurufulum</i>	MFLUCC 12-0567	KJ546129	KJ526126	KJ546124	NA	Thambugala et al. (2016)
<i>Rhytidhysterion neurufulum</i>	MFLUCC 12-0569	KJ546131	KJ526128	KJ546126	NA	Thambugala et al. (2016)
<i>Rhytidhysterion neurufulum</i>	EB 0381	GU397366	GU397351	NA	NA	Thambugala et al. (2016)
<i>Rhytidhysterion neurufulum</i>	MFLUCC 21-0035	MZ346025	MZ346015	MZ346020	MZ356249	This study
<i>Rhytidhysterion opuntiae</i>	GKM 1190	NA	GQ221892	NA	GU397341	Mugambi et al. (2009)
<i>Rhytidhysterion rufulum</i>	MFLUCC 14-0577 ^T	KU377570	KU377565	KU377560	KU510399	Thambugala et al. (2016)
<i>Rhytidhysterion rufulum</i>	EB 0384	GU397368	GU397354	NA	NA	Boehm et al. (2009b)
<i>Rhytidhysterion rufulum</i>	EB 0382	NA	GU397352	NA	NA	Boehm et al. (2009b)
<i>Rhytidhysterion rufulum</i>	EB 0383	GU397367	GU397353	NA	NA	Boehm et al. (2009b)
<i>Rhytidhysterion rufulum</i>	MFLUCC 12-0013	KJ418113	KJ418111	KJ418112	NA	de Silva et al. (2020)
<i>Rhytidhysterion tectonae</i>	MFLUCC 13-0710 ^T	KU712457	KU764698	KU144936	KU872760	Doilom et al. (2017)
<i>Rhytidhysterion tectonae</i>	MFLUCC 21-0037	MZ346023	MZ346013	MZ346018	MZ356247	This study
<i>Rhytidhysterion tectonae</i>	MFLUCC 21-0034	MZ346024	MZ346014	MZ346019	MZ356248	This study
<i>Rhytidhysterion thailandicum</i>	MFLUCC 14-0503 ^T	KU377569	KU377564	KU377559	KU497490	Thambugala et al. (2016)

Taxon	Strain number	GenBank accession numbers				Reference
		SSU	LSU	ITS	<i>tef1-α</i>	
<i>Rhytidhysteron thailandicum</i>	MFLUCC 12-0530	KJ546128	KJ526125	KJ546123	NA	Thambugala et al. (2016)
<i>Rhytidhysteron thailandicum</i>	MFLU17-0788	MT093495	MT093472	MT093733	NA	de Silva et al. (2020)
<i>Rhytidhysteron xiaokongense</i>	KUMCC 20-0158	MZ346021	MZ346011	MZ346016	MZ356245	This study
<i>Rhytidhysteron xiaokongense</i>	KUMCC 20-0160^T	MZ346022	MZ346012	MZ346017	MZ356246	This study

Ex-type strains are indicated with superscript “T”, and newly generated sequences are shown in bold. NA represents sequences that are unavailable in GenBank.

Phylogenetic analyses

Representative species used in the phylogenetic analyses were selected based on previous publications (Thambugala et al. 2016; Mapook et al. 2020; Wanasinghe et al. 2021). Sequences were downloaded from GenBank (<http://www.ncbi.nlm.nih.gov/>) and their accession numbers are listed in Table 1. The newly generated sequences in this study were assembled by BioEdit 7.0.9.0 (Hall 1999). Individual gene regions were separately aligned in MAFFT v.7 web server (<http://mafft.cbrc.jp/alignment/server/>) (Kato et al. 2019). The alignments of each gene were improved by manually deleting the ambiguous regions and gaps, and then combined using BioEdit 7.2.3. Final alignments containing SSU, LSU, ITS, and *tef1- α* were converted to NEXUS format (.nxs) using CLUSTAL X (2.0) and PAUP v. 4.0b10 (Thompson et al. 1997; Swofford 2002) and processed for Bayesian and maximum parsimony analysis. The FASTA format was changed into PHYLIP format via the Alignment Transformation Environment (ALTER) online program (<http://www.sing-group.org/ALTER/>) and used for maximum likelihood analysis (ML).

ML was carried out in CIPRES Science Gateway v.3.3 (<http://www.phylo.org/portal2/>; Miller et al. 2010) using RAxML-HPC2 on XSEDE (8.2.12) (Stamatakis 2014) with the GTRGAMMA substitution model and 1,000 bootstrap iterations. Maximum parsimony analysis (MP) was performed in PAUP v. 4.0b10 (Swofford 2002) with the heuristic search option and Tree-Bisection-Reconnection (TBR) of branch-swapping algorithm for 1,000 random replicates. Branches with a minimum branch length of zero were collapsed and gaps were treated as missing data (Hillis and Bull 1993). ML and MP bootstrap values (ML) $\geq 75\%$ are given above each node of the phylogenetic tree (Fig. 1).

Bayesian analysis was executed in MrBayes v.3.2.2 (Ronquist et al. 2012). The model of evolution was estimated using MrModeltest v. 2.3 (Nylander et al. 2008) via PAUP v. 4.0b10 (Ronquist and Huelsenbeck 2003). The HKY+I for SSU; GTR+I+G for ITS, LSU and *tef1- α* were used in the final command. Markov chain Monte Carlo sampling (MCMC) in MrBayes v.3.2.2 (Ronquist et al. 2012) was used to determine posterior probabilities (PP) (Rannala and Yang 1996; Zhaxybayeva and Gogarten 2002). Bayesian analyses of six simultaneous Markov chains were run for 2,000,000 generations and trees were sampled every 200 generations (resulting in 10,001 total

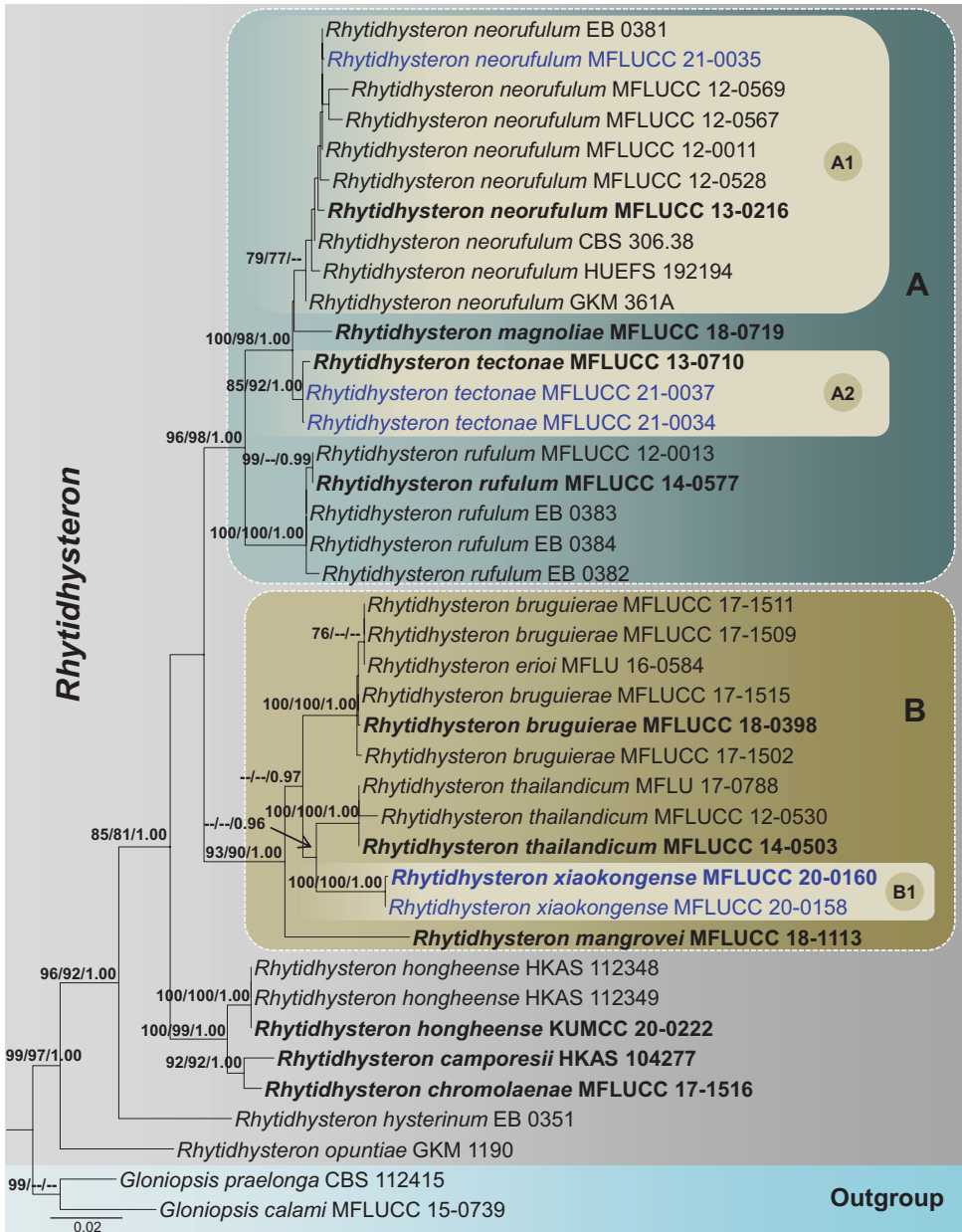


Figure 1. RAxML tree based on a combined dataset of partial SSU, LSU, ITS, and *tef1-α* sequence analyses. Bootstrap support values for ML and MP equal to or higher than 75% and Bayesian PP equal to or greater than 0.95 are shown at the nodes. Hyphens (--) represent support values less than 75% / 0.95 BYPP. The ex-type strains are in bold and the new isolate in this study is in blue. The tree is rooted with *Gloniopsis calami* (MFLUCC 15-0739) and *G. praelonga* (CBS 112415).

trees). The first 25% of sampled trees were discarded as part of the burn-in procedure, the remaining 7,501 trees were used to create the consensus tree, and the average standard deviation of split frequencies was set as 0.01. Branches with Bayesian posterior probabilities (BYPP) ≥ 0.95 are indicated above each node of the phylogenetic tree (Fig. 1). Phylogenetic trees were visualized in FigTree v1.4.0 (<http://tree.bio.ed.ac.uk/software/figtree/>; Rambaut 2012). The tree was edited using Microsoft PowerPoint before being, then saved in PDF format and finally converted to JPG format using Adobe Illustrator CS6 (Adobe Systems, USA). The finalized alignments and trees were deposited in TreeBASE, submission ID: TB2:S28620 (<http://purl.org/phylo/treebase/phylovs/study/TB2:S28620>).

Results

Phylogenetic analysis

The phylogenetic analysis was conducted using 38 strains in *Rhytidhysteron*, and two out-group taxa viz. *Gloniopsis calami* (MFLUCC 15-0739) and *G. praelonga* (CBS 112415) in Pleosporales (Table 1). The aligned sequence matrix comprised four gene regions (SSU: 1018 bp, LSU: 891 bp, ITS: 742 bp and *tef1*- α : 953 bp) and a total of 3,604 characters (including gaps), of which 3,095 characters were constant, 161 variable characters were parsimony-uninformative and 348 characters were parsimony-informative. The Kishino-Hasegawa test shows length = 928 steps with CI = 0.696, RI = 0.846, RC = 0.589 and HI = 0.304. The RAxML analysis of the combined dataset yielded a best-scoring tree with a final ML optimization likelihood value of -10181.226009. The matrix had 723 distinct alignment patterns, with 26.6% of undetermined characters or gaps. Estimated base frequencies were as follows: A = 0.242390, C = 0.244261, G = 0.276352, T = 0.236997; substitution rates AC = 1.457846, AG = 2.708684, AT = 1.298658, CG = 0.909442, CT = 6.323746, GT = 1.00; gamma distribution shape parameter $\alpha = 0.02$.

Topologies of the phylogenetic trees under ML, MP and BI criteria recovered for each gene dataset were visually compared, and the overall tree topology was similar to those obtained from the combined dataset (Figure 1). Our analyzed molecular data generated phylogeny of *Rhytidhysteron* species was consistent with those of Wanasinghe et al. (2021). The maximum likelihood tree generated based on sequence analysis of the combined (ribosomal DNA: SSU, LSU and ITS; and protein coding gene: *tef1*- α) dataset recovered three major monophyletic clades within *Rhytidhysteron* (A-C, Figure 1) and two basal lineages viz. *R. hysterinum* (EB 0351) and *R. opuntiae* (GKM 1190). Clade A comprises *Rhytidhysteron magnoliae*, *R. neorufulum*, *R. rufulum* and *R. tectonae* with 96% ML, 98% MP and 1.00 BYPP support values.

One of our new isolates, MFLUCC 21-0035 grouped with another nine *Rhytidhysteron neorufulum* strains (CBS 306.38, EB 0381, GKM 361A, HUEFS 192194,

MFLUCC 12-0011, MFLUCC 12-0528, MFLUCC 12-0567, MFLUCC 12-0569, MFLUCC 13-0216, MFLUCC 21-0035). However, this relationship is not statistically supported in Bayesian analysis, retrieving 79% and 77% support values in ML and MP, respectively (sub clade A1, Figure 1). *Rhytidhysterion magnoliae* (MFLUCC 18-0719) constitutes an independent lineage and is a sister taxon to others in sub clade A1, and this was not statistically supported.

Two newly generated sequences MFLUCC 21-0034 and MFLUCC 21-0037 grouped with the type strain of *Rhytidhysterion tectonae* (MFLUCC 13-0710) as a monophyletic clade within Clade A (subclade A2, Figure 1). This association was supported by 85% ML, 92% MP and 1.00 BYPP bootstrap values (subclade A2, Figure 1). Five strains of *Rhytidhysterion rufulum* (EB 0382, EB 0383, EB 0384, MFLUCC 12-0013, MFLUCC 14-0577) constitute another strongly monophyletic group basal to Clade A.

Two of our newly generated sequences, *Rhytidhysterion xiaokongense* (KUMCC 20-0158, KUMCC 20-0160), grouped with *R. bruguierae* (MFLUCC 17-1511, MFLUCC 17-1502, MFLUCC 17-1509, MFLUCC 17-1515, MFLUCC 18-0398), *R. erioi* (MFLU 16-0584), *R. mangrovei* (MFLUCC 18-1113) and *R. thailandicum* (MFLU 17-0788, MFLUCC 12-0530, MFLUCC 14-0503). These taxa form a monophyletic clade (Clade B) in *Rhytidhysterion* with 93% ML, 91% MP and 1.00 BYPP bootstrap values. Within this clade (Clade B), *Rhytidhysterion xiaokongense* (KUMCC 20-0158 and KUMCC 20-0160) clusters together (subclade B1) with high bootstrap values (100% ML, 100% MP and 1.00 BYPP) and is sister to *Rhytidhysterion thailandicum*. However, the latter relationship was only supported by BI analysis with 0.96 BYPP.

Rhytidhysterion camporesii (HKAS104277), *R. chromolaenae* (MFLUCC 17-1516) and *R. hongheense* (HKAS112348, HKAS112349, KUMCC 20-0222) grouped as a monophyletic clade. This relationship is statistically supported with 100% ML, 99% MP and 1.00 BYPP values (Figure 1). *Rhytidhysterion hysterinum* (EB 0351) and *R. opuntiae* (GKM 1190) nested as basal lineages in *Rhytidhysterion* (Figure 1).

Taxonomy

Rhytidhysterion xiaokongense G.C. Ren & K.D. Hyde, sp. nov.

MycoBank No: 558453

Facesoffungi Number No: FoF09903

Figure 2

Etymology. The species epithet reflects the location where the species was collected.

Holotype. HKAS 112728.

Diagnosis. Similar to *R. hysterinum* and *R. rufulum*, but differs in some conidial features.

Description. *Saprobic* on woody litter of *Prunus* sp. **Sexual morph** Undetermined. **Asexual morph** *Conidiomata* 448–464 × 324–422 μm (\bar{x} = 454 × 378 μm, n = 5),

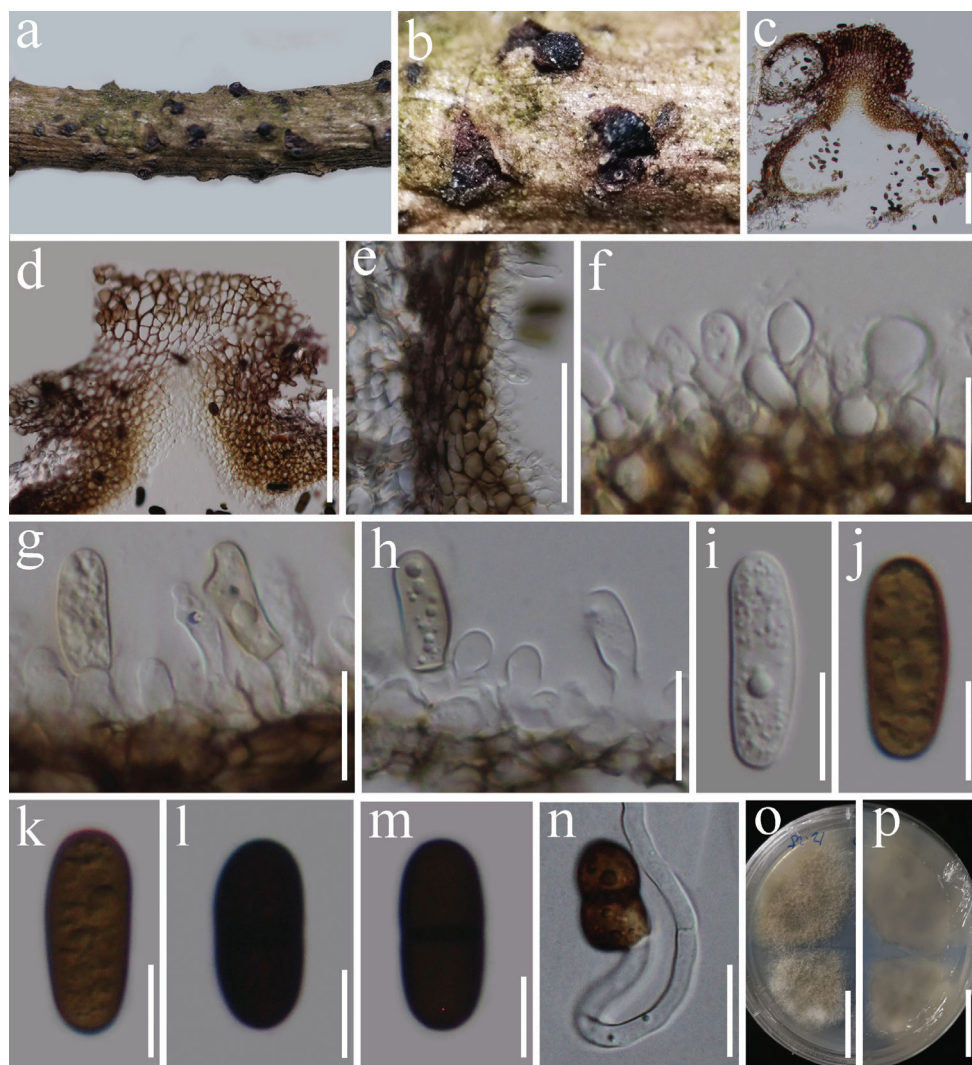


Figure 2. *Rhytidhysteron xiaokongense* (HKAS 112728, holotype) **a, b** conidiomata on natural wood surface **c** sections through conidioma **d** ostiolar neck **e** conidioma wall **f–h** conidiogenous cells and developing conidia **i–m** conidia **n** germinated conidium **o, p** culture characters on PDA (**o** = above, **p** = reverse). Scale bars: 100 μm (**c, d**); 50 μm (**e**); 15 μm (**f–h**); 10 μm (**i–m**); 20 μm (**n**); 25 mm (**o, p**).

solitary, scattered, semi-immersed in the host, black, unilocular, subglobose to ampulliform. *Ostioles* 178–227 \times 166–234 μm (\bar{x} = 205 \times 198 μm , n = 6), central, short papillate. *Conidiomata wall* 30–40 μm thick, 4–6 layers, reddish-brown to dark brown cells of *textura angularis*. *Conidiogenous cells* 5–8 \times 3–6 μm (\bar{x} = 6.8 \times 4.5 μm , n = 10), subglobose or ellipsoidal, hyaline, smooth, forming in a single layer over the entire inner surface of the wall, discrete, producing a single conidium at the apex. *Conidia* 20–25 \times 8–10 μm (\bar{x} = 22 \times 9 μm , n = 20), hyaline to yellowish-brown

when immature, becoming brown to dark brown at maturity, oblong to ellipsoidal, with rounded ends, straight to slightly curved, aseptate when immature, becoming 1-septate when mature, with granular appearance, slightly constricted at septa.

Habitat and distribution. Known to inhabit woody litter of *Prunus* sp. (Yunnan, China) (this study).

Material examined. China, Yunnan Province, Kunming city, Xiaokong Mountain (25.171311°N, 102.703690°E), on dead wood of *Prunus* sp. (Rosaceae), 21-Dec-2019, G.C. Ren, KM18 (HKAS 112728, holotype), ex-type living culture KUMCC 20-0160; KM17 (HKAS 112727, paratype), ex-paratype living culture KUMCC 20-0158.

Notes. *Rhytidhysteron xiaokongense* is similar to *R. hysterinum* and *R. rufulum* in having black, unilocular, subglobose conidiomata and dark brown, 1-septate conidia. However, some of the conidia features in these species are different: *R. xiaokongense* has oblong to ellipsoidal conidia with rounded ends, whereas the conidia of *R. rufulum* and *R. hysterinum* have a truncated base with a pore in the middle of the septum (Samuels and Müller 1979). In the phylogenetic analyses, *R. xiaokongense* is distinct from *R. rufulum* and *R. hysterinum* and is more closely related to *R. thailandicum*. *Rhytidhysteron xiaokongense* has 1-septate, dark brown, oblong to ellipsoidal conidia, while *R. thailandicum* has globose to subglobose, hyaline conidia (Thambugala et al. 2016). The sequence data from both mycelium and fruiting bodies confirms that single spore isolation was successfully performed.

***Rhytidhysteron tectonae* Doilom & K.D. Hyde, Fungal Diversity. 82: 107–182 (2017)**

MycoBank No: 551964

Facesoffungi number No: FoF01849

Figure 3

Description. *Saprobic* on decaying wood. **Sexual morph** *Hysterothecia* 550–950 µm long, 450–600 µm high, 400–500 diam. (\bar{x} = 800 × 500 × 450 µm, n = 5), semi-immersed to superficial, scattered, apothecial, erumpent from the substrate, dark brown to black, coriaceous, elongate with a longitudinal slit. *Exciple* 70–110 µm (\bar{x} = 90 µm, n = 15), thick-walled, composed of brown to dark brown cells of *textura globulosa* to *angularis*. *Hamathecium* comprising 1–2 µm wide, numerous, septate, branched, pseudoparaphyses. *Asci* 170–200 × 10–12 µm (\bar{x} = 190 × 11, n = 15), 8-spored, bitunicate, cylindrical, with short pedicel, rounded at the apex, with an ocular chamber. *Ascospores* 25–29 × 8–10 µm (\bar{x} = 27 × 9 µm, n = 20), uniseriate, hyaline to brown, 1–3-septate, smooth-walled, ellipsoidal to fusoid, straight or curved, rounded to slightly pointed at both ends, guttulate. **Asexual morph** Undetermined.

Habitat and distribution. Known to inhabit dead branches of *Tectona grandis*, *Betula* sp. (Betulaceae) and Fabaceae sp (Thailand) (Doilom et al. 2017; this study).

Material examined. Thailand, Chiang Rai Province, Mae Yao District, on dead woody twigs of *Betula* sp. (Betulaceae), 23-Sep-2019, G.C. Ren, MY09 (HKAS 115533), living culture MFLUCC 21-0037; Thailand, Chiang Rai Province, Mae Fah



Figure 3. *Rhytidhysteron tectonae* (HKAS 115533) **a, b** *Hysterothecium* on wood **c** vertical section through hysterothecia **d** exciple **e** pseudoparaphyses **f-i** immature and mature asci **j** ocular chamber. **k-r** immature and mature ascospores **s** Germinating ascospore **t, u** culture characters on PDA (**t** = above view, **u** = reverse view). Scale bars: 300 μ m (**c**); 50 μ m (**d**); 30 μ m (**e**); 50 μ m (**f-i**); 10 μ m (**j-r**); 15 μ m (**s**); 25 mm (**t, u**).

Luang University, on dead woody twigs of Fabaceae, 5-Jul-2019, G.C. Ren, RMF-LU19001 (HKAS 115532), living culture MFLUCC 21-0034.

Notes. *Rhytidhysteron tectonae* was introduced by Doilom et al. (2017) based on morphological and phylogenetic analyses from dead branches of *Tectona grandis* in Thailand. Based on our phylogenetic analysis of the combined SSU, LSU, ITS, and *tefl*- α sequence data, our collections (MFLUCC 21-0034 and MFLUCC 21-0037) cluster with the strain of *R. tectonae* (MFLUCC 13-0710) with 85% ML, 92% MP, 1.00 PP bootstrap support (Figure 1). Our collection shares similar morphological features with *R. tectonae* (MFLU 14-0607). However, our new collection has smaller hysterothecia ($800 \times 500 \times 450 \mu\text{m}$ vs $2175 \times 585 \times 523 \mu\text{m}$) and longer asci ($190 \mu\text{m}$ vs $155 \mu\text{m}$) in comparison to the type. Based on morphological characteristics and phylogenetic analysis, we introduce MFLUCC 21-0034 and MFLUCC 21-0037 as new host records of *R. tectonae* from decaying wood of *Betula* sp. and Fabaceae sp. in Thailand.

***Rhytidhysteron neorufulum* Thambugala & K.D. Hyde, Cryptog. Mycol. 37(1): 110 (2016)**

MycoBank No: 551865

Facesoffungi number No: FoF01840

Figure 4

Description. *Saprobic* on decaying wood of *Tectona grandis*. **Sexual morph** *Hysterothecia* 1400–2100 μm long, 350–500 μm high, 600–1000 μm diam. ($\bar{x} = 1780 \times 400 \times 700 \mu\text{m}$, $n = 5$), superficial, black, solitary to aggregated, coriaceous, smooth, elliptical or irregular in shape, elongated with a longitudinal slit. *Exciple* 75–115 μm ($\bar{x} = 90$, $n = 20$) wide, composed of several layers of brown to dark brown, thick-walled cells of *textura angularis*. *Hamathecium* 2–3.5 μm wide, dense, septate pseudoparaphyses, constricted at the septum, filiform, pale-yellow pigmented, forming epithecium above the asci and enclosed in a gelatinous matrix. *Asci* 190–260 \times 13–18 μm ($\bar{x} = 230 \times 16 \mu\text{m}$, $n = 10$), 8-spored, bitunicate, clavate to cylindrical, with a short furcate pedicel, apically rounded, without a distinct ocular chamber. *Ascospores* 36–44 \times 11–17 μm ($\bar{x} = 41 \times 13 \mu\text{m}$, $n = 30$), uni-seriate, yellowish to brown, with 1–3-septa, ellipsoidal to fusiform, slightly rounded or pointed at both ends, constricted at the central septum, with granular appearance. **Asexual morph** Undetermined.

Habitat and distribution. *Bursera* sp (Mexico), *Hevea brasiliensis* and *Tectona grandis* (Thailand) (Thambugala et al. 2016; Cobos-Villagran et al. 2020; this study).

Material examined. Thailand, Tak Province, Mogro District, Amphoe Umphang, on dead woods of *Tectona grandis* (Lamiaceae), 20-Aug-2019, G.C. Ren, T203 (HKAS 115534), living culture MFLUCC 21-0035.

Notes. *Rhytidhysteron neorufulum* was introduced by Thambugala et al. (2016) based on both morphological and phylogenetic analyses of a combined dataset of LSU, SSU and *tefl*- α sequence data. Thambugala et al. (2016) accounted *R. neorufulum* (MFLUCC 13-0216) from decaying woody stems and twigs in Thailand. Our new collection shares similar morphology to that of the type description of *Rhytidhysteron neorufulum*

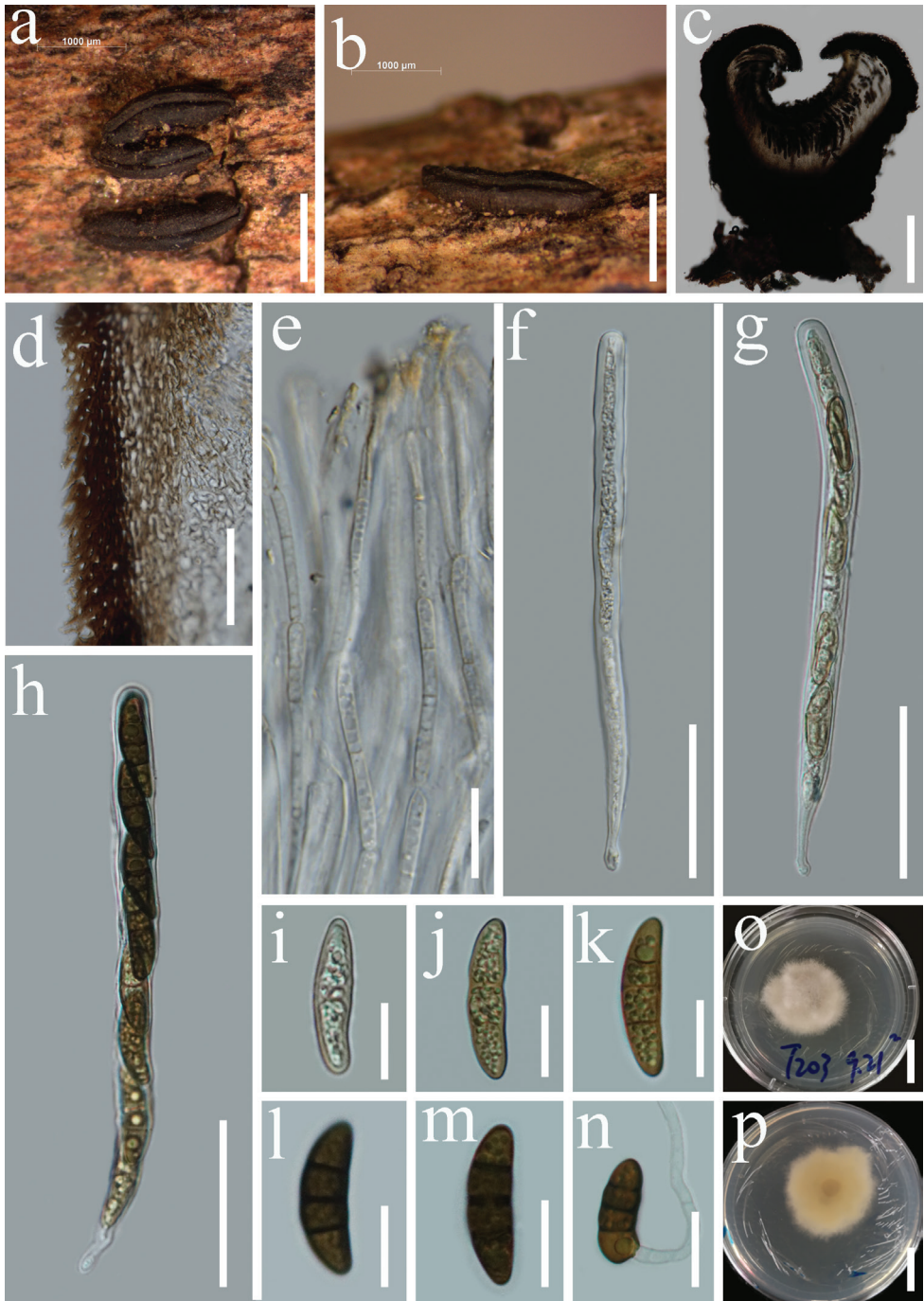


Figure 4. *Rhytidhysteron neorufulum* (HKAS 115534) **a, b** *Hysterothecium* on wood **c** vertical section through hysterothecia **d** exciple **e** pseudoparaphyses **f-h** immature asci and mature asci **i-m** immature ascospores and mature ascospores **n** germinating ascospore **o, p** culture characters on PDA (**o** = above view, **p** = reverse view). Scale bars: 1000 μ m (**a, b**); 200 μ m (**c**); 15 μ m (**d**); 20 μ m (**e**); 50 μ m (**f-h**); 10 μ m (**i-m**); 20 μ m (**n**); 20 mm (**o, p**).

(MFLUCC 13-0216) in having superficial, coriaceous, elliptical or irregular, elongated hysterothecia with a longitudinal slit, bitunicate, cylindrical, short furcate pedicel asci and yellowish to brown, ellipsoidal to fusiform ascospores with 1–3-septa (Thambugala et al. 2016). However, our new collection has larger asci (190–260 × 13–18 µm vs 185–220 × 9.5–13 µm) and ascospores (36–44 × 11–17 µm vs 19–31 × 8–13 µm) in comparison to the type of *Rhytidhysterion neurufulum* (MFLUCC 13-0216). The multi-gene phylogenetic analysis based on combined SSU, LSU, ITS, and *tefl-α* sequence data showed that our collection is related to *Rhytidhysterion neurufulum* (Figure 1).

Key to asexual morphs of *Rhytidhysterion* species

- | | | |
|---|--|------------------------|
| 1 | Asexual morph has two types of conidia..... | 2 |
| – | Asexual morph has only one type of conidia | 3 |
| 2 | Comprising paraphyses..... | <i>R. hysterinum</i> |
| – | Paraphyses are absent..... | <i>R. rufulum</i> |
| 3 | Diplodia-like conidia | <i>R. xiaokongense</i> |
| – | Aposphaeria-like conidia..... | <i>R. thailandicum</i> |

Discussion

Rhytidhysterion is one of the first genera that trainee mycologists working on microfungi find in nature, as the hysterothecia are conspicuous (Hyde et al. 2020a). Species also easily germinate in culture and can easily be sequenced (Hyde et al. 2020a). Thus, it is even more remarkable that we found a new species in this study, indicating we are far from finding all species in this genus, and that more collections need be done on other continents (Hyde et al. 2020c). Most of *Rhytidhysterion* species are saprobes, which are essential for ecosystems functioning in terrestrial habitats and are commonly recognized as key biotic agents of wood decomposition, playing a vital role in carbon and nitrogen cycling in arid ecosystems, soil stability, plant biomass decomposition, and endophytic interactions with plants (Lustenhouwer et al. 2020; Dossa et al. 2021). Furthermore, *Rhytidhysterion* species have numerous antimicrobial and antifungal applications (Murillo et al. 2009; Mapook et al. 2020), and the discovery of new species provides new resources for future applied research in the field of biotechnology and industry.

Since the genus was established in 1881, a total of 24 species have been found to date, and the most commonly encountered species are *Rhytidhysterion neurufulum* and *R. rufulum*, so it might be difficult for mycologists to find new species within *Rhytidhysterion*. *Rhytidhysterion* is mainly identified via its sexual morph (Dayarathne et al. 2020; de Silva et al. 2020; Hyde et al. 2020a, b; Mapook et al. 2020; Wanasinghe et al. 2021). The asexual morphs of *Rhytidhysterion* have been reported as aposphaeria-like or diplodia-like, including *R. hysterinum* and *R. rufulum* (Samuels and Müller 1979).

Thambugala et al. (2016) confirmed the asexual-sexual morph connection for *R. thailandicum* by aposphaeria-like asexual morphs forming in culture on PDA. Herein, we found a diplodia-like asexual morph of *Rhytidhysteron* from woody litter of *Prunus* sp. in China. In comparison to the occurrence of the sexual morph of *Rhytidhysteron*, asexual morphs seldom form under natural conditions. The discovery of this new species provides an important reference for the study of the asexual morphs of *Rhytidhysteron*. Moreover, findings from this study further enrich GMS *Rhytidhysteron* species diversity.

In our phylogenetic analyses, the new species, *Rhytidhysteron xiaokongense* was basal to *R. thailandicum* (Fig. 1). Although species in *Rhytidhysteron* are morphologically similar, our new species is an asexual form of the species found in nature, so it is easy to distinguish from other species excluding the asexual forms of *R. hysterinum*, *R. rufulum* and *R. thailandicum*. *Rhytidhysteron xiaokongense* shares similar morphological characters to *R. hysterinum* and *R. rufulum* in having black, unilocular, subglobose conidiomata and dark brown, 1-septate conidia but conidial features differ (Samuels and Müller 1979). *Rhytidhysteron thailandicum* can be differentiated from *R. xiaokongense* with respects to its globose to subglobose, hyaline conidia (Thambugala et al. 2016). To further support the establishment of the new taxon as proposed by Jeewon and Hyde (2016), we examined the nucleotide differences within the ITS regions (ITS1-5.8S-ITS2) gene region. Comparison of the 507 nucleotides across the ITS regions reveals 39 bp (7.7%) differences between *Rhytidhysteron thailandicum* and *R. xiaokongense*.

Rhytidhysteron species are widely distributed throughout the globe (de Silva et al. 2020); however, they appear to be particularly abundant in Asia, where they are well studied. There is an abundance of species and collections in the Greater Mekong Subregion (China and Thailand), such as *R. brasiliense*, *R. camporesii*, *R. chromolaenae*, *R. erioi*, *R. hongbeense*, *R. hysterinum*, *R. magnoliae*, *R. mangrovei*, *R. neorufulum*, *R. tectonae* and *R. thailandicum* (Thambugala et al. 2016; Doilom et al. 2017; Soto-Medina et al. 2017; Kumar et al. 2019; Cobos-Villagran et al. 2020; Dayarathne et al. 2020; de Silva et al. 2020; Hyde et al. 2020a; Mapook et al. 2020; Wanasinghe et al. 2021). We provide morphological and phylogenetic data for three species of *Rhytidhysteron* collected from the Greater Mekong Subregion: one new species, *Rhytidhysteron xiaokongense*, as a geographical record from China, two new host records of *R. tectonae* from woody litter of *Betula* sp and Fabaceae sp, and one new host record of *R. neorufulum* from woody litter of *Tectona grandis*. Based on our current work and that of past studies (de Silva et al. 2020; Hyde et al. 2020a, b; Mapook et al. 2020; Wanasinghe et al. 2021), it is clear that species within *Rhytidhysteron* are likely cosmopolitan and not host-specific, with evidence of the same species being found on a number of different hosts. Importantly, the morphology of a single species sometimes shows slight variations under different environmental conditions, geographical regions, hosts and different life modes (Senanayake et al. 2020). It is therefore crucial to collect more species of *Rhytidhysteron* across different geographic regions and hosts, obtain more cultures and sequence data, and describe their morphology to improve knowledge of taxonomy and phylogeny.

Acknowledgements

This work was supported by the Strategic Priority Research Program of Chinese Academy of Sciences (Grant No. XDA2602020). We thank the support from the National Natural Science Foundation of China (NSFC32001296). We also would like to thank the Thailand Research Fund for the grant entitled Impact of climate change on fungal diversity and biogeography in the Greater Mekong Subregion (No. RDG6130001). Dhanushka Wanasinghe thanks the CAS President's International Fellowship Initiative (PIFI) for funding his postdoctoral research (number 2021FYB0005), the Postdoctoral Fund from Human Resources and Social Security Bureau of Yunnan Province and the National Science Foundation of China, High-End Foreign Experts" in the High-Level Talent Recruitment Plan of Yunnan Province (2021) and Chinese Academy of Sciences (grant no. 41761144055) for financial support. Austin G. Smith at World Agroforestry (ICRAF), Kunming Institute of Botany, China, is thanked for English editing.

References

- Bao DF, Hyde KD, Luo ZL, Su HY, Nalumpang S (2019) *Minutisphaera aquaticum* sp. nov. increases the known diversity of Minutisphaeraceae. *Asian Journal of Mycology* 2: 306–314. <http://doi.org/10.5943/ajom/2/1/21>
- Barr ME (1990) *Rhytidhysterion opuntiae*. *Memoirs of the New York Botanical Garden* 62: e72.
- Boehm EW, Mugambi GK, Miller AN, Huhndorf SM, Marincowitz S, Spatafora JW, Schoch CL (2009a) A molecular phylogenetic reappraisal of the Hysteriaceae, Mytiliniaceae and Gloniaceae (Pleosporomycetidae, Dothideomycetes) with keys to world species. *Studies in Mycology* 64: 49–83. <http://doi.org/10.3114/sim.2009.64.03>
- Boehm EWA, Schoch CL, Spatafora JW (2009b) On the evolution of the Hysteriaceae and Mytiliniaceae (Pleosporomycetidae, Dothideomycetes, Ascomycota) using four nuclear genes. *Mycological Research* 113: 461–479. <http://doi.org/10.1016/j.mycres.2008.12.001>
- Chevallier FF (1826) *Flore générale des environs de Paris*, vol I. Ferra Librairie-Editeur, Paris.
- Clements FE, Shear CL (1931) *The Genera of Fungi*; Hafner Publishing Co.: New York, NY, USA, 632 pp.
- Cobos-Villagrán A, Hernández-Rodríguez C, Valenzuela R, Villa-Tanaca L, Calvillo-Medina RP, Mateo-Cid LE, Martínez-Pineda M, Raymundo T (2020) The genus *Rhytidhysterion* (Dothideomycetes, Ascomycota) in Mexico. *Acta Botanica Mexicana* 127: e1675. <http://doi.org/10.21829/abm127.2020.1675>
- Dayarathne MC, Jones EBG, Maharachchikumbura SSN, Devadatha B, Sarma VV, Khongphinitbunjong K, Chomnunti P, Hyde KD (2020) Morpho-molecular characterization of microfungi associated with marine based habitats. *Mycosphere* 11: 1–188. <http://doi.org/10.5943/mycosphere/11/1/1>
- De Silva NI, Tennakoon DS, Thambugala KM, Karunarathna SC, Lumyong S, Hyde KD (2020) Morphology and multigene phylogeny reveal a new species and a new record of *Rhytidhysterion* (Dothideomycetes, Ascomycota) from China. *Asian Journal of Mycology* 3: 295–306. <http://doi.org/10.5943/ajom/3/1/4>

- Doilom M, Dissanayake AJ, Wanasinghe DN, Boonmee S, Liu JK, Bhat DJ, Taylor JE, Bahkali AH, McKenzie EHC, Hyde KD (2016) Micro fungi on *Tectona grandis* (teak) in Northern Thailand. *Fungal Diversity* 82: 107–182. <http://doi.org/10.1007/s13225-016-0368-7>
- Dong W, Wang B, Hyde KD, McKenzie EHC, Raja HA, Tanaka K, Abdel-Wahab MA, Abdel-Aziz FA, Doilom M, Phookamsak R, Hongsanan S, Wanasinghe DN, Yu XD, Wang GN, Yang H, Yang J, Thambugala KM, Tian Q, Luo ZL, Yang JB, Miller AN, Fournier J, Boonmee S, Hu DM, Nalumpang S, Zhang H (2020) Freshwater Dothideomycetes. *Fungal Diversity* 105: 319–575. <http://doi.org/10.1007/s13225-020-00463-5>
- Dossa GGO, Yang YQ, Hu W, Paudel E, Schaefer D, Yang YP, Cao KF, Xu JC, Bushley KE, Harrison RD (2021) Fungal succession in decomposing woody debris across a tropical forest disturbance gradient. *Soil Biology and Biochemistry* 155: e108142. <http://doi.org/10.1016/j.soilbio.2021.108142>
- Hall TA (1999) BioEdit: a user-friendly biological sequence alignment editor and analysis program for Windows 95/98/NT. *Nucleic Acids Symposium Series* 41: 95–98.
- Hillis DM, Bull JJ (1993) An empirical test of bootstrapping as a method for assessing confidence in phylogenetic analysis. *Systematic Biology* 42: 182–192. <http://doi.org/10.1093/sysbio/42.2.182>
- Hongsanan S, Hyde KD, Phookamsak R, Wanasinghe DN, McKenzie EHC, Sarma VV, Boonmee S, Lücking R, Bhat DJ, Liu NG, Tennakoon DS, Pem D, Karunarathna A, Jiang SH, Jones EBG, Phillips AJL, Manawasinghe IS, Tibpromma S, Jayasiri SC, Sandamali DS, Jayawardena RS, Wijayawardene NN, Ekanayaka AH, Jeewon R, Lu YZ, Dissanayake AJ, Zeng XY, Luo ZL, Tian Q, Phukhamsakda C, Thambugala KM, Dai DQ, Chethana KWT, Samarakoon MC, Ertz D, Bao DF, Doilom M, Liu JK, Pérez-Ortega S, Suija A, Senwana C, Wijesinghe SN, Konta S, Niranjana M, Zhang SN, Ariyawansa HA, Jiang HB, Zhang JF, Norphanphoun C, de Silva NI, Thiyagaraja V, Zhang H, Bezerra JDP, Miranda-González R, Aptroot A, Kashiwadani H, Harishchandra D, Sérusiaux E, Aluthmuhandiram JVS, Abeywickrama PD, Devadatha B, Wu HX, Moon KH, Gueidan C, Schumm F, Bundhun D, Mapook A, Monkai J, Chomnunti P, Suetrong S, Chaiwan N, Dayarathne MC, Yang J, Rathnayaka AR, Bhunjun CS, Xu JC, Zheng JS, Liu G, Feng Y, Xie N (2020) Refined families of Dothideomycetes: Dothideomycetidae and Pleosporomycetidae. *Mycosphere* 11: 1553–2107. <http://doi.org/10.5943/mycosphere/11/1/13>
- Hyde KD, Dong Y, Phookamsak R, Jeewon R, Bhat DJ, Jones EBG, Liu NG, Abeywickrama PD, Mapook A, Wei D, Perera RH, Manawasinghe IS, Pem D, Bundhun D, Karunarathna A, Ekanayaka AH, Bao DF, Li J, Samarakoon MC, Chaiwan N, Lin CG, Phuththacharoen K, Zhang SN, Senanayake IC, Goonasekara ID, Thambugala KM, Phukhamsakda C, Tennakoon DS, Jiang HB, Yang J, Zeng M, Huanraluek N, Liu JK, Wijesinghe SN, Tian Q, Tibpromma S, Brahmanage RS, Boonmee S, Huang SK, Thiyagaraja V, Lu YZ, Jayawardena RS, Dong W, Yang EF, Singh SK, Singh SM, Rana S, Lad SS, Anand G, Devadatha B, Niranjana M, Sarma VV, Liimatainen K, Aguirre-Hudson B, Niskanen T, Overall A, Alvarenga RLM, Gibertoni TB, Pfliegler WP, Horváth E, Imre A, Alves AL, da Silva Santos AC, Tiago PV, Bulgakov TS, Wanasinghe DN, Bahkali AH, Doilom M, Elgorban AM, Maharachchikumbura SSN, Rajeshkumar KC, Haelewaters D, Mortimer PE, Zhao Q, Lumyong S, Xu J, Sheng J (2020a) Fungal diversity notes 1151–1276: taxonomic and phylogenetic contributions on genera and species of fungal taxa. *Fungal Diversity* 100: 5–277. <http://doi.org/10.1007/s13225-020-00439-5>

- Hyde KD, de Silva N, Jeewon R, Bhat DJ, Phookamsak R, Doilom M, Boonmee S, Jayawardena RS, Maharachchikumbura SSN, Senanayake IC, Manawasinghe IS, Liu NG, Abeywickrama PD, Chaiwan N, Karunarathna A, Pem D, Lin CG, Sysouphanthong P, Luo ZL, Wei DP, Wanasinghe DN, Norphanphoun C, Tennakoon DS, Samarakoon MC, Jayasiri SC, Jiang HB, Zeng XY, Li JF, Wijesinghe SN, Devadatha B, Goonasekara ID, Brahmanage RS, Yang EF, Aluthmuhandiram JVS, Dayarathne MC, Marasinghe DS, Li WJ, Dissanayake LS, Dong W, Huanraluek N, Lumyong S, Liu JK, Karunarathna SC, Jones EBG, Al-Sadi AM, Xu JC, Harishchandra D, Sarma VV (2020b) AJOM new records and collections of fungi: 1–100. *Asian Journal of Mycology* 3: 22–294 <http://doi.org/10.5943/ajom/3/1/3>
- Hyde KD, Jeewon R, Chen YJ, Bhunjun CS, Calabon MS, Jiang HB, Lin CG, Norphanphoun C, Sysouphanthong P, Pem D, Tibpromma S, Zhang Q, Doilom M, Jayawardena RS, Liu JK, Maharachchikumbura SSN, Phukhamsakda C, Phookamsak R, Al-Sadi AM, Naritsada Thongklang N, Wang Y, Gafforov Y, Jones EBG, Lumyong S (2020c) The numbers of fungi: is the descriptive curve flattening? *Fungal Diversity* 103: 219–271. <http://doi.org/10.1007/s13225-020-00458-2>
- Hyde KD, Hongsanan S, Jeewon R, Bhat DJ, McKenzie EHC, Jones EBG, Phookamsak R, Ariyawansa HA, Boonmee S, Zhao Q, Abdel-Aziz FA, Abdel-Wahab MA, Banmai S, Chomnunti P, Cui BK, Daranagama DA, Das K, Dayarathne MC, de Silva NI, Dissanayake AJ, Doilom M, Ekanayaka AH, Gibertoni TB, Góes- Neto A, Huang SK, Jayasiri SC, Jayawardena RS, Konta S, Lee HB, Li WJ, Lin CG, Liu JK, Lu YZ, Luo ZL, Manawasinghe IS, Manimohan P, Mapook A, Niskanen T, Norphanphoun C, Papizadeh M, Perera RH, Phukhamsakda C, Richter C, Santiago ALCMA, Drechsler-Santos ER, Senanayake I, Tanaka K, Tennakoon TMDS, Thambugala KM, Tian Q, Tibpromma S, Thongbai B, Vizzini A, Wanasinghe DN, Wijayawardene NN, Wu HX, Ynag J, Zeng XY, Zhang H, Zhang JF, Bulgakov TS, Camporesi E, Bahkali AH, Amoozegar MA, Araujo-Neta LS, Ammirati JF, Baghela A, Bhatt RP, Bojantchev D, Buyck B, da Silva GA, de Lima CLF, de Oliveira RJV, de Souza CAF, Dai YC, Dima B, Duong TT, Ercole E, Mafalda-Freire F, Ghosh A, Hashimoto A, Kamolhan S, Kang JC, Karunarathna SC, Kirk PM, Kytövuori I, Lantieri A, Liimatainen K, Liu ZY, Liu XZ, Lücking R, Medardi G, Mortimer PE, Nguyen TTT, Promputtha I, Raj KNA, Reck MA, Lumyong S, Shahzadeh-Fazeli SA, Stadler M, Soudi MR, Su HY, Takahashi T, Tangthirasunun N, Uniyal P, Wang Y, Wen TC, Xu JC, Zhang ZK, Zhao YC, Zhou JL, Zhu L (2016) Fungal diversity notes 367–490: taxonomic and phylogenetic contributions to fungal taxa. *Fungal Diversity* 80: 1–270. <http://doi.org/10.1007/s13225-016-0373-x>
- Jayasiri SC, Hyde KD, Jones EBG, McKenzie EHC, Jeewon R, Phillips AJL, Bhat DJ, Wanasinghe DN, Liu JK, Lu YZ, Kang JC, Xu J, Karunarathna SC (2019) Diversity, morphology and molecular phylogeny of Dothideomycetes on decaying wild seed pods and fruits. *Mycosphere* 10: 1–186. <http://doi.org/10.5943/mycosphere/10/1/1>
- Jeewon R, Hyde KD (2016) Establishing species boundaries and new taxa among fungi: recommendations to resolve taxonomic ambiguities. *Mycosphere* 7: 1669–1677. <http://doi.org/10.5943/mycosphere/7/1/1/4>
- Katoh K, Rozewicki J, Yamada KD (2019) MAFFT online service: multiple sequence alignment, interactive sequence choice and visualization. *Briefings in bioinformatics* 20: 1160–1166. <http://doi.org/10.1093/bib/bbx108>

- Kumar V, Cheewangkoon R, Thambugala KM, Jones GEB, Brahmanage RS, Doilom M, Jeewon R, Hyde KD (2019) *Rhytidhysteron mangrovei* (Hysteriaceae), a new species from mangroves in Phetchaburi Province, Thailand. *Phytotaxa* 401: 166–178. <http://doi.org/10.11646/phytotaxa.401.3.2>
- Kutorga E, Hawksworth DL (1997) A re-assessment of the genera referred to the family Patellariaceae (Ascomycota). *Systema Ascomycetum* 15: 1–110.
- Li H, Guo J, Karunaratna SC, Ye L, Xu J, Hyde KD, Mortimer PE (2018) Native Forests Have a Higher Diversity of Macrofungi Than Comparable Plantation Forests in the Greater Mekong Subregion. *Forests* 9: e402. <http://doi.org/10.3390/f9070402>
- Luo Z, Hyde KD, Bhat DJ, Jeewon R, Maharachchikumbura SSN, Bao DF, Li WL, Su XJ, Yang XY, Su HY (2018) Morphological and molecular taxonomy of novel species Pleurotheciaceae from freshwater habitats in Yunnan, China. *Mycological Progress* 17: 511–530. <http://doi.org/10.1007/s11557-018-1377-6>
- Lustenhauer N, Maynard DS, Bradford MA, Lindner DL, Oberle B, Zanne AE, Crowther TW (2020) A trait-based understanding of wood decomposition by fungi. *Proceedings of the National Academy of Sciences* 117: 11551–11558. <https://doi.org/10.1073/pnas.1909166117>
- Monkai J, Boonmee S, Ren GC, Wei DP, Phookamsak R, Mortimer PE (2020) *Distoseptispora hydei* sp. nov. (Distoseptisporaceae), a novel lignicolous fungus on decaying bamboo in Thailand. *Phytotaxa* 459: 093–107. <http://doi.org/10.11646/phytotaxa.459.2.1>
- Monkai J, Wanasinghe DN, Jeewon R, Promputtha I, Phookamsak R (2021) Morphological and phylogenetic characterization of fungi within Bambusicolaceae: introducing two new species from the Greater Mekong Subregion. *Mycological Progress* 20: 721–732. <http://doi.org/10.1007/s11557-021-01694-9>
- Mapook A, Hyde KD, McKenzie EHC, Jones EBG, Bhat DJ, Jeewon R, Stadler M, Samarakoon MC, Malaithong M, Tanunchai B, Buscot F, Wubet T, Purahong W (2020) Taxonomic and phylogenetic contributions to fungi associated with the invasive weed *Chromolaena odorata* (Siam weed). *Fungal Diversity* 101: 1–175. <http://doi.org/10.1007/s13225-020-00444-8>
- Murillo C, Albertazzi FJ, Carranza J, Lumbsch HT, Tamayo G (2009) Molecular data indicate that *Rhytidhysteron rufulum* (ascomycetes, Patellariales) in Costa Rica consists of four distinct lineages corroborated by morphological and chemical characters. *Mycological Research* 113: 405–16. <http://doi.org/10.1016/j.mycres.2008.09.003>
- Mugambi GK, Huhndorf SM (2009) Parallel evolution of hysterothecial ascomata in ascolocularous fungi (Ascomycota, Fungi). *Systematics and Biodiversity* 7: 453–464. <http://doi.org/10.1017/S147720000999020X>
- Miller MA, Pfeiffer W, Schwartz T (2010) Creating the CIPRES Science Gateway for inference of large phylogenetic trees. In: *Proceedings of the Gateway Computing Environments Workshop (GCE)*. New Orleans, LA, 1–8. <http://doi.org/10.1109/GCE.2010.5676129>
- Niranjan M, Tiwari S, Baghela A, Sarma VV (2018) New records of Ascomycetous fungi from Andaman Islands, India and their molecular sequence data. *Current Research in Environmental & Applied Mycology* 8: 331–350. <http://doi.org/10.5943/cream/8/3/5>
- Nylander JAA, Wilgenbusch JC, Warren DL, Swofford DL (2008) AWTY: a system for graphical exploration of MCMC convergence in Bayesian phylogenetics. *Bioinformatics* 24: 581–583. <http://doi.org/10.1093/bioinformatics/btm388>

- Pem D, Hongsanan S, Doilom M, Tibpromma S, Wanasinghe DN, Dong W, Ningguo L, Phookamsak R, Phillips AJL, Jeewon R, Hyde KD (2019) <https://www.dothideomycetes.org>: An online taxonomic resource for the classification, identification, and nomenclature of Dothideomycetes. *Asian Journal of Mycology* 2: 287–297. <http://doi.org/10.5943/ajom/2/1/19>
- Rambaut A (2012) FigTree version 1.4.0. <http://tree.bio.ed.ac.uk/software/figtree> [Accessed 1 May 2020]
- Rannala B, Yang Z (1996) Probability distribution of molecular evolutionary trees: a new method of phylogenetic inference. *Journal of Molecular Evolution* 43: 304–311. <http://doi.org/10.1007/BF02338839>
- Rehner SA, Buckley E (2005) A *Beauveria* phylogeny inferred from nuclear ITS and EF1- α sequences: evidence for cryptic diversification and links to *Cordyceps* teleomorphs. *Mycologia* 97: 84–98. <http://doi.org/10.1080/15572536.2006.11832842>
- Ronquist F, Huelsenbeck JP (2003) MrBayes 3: Bayesian phylogenetic inference under mixed models. *Bioinformatics* 19: 1572–1574. <http://doi.org/10.1093/bioinformatics/btg180>
- Ronquist F, Teslenko M, van der Mark P, Ayres DL, Darling A, Höhna S, Larget B, Liu L, Suchard MA, Huelsenbeck JP (2012) MrBayes 3.2: efficient Bayesian phylogenetic inference and model choice across a large model space. *Systematic Biology* 61: 539–542. <http://doi.org/10.1093/sysbio/sys029>
- Samuels GJ, Müller E (1979) Life-history studies of Brazilian ascomycetes. 7. *Rhytidhysterion rufulum* and the genus *Eutrybliidiella*. *Sydowia* 32: 277–292.
- Senanayake IC, Rathnayaka AR, Marasinghe DS, Calabon MS, Gentekaki E, Lee HB, Hurdeal VG, Pem D, Dissanayake LS, Wijesinghe SN, Bundhun D, Nguyen TT, Goonasekara ID, Abeywickrama PD, Bhunjun CS, Jayawardena RS, Wanasinghe DN, Jeewon R, Bhat DJ, Xiang MM (2020) Morphological approaches in studying fungi: collection, examination, isolation, sporulation and preservation. *Mycosphere* 11: 2678–2754. <http://doi.org/10.5943/mycosphere/11/1/20>
- Soto EM, Lücking R (2017) A new species of *Rhytidhysterion* (Ascomycota: Patellariaceae) from Colombia, with a provisional working key to known species in the world Artículo original. *Revista de la Academia Colombiana de Ciencias Exactas, Físicas y Naturales* 41: 59–63. <http://doi.org/10.18257/raccefyn.423>
- Spegazzini C (1881) Fungi argentini additis nonnullis brasiliensibus montevidensibusque. *Pugillus quartus* (Continuacion). *An Soc Cient Argent* 12: 174–189.
- Species Fungorum (2021) Species Fungorum. <http://www.speciesfungorum.org/Names/Names.asp>
- Stamatakis A (2014) RAxML Version 8: A tool for Phylogenetic Analysis and Post-Analysis of Large Phylogenies. *Bioinformatics* 30: 1312–1313. <http://doi.org/10.1093/bioinformatics/btu033>
- Swofford DL (2002) PAUP: phylogenetic analysis using parsimony, version 4.0 b10. Sinauer Associates, Sunderland, 56(9): 1776–1778. <http://doi.org/10.1111/j.0014-3820.2002.tb00191.x>
- Thambugala KM, Hyde KD, Eungwanichayapant PD, Romero AI, Liu ZY (2016) Additions to the Genus *Rhytidhysterion* in Hysteriaceae. *Cryptogamie, Mycologie* 37: 99–116. <http://doi.org/10.7872/crym/v37.iss1.2016.99>
- Thompson JD, Gibson TJ, Plewniak F, Jeanmougin F, Higgins DG (1997) The ClustalX windows interface: flexible strategies for multiple sequence alignment aided by quality analysis tools. *Nucleic Acids Research* 24: 4876–4882. <https://doi.org/10.1093/nar/25.24.4876>

- Vilgalys R, Hester M (1990) Rapid genetic identification and mapping of enzymatically amplified ribosomal DNA from several *Cryptococcus* species. *Journal of Bacteriology* 172: 4238–4246. <http://doi.org/10.1128/jb.172.8.4238-4246.1990>
- Wanasinghe DN, Wijayawardene NN, Xu JC, Cheewangkoon R, Mortimer PE (2020) Taxonomic novelties in Magnolia-associated pleosporalean fungi in the Kunming Botanical Gardens (Yunnan, China). *PLoS ONE* 15: e0235855. <http://doi.org/10.1371/journal.pone.0235855>
- Wanasinghe DN, Mortimer PE, Xu J (2021) Insight into the systematics of microfungi colonizing dead woody twigs of *Dodonaea viscosa* in Honghe (China). *Journal of Fungi* 7: e180. <http://doi.org/10.3390/jof7030180>
- White TJ, Bruns T, Lee S, Taylor JW (1990) Amplification and direct sequencing of fungal ribosomal RNA genes for phylogenetics. *PCR protocols: A Guide to Methods and Applications*. Academic Press, San Diego, 315–322. <http://doi.org/10.1016/B978-0-12-372180-8.50042-1>
- Wijayawardene NN, Hyde KD, Al-Ani LKT, Tedersoo L, Haelewaters D, Rajeshkumar KC, Zhao RL, Aptroot A, Leontyev DV, Saxena RK, Tokarev YS, Dai DQ, Letcher PM, Stephenson SL, Ertz D, Lumbsch HT, Kukwa M, Issi IV, Madrid H, Phillips AJL, Selbmann L, Pfliegler WP, Horváth E, Bensch K, Kirk PM, Kolaříková K, Raja HA, Radek R, Papp V, Dima V, Ma J, Malosso E, Takamatsu S, Rambold G, Gannibal PB, Triebel D, Gautam AK, Avasthi S, Suetrong S, Timdal E, Fryar SC, Delgado G, Réblová M, Doilom M, Dolatabadi S, Pawłowska JZ, Humber RA, Kodsueb R, Sánchez-Castro I, Goto BT, Silva DKA, de Souza FA, Oehl F, da Silva GA, Silva IR, Błaszczowski J, Jobim K, Maia LC, Barbosa FR, Fiuza PO, Divakar PK, Shenoy BD, Castañeda-Ruiz RF, Somrithipol S, Lateef AA, Karunarathna SC, Tibpromma S, Mortimer PE, Wanasinghe DN, Phookamsak R, Xu J, Wang Y, Tian F, Alvarado P, Li DW, Kušan I, Matočec N, Mešić A, Tkalčec Z, Maharachchikumbura SSN, Papizadeh M, Heredia G, Wartchow F, Bakhshi M, Boehm E, Youssef N, Hustad VP, Lawrey JD, Santiago ALCMA, Bezerra JDP, Souza-Motta CM, Firmino AL, Tian Q, Houbraken J, Hongsanan S, Tanaka K, Dissanayake AJ, Monteiro JS, Grossart HP, Suija A, Weerakoon G, Etayo J, Tsurukau A, Vázquez V, Mungai P, Damm U, Li QR, Zhang H, Boonmee S, Lu YZ, Becerra AG, Kendrick B, Brearley FQ, Motiejūnaitė J, Sharma B, Khare R, Gaikwad S, Wijesundara DSA, Tang LZ, He MQ, Flakus A, Rodriguez-Flakus P, Zhurbenko MP, McKenzie EHC, Stadler M, Bhat DJ, Liu JK, Raza M, Jeewon R, Nassonova ES, Prieto M, Jayalal RGU, Erdoğan M, Yurkov A, Schnittler M, Shchepin ON, Novozhilov YK, Silva-Filho AGS, Gentekaki E, Liu P, Cavender JC, Kang Y, Mohammad S, Zhang LF, Xu RF, Li YM, Dayarathne MC, Ekanayaka AH, Wen TC, Deng CY, Pereira OL, Navathe S, Hawksworth DL, Fan XL, Dissanayake LS, Kuhnert E, Grossart HP, Thines M (2020) Outline of Fungi and fungus-like taxa. *Mycosphere* 11: 1060–1456. <http://doi.org/10.5943/mycosphere/11/1/8>
- Yasanthika E, Dissanayake LS, Wanasinghe DN, Karunarathna SC, Mortimer PE, Samarakoon BC, Monkai J, Hyde KD (2020) *Lonicericola fuyuanensis* (Parabambusicolaceae) a new terrestrial pleosporalean ascomycete from Yunnan Province, China. *Phytotaxa* 446: 103–113. <http://doi.org/10.11646/phytotaxa.446.2.3>
- Zhaxybayeva O, Gogarten JP (2002) Bootstrap, Bayesian probability and maximum likelihood mapping: exploring new tools for comparative genome analyses. *BMC Genomics* 3: 1–4. <http://doi.org/10.1186/1471-2164-3-4>

Redelimitation of *Heteroradulum* (Auriculariales, Basidiomycota) with *H. australiense* sp. nov.

Qian-Zhu Li^{1,2,3}, Shi-Liang Liu¹, Xue-Wei Wang^{1,3}, Tom W. May⁴, Li-Wei Zhou^{1,2}

1 State Key Laboratory of Mycology, Institute of Microbiology, Chinese Academy of Sciences, Beijing, 100101, China **2** Institute of Applied Ecology, Chinese Academy of Sciences, Shenyang, 110016, China **3** University of Chinese Academy of Sciences, Beijing, 100049, China **4** Royal Botanic Gardens Victoria, Birdwood Avenue, Melbourne, 3004, Australia

Corresponding authors: Tom W. May (tom.may@rbg.vic.gov.au), Li-Wei Zhou (liwei_zhou1982@im.ac.cn)

Academic editor: R. H. Nilsson | Received 12 October 2021 | Accepted 11 January 2022 | Published 19 January 2022

Citation: Li Q-Z, Liu S-L, Wang X-W, May TW, Zhou L-W (2022) Redelimitation of *Heteroradulum* (Auriculariales, Basidiomycota) with *H. australiense* sp. nov.. MycoKeys 86: 87–101. <https://doi.org/10.3897/mycokeys.86.76425>

Abstract

Auriculariales accommodates species with diverse basidiomes and hymenophores. From morphological and phylogenetic perspectives, we perform a taxonomic study on *Heteroradulum*, a recently validated genus within the *Auriculariales*. The genus *Grammatus* is merged into *Heteroradulum*, and thus its generic type *G. labyrinthinus* is combined with *Heteroradulum* and *G. semis* is reaccepted as a member of *Heteroradulum*. *Heteroradulum australiense* is newly described on the basis of three Australian specimens. *Heteroradulum yunnanense* is excluded from this genus and its taxonomic position at the generic level is considered uncertain. Accordingly, the circumscription of *Heteroradulum* is re-delimited and the concept of this genus is adjusted by including irpicoid to poroid hymenophores and a hyphal system with clamp connections or simple septa. A key to all nine accepted species of *Heteroradulum* is presented.

Keywords

Agaricomycetes, Australia, *Grammatus*, heterobasidiomycetes, two new taxa, wood-inhabiting fungi

Introduction

Auriculariales (*Agaricomycetes*, *Basidiomycota*) is characterized by a wood-inhabiting habit and longitudinally or transversely septate basidia (Weiß and Oberwinkler 2001). While the type genus *Auricularia* Bull. and a number of additional genera accommodate “jelly fungi” with gelatinous basidiomes, some other genera in this order have tough

basidiomes with smooth, hydroid, poroid or lamellate hymenophores (Weiß and Oberwinkler 2001; Zhou and Dai 2013; Malysheva and Spirin 2017; Malysheva et al. 2018). The diverse macromorphological characters result in the taxonomy of *Auriculariales* having rarely focused on the whole order. Therefore, within this order, the intergeneric relationships, viz. their taxonomic positions at the family level, are not clear; moreover, the independence and monophyly of certain genera still needs to be addressed (Zhou and Dai 2013; Malysheva and Spirin 2017).

Weiß and Oberwinkler (2001) performed the first comprehensive phylogenetic analysis of *Auriculariales*. The redefined *Auriculariales* was composed of five well supported groups, but the monophyly of this order even as represented by limited samples was not statistically supported (Weiß and Oberwinkler 2001). With this phylogenetic frame as a main reference, the taxonomy and phylogeny of poroid and lamellate species were further explored (Miettinen et al. 2012; Zhou and Dai 2013; Sotome et al. 2014; Wu et al. 2017; Spirin et al. 2019a). In addition, the knowledge of the diversity of species with gelatinous basidiomes has been extremely enriched recently (Bandara et al. 2015; Wu et al. 2015a, b; Malysheva et al. 2018; Spirin et al. 2018, 2019b; Chen et al. 2020; Ye et al. 2020; Wang and Thorn 2021).

On the basis of morphology, the non-gelatinous species of *Auriculariales* that are resupinate with or without a narrow reflexed pileus (i.e., corticioid or stereoid) have been placed in the genera *Eichleriella* Bres., *Exidiopsis* (Bref.) Möller and *Heterochaete* Pat. (Bodman 1952; Wells 1961; Wells and Raitviir 1977, 1980). Circumscriptions of the genera changed over time, but according to Wells and Raitviir (1977, 1980) the distinguishing character of *Eichleriella* was the presence of a basal layer of thick-walled, brown hyphae, while the delimitation of *Heterochaete* relied on the presence of minute, sterile spines (hyphal pegs) on the hymenophore. With the integration of molecular data into phylogenies including these and related genera, *Hirneolina* (Pat.) Bres. and *Tremellochaete* Raitv. have been reinstated and a number of novel genera have been introduced, including *Adustochaete* Alvarenga & K.H. Larss., *Amphistereum* Spirin & Malysheva, *Crystalloodon* Alvarenga (Alvarenga and Gibertoni 2021), *Heteroradulum* Lloyd ex Spirin & Malysheva, *Proterochaete* Spirin & Malysheva and *Sclerotrema* Spirin & Malysheva (Malysheva and Spirin 2017; Alvarenga et al. 2019). After transfer of some species to these novel genera, *Eichleriella* (as far as sequenced species go) is monophyletic, but *Exidiopsis* is currently polyphyletic. The only species remaining in *Heterochaete* for which sequences are available is the type (*H. andina* Pat. & Lagerh.) and this is close to the type of *Exidiopsis* [*E. effusa* (Bref. ex Sacc.) Möller], leading Malysheva and Spirin (2017) to suggest that the two genera may be synonymous. Numerous species remain in *Heterochaete* that are yet to be sequenced, while those that have been sequenced, apart from *H. andina*, are placed in *Crystalloodon*, *Eichleriella* and *Heteroradulum*.

Heteroradulum, typified by *H. kmetii* (Bres.) Spirin & Malysheva, was validated by Malysheva and Spirin (2017), who included seven species in this genus. Later, the new genus *Grammatus* H.S. Yuan & Decock was introduced, typified by *G. labyrinthinus* H.S. Yuan & Decock, and *H. semis* was transferred to *Grammatus* (Yuan et al. 2018). However, the phylogenetic analysis of Yuan et al. (2018) did not recover a monophyletic

group for the remaining sampled species of *Heteroradulum*. Recently, *Heteroradulum yunnanense* C.L. Zhao (as 'yunnanensis') was newly described in *Heteroradulum* (Guan et al. 2020) but the phylogeny sampled only *Heteroradulum* as ingroup taxa and the analysis cannot properly determine whether *H. yunnanense*, which had a basal phylogenetic position, belongs to *Heteroradulum* or not. Therefore, questions remain about the delimitation of *Heteroradulum* from a phylogenetic perspective.

During field trips in Australia, three specimens bearing corticioid basidiomes and longitudinally septate basidia were collected. Based on these specimens, a new species of *Heteroradulum* was identified and is presented below along with a revised phylogeny of the genus and its relatives based on molecular data. This phylogenetic analysis leads to a revised circumscription of *Heteroradulum*.

Materials and methods

Morphological examination

The studied specimens are preserved at the Fungarium, Institute of Microbiology, Chinese Academy of Sciences (HMAS), Beijing, China and the National Herbarium of Victoria (MEL), Melbourne, Australia. The hymenial surfaces of basidiomes were observed and photographed with the aid of a stereomicroscope (LEICA M125). Special color terms follow Petersen (1996). Microscopic procedure followed Wang et al. (2020). A Nikon Eclipse 80i light microscope (Tokyo, Japan) was used at magnifications up to 1000 \times . Specimen sections were prepared with Cotton Blue (CB), Melzer's reagent (IKI) and 5% potassium hydroxide (KOH) for observation. All measurements were taken from materials mounted in CB. Drawings were made with the aid of a drawing tube. When presenting the variation of basidiospore sizes, 5% of the measurements were excluded from each end of the range and are given in parentheses. The following abbreviations are used in the text: L = mean basidiospore length (arithmetic average of all measured basidiospores), W = mean basidiospore width (arithmetic average of all measured basidiospores), Q = variation in the L/W ratios between the specimens studied, and (a/b) = number of basidiospores (a) measured from given number (b) of specimens.

Molecular sequencing

Crude DNA was extracted from basidiomes of dry specimens using FH Plant DNA Kit (Beijing Demeter Biotech Co., Ltd., Beijing, China), and then directly used as template for subsequent PCR amplifications. The primer pairs ITS5/ITS4 (White et al. 1990) and LR0R/LR7 (Vilgalys and Hester 1990) were selected for amplifying the ITS and nLSU regions, respectively. The PCR procedures are as follows: for the ITS region, initial denaturation at 95 °C for 3 min, followed by 34 cycles at 94 °C for 40 s, 57.2 °C for 45 s and 72 °C for 1 min, and a final extension at 72 °C for 10 min, while for the nLSU

region, initial denaturation at 94 °C for 1min, followed by 34 cycles at 94 °C for 30 s, 47.2 °C for 1 min and 72 °C for 1.5 min, and a final extension at 72 °C for 10 min. The PCR products were sequenced with the same primers as those used in amplifications at the Beijing Genomics Institute, Beijing, China. The newly generated sequences were deposited in GenBank (<https://www.ncbi.nlm.nih.gov/genbank/>; Table 1).

Table 1. Information on species and specimens used in the phylogenetic analysis. The newly generated sequences are in boldface. Type specimens are indicated with an asterisk (*).

Species	Voucher number	GenBank accession number	
		ITS	nLSU
<i>Amphistereum leveilleanum</i>	FP-106715	KX262119	KX262168
<i>A. schrenkii</i>	HHB8476	KX262130	KX262178
<i>Aporpium hexagonoides</i>	ML297	AB871754	AB871735
<i>Auricularia mesenterica</i>	FO25132	AF291271	AF291292
<i>A. mesenterica</i>	TUFC12805	AB915192	AB915191
<i>A. polytricha</i>	TUFC12920	AB871752	AB871733
<i>Basidiodendron eyrei</i>	TUFC14484	AB871753	AB871734
<i>Eichleriella bactriana</i>	TAAM55071*	KX262121	KX262170
<i>E. leucophaea</i>	LE303261	KX262111	KX262161
<i>Elmerina caryae</i>	WD2207	AB871751	AB871730
<i>E. foliacea</i>	Yuan 5691	JQ764666	JQ764644
<i>E. hispida</i>	WD548	AB871768	AB871749
	E701	AB871767	AB871748
<i>Exidia glandulosa</i>	TUFC34008	AB871761	AB871742
<i>E. glandulosa</i>	MW355	AF291273	AF291319
<i>E. pithya</i>	MW313	AF291275	AF291321
<i>Exidiopsis calcea</i>	MW331	AF291280	AF291326
<i>E. effusa</i>	OM19136	KX262145	KX262193
<i>E. grisea</i>	RoKi162	AF291281	AF291328
<i>E. grisea</i>	TUFC100049	AB871765	AB871746
<i>Exidia</i> sp.	TUFC34333	AB871764	AB871745
	FO46291	AF291282	AF291329
<i>Heteroradulum adnatum</i>	LR23453*	KX262116	KX262165
<i>H. australiense</i>	LWZ 20180512–20*	MZ325254	MZ310424
	LWZ 20180512–25*	MZ325255	MZ310425
	LWZ 20180515–26*	MZ325256	MZ310426
<i>H. deglubens</i>	FO12006	AF291272	AF291318
	LE38182	KX262112	KX262162
	LE225523	KX262113	KX262163
	TAAM064782	KX262101	KX262148
	Solheim1864	KX262133	KX262181
<i>H. kmetii</i>	Kmet*	KX262124	KX262173
	VS8858	KX262105	KX262154
	VS8864	KX262106	KX262155
	VS8981	KX262132	KX262180
	VS8988	KX262107	KX262156
	LE38181	KX262109	KX262159
	DAOM145605	KX262135	KX262183
	DAOM31292	KX262134	KX262182
	OF-295640	KX262122	KX262171
	OF-295641	KX262117	KX262166

Species	Voucher number	GenBank accession number	
		ITS	nLSU
<i>H. kmetii</i>	OF-295639	KX262128	KX262177
	VS7967	KX262108	KX262157
	TAAM9847	KX262125	KX262174
	VS6466	KX262104	KX262152
	LE303456	KX262103	KX262151
	TAAM149179	KX262102	KX262149
	CWU4563	KX262127	KX262176
	CWU6152	KX262126	KX262175
	LR14389	KX262131	KX262179
	<i>H. labyrinthinum</i>	Yuan 1759*	KM379137
Yuan 1600*		KM379139	KM379140
<i>H. semis</i>	OM10618*	KX262146	KX262194
<i>H. yunnanense</i>	CLZhao 4023*	MT215568	MT215564
	CLZhao 8106*	MT215569	MT215565
	CLZhao 9132*	MT215570	MT215566
	CLZhao 9200*	MT215571	MT215567
<i>Heteroradulum</i> sp.	USJ55639	AF291285	AF291336
<i>Hirneolina birneoloides</i>	USJ55480	AF291283	AF291334
<i>Sclerotrema griseobrunneum</i>	VS7674	KX262140	KX262188
<i>Sistotrema brinkmannii</i>	236	JX535169	JX535170
<i>Tremellochaete japonica</i>	LE303446	KX262110	KX262160

Phylogenetic analysis

Besides the newly sequenced specimens, additional taxa representing all main lineages within the *Auriculariales* were also included in the current phylogenetic analysis, and *Sistotrema brinkmannii* (Bres.) J. Erikss. within the *Cantharellales* was selected as an outgroup taxon following Malysheva and Spirin (2017) (Table 1). The datasets of ITS and nLSU regions were aligned separately using MAFFT version 7 (Katoh and Standley 2013) with the G-INS-i strategy (Katoh et al. 2005). Then, the two resulting alignments were concatenated as a single alignment for subsequent phylogenetic analysis. This alignment was submitted to TreeBASE (<http://www.treebase.org>; accession number S28342) and its best-fit evolutionary model was estimated using jModelTest (Guindon and Gascuel 2003; Posada 2008) with calculation under the Akaike information criterion. Following the resulting evolutionary model SYM + I + G, Maximum Likelihood (ML) and Bayesian Inference (BI) analyses were performed. The ML analysis was conducted using raxmlGUI 1.2 (Silvestro and Michalak 2012; Stamatakis 2006) with the calculation of bootstrap (BS) replicates under the auto FC option (Pattengale et al. 2010). The BI analysis was conducted using MrBayes 3.2 (Ronquist et al. 2012) with two independent runs, each including four chains of 10 million generations and starting from random trees. Trees were sampled every 1000th generation. The first 25% of the resulting trees was discarded as burn-in, while the remaining 75% were used for constructing a 50% majority consensus tree and calculating Bayesian posterior probabilities (BPPs). Chain convergence was determined using Tracer 1.5 (<http://tree.bio.ed.ac.uk/software/tracer/>).

Results

Three ITS and three nLSU sequences were newly generated from three Australian specimens of *Heteroradulum* for this study. The alignment used for phylogenetic analysis has 62 collections and 1583 characters. The ML analysis ended after 300 BS replicates. The BI analysis converged after 10 million generations as indicated by an average standard deviation of split frequencies = 0.004375, the effective sample sizes of all parameters above 4960 and the potential scale reduction factors equal to 1.000. The ML and BI analyses generated similar topologies in main lineages, and thus the topology generated from ML analysis is presented along with BS values above 50% and BPPs above 0.8 at the nodes (Figure 1).

The current phylogeny groups *Grammatus* and *Heteroradulum*, with the exception of *H. yunnanense*, as a strongly supported clade (BS = 94%, BPP = 1; Figure 1). Within this clade, the three newly sequenced Australian specimens grouped as a fully supported lineage, as sister to the two species formerly placed in the genus *Grammatus*, forming a strongly supported subclade (BS = 92%, BPP = 1), while the monophyly of the subclade including the remaining species of *Heteroradulum*, viz. *H. adnatum* Spirin & Malysheva, *H. deglubens* (Berk. & Broome) Spirin & Malysheva and *H. kmetii*, did not receive reliable statistical support (Figure 1). This topology means that the subclades containing the types of *Grammatus* and *Heteroradulum* respectively are not reciprocally monophyletic within the strongly supported clade. *Heteroradulum yunnanense* falls outside of the *Heteroradulum* clade as a well-supported sister to a clade comprised of three taxa currently placed in *Exidiopsis* (Figure 1).

Taxonomy

***Heteroradulum* Lloyd ex Spirin & Malysheva, in Malysheva & Spirin, Fungal Biology 121(8): 709 (2017)**

= *Grammatus* H.S. Yuan & Decock, in Yuan, Lu & Decock, MycoKeys 35: 32 (2018)

Remarks. Following the phylogenetic analysis, we treat *Grammatus* and *Heteroradulum* as a single genus, for which *Heteroradulum* has priority. The newly revealed Australian lineage is described as the new species *Heteroradulum australiense* below. In addition, *G. labyrinthinus* is combined to *Heteroradulum* and *G. semis* (Spirin & Malysheva) H.S. Yuan & Decock is reaccepted as a member of *Heteroradulum*.

Malysheva and Spirin (2017) defined the morphological characters of *Heteroradulum* according to the seven accepted species at that time, viz. *H. adnatum*, *H. brasiliense* (Bodman) Spirin & Malysheva, *H. deglubens*, *H. kmetii*, *H. lividofuscum* (Pat.) Spirin & Malysheva, *H. semis* and *H. spinulosum* (Berk. & M.A. Curtis) Spirin & Malysheva.

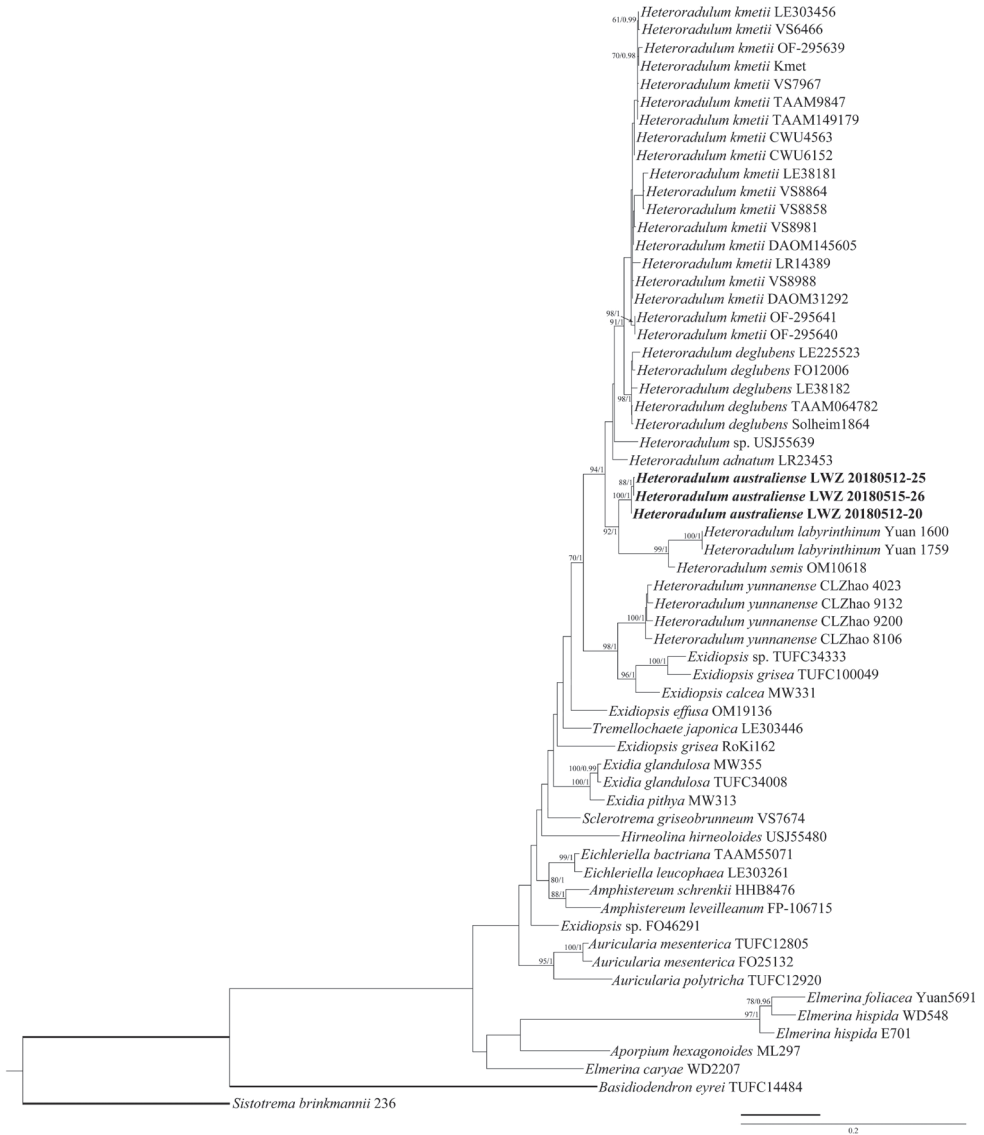


Figure 1. Phylogenetic delimitation of *Heteroradulum* within the *Auriculariales* inferred from the combined dataset of ITS and nLSU regions. The topology generated by the maximum likelihood analysis is presented along with bootstrap values and Bayesian posterior probabilities above 50% and 0.8, respectively, at the nodes. The specimens of the newly described species are in boldface.

The concept of this genus was adjusted by below including *H. australiense* with generative hyphae bearing a mixture of simple septa and clamp connections and *H. labyrinthinus* with irpicoid to poroid hymenophores.

***Heteroradulum australiense* L.W. Zhou, Q.Z. Li & S.L. Liu, sp. nov.**

MycoBank: 842485

Figures 2, 3

Etymology. *australiense* (Lat.), refers to Australia.**Type.** Australia, Tasmania, Tahune Adventures, Arve River Picnic Area, on fallen angiosperm branch, 15 May 2018, L.W. Zhou, LWZ 20180515–26 (holotype in MEL, isotype in HMAS).**Diagnosis.** *Heteroradulum australiense* differs from other species in this genus by the generative hyphae having a mixture of simple septa and clamp connections.**Description.** Basidiomes annual, resupinate, adnate, without odor or taste when fresh, leathery, covering 24.5 cm in widest dimension and up to 0.4 mm thick. Hymenophore odontoid, covered by irregularly arranged spines, up to 0.2 mm long, 3–5 per mm, pale red to reddish lilac when fresh, pale orange to brownish gray upon drying. Margin smooth, adnate, yellowish white, 0.5 mm wide.

Hyphal system dimitic; generative hyphae with simple septa or clamp connections; skeletal hyphae IKI–, CB+; tissue unchanged in KOH. Subicular generative hyphae hyaline, thin to thick-walled, rarely branched, 2–4 µm in diam; skeletal hyphae hyaline to brownish, thick-walled, interwoven, occasionally branched, 2.5–4 µm in diam, sometimes irregularly inflated up to 6 µm. Subhymenial generative hyphae hyaline to brownish, thin-to slightly thick-walled, 2–3.5 µm in diam; skeletal hyphae brownish, thick-walled, encrusted by grainy crystals, subparallel and vertical along substrate, compact, 2–4.5 µm in diam. Clavate to subcylindrical cystidia abundant, septate with or without clamp connections, thin-walled, 24–56 × 3–8 µm. Skeletocystidia present as endings of subicular skeletal hyphae, distinctly thick-walled, heavily encrusted by grainy crystals, 4–7 µm in diam. Dendrohyphidia abundant, scattered among hymenial cells, covering the hymenial surface, branched, up to 54 µm long, 2–3 µm in diam. Basidia narrowly ovoid to obconical, longitudinally septate, four-celled, 29–34.5 × 10–13.5 µm, with enucleate stalk up to 14 × 4 µm. Basidiospores cylindrical, slightly or distinctly curved, hyaline, thin-walled, smooth, occasionally with oily inclusions, IKI–, CB–, (14.5–)15–20(–20.5) × 5–7(–7.5) µm, L = 17.0 µm, W = 6.2 µm, Q = 2.66–2.88 (n = 90/3).

Specimens (paratypes) examined. Australia, Victoria, Yarra Ranges National Park, Dandenong Ranges Botanic Garden, on a fallen branch of *Eucalyptus*, 12 May 2018, L.W. Zhou, LWZ 20180512–20 (HMAS), on fallen angiosperm branch, 12 May 2018, L.W. Zhou, LWZ 20180512–25 (HMAS).**Remarks.** *Heteroradulum australiense* is characterized by pale red to reddish lilac basidiomes, a dimitic hyphal system, generative hyphae with simple septa or clamp connections, abundant skeletocystidia in the hymenium, and basidia with an enucleate stalk. *Heteroradulum kmetii* and *H. spinulosum* resemble *H. australiense* by odontoid hymenophores, a dimitic hyphal system and the presence of skeletocystidia (Malysheva and Spirin 2017). However, *H. kmetii* has longer spines (up to 1 mm long) and slightly larger basidiospores (14.3–22.3 × 6–9.2 µm), and generative hyphae always with clamp connections; and *H. spinulosum* differs by basidia with a shorter enucleate stalk (up to 6 µm long) and generative hyphae always with clamp connections (Malysheva and Spirin 2017).



Figure 2. Basidiomes of *Heteroradulum australiense*. **A–B** LWZ 20180515–26 (holotype) **C** LWZ 20180512–20 (paratype) **D** LWZ 20180512–25 (paratype). Scale bars: 2 mm (**A**); 1 cm (**B–D**).

In regard to previously described Australian species against which *H. australiense* should be compared, the coriaceous, resupinate species of the *Auriculariales* are poorly sampled from Australia. May et al. (2003) listed records from Australia of a number of species of *Eichleriella*, *Exidiopsis* and *Heterochaete* that were originally described from the Northern Hemisphere. Such records remain suspect unless confirmed. Only two new species have been described on the basis of type materials from Australia that may fall within these three genera: *Heterochaete cheesmanii* Wakef. and *Irpex depauperatus* Masee.

Heterochaete cheesmanii was described by Wakefield (1915) from a collection on wood from New South Wales, characterized by the thin, orbicular basidiomes with a shortly reflexed margin, the pale hymenium with sparse, minute spines, the soft fulvous context, with 4-spored, cruciate basidia $15 \times 10\text{--}12 \mu\text{m}$, and curved, cylindrical spores, $14\text{--}15 \times 5\text{--}5.5 \mu\text{m}$, and hyphae $1.5\text{--}4 \mu\text{m}$ diameter. Reid (1957) examined the type at K and noted the presence of “conspicuous branched paraphyses”. *Heterochaete cheesmanii* differs from *H. australiense* by the shorter basidiospores. It will be necessary to obtain sequences from *H. cheesmanii* to ascertain its correct generic placement, but it could well be a member of *Heteroradulum*.

Irpex depauperatus was introduced by Masee (1901) with a short description, based on a collection on dead bark by Rodway from Tasmania. Note that due to existence of the previously described *Irpex depauperatus* Berk. & Broome, the replacement name *Irpex tasmanicus* Syd. & P. Syd. was introduced for *I. depauperatus* Masee. According to Masee (1901), *Irpex depauperatus* Masee was characterized by the tawny hymenium with short, laterally incised spines forming orbicular then confluent patches with a

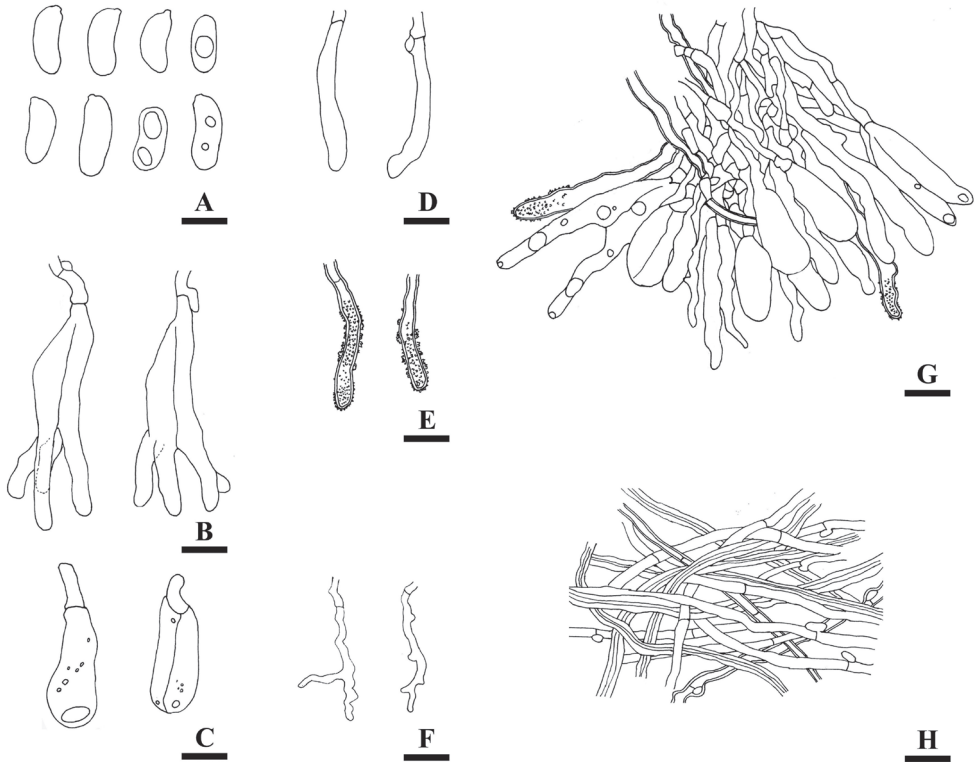


Figure 3. Microscopic structures of *Heteroradulum australiense* (drawn from the holotype, LWZ 20180515–26). **A** basidiospores **B, C** basidia and basidioles **D** cystidia **E** skeletocystidia **F** dendrohyphidia **G** hymenium **H** subicular hyphae. Scale bars: 10 μm (**A–H**).

white edge and basidiospores of $6 \times 3\text{--}4 \mu\text{m}$. No comparison against other species was provided in the protologue. Both Bodman (1952) and Reid (1957) placed *I. depauperatus* as a synonym of other species. Without examining the type, Bodman (1952) listed *I. depauperatus* as a possible synonym of *Heterochaete delicata* (Klotzsch) Bres. However, Reid (1957) considered that *I. depauperatus* was a synonym of *Eichleriella spinulosa* (Berk. & M.A. Curtis) D.A. Reid (basionym *Radulum spinulosum* Berk. & M.A. Curtis, now accepted as *Heteroradulum spinulosum*). Reid (1957) provided a description of *E. spinulosa* (with *I. depauperatus* listed as synonym) that is evidently based on the cited Australian specimen (*Miller s.n.*, K, Herb. F.P.S.M. No. 4996). Despite the fact that Masee (1901) originally described *I. depauperatus* as having basidiospores of $6 \times 3\text{--}4 \mu\text{m}$, Reid (1957) found that the type at K has basidiospores of $19 \times 7 \mu\text{m}$, matching the basidiospores from the Australian collection by Miller in 1954, but he did not provide any further details of the characters of the type collection of *I. depauperatus*.

Irpex depauperatus potentially belongs in *Heteroradulum* but due to slight morphological differences between species such as *H. australiense* and *H. spinulosum*, and the potential for further species to occur in the region, DNA sequences would be ideal to assist in interpretation of the old name. However, it is unlikely to be able

to readily obtain DNA from the more than 100-year old type of *Irpex depauperatus*, which is borne out by unsuccessful attempts to amplify ITS and LSU sequences from several Australian collections in MEL filed under *Heterochaete*, collected in the 1950s and 1960s. Collections for which DNA amplification was unsuccessful included MEL 2313650 (which is a duplicate of the K collection *Miller s.n.*, Herb. F.P.S.M. No. 4996). The morphology of *Miller s.n.* as recorded by Reid (1957) matches *H. australiense* in basidiospore size and shape and presence of skeletocystidia. However, the connection between this collection and the type of *Irpex depauperatus* is not definite, as only basidiospore dimensions of the latter were provided by Reid (1957). It remains possible that *Irpex tasmanicus* (= *I. depauperatus*) represents an earlier name for *Heteroradulum australiense*. Given the lack of a sequence from the type and the meagre morphological details available, we choose to introduce a new species, well-characterized by the combination of morphology and sequence data. Perhaps with the application of next generation sequencing, it may become possible to recover sequences from older types more routinely as has been done already in some cases, such as by Delgat et al. (2019).

***Heteroradulum labyrinthinum* (H.S. Yuan & C. Decock) L.W. Zhou, comb. nov.**
MycoBank: 842486

Basionym. *Grammatus labyrinthinus* H.S. Yuan & Decock, in Yuan, Lu & Decock, MycoKeys 35: 32 (2018)

Remarks. *Heteroradulum labyrinthinum* was placed in the new genus *Grammatus* as the generic type (Yuan et al. 2018). The main reason for introducing *Grammatus* was its irregularly irpicoid to poroid hymenophores, from a morphological perspective (Yuan et al. 2018). However, the morphological difference of hymenophores is not a reliable taxonomic character at the generic level within the *Auriculariales*. For example, *Protomerulius* Möller was recently shown to accommodate species with various kinds of hymenophore (Spirin et al. 2019a). This phenomenon also occurs in other groups of wood-inhabiting fungi (Wang et al. 2021). Moreover, taking the current phylogenetic evidence into consideration (Figure 1), we propose to treat *Grammatus* as a later synonym of *Heteroradulum*. Therefore, *G. labyrinthinus* is transferred to *Heteroradulum*, and *Heteroradulum semis*, that was moved to *Grammatus* (Yuan et al. 2018), is reaccepted as a member of *Heteroradulum*.

Species excluded from *Heteroradulum*

***Heteroradulum yunnanense* C.L. Zhao [as ‘yunnanensis’], in Guan, Liu, Zhao & Zhao, Phytotaxa 437(2): 57 (2020)**

Remarks. *Heteroradulum yunnanense* has a white to gray hymenophore and colorless hyphae (Guan et al. 2020), which do not fit well with the concept of *Heteroradulum* sensu Malysheva and Spirin (2017). According to the current phylogenetic evidence, we propose to exclude *H. yunnanense* from *Heteroradulum*.

A key to species of *Heteroradulum*

1	Hymenophore irpicoid to poroid.....	<i>H. labyrinthinum</i>
–	Hymenophore grandinioid to odontoid.....	2
2	Hyphal system monomitic.....	3
–	Hyphal system dimitic.....	4
3	Basidiospores up to 14.2 µm long.....	<i>H. adnatum</i>
–	Basidiospores up to 20.4 µm long.....	<i>H. deglubens</i>
4	Basidiomes perennial.....	<i>H. kmetii</i>
–	Basidiomes annual.....	5
5	Skeletocystidia present.....	6
–	Skeletocystidia absent.....	7
6	Generative hyphae septa with or without clamp connections....	<i>H. australiense</i>
–	Generative hyphae septa with clamp connections.....	<i>H. spinulosum</i>
7	Cystidia absent.....	<i>H. brasiliense</i>
–	Cystidia present.....	8
8	Basidiospores more than 15 µm long.....	<i>H. lividofuscum</i>
–	Basidiospores less than 15 µm long.....	<i>H. semis</i>

Discussion

In this study, the circumscription of *Heteroradulum* is emended by merging the genus *Grammatus*, adding the newly described species *H. australiense* and excluding the species *H. yunnanense*.

Recently, the concept of *Protomerulius*, another genus of the *Auriculariales*, was redefined to accommodate species bearing smooth, poroid and spiny hymenophores (Spirin et al. 2019a). The merging of *Grammatus* into *Heteroradulum* further indicates that while hymenophoral characters may be used to distinguish species they are not reliable characters at genera rank within the *Auriculariales*. In the case of the highly diverse macromorphological characters of species within the *Auriculariales*, the generic and, especially, familial delimitations should be cautiously explored with the aid of as comprehensive phylogenetic samplings as possible. Ideally, the construction of an order-level phylogenetic framework with wider taxon sampling and multimarker sequencing will help exactly clarify the higher-level relationships.

Heteroradulum yunnanense was placed in *Heteroradulum* based on a quite simple phylogeny with limited samples (Guan et al. 2020). Guan et al. (2020) stated that *H. yunnanense* grouped together with *H. adnatum*, but it actually was separated from all sampled species of *Heteroradulum*. The improper selection of outgroup taxa and absence of additional ingroup taxa lead to the inaccurate taxonomic placement of *H. yunnanense*. In the current phylogeny, *H. yunnanense* has a closer relationship with *Exidiopsis calcea* (Pers.) K. Wells, *E. grisea* (Bres.) Bourdot & Maire (TUFC100049) and an unnamed taxon of *Exidiopsis* (Figure 1). However, the generic type of *Exidiopsis*, *E. effusa*, is separated from

the three so-called taxa of *Exidiopsis*. Consequently, it is premature to transfer *H. yunnanense* to another genus at this stage, but it clearly does not belong in *Heteroradulum*. A wider sampling of species related to *H. yunnanense* and disposition of species of *Exidiopsis* not conspecific with the type is needed to reveal its taxonomic position at a generic level.

Acknowledgements

The research was financed by the National Natural Science Foundation of China (Project Nos. 31970012 & 31770008).

References

- Alvarenga RLM, Gibertoni TB (2021) *Crystallodon* Alvarenga gen. nov., a new genus of the Auriculariales from the Neotropics. *Cryptogamie Mycologie* 42: 17–24. <https://doi.org/10.5252/cryptogamie-mycologie2021v42a2>
- Alvarenga RLM, Spirin V, Malysheva V, Gibertoni TB, Larsson KH (2019) Two new genera and six other novelties in *Heterochaete* sensu lato (Auriculariales, Basidiomycota). *Botany* 97: 439–451. <https://doi.org/10.1139/cjb-2019-0046>
- Bandara A, Chen J, Karunarathna S, Hyde KD, Kakumyan P (2015) *Auricularia thailandica* sp. nov. (Auriculariaceae, Auriculariales) a widely distributed species from Southeastern Asia. *Phytotaxa* 208: 147–156. <http://doi.org/10.11646/phytotaxa.208.2.3>
- Bodman MC (1952) A taxonomic study of the genus *Heterochaete*. *Lloydia* 15: 193–233.
- Chen YL, Su MS, Zhang LP, Zou Q, Wu F, Zeng NK, Liu M (2020) *Pseudohydnum brunneiceps* (Auriculariales, Basidiomycota), a new species from Central China. *Phytotaxa* 441: 87–94. <https://doi.org/10.11646/phytotaxa.441.1.8>
- Delgat L, Dierickx G, De Wilde S, Angelini C, De Crop E, De Lange R, Halling R, Manz C, Nuytinck J, Verbeken A (2019) Looks can be deceiving: the deceptive milkcaps (*Lactifluus*, Russulaceae) exhibit low morphological variance but harbour high genetic diversity. *IMA Fungus* 10: e14. <https://doi.org/10.1186/s43008-019-0017-3>
- Guan QX, Liu CM, Zhao TJ, Zhao CL (2020) *Heteroradulum yunnanensis* sp. nov. (Auriculariales, Basidiomycota) evidenced by morphological characters and phylogenetic analyses in China. *Phytotaxa* 437: 51–59. <https://doi.org/10.11646/phytotaxa.437.2.1>
- Guindon S, Gascuel O (2003) A simple, fast and accurate algorithm to estimate large phylogenies by maximum likelihood. *Systematic Biology* 52: 696–704. <https://doi.org/10.1080/10635150390235520>
- Katoh K, Kuma K, Toh H, Miyata T (2005) MAFFT version 5: improvement in accuracy of multiple sequence alignment. *Nucleic Acids Research* 33: 511–518. <https://doi.org/10.1093/nar/gki198>
- Katoh K, Standley DM (2013) MAFFT multiple sequence alignment software version 7: improvements in performance and usability. *Molecular Biology and Evolution* 30: 772–780. <https://doi.org/10.1093/molbev/mst010>

- Malysheva V, Spirin V (2017) Taxonomy and phylogeny of the *Auriculariales* (Agaricomycetes, Basidiomycota) with stereoid basidiocarps. *Fungal Biology* 121: 689–715. <http://doi.org/10.1016/j.funbio.2017.05.001>
- Malysheva V, Spirin V, Miettinen O, Motato-Vásquez V, Hernawati, Seelan JSS, Larsson KH (2018) Revision of *Protohydnum* (Auriculariales, Basidiomycota). *Mycological Progress* 17: 805–814. <https://doi.org/10.1007/s11557-018-1393-6>
- Massee G (1901) Fungi exotici, III. *Bulletin of Miscellaneous Information* 1901: 150–169. <https://doi.org/10.2307/4114928>
- May TW, Milne J, Shingles S, Jones RH (2003) Catalogue and bibliography of Australian fungi. 2. Basidiomycota p.p. & Myxomycota p.p. *Fungi of Australia Volume 2B*. ABRS/CSIRO Publishing, Melbourne, 452pp.
- Miettinen O, Spirin V, Niemelä T (2012) Notes on the genus *Aporpium* (Auriculariales, Basidiomycota), with a new species from temperate Europe. *Annales Botanici Fennici* 49: 359–368. <https://doi.org/10.5735/085.049.0607>
- Pattengale ND, Alipour M, Bininda-Emonds ORP, Moret BME, Stamatakis A (2010) How many bootstrap replicates are necessary? *Journal of Computational Biology* 17: 337–354. <https://doi.org/10.1089/cmb.2009.0179>
- Petersen JH (1996) Farvekort. The Danish Mycological Society's colour chart. Foreningen til Svampekundskabens Fremme, Greve.
- Posada D (2008) jModelTest: phylogenetic model averaging. *Molecular Biology and Evolution* 25: 1253–1256. <https://doi.org/10.1093/molbev/msn083>
- Reid DA (1957) New or interesting records of Australasian basidiomycetes: III. *Kew Bulletin* 1957: 127–143. <https://doi.org/10.2307/4109115>
- Ronquist F, Teslenko M, van der Mark P, Ayres D, Darling A, Höhna S, Larget B, Liu L, Suchard MA, Huelsenbeck JP (2012) MrBayes 3.2: efficient Bayesian phylogenetic inference and model choice across a large model space. *Systematic Biology* 61: 539–542. <https://doi.org/10.1093/sysbio/sys029>
- Silvestro D, Michalak I (2012) RAxMLGUI: a graphical front-end for RAxML. *Organisms, Diversity & Evolution* 12: 335–337. <https://doi.org/10.1007/s13127-011-0056-0>
- Sotome K, Maekawa N, Nakagiri A, Lee SS, Hattori T (2014) Taxonomic study of Asian species of poroid Auriculariales. *Mycological Progress* 13: 987–997. <https://doi.org/10.1007/s11557-014-0984-0>
- Spirin V, Malysheva V, Larsson KH (2018) On some forgotten of *Exidia* and *Myxarium* (Auriculariales, Basidiomycota). *Nordic Journal of Botany* 36: e01601. <https://doi.org/10.1111/njb.01601>
- Spirin V, Malysheva V, Miettinen O, Vlasák J, Alvarenga RLM, Gibertoni TB, Ryvarden L, Larsson KH (2019a) On *Protomerulius* and *Heterochaetella* (Auriculariales, Basidiomycota). *Mycological Progress* 18: 1079–1099. <https://doi.org/10.1007/s11557-019-01507-0>
- Spirin V, Malysheva V, Roberts P, Trichies G, Savchenko A, Larsson KH (2019b) A convolute diversity of the *Auriculariales* (Agaricomycetes, Basidiomycota) with sphaeropedunculate basidia. *Nordic Journal of Botany* 37: e02394. <https://doi.org/10.1111/njb.02394>
- Stamatakis A (2006) RAxML-VI-HPC: maximum likelihood-based phylogenetic analyses with thousands of taxa and mixed models. *Bioinformatics* 22: 2688–2690. <https://doi.org/10.1093/bioinformatics/btl446>

- Vilgalys R, Hester M (1990) Rapid genetic identification and mapping of enzymatically amplified ribosomal DNA from several *Cryptococcus species*. *Journal of Bacteriology* 172: 4238–4246. <https://doi.org/10.1128/jb.172.8.4238-4246.1990>
- Wakefield E (1915) On a collection of fungi from Australia and New Zealand. *Bulletin of Miscellaneous Information* 1915: 361–376. <https://doi.org/10.2307/4104559>
- Wang S, Thorn RG (2021) *Exidia qinghaiensis*, a new species from China. *Mycoscience* 62: 212–216. <https://doi.org/10.47371/mycosci.2021.03.002>
- Wang XW, Jiang JH, Zhou LW (2020) *Basidioradulum mayi* and *B. tasmanicum* spp. nov. (*Hymenochaetales*, *Basidiomycota*) from both sides of Bass Strait, Australia. *Scientific Reports* 10: e102. <https://doi.org/10.1038/s41598-019-57061-y>
- Wang XW, May TW, Liu SL, Zhou LW (2021) Towards a natural classification of *Hyphodontia* sensu lato and the trait evolution of basidiocarps within *Hymenochaetales* (*Basidiomycota*). *Journal of Fungi* 7: e478. <https://doi.org/10.3390/jof7060478>
- Wei M, Oberwinkler F (2001) Phylogenetic relationships in *Auriculariales* and related groups - hypotheses derived from nuclear ribosomal DNA sequences. *Mycological Research* 105: 403–415. <https://doi.org/10.1017/S095375620100363X>
- Wells K (1961) Studies of some Tremellaceae. IV. *Exidiopsis*. *Mycologia* 53: 317–370. <https://doi.org/10.1080/00275514.1961.12017967>
- Wells K, Raitviir A (1977) The species of *Exidiopsis* (Tremellaceae) of the USSR. *Mycologia* 69: 987–1007. <https://doi.org/10.2307/3758782>
- Wells K, Raitviir A (1980) The species of *Eichleriella* (Tremellaceae) of the USSR. *Mycologia* 72: 564–577. <https://doi.org/10.1080/00275514.1980.12021219>
- White TJ, Bruns T, Lee S, Taylor J (1990) Amplification and direct sequencing of fungal ribosomal RNA genes for phylogenetics. In: Innis MA, Gelfand DH, Sninsky JJ, White TJ (Eds) *PCR protocols: a guide to methods and applications*. Academic Press, San Diego, 315–322. <https://doi.org/10.1016/B978-0-12-372180-8.50042-1>
- Wu F, Yuan Y, He SH, Bandara AR, Hyde KD, Malysheva VF, Li DW, Dai YC (2015a) Global diversity and taxonomy of the *Auricularia auricula-judae* complex (*Auriculariales*, *Basidiomycota*). *Mycological Progress* 14: e95. <https://doi.org/10.1007/s11557-015-1113-4>
- Wu F, Yuan Y, Rivoire B, Dai YC (2015b) Phylogeny and diversity of the *Auricularia mesenterica* (*Auriculariales*, *Basidiomycota*) complex. *Mycological Progress* 14: e42. <https://doi.org/10.1007/s11557-015-1065-8>
- Wu F, Zhou LW, Yuan Y, Dai YC (2017) *Aporpium miniporum*, a new polyporoid species with vertically septate basidia from southern China. *Phytotaxa* 317: 137–143. <https://doi.org/10.11646/phytotaxa.317.2.6>
- Ye SY, Zhang YB, Wu F, Liu HX (2020) Multi-locus phylogeny reveals two new species of *Exidia* (*Auriculariales*, *Basidiomycota*) from China. *Mycological Progress* 19: 859–868. <https://doi.org/10.1007/s11557-020-01601-8>
- Yuan HS, Lu X, Decock C (2018) Molecular and morphological evidence reveal a new genus and species in *Auriculariales* from tropical China. *MycKeys* 35: 27–39. <https://doi.org/10.3897/mycokeys.35.25271>
- Zhou LW, Dai YC (2013) Phylogeny and taxonomy of poroid and lamellate genera in the *Auriculariales* (*Basidiomycota*). *Mycologia* 105: 1219–1230. <https://doi.org/10.3852/12-212>

New and interesting species of *Penicillium* (Eurotiomycetes, Aspergillaceae) in freshwater sediments from Spain

Daniel Torres-García¹, Josepa Gené¹, Dania García¹

¹ *Universitat Rovira i Virgili, Unitat de Micologia, Facultat de Medicina i Ciències de la Salut and IISPV, 43201-Reus, Spain*

Corresponding author: Dania García (danial.garcias@urv.cat)

Academic editor: D. Haelewaters | Received 2 September 2021 | Accepted 10 January 2022 | Published 1 February 2022

Citation: Torres-García D, Gené J, García D (2022) New and interesting species of *Penicillium* (Eurotiomycetes, Aspergillaceae) in freshwater sediments from Spain. MycoKeys 86: 103–145. <https://doi.org/10.3897/mycokeys.86.73861>

Abstract

Penicillium species are common fungi found worldwide from diverse substrates, including soil, plant debris, food products and air. Their diversity in aquatic environments is still underexplored. With the aim to explore the fungal diversity in Spanish freshwater sediments, numerous *Penicillium* strains were isolated using various culture-dependent techniques. A preliminary sequence analysis of the β -tubulin (*tub2*) gene marker allowed us to identify several interesting species of *Penicillium*, which were later characterized phylogenetically with the barcodes recommended for species delimitation in the genus. Based on the multi-locus phylogeny of the internal transcribed spacer region (ITS) of the ribosomal DNA, and partial fragments of *tub2*, calmodulin (*cmdA*), and the RNA polymerase II largest subunit (*rpb2*) genes, in combination with phenotypic analyses, five novel species are described. These are *P. ausonianum* in section *Lanata-Divaricata*, *P. guarroi* in sect. *Gracilentia*, *P. irregulare* in sect. *Canescentia*, *P. sicoris* in sect. *Paradoxa* and *P. submersum* in sect. *Robsamsonia*. The study of several isolates from samples collected in different locations resulted in the reinstatement of *P. vaccaeorum* into section *Citrina*. Finally, *P. heteromorphum* (sect. *Exilicaulis*) and *P. tardochrysogenum* (sect. *Chrysogena*) are reported, previously only known from Antarctica and China, respectively.

Keywords

5 new species, Ascomycota, Eurotiales, fluvial sediments, phylogeny, species delimitation, taxonomy

Introduction

Fungi make up a significant component of the benthic microbial biomass in freshwater ecosystems, and play a pivotal role in decomposing organic matter in river habitats (Pascoal and Cassio 2004; Zhang et al. 2013). In general, representatives of Ascomycota account for the largest number of species recovered from water systems (Kelley et al. 2001; Liu et al. 2015; Khomich et al. 2017; Sutcliffe et al. 2018; Samson et al. 2020), their asexual forms with stauro- or scoleococonidia (aquatic hyphomycetes) being the most representative fungal group in freshwater environments (Pascoal et al. 2005; Jones and Pang 2012). Although common Ascomycota like *Penicillium* species are not considered aquatic fungi, they are one of the most common genera identified from freshwater (Pitt 1979; Hageskal et al. 2006; Sonjak et al. 2006; Samson et al. 2010; Heo et al. 2019; Pangging et al. 2019) and recently were also reported in marine environments (Kirichuk et al. 2017; Gonçalves et al. 2019; Grossart et al. 2019). However, in almost all of those reports, little attention has been paid to the study of river sediments as a reservoir of taxonomically interesting penicillia.

Penicillium (Eurotiomycetes, Eurotiales, Aspergillaceae) is a ubiquitous genus recovered from a wide range of substrates—including soil, plant material, indoor and outdoor air environments, a variety of food products, herbivore dung and water (Visagie et al. 2014a; Barbosa et al. 2018; Grossart et al. 2019; Guevara-Suarez et al. 2020; Rodriguez-Andrade et al. 2021). *Penicillium* species have a great impact on human life as agents of food spoilage, causal agents of pre- and postharvest diseases on crops (Frisvad et al. 2004; Pitt and Hocking 2009; Samson et al. 2010), and their ability to produce toxic compounds like mycotoxins (Frisvad et al. 2004; Perrone and Susca 2017), which can be a serious threat to human and animal health worldwide. On the contrary, positive impacts of these fungi include their use in food fermentations, the production of many bioactive compounds of medical interest (antimicrobial agents, immunosuppressants), and the production of enzymes with a variety of industrial applications (Houbraken et al. 2014; Visagie et al. 2014a; Abdelwahab et al. 2018; Park et al. 2019; Ogaki et al. 2020a, b). Other recent applications are the potential use of some species as biocontrol agents against plant pathogens or for bioremediation in polluted environments (Guijarro et al. 2017; Cecchi et al. 2019; Behera et al. 2020; Thambugala et al. 2020; Liang et al. 2021). The discovery of novel lineages in the genus *Penicillium*, therefore, represents an opportunity to find and characterize new fungi or molecules with a wide range of applications. As an example, more than 390 novel natural products have been isolated in recent years from marine-derived *Penicillium* fungi, many of which possess biological activity with potential application in new drug developments (Yang et al. 2021).

Limitations in establishing species boundaries by morphological and even molecular data are well-known in Ascomycota, mainly in those genera that comprise a huge number of species such as *Aspergillus*, *Fusarium* and *Trichoderma*, among many others. Therefore, the use of an integrative taxonomy that combines

morphometric, phylogenetic, chemical and ecological data provides support for accurate species delimitation and formal description of novel taxa (Haelewaters et al. 2018; Aime et al. 2021; Maharachchikumbura et al. 2021). Species delimitation in *Penicillium* is currently based on an integrative or polyphasic approach, which usually includes morphological features, extrolite profiles (when available), and multi-locus phylogenies (Visagie et al. 2014a). Phylogenetic markers used for this purpose include β -tubulin (*tub2*), the internal transcribed spacer region (ITS) of the ribosomal RNA gene (rDNA) and the calmodulin (*cmdA*) and the RNA polymerase II largest subunit (*rpb2*) genes. More than 480 species are accepted in the genus, distributed across 32 sections (Houbraken and Samson 2011; Visagie et al. 2014a; Houbraken et al. 2020). More recently, in a phylogenetic re-evaluation of various genera in the order Eurotiales, Houbraken et al. (2020) reinstated a series classification, and in particular for *Penicillium* recognized 89 series, contributing in this way to work easily with phylogenetic clades instead of large sections.

In this context, in an ongoing study of microfungal diversity from freshwater sediments collected from rivers or streams in different Spanish regions, we found several isolates of *Penicillium*, which could represent putative new or uncommon species of penicillia based on the sequence analysis of the recommended secondary identification marker *tub2* (Visagie et al. 2014a). The present work aims to resolve the taxonomy of those isolates by using the above-mentioned polyphasic approach and following the Genealogical Concordance Phylogenetic Species Recognition (GCPSR) criterion (Taylor et al. 2000).

Materials and methods

Sampling and fungal isolation

Sediment samples were collected between February 2018 and December 2020 from rivers and streams in natural and rural areas from various Spanish provinces (Balears, Barcelona, Lleida, Madrid, and Tarragona) (Table 1). Sterile 100 ml plastic containers were used for collecting samples from the bunk beds or edges of the rivers selected ca 10 cm below the surface layer. Samples were transported in a refrigerated container and immediately processed in the laboratory. Samples were shaken vigorously in the same containers and, after leaving them for 1 min to settle, the water was decanted, and the sediment poured onto several layers of sterile filter paper on plastic trays to remove any water excess (Ulfig et al. 1997). To isolate a wide range of fungal species, each sample was cultured as follows: 1 g of sediment was distributed across three Petri dishes and mixed with dichloran rose-bengal-chloramphenicol agar (DRBC; 2.5 g peptone, 5 g glucose, 0.5 g KH₂PO₄, 0.25 g MgSO₄, 12.5 mg Rose Bengal, 100 mg chloramphenicol, 1 mg dichloran, 10 g agar, 500 mL distilled water) melted at 45 °C; and in parallel, another 1 g was distributed in three other Petri dishes and mixed with

melted potato dextrose agar (PDA; Pronadisa) supplemented with 2 g/L of chloramphenicol and 2 g/L of cycloheximide. Once solidified, the cultures were incubated at room temperature (22–25 °C) and examined weekly with a stereomicroscope for up to 4–5 weeks. To achieve pure cultures, conidia of *Penicillium* colonies were transferred with a sterile dissection needle to plates with PDA supplemented with chloramphenicol and incubated at 25 °C in darkness.

All isolates were preserved and deposited into the fungal collection of the Faculty of Medicine, Reus (FMR). Those isolates that were representative of novel species, ex-type cultures and holotypes (dried cultures) were prepared and deposited at the Westerdijk Fungal Biodiversity Institute (CBS, Utrecht, The Netherlands).

DNA extraction, sequencing and phylogenetic analysis

Isolates were cultured on PDA for 7–14 days at 25 °C in darkness. The DNA was extracted through the modified protocol of Werner et al. (1998). Preliminary species identifications were carried out by similarity searches of obtained *tub2* DNA sequences against reference sequences on GenBank. In the case of putative new species, the ITS region and fragments of *cmdA* and *rpb2* genes were amplified and sequenced (Visagie et al. 2014b). The primer pairs used for gene amplifications were: Bt2a/Bt2b for *tub2* (Glass and Donaldson 1995), ITS5/ITS4 for ITS (White et al. 1990), CMD5/CMD6 for *cmdA* (Hong et al. 2006) and RPB2–5F/RPB2–7Cr for *rpb2* (Liu et al. 1999). The PCR conditions were carried out using primers and methods previously described (Peterson 2008; Houbraeken and Samson 2011; Visagie et al. 2014a). Amplified products were purified and sequenced at Macrogen (Madrid, Spain). Consensus sequences were obtained using SeqMan v. 7.0.0 (DNAStar Lasergene, Madison, WI, USA).

Sequences for phylogenies of *Penicillium* sections and series included in the study were retrieved from NCBI GenBank (<https://www.ncbi.nlm.nih.gov/genbank/>), considering the accepted species of penicillia included in the last update of the International Commission of *Penicillium* and *Aspergillus* database (<http://www.aspergillus-penicillium.org>), and those more recently published (Houbraeken et al. 2020; Visagie et al. 2021). Initially, a preliminary phylogenetic analysis with *tub2* sequences was carried out to resolve the taxonomic position of our isolates at section level. Thereafter, single and concatenated phylogenetic analyses for each section were calculated to allocate the isolates at series level and establish phylogenetic relationships among closely related species. Individual analyses of the alternative molecular markers of the series in which the isolates under study belong are included as supplementary material.

Datasets for each locus were aligned individually in MEGA (Molecular Evolutionary Genetic Analysis) software v. 6.0. (Tamura et al. 2013) using the CLUSTALW algorithm (Thompson et al. 1994) and refined with MUSCLE (Edgar 2004) or manually adjusted, if necessary, on the same platform. Phylogenetic concordance of the four-

locus datasets was evaluated individually through visual comparison of each single-locus phylogeny to assess any incongruent results among nodes with high statistical support. Once the lack of incongruence was confirmed, individual alignments were concatenated into a single data matrix with SequenceMatrix (Vaidya et al. 2011). The best substitution model for all gene matrices was estimated using MEGA software for Maximum Likelihood (ML) analysis, while for the Bayesian Inference (BI) analysis it was estimated using jModelTest v.2.1.3 according to the Akaike criterion (Guindon and Gascuel 2003; Darriba et al. 2012). The phylogenetic reconstructions were made with the combined genes using ML under RAxML-HPC2 on XSEDE v-8.2.12 (Stamatakis et al. 2014) on the CIPRES Science gateway portal (Miller et al. 2012) and BI with MrBayes v.3.2.6 (Ronquist et al. 2012).

For ML, phylogenetic support for internal branches was assessed by 1,000 ML bootstrapped pseudoreplicates and bootstrap support (bs) ≥ 70 was considered significant (Hillis and Bull 1993). The phylogenetic reconstruction by BI was carried out using 5 million Markov chain Monte Carlo (MCMC) generations, with four runs (one cold chain and three heated chains), and samples were stored every 1,000 generations. The 50% majority-rule consensus tree and posterior probability (pp) values were calculated after discarding the first 25% of samples. A pp value of ≥ 0.95 was considered significant (Hespanhol et al. 2019). The resulting trees were plotted using FigTree v.1.3.1 (<http://tree.bio.ed.ac.uk/software/figtree/>).

The DNA sequences and alignments generated in this study were deposited in GenBank (Table 1) and in TreeBASE under the submission number: 28954 (<http://treebase.org>), respectively.

Phenotypic study

Phenotypic characterization of the strains was made using standard growth conditions established previously (Visagie et al. 2014a). Strains were inoculated in three-point fashion onto Czapek Yeast Autolysate agar (CYA; Pitt 1979), 2% Malt Extract Agar (MEA; Samson et al. 2010), Yeast Extract Sucrose agar (YES; Frisvad 1981), Oatmeal agar (OA; Samson et al. 2010), Dichloran 18% Glycerol agar (DG18; Hocking and Pitt 1980) and Creatine Sucrose agar (CREA; Frisvad 1981) and incubated at 25 °C for 7d in darkness, with the exception of FMR 16948 which was incubated for 14d for sporulation to occur. Colony growth rates were measured after 7 d at 5, 15, 20, 30, 35, 37, and 40 °C on CYA. Color annotations in descriptions follow Kornerup and Wanscher (1978). Microscopic measurements and features were described from colonies grown on MEA after 7 d (14 d for FMR 16948) of incubation. Microscopic slides were mounted with Shear's solution, after prior removal of the excess conidia with 70% ethanol. Photomicrographs were obtained using a Zeiss Axio-Imager M1 light microscope (Zeiss, Oberkochen, Germany) with a DeltaPix Infinity x digital camera. Photoplates were assembled from separate photographs using PhotoShop CS6.

Results

Phylogenetic analyses

Among the penicillium-like fungi found, we recovered 15 isolates (12 from PDA at 0.2% cycloheximide; three from DRBC), which preliminary identification, having compared their *tub2* sequences through BLAST search, revealed as possibly representing putative novel or uncommon species of penicillia (Table 1). According to the *tub2* phylogeny, *Penicillium* isolates were distributed over two major clades corresponding to the two subgenera of *Penicillium* (i.e. *Aspergilloides* and *Penicillium*) and all sections included in the analysis were well delineated (Suppl. material 1: Fig. S1). Five of the isolates under study, which were distributed in the sections *Robsamsonia* (FMR 17140), *Paradoxa* (FMR 18076), *Canescentia* (FMR 17859), *Lanata-Divaricata* (FMR 16948) and *Gracilentia* (FMR 17747), could not be assigned to any currently accepted species in the genus. Another eight isolates, which belong to the section *Citrina* (FMR 17531, FMR 17534, FMR 17616, FMR 17617, FMR 17619, FMR 17967, FMR 18100 and FMR 18123), were closely related to the ex-type strains of *P. sanguifluum*, *P. roseopurpureum* and *P. vaccaeorum*, the latter species currently considered synonym of *P. sanguifluum* (Houbraken et al. 2011). The other two isolates, FMR 17137 and FMR 18043, were placed in sections *Chrysogena* and *Exilicaulis*, respectively. However, the *tub2* marker did not show enough discriminatory power to resolve the identity of both isolates concerning their counterparts, which were the ex-type strains of *P. chrysogenum*, *P. tardochrysogenum* and *P. rubens* for FMR 17137, and *P. restrictum* and *P. heteromorphum* for FMR 18043. Phylogenetic analyses and species delimitation were performed using ITS, *tub2*, *cmdA*, and *rpb2*. Dataset characteristics and substitution models for each data partition are summarized in Table 2. Since tree topologies were similar and congruent between the ML and BI analyses in all cases, we selected ML trees to represent section results. Bootstrap support values $\geq 70\%$ and BI posterior probability values ≥ 0.95 are indicated on branches.

The concatenate phylogeny for the section *Chrysogena* was constructed with ITS, *tub2* and *cmdA* markers since *rpb2* was not available for FMR 17137. This isolate was placed in a fully-supported clade (100 bs/1 pp) with the ex-type strain of *P. tardochrysogenum* (Fig. 1). Both specimens showed a high sequence similarity (99.2% for *tub2*, 98.9% *cmdA*, and 99.8% ITS). It is closely related to the type species of the section *P. chrysogenum* and its relatives (*P. rubens*, *P. allii-sativa*, *P. rubens* and *P. vanluytii*). Additional analyses of the series *Chrysogena* with *tub2* and *cmdA* sequences, including ex-type strains and more reference strains of those mentioned species, confirmed the identity of the sediment isolate (Suppl. material 1: Fig. S2). *Penicillium tardochrysogenum* has so far been isolated exclusively from soil and rock samples in Antarctica (Houbraken et al. 2012; Alves et al. 2019), and our specimen is thus the first report of the species from temperate regions.

Phylogenetic reconstruction of section *Robsamsonia* with the four markers (Fig. 2) showed the unidentified isolate FMR 17140 grouped with the ex-type strain

Table 1. Strain information and GenBank/EMBL accession numbers of the *Penicillium* species investigated in this study.

Species	Section	Strain no. ¹	Substrate and Origin	GenBank nucleotide accession no. ²		Citation
				<i>trb2</i>	<i>emd4</i> ITS <i>trp62</i>	
<i>P. ansomannum</i>	<i>Lanata-Divariata</i>	FMR 16948 ^T	Fluvial sediment, stream of the Guillerries National Park, Barcelona, Catalonia, Spain	LR655809	LR655808	LR655811 This study
<i>P. guarroi</i>	<i>Gracilentia</i>	FMR 17747 ^T	Fluvial sediment, Brugent River, Tarragona, Catalonia, Spain	LR814134	LR814139	LR814145 This study
<i>P. heteromorphum</i>	<i>Exalicaulis</i>	CBS 226.89 ^T	Soil, China	KJ834455	KC411702	JN406605 Visgüe et al. 2014a
	<i>Exalicaulis</i>	FMR 18043	Fluvial sediment, stream of the Cadí-Moixeró Natural Park, Lleida, Catalonia, Spain	LR861780	LR861783	LR861784 This study
<i>P. irregularare</i>	<i>Canescentia</i>	FMR 17859 ^T	Fluvial sediment, Miraflores River, Community of Madrid, Spain	LR814144	LR814181	LR814182 This study
<i>P. songnifluum</i>	<i>Citrina</i>	CBS 127032 ^T	Soil, Calahonda, Costa del Sol, Spain	JN606819	JN617681	– Houbraken et al. 2011
	<i>Citrina</i>	FMR 17617	Fluvial sediment, Mallorca Island, Spain	LR861778	LR861779	– This study
<i>P. sticoris</i>	<i>Citrina</i>	FMR 17619	Fluvial sediment, Mallorca Island, Spain	OU375375	–	– This study
<i>P. sticoris</i>	<i>Paradoxa</i>	FMR 18076 ^T	Fluvial sediment, Segre River, Lleida, Catalonia, Spain	LR884494	LR884496	LR884497 LR884495 This study
	<i>Robsamsonia</i>	FMR 17140 ^T	Fluvial sediment, stream of the Montsant Natural Park, Tarragona, Catalonia, Spain	LR814187	LR814188	LR814194 LR814195 This study
<i>P. tardochrysoeum</i>	<i>Chrysoeum</i>	CBS 132200 ^T	Soil, McMurdoo Dry Valley, Antarctica	JX996898	JX997028	JX996634 Houbraken et al. 2012
	<i>Chrysoeum</i>	FMR 17137	Fluvial sediment, stream of the Montsant Natural Park, Tarragona, Catalonia, Spain	HG996463	HG996465	HG996464 This study
<i>P. vaccaeorum</i>	<i>Citrina</i>	CBS 148.83 ^T	Sandy soil under pine tree, Valladolid, Spain	JN606846	JN606543	MH861558 – Houbraken et al. 2011
	<i>Citrina</i>	FMR 17967	Fluvial sediment, Basque Country, Spain	LR814226	LR814227	LR814235 – This study
	<i>Citrina</i>	FMR 17531	Fluvial sediment, stream of Montseny National Park, Barcelona, Spain	LR814203	LR814204	LR814213 – This study
	<i>Citrina</i>	FMR 17534	Fluvial sediment, stream of Montseny National Park, Barcelona, Spain	OU375168	OU375273	OU375272 – This study
	<i>Citrina</i>	FMR 17616	Fluvial sediment, stream of Serra de Tramontana, Mallorca, Spain	LR814212	LR814218	LR814217 – This study
	<i>Citrina</i>	FMR 18100	Fluvial sediment, Segre River, Lleida, Spain	LR814234	LR814242	LR814241 – This study
	<i>Citrina</i>	FMR 18123	Fluvial sediment, Segre River, Lleida, Spain	LR814265	LR814264	LR814273 – This study
	<i>Citrina</i>	CBS 110.64	Forest soil, Erzurum, Turkey	JN606829	JN606533	MH858377 – Houbraken et al. 2011
	<i>Citrina</i>	CBS 441.88	Sandy soil, Chile	JN606846	JN606568	– Houbraken et al. 2011
	<i>Citrina</i>	CBS 643.73	Sandy soil, Manitoba, Canada	–	JN606576	– Houbraken et al. 2011
	<i>Citrina</i>	CBS 644.73	Sandy soil, Manitoba, Canada	LR814213	JN606577	– Houbraken et al. 2011
	<i>Citrina</i>	CBS 685.85 (Type of <i>P. lacusarmantae</i>)	Sandy soil, Torres del Paine National Park, Tierra del Fuego, Chile	JN606855	JN606533	JN617711 – Houbraken et al. 2011
<i>Citrina</i>	CBS 300.67	Sandy greenhouse soil, The Netherlands	–	JN606561	– Houbraken et al. 2011	
<i>Citrina</i>	CBS 127029	Forest soil, Los Alerces National Park, Argentina	JN606814	–	MH864309 – Houbraken et al. 2011	
<i>Citrina</i>	CBS 118024	Ants (<i>Camponotus</i> spp.), New Brunswick, Canada	JN606833	JN606537	– Houbraken et al. 2011	

CBS: Culture collection of the Westerdijk Fungal Biodiversity Institute, Utrecht, The Netherlands; FMR: Facultat de Medicina i Ciències de la Salut, Reus, Spain. ¹ Indicate ex-type strains. ² Strain no.: strain number. ³ *trb2*; *β*-tubulin; *emd4*; calmodulin; ITS: Internal transcribed spacer regions of the rDNA and 5.8S region; *trp62*: the DNA dependent RNA polymerase II largest subunit. Novelities and sequences generated in this study are in bold.

Table 2. Overview and details used for phylogenetic analyses in sections of *Penicillium* analysed in this study.

Dataset		Sections							
		<i>Chrysogena</i>	<i>Robsamsonia</i>	<i>Paradoxal/ Turbata</i>	<i>Canescentia</i>	<i>Exilicaulis</i>	<i>Lan.-Div.</i>	<i>Gracilentia</i>	<i>Citrina</i>
<i>tub2</i>	Length (bp)	499	468	493	431	503	547	508	470
<i>tub2</i>	Pvar	113	171	173	161	254	307	189	240
<i>tub2</i>	Pi	65	103	108	101	205	257	93	207
<i>tub2</i>	Model*	K2+G	K2+G	K2+G	K2+G	HKY+G+I	HKY+G+I	HKY+G	HKY+G+I
<i>tub2</i>	Model**	K2+G	K2+G	K2+G	K2+G	K2+G	K2+G+I	TN93+G	K2+G
<i>cmdA</i>	Length (bp)	531	542	529	560	604	626	642	626
<i>cmdA</i>	Pvar	177	202	221	189	302	392	264	378
<i>cmdA</i>	Pi	93	124	136	95	349	329	145	337
<i>cmdA</i>	Model*	K2+G	K2+I	SYM+G	K2+G	SYM+G+I	HKY+G+I	K2+I	SYM+G+I
<i>cmdA</i>	Model**	K2+G	K2+G	K2+I	K2+G	K2+G+I	K2+G+I	K2+I	K2+G+I
ITS	Length (bp)	580	605	572	610	576	559	566	566
ITS	Pvar	25	60	39	45	102	180	44	119
ITS	Pi	7	17	21	33	60	154	20	99
ITS	Model*	K2+G	K2+G	K2+I	K2	K2+G+I	GTR+G+I	GTR+I	GTR+G+I
ITS	Model**	T92	JC+G	K2+I	T92	K2+G+I	GTR+G+I	T92+I	K2+G+I
<i>rpb2</i>	Length (bp)	-	936	929	915	950	837	978	-
<i>rpb2</i>	Pvar	-	249	256	230	360	345	294	-
<i>rpb2</i>	Pi	-	176	183	121	306	313	113	-
<i>rpb2</i>	Model*	-	SYM+G	SYM+G	K2+G	SYM+G+I	GTR+G+I	SYM+G	-
<i>rpb2</i>	Model**	-	K2+G	K2+I	K2+G	K2+G+I	K2+G+I	TN93+G	-
Concatenated	Length (bp)	1610	2551	2523	2516	2633	2569	2694	1662
Concatenated	Pvar	315	628	689	625	1018	1224	791	737
Concatenated	Pi	165	420	448	350	820	1053	371	643
Concatenated	Model*	K2+G+I	SYM+G	SYM+G	K2+G+I	HKY+G+I	GTR+G+I	GTR+G	SYM+G+I
Concatenated	Model**	K2+G	K2+G	K2+G	K2+G	K2+G+I	GTR+G+I	K2+I	K2+G

Lan.-Div. = sect. *Lanata-Divariata*; Pvar = variable sites; Pi = phylogenetic informative sites; * = substitution model for Bayesian inference; ** = substitution model for ML analysis; K2 = Kimura 2-parameter; HKY = Hasegawa-Kishino-Yano; SYM = Symmetrical; GTR = General Time Reversible; TN93 = Tamura-Nei; T92 = Tamura 3-parameter; JC = Jukes-Cantor; G = Gamma Distributed; I = Invariant Sites.

of *P. griseofulvum* in a fully-supported terminal clade (100 bs/1 pp), but forming an independent and single branch with enough genetic distance (97.0% *tub2*, 97.7% *cmdA*, 99.6% ITS, and 97.2% *rpb2* similarity) with the ex-type of *P. griseofulvum* to be considered a distinct phylogenetic species. In order to evaluate possible inter- and intraspecific variability regarding closely related species, we carried out additional analyses with *tub2*, *cmdA* and *rpb2* markers of the species in series *Urticicola* (Suppl. material 1: Fig. S3), including more sequences of *P. griseofulvum* retrieved from GenBank. These analyses showed that our isolate was always placed distant to the clade representative of *P. griseofulvum*. Therefore, genetic and phenotypic differences, such as a faster growth rate on CYA and strong acid production compared to *P. griseofulvum*, allow us to propose the novel species *Penicillium submersum*.

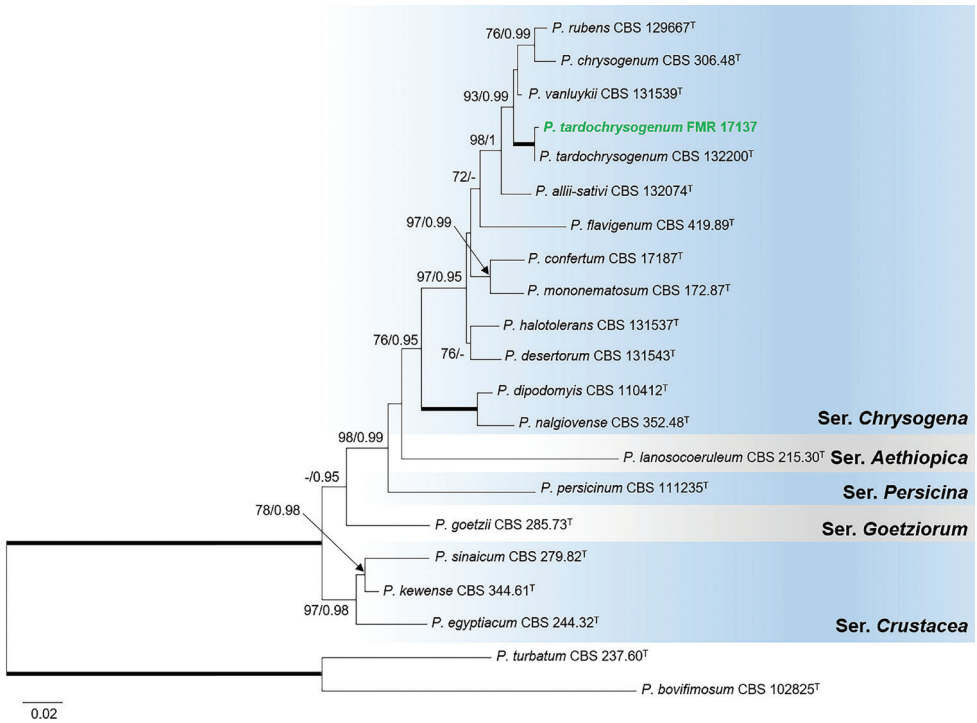


Figure 1. Phylogenetic tree of *Penicillium* section *Chrysogena* based on ML analysis obtained by RAxML inferred from the combined *tub2*, *cmdA* and ITS loci. Branch lengths are proportional to phylogenetic distance. Bootstrap support values/Bayesian posterior probability scores above 70%/0.95 are indicated on the nodes. Bold branches indicate bs/pp values 100/1. The tree is rooted to *P. turbatum* CBS 237.60 and *P. bovisfimosum* CBS 102825. The name in green is the strain of *P. tardochrysogenum* included in this study. ^T= Ex-type strain.

The concatenated dataset for section *Paradoxa* (Fig. 3) revealed that FMR 18076 belonged to the series *Atramentosa* and was closely related to the lineage representative of *P. mexicanum*, a species recently described from house dust of which only two specimens are known (Visagie et al. 2014c; Park et al. 2019). Both lineages were also well differentiated when additional analyses of the series were carried out with the three alternative markers (*tub2*, *cmdA* and *rpb2*) and more representative sequences of the species in the series (Suppl. material 1: Fig. S4). The genetic distance with the ex-type strain of *P. mexicanum* (96.5%, 94.3% 98.2%, and 97.6% sequence similarity for *tub2*, *cmdA*, ITS, and *rpb2*, respectively) and their morphological differences in colony color, growth rates, and conidial shape (see Taxonomy section) allow to propose FMR 18076 as *Penicillium sicoris*.

The phylogeny constructed for section *Canescentia* (Fig. 4) placed FMR 17859 in a divergent lineage closely related to the ex-type strains of *P. arizonense* and *P. yarmokense*, the three forming a terminal clade only supported with BI analysis (- bs/0.99 pp).

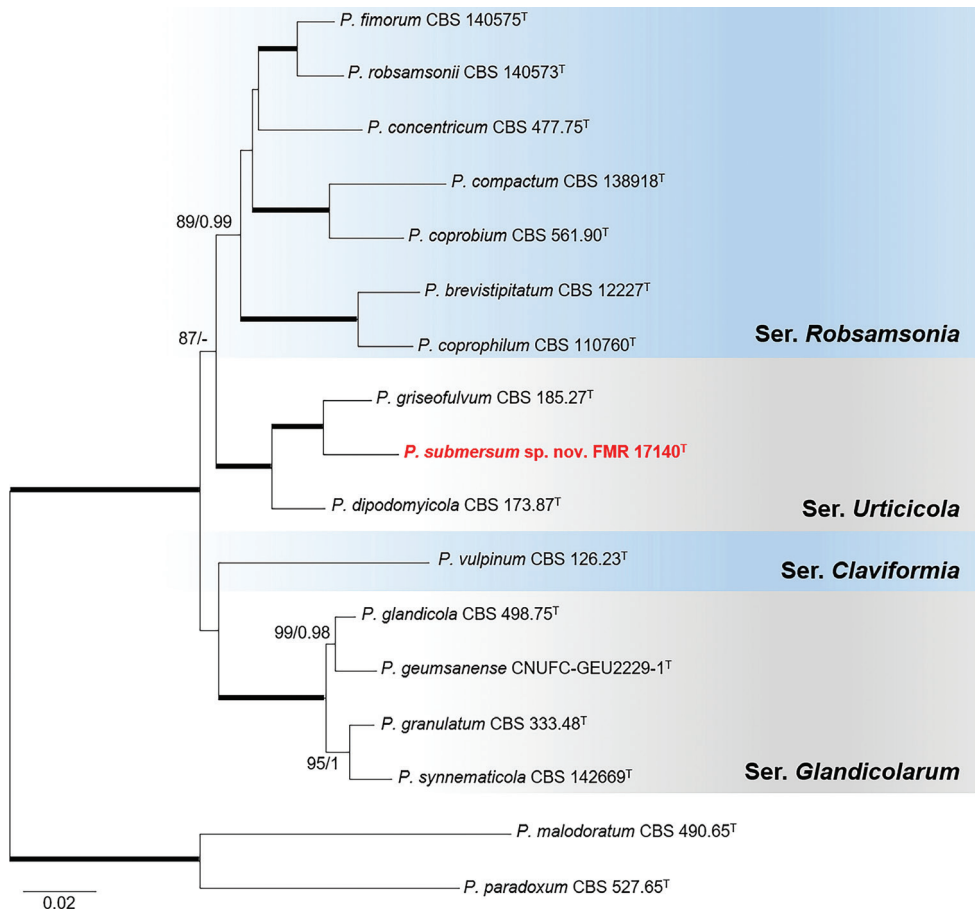


Figure 2. Phylogenetic tree of *Penicillium* section *Robsamsonia* based on ML analysis obtained by RAxML inferred from the combined *tub2*, *cmdA*, ITS, and *rpb2* loci. Branch lengths are proportional to phylogenetic distance. Bootstrap support values/Bayesian posterior probability scores above 70%/0.95 are indicated on the nodes. Bold branches indicate bs/pp values 100/1. The tree is rooted to *P. paradoxum* CBS 527.65 and *P. malodoratum* CBS 490.65. The name in red is the new species described in this study. T= Ex-type strain.

In order to elucidate possible inter- and intraspecific variability among these close relatives, additional analyses of the series with the three alternative markers and with more sequences of reference strains of those mentioned species were carried out (Suppl. material 1: Fig. S5). All revealed that *P. arizonense* was the closest relative and FMR 17859 being always placed in a distant branch. Phylogenetic and phenotypic differences like stipe and metulae length, its ability to grow at 37 °C and its reverse color on CYA support the proposal of the novel species *Penicillium irregulare*.

Identification of FMR 18043 as *P. heteromorphum* was confirmed with the multi-locus phylogeny of section *Exilicaulis* (Fig. 5). This species belongs to series *Restricta*, which includes species with still unresolved phylogeny (Visagie et al. 2016). In the tree, our isolate grouped in a strongly supported terminal clade (98 bs/0.99 pp) with the

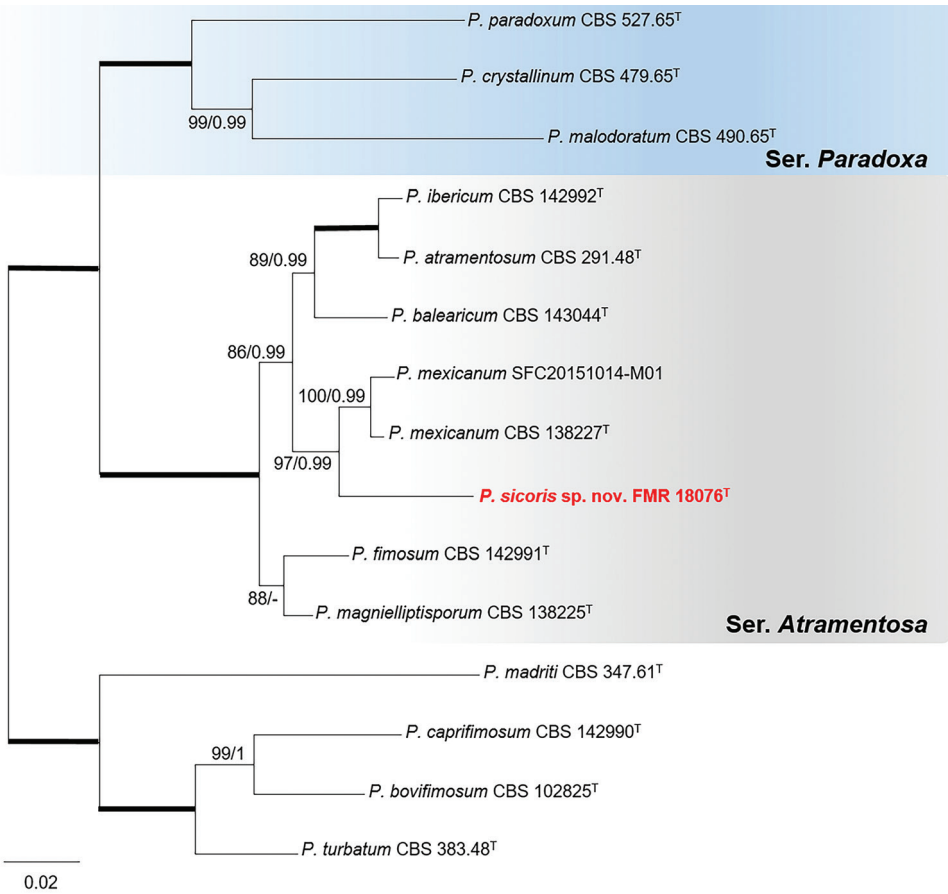


Figure 3. Phylogenetic tree of *Penicillium* section *Paradoxa* based on ML analysis obtained by RAxML inferred from the combined *tub2*, *cmdA*, ITS, and *rpb2* loci. Branch lengths are proportional to phylogenetic distance. Bootstrap support values/Bayesian posterior probability scores above 70%/0.95 are indicated on the nodes. Bold branches indicate bs/pp values 100/1. The tree is rooted to *Penicillium* species belonging to section *Turbata* (*P. madriti* CBS 347.61, *P. caprifimosum* CBS 142990, *P. bovisfimosum* CBS 102825 and *P. turbatum* CBS 383.48). The name in red is the new species described in this study. ^T= Ex-type strain.

monotypic species *P. heteromorphum* (Kong and Qi 1988). However, despite the high genetic similarity of both strains in *tub2*, *cmdA*, ITS, and *rpb2* (99.2%, 99.8%, 99.6% and 99.4%, respectively), we observed morphological differences regarding ornamentation of conidia, length of conidiophores and its growth at 37 °C. These differences are described in the Taxonomy section. Additional analyses with more sequences of representative strains of its closely related species in series *Restricta* also supported the identification of our sediment isolate (Suppl. material 1: Fig. S6).

Phylogenetic reconstruction of section *Lanata-Divaricata* (Fig. 6) resolved FMR 16948 in series *Dalearum* closely related to the ex-type strains of *P. amphipolaria* and *P. viridissimum* (78 bs/0.98 pp), but the three specimens were placed in distant

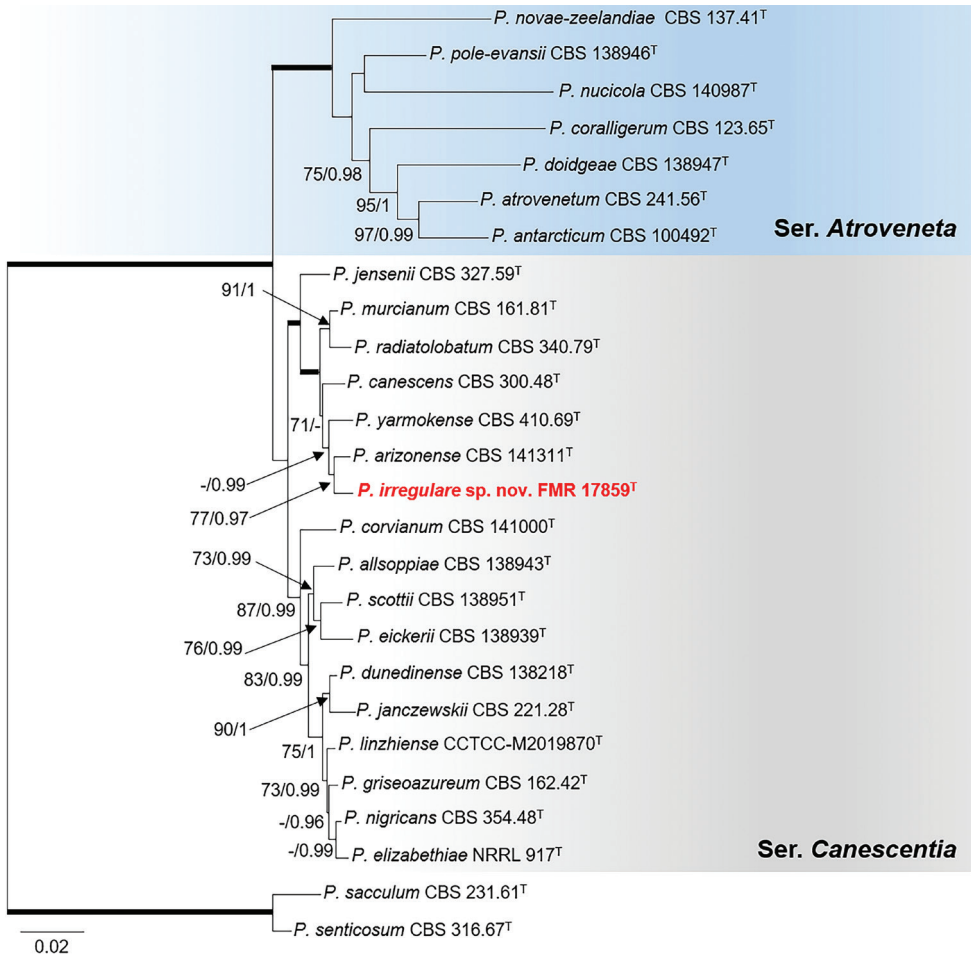


Figure 4. Phylogenetic tree of *Penicillium* section *Canescentia* based on ML analysis obtained by RAxML inferred from the combined *tub2*, *cmdA*, ITS, and *rpb2* loci. Branch lengths are proportional to phylogenetic distance. Bootstrap support values/Bayesian posterior probability scores above 70%/0.95 are indicated on the nodes. Bold branches indicate bs/pp values 100/1. The tree is rooted to *P. sacculum* CBS 231.61 and *P. senticosum* CBS 316.67. The name in red is the new species described in this study. ^T= Ex-type strain.

lineages. In addition, FMR 16948 showed a similarity of 97.1% *tub2*, 97.2% *cmdA* and 97.4% *rpb2* with the ex-type strain of *P. amphipolaria* and of 97.8% *tub2*, 97.7% *cmdA* and 98.4% *rpb2* with the ex-type of *P. viridissimum*. Similar results were obtained in analyses of the series with alternative markers and more sequences of representative strains of its closest relatives (Suppl. material 1: Fig. S7). Our isolate also differed from its relatives by strong acid production and by the predominance of mono- and biverticillate conidiophores. Therefore, morphological and phylogenetic differences support to propose our isolate as *Penicillium ausonianum*.

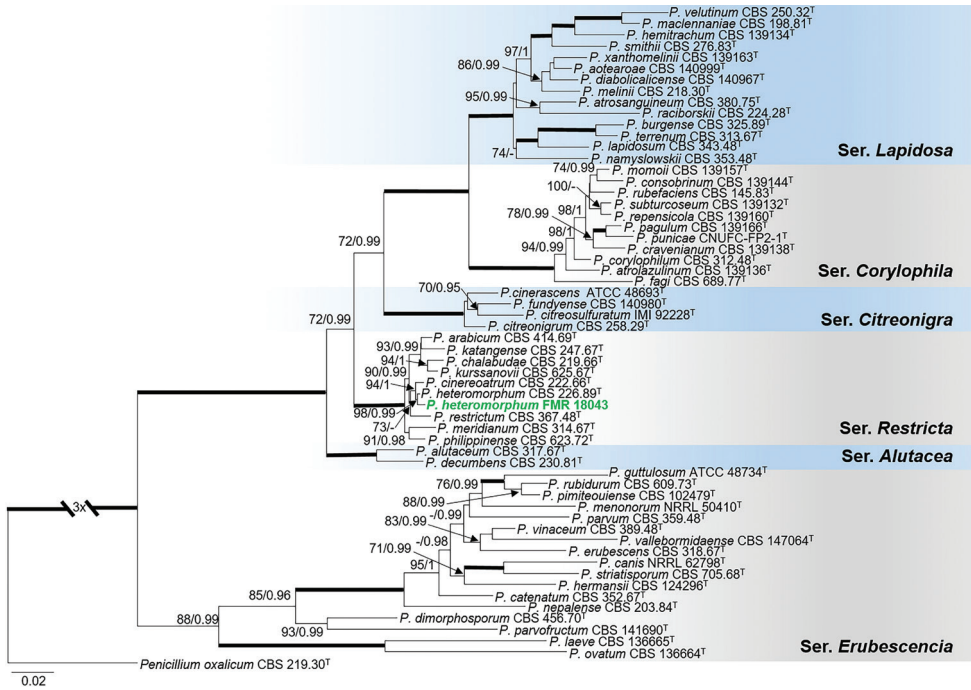


Figure 5. Phylogenetic tree of *Penicillium* section *Exilicaulis* based on ML analysis obtained by RAxML inferred from the combined *tub2*, *cmdA*, ITS, and *rpb2* loci. Branch lengths are proportional to phylogenetic distance. Bootstrap support values/Bayesian posterior probability scores above 70%/0.95 are indicated on the nodes. Bold branches indicate bs/pp values 100/1. The tree is rooted to *P. oxalicum* CBS 219.30. The name in green is the strain of *P. heteromorphum* included in this study. ^T= Ex-type strain.

The phylogenetic analysis of section *Gracilentia* (Fig. 7), comprising the six species *P. aquaticum*, *P. angustiporcatum*, *P. apimei*, *P. estinogenum*, *P. gracilentum* and *P. macroesclerotiorum* with considerable genetic distance between them, revealed that FMR 17747 did not belong to any of the lineages of these known species and formed a basal and distant branch neighboring the fully-supported clade representative of *P. estinogenum*. Similarity values of the sediment isolate with respect to the ex-type strain of this latter species were 86.5% for *tub2*, 82.5% for *cmdA*, and 96.8% for ITS. *Rpb2* sequences of *P. estinogenum* were not available for comparison. Individual analyses of the alternative gene markers including sequences of all reference strains available for the species in the section are shown in Suppl. material 1: Fig. S8. This undescribed monophyletic lineage is proposed as *Penicillium guarroi*, which differed morphologically from its counterpart mainly by its smooth-walled globose conidia.

The concatenated alignment for section *Citrina* (Fig. 8) was carried out with *tub2*, *cmdA* and ITS loci, since sequences of the *rpb2* marker were not available for many species in the section. This multi-locus analysis placed the sediment isolates (FMR 17531, FMR 17534, FMR 17616, FMR 17967, FMR 18100 and FMR

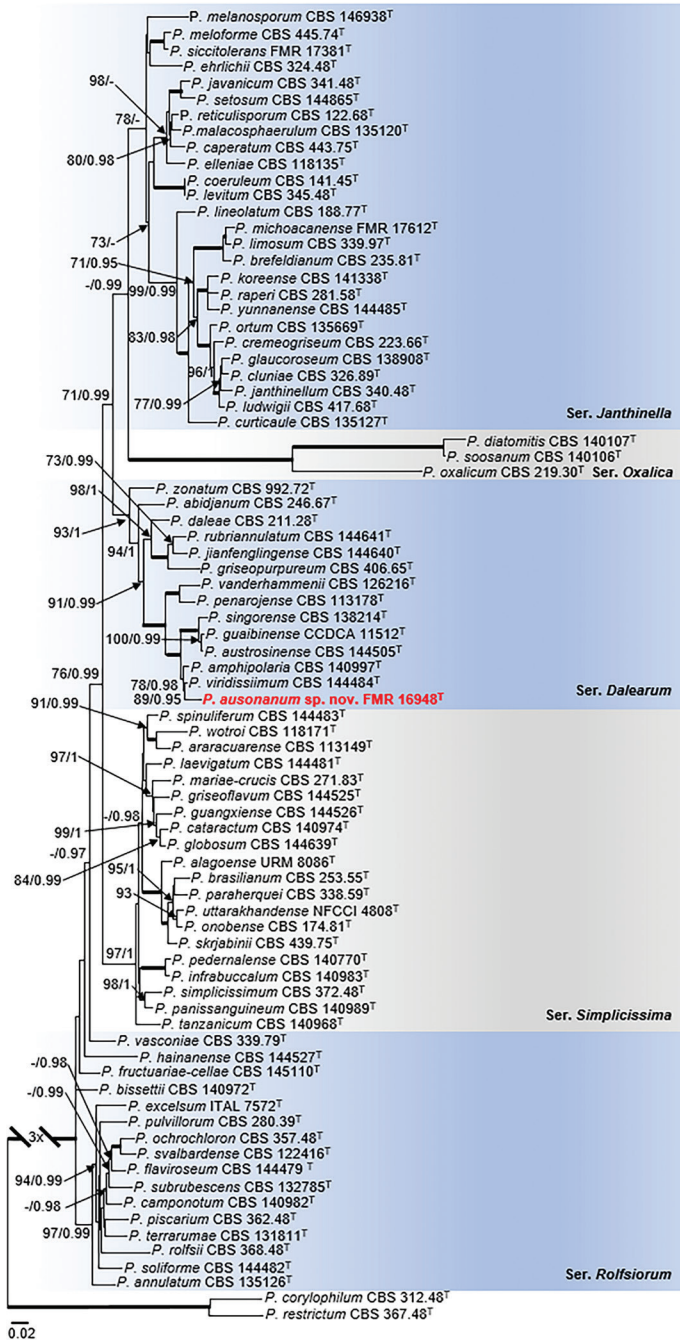


Figure 6. Phylogenetic tree of *Penicillium* section *Lanata-Divaricata* based on ML analysis obtained by RAxML inferred from the combined *tub2*, *cmdA*, ITS, and *rpb2* loci. Branch lengths are proportional to phylogenetic distance. Bootstrap support values/Bayesian posterior probability scores above 70%/0.95 are indicated on the nodes. Bold branches indicate bs/pp values 100/1. The tree is rooted to *P. restrictum* CBS 367.48 and *P. corylophilum* CBS 312.48. The name in red is the new species described in this study. ^T = Ex-type strain.

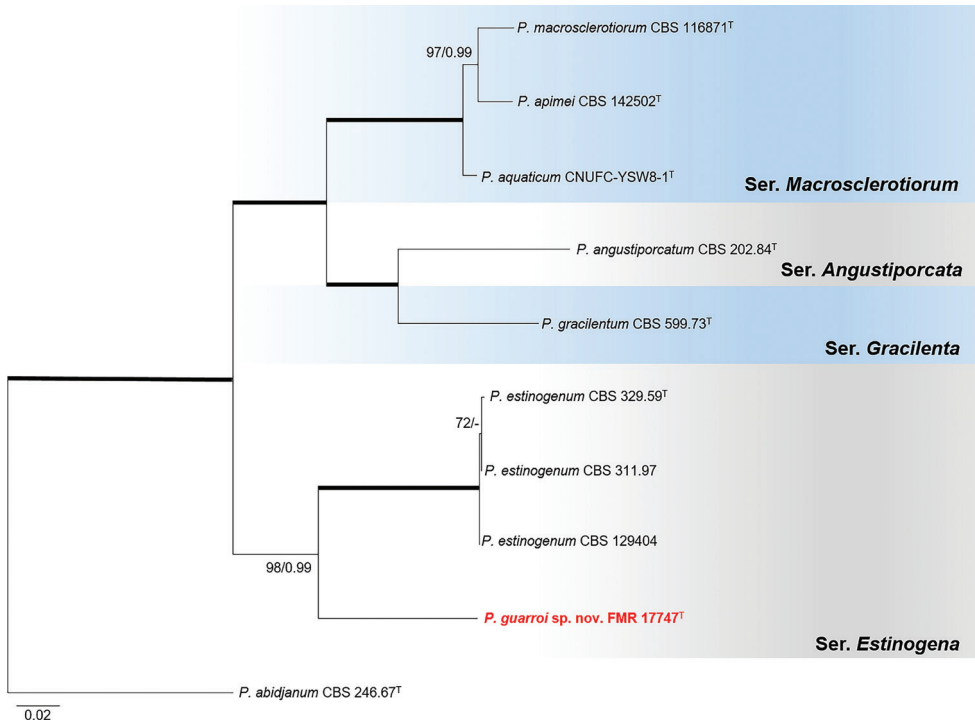


Figure 7. Phylogenetic tree of *Penicillium* section *Gracilentia* based on ML analysis obtained by RAxML inferred from the combined *tub2*, *cmdA*, ITS, and *rpb2* loci. Branch lengths are proportional to phylogenetic distance. Bootstrap support values/Bayesian posterior probability scores above 70%/0.95 are indicated on the nodes. Bold branches indicate bs/pp values 100/1. The tree is rooted to *P. abidjanum* CBS 246.67. The name in red is the new species described in this study. ^T = Ex-type strain.

18123) in the series *Roseopurpurea* and grouped them in a well-supported clade (98 bs/1 pp) with the ex-type strains of *P. vaccaeorum* (CBS 148.83) and *P. lacussarmientei* (CBS 685.85), together with other strains (CBS 110.64, CBS 127029, CBS 441.88, CBS 300.67, CBS 118024, CBS 644.73, CBS 643.73) from soil and insects of different countries, and previously considered as *P. sanguifluum* by Houbraken et al. (2011). This terminal clade was sister to the also strongly supported clade with the ex-type strain of *P. sanguifluum* (CBS 127032) and other reference strains from different origins, including some collected in our survey from Spanish fluvial sediments (FMR 17617 and 17619). Both monophyletic lineages showed a genetic distance of 3.4%, which supports considering them distinct species. This result was corroborated with additional analyses of the alternative markers *tub2* and *cmdA*, including more sequences of reference strains for the species in the series (Suppl. material 1: Fig. S9). In addition, features such as faster growth on YES agar, the ability to grow at 35 °C and longer stipes, allow us to distinguish the clade represented by *P. vaccaeorum* from that of *P. sanguifluum*. Since we accept *P. vaccaeorum* as a distinct species, a detailed description is provided below.

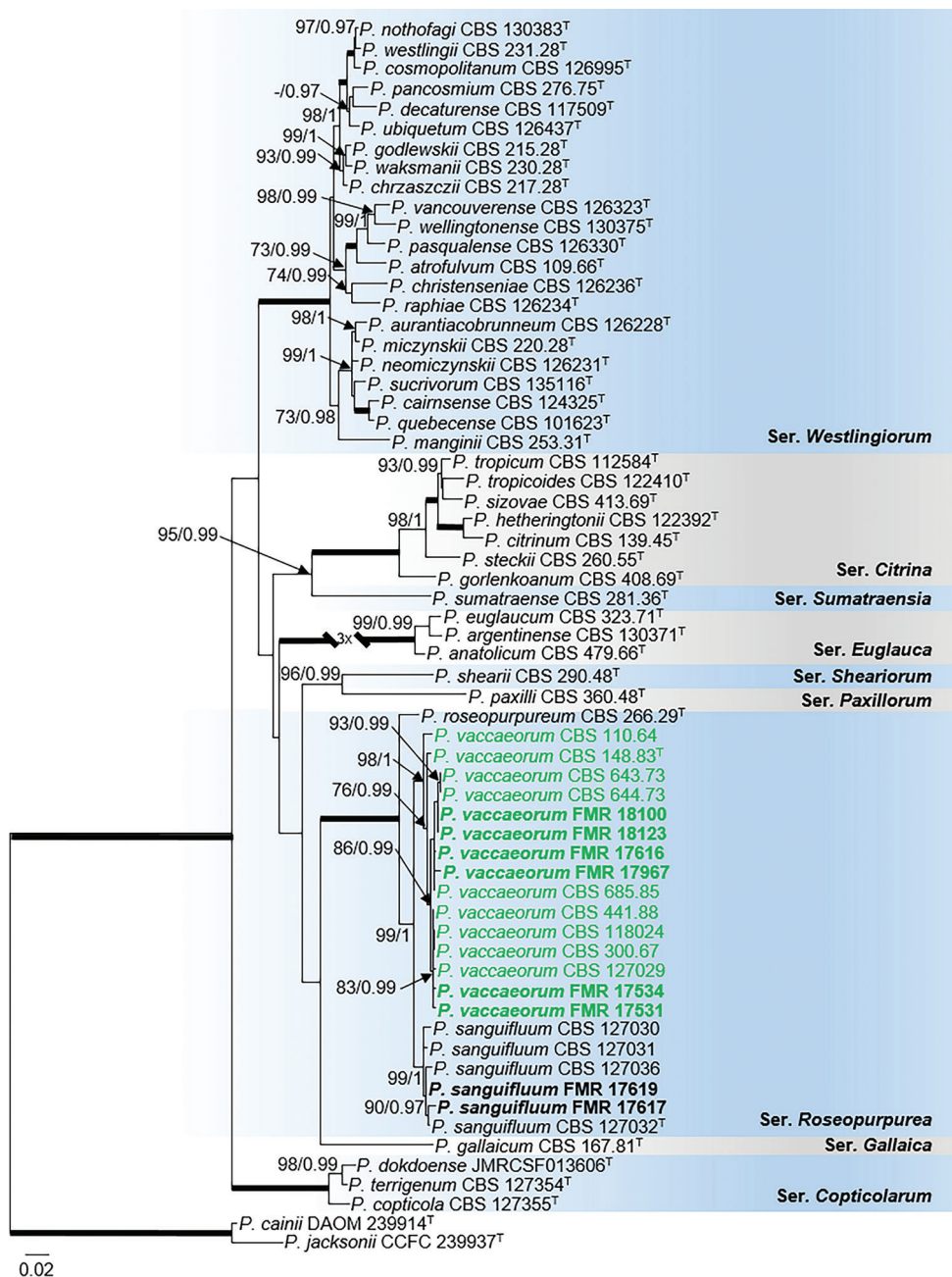


Figure 8. Phylogenetic tree of *Penicillium* section *Citrina* based on ML analysis obtained by RAxML inferred from the combined *tub2*, *cmdA*, and ITS loci. Branch lengths are proportional to phylogenetic distance. Bootstrap support values/Bayesian posterior probability scores above 70%/0.95 are indicated on the nodes. Bold branches indicate bs/pp values 100/1. The tree is rooted to *P. cainii* DAOM 239914 and *P. jacksonii* CCFC 239937. The name in green is the resurrected species *P. vaccaeorum* included in this study. ^T = Ex-type strain.

Taxonomy

Penicillium ausonianum Torres-Garcia, Gené and Dania García, sp. nov.

Mycobank No: 840556

Figure 9

Etymology. Referring to *Ausona* (Osona), the region of Catalonia where the fungus was collected.

Type. SPAIN, Catalonia, Osona, Guillerics-Savassona Natural Park, Malafogassa, Major Stream, from sediments, Nov. 2018, E. Carvalho & J. Gené (**holotype** CBS H-24781, cultures ex-type CBS 148237 = FMR 16948).

Subgeneric classification. Subgenus *Aspergilloides*, section *Lanata-Divaricata*, series *Dalearum*.

Description. *Mycelium* superficial and immersed, composed of septate, smooth-walled, hyaline hyphae, 2–3 µm wide. *Conidiophores* monoverticillate and divaricate, minor proportion biverticillate; *stipes* smooth-walled, 20–120 × 2–2.5 µm; *metulae* slightly appressed to divergent, mostly 2, occasionally 3 per stipe, 10–18 × 2–3 µm, occasionally a solitary phialide borne on the same level as metulae; *phialides* 2–5 per stipe/metula, ampulliform to cylindrical, 9–12 × 2–3 µm; *conidia* smooth-walled, globose to subglobose, 2–3 × 2–3 µm.

Culture characteristics (14 d at 25 °C). Colonies on CYA, 58–59 mm diam., slightly radially and concentrically sulcate, velvety to floccose, whitish (5A1), margins regular and slightly fimbriate, sporulation absent to sparse, when present conidial masses brownish gray (6C2); reverse grayish yellow (4B4); little production of exudates hyaline, soluble pigment absent. On MEA, 61–62 mm diam., slightly raised, floccose, white (3A1), margins fimbriate, sporulation absent to sparse, conidial masses brownish gray (5E3); reverse light yellow (4A4); exudate absent, soluble pigment absent. On YES, 67–71 mm diam., slightly raised, radially sulcate, randomly furrowed as well, velvety to floccose, dull yellow (3B3) at center and white (3B1) towards periphery, margins slightly fimbriate, sporulation absent to sparse, conidial masses grayish to dull green (25C4–5C); reverse brownish yellow (5C8), exudates and soluble pigment absent. On OA, 63–65 mm diam., slightly raised, white (3A1) with gray (3E1) to olive (3F3) areas, velvety, margins slightly fimbriate, sporulation abundant, conidial masses grayish to dull green (25C5–D5); reverse grayish-yellow (3B5); exudates and soluble pigment absent. On DG18, 10–12 mm diam., randomly furrowed at the center, radially sulcate towards periphery, velvety, yellowish gray (2B2), margins entire, sporulation absent to sparse, conidial masses grayish to dull green (25C4–5C); reverse grayish yellow (2C3); exudates and soluble pigment absent. On CREA, 61–63 mm diam., slightly raised, floccose, gray (4B1) at center to yellowish gray (4B2) and white (4A1) towards periphery, margins slightly fimbriate, sporulation abundant, conidial masses brownish gray (6C2); reverse vivid yellow (3A8); exudates absent, acid production strong.

Colony diameter on CYA after 7 d (mm). 5 °C 3–2, 15 °C 41–43, 20 °C 46–48, 30 °C 56–57, 35 °C 50–51, 37 °C 38–39, 40 °C no growth.



Figure 9. Morphological characters of *Penicillium ausonianum* sp. nov. (ex-type FMR 16948). **A** colonies from left to right (top row) CYA, MEA, YES, and OA; (bottom row) CYA reverse, MEA reverse, DG18, and CREA **B** colony on OA under stereoscopic magnifying glass **C–H** conidiophores **I** conidia. Scale Bars: 25 μm (**C**), 10 μm (**D–I**).

Distribution. Spain.

Notes. *Penicillium ausonianum* formed a phylogenetically supported group together with *P. amphipolaria* and *P. viridissimum* in series *Dalearum* (Fig. 6). These are two species recently described, the former from soil in Antarctica and Canada, and the latter from acidic and forest soil from China (Visagie et al. 2016a, Diao et al. 2019). The new species can be morphologically differentiated from them by its equal proportion of monoverticillate and divaricate conidiophores, which are mostly with a complex branching pattern in *P. amphipolaria* (biverticillate and divaricate) (Visagie et al. 2016a), and mono- to terverticillate in *P. viridissimum* (Diao et al. 2019). Both *P. amphipolaria* (6.5–10 μm) and *P. viridissimum* (6.5–10 μm) have slightly shorter

phialides than *P. ausonianum* (9–12 µm). Also, *P. amphipolaria* (240–460 µm) and *P. viridissimum* (40–125 µm) have longer stipes (Visagie et al. 2016a, Diao et al. 2019) in comparison to those of *P. ausonianum* (20–120 µm). Furthermore, the three species also differed in acid production on CREA, which is strong in *P. ausonianum*, moderate in *P. amphipolaria* and absent in the neighboring species *P. viridissimum*.

***Penicillium guarroi* Torres-García, Gené and Dania García, sp. nov.**

Mycobank No: 840567

Figure 10

Etymology. Named in honor of Josep Guarro for his contributions to our knowledge of microfungi.

Type. SPAIN, Catalonia, Alt Camp, Alcover, Brugent River, sediments, Mar. 2019, D. Torres & J. Gené (*holotype* CBS H-24782, cultures ex-type CBS 148238 = FMR 17747).

Subgeneric classification. Subgenus *Aspergilloides*, section *Gracilenta*, series *Estinogena*.

Description. *Mycelium* superficial and immersed, composed of septate, smooth-walled, hyaline hyphae, 2.5–3.5 µm wide. *Conidiophores* predominantly symmetrically biverticillate, occasionally with subterminal branches; *stipes* smooth- to rough-walled, 88–215 × 3–4 µm; *metulae* appressed, 2–4 per stipe, vesiculate, 5–10 × 2–4.5 µm (vesicle up to 5.5 µm wide); *phialides* 3–6 per metula, ampulliform, 6–9 × 1.5–3 µm; *conidia* smooth-walled, globose, 2–2.5 × 2–2.5 µm.

Culture characteristics (7 d at 25 °C). Colonies on CYA, 38–40 mm diam., slightly raised at center, radially sulcate, velvety, brownish gray (6C2) and white (1A1) towards periphery, margins fimbriate, sporulation moderate, conidial masses greenish gray (28C2); reverse dark brown (6F6) and light brown (6D6) at periphery, becoming entirely brown after 14 d; soluble pigment absent. On MEA, 41–43 mm diam., slightly raised, granular, yellowish green (29B7) and white (1A1) towards periphery, margins slightly fimbriate, sporulation moderate, conidial masses grayish green (28D2); reverse yellowish brown (5E6) at center to grayish yellow at periphery; soluble pigment absent. On YES, 49–51 mm diam., raised at center, radially sulcate, velvety, brownish gray (5C2) and white (1A1) at periphery, margins entire, sporulation sparse, conidial masses greenish gray (28D2); reverse dark green (30F5) and yellowish brown (5D5) towards periphery; soluble pigment absent. On OA, 24–26 mm diam., elevated at center, velvety, white (1A1) at center and dull green (25E3) towards periphery, margins regular, sporulation moderate, conidial masses dull green (25D4); reverse brown (6E4) and yellowish gray (4B2) at periphery; soluble pigment absent. On DG18, 22–25 mm diam., flattened, granular, grayish green (30C3) at center, and dull green (29D49) towards periphery, margins fimbriate, sporulation moderate, conidial masses greenish gray (27D2); reverse grayish green (30E5) and white (1A1) at periphery, soluble pigment absent. On CREA, 22–25 mm diam., flattened, floccose, yellowish green (29B7) and white (1A1)

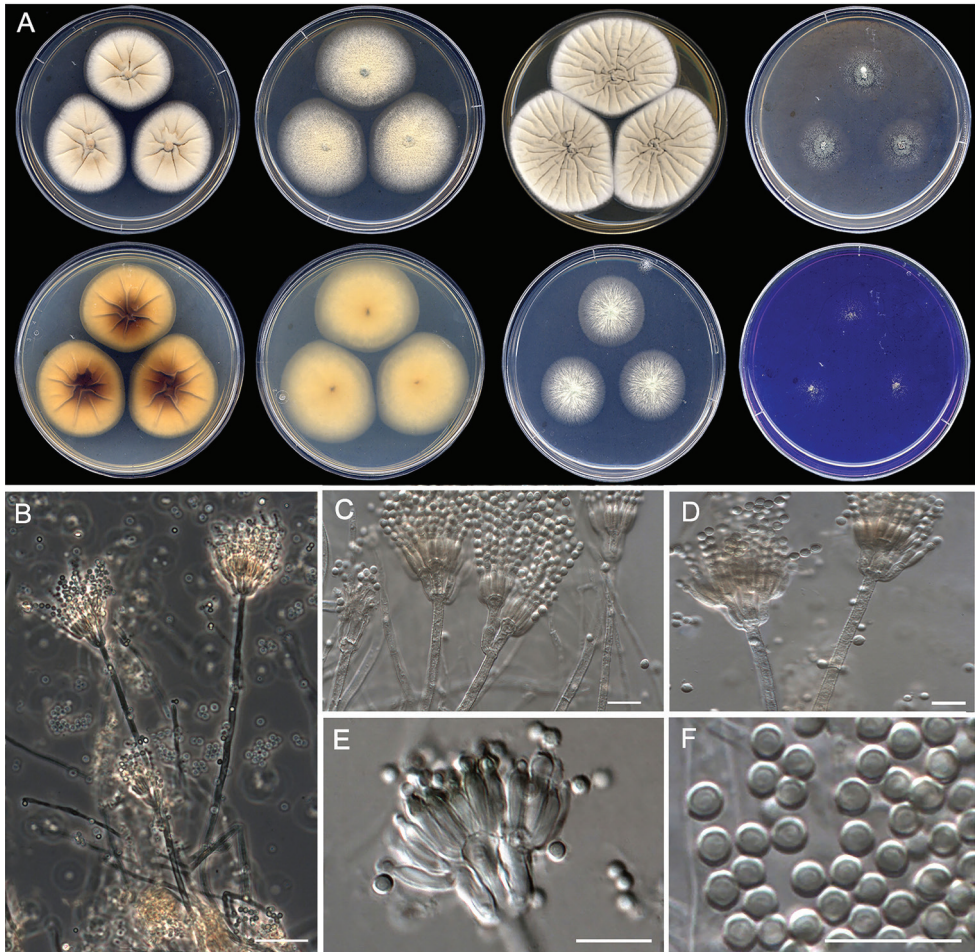


Figure 10. Morphological characters of *Penicillium guarroi* sp. nov. (ex-type FMR 17747). **A** colonies from left to right (top row) CYA, MEA, YES, and OA; (bottom row) CYA reverse, MEA reverse, DG18, and CREA **B–E** conidiophores on MEA **F** conidia. Scale Bars: 25 µm (**B**), 10 µm (**C–F**).

at periphery, margins irregular, sporulation moderate, conidial masses grayish green (27B3–D3); reverse dark gray (1F1); soluble pigment absent, no acid production.

Colony diameter on CYA after 7d (mm). 5 °C no growth, 15 °C 17–19, 20 °C 26–28, 30 °C 34–36, 35 °C 4–5, 37 °C no growth, 40 °C no growth.

Distribution. Spain.

Notes. *Penicillium guarroi* is the second species included in section *Gracilentia* series *Estinogena* (Fig. 7). This species shows morphological attributes of the series based on its type *P. estinogenum*, namely that both have symmetrically appressed biverticillate conidiophores with rough-walled stipes (Houbraken et al. 2020). However, *P. guarroi* mainly differs from *P. estinogenum* by producing strictly smooth-walled globose conidia, which are ellipsoidal to ovate and with smooth to finely roughened walls in the latter

(Abe 1956; Houbraken et al. 2020). In addition to their phylogenetic distance, other members of section *Gracilentia* (i.e., series *Gracilentia* and *Macrosclerotiorum*) can be differentiated morphologically by the production of monoverticillate conidiophores and the lack of growth at 37 °C, with the exception of *P. apimei* and *P. aquaticum*, which are able to grow at this temperature (Barbosa et al. 2018; Houbraken et al. 2020). *Penicillium guarroi* was unable to grow at 37 °C, but it shows a maximum temperature for growth at 35 °C (4–5 mm), like other members in the section (i.e., *P. macrosclerotiorum*, *P. angustiporcatum*, *P. gracilentum* and *P. estinogenum*).

***Penicillium heteromorphum* H.Z. Kong and Z.T. Qi. Mycosystema 1:107. 1988.**

Figure 11

Subgeneric classification. Subgenus *Aspergilloides*, section *Exilicaulis*, series *Restricta*.

Description. *Mycelium* superficial and immersed, composed of septate, smooth-walled, hyaline hyphae, 1.5–3 µm wide. *Conidiophores* monoverticillate, occasionally irregularly branched; *stipes* smooth-walled, thin, 6–47.5 × 1.5–2 µm; *phialides* 2–3 per stipe, ampulliform, 3–7 × 1.5–2.5 µm; *conidia* roughened, globose to subglobose, 2.5–3 × 2.5–3 µm, occasionally conidia up to 5 µm were observed.

Culture characteristics (7 d at 25 °C). Colonies on CYA, 19–20 mm diam., slightly raised at center, velvety, radially sulcate, yellowish gray (4B2) at center and white (1A1) at periphery, margins slightly undulate, sporulation absent; reverse pale yellow (4A3); soluble pigment absent. On MEA, 27–28 mm diam., slightly raised at center, velvety, white (1A1) at center, ash blond (3C3) towards periphery, margins entire, sporulation absent; reverse champagne colored (4A4) at center, pastel yellow (3A4) towards periphery; soluble pigment absent. On YES, 22–21 mm diam., slightly raised at center, velvety, radially sulcate, yellowish gray (4B2) and Sahara colored (6C5), margins entire, sporulation absent; reverse grayish orange (5B5) at center and champagne colored (4B4) towards periphery; soluble pigment absent. On OA, 23–24 mm diam., slightly elevated at center, floccose, greenish gray (28B2) at center and beige (4C3) towards periphery, margins fimbriate, sporulation abundant, conidial masses dull green (29E3); reverse beige (4C3); soluble pigment absent. On DG18, 14–15 mm diam., slightly raised at center, velvety, yellowish white (1A2) at center and white (1A1) towards periphery, margins regular, sporulation absent; reverse wine yellow (3B3) at center and yellowish white (3A2) towards periphery; soluble pigment absent. On CREA reaching 17–19 mm diam., slightly raised at center, floccose, white (1A1) at center and lemon yellow (3B8) towards periphery, margins fimbriate, sporulation absent; reverse lemon yellow (3B8); soluble pigment absent and acid production moderate. Colonies on Czapek's agar reaching 13–14 mm diam., flattened, floccose, white (1A1) at center to ash gray (1B2) towards periphery, margins entire, sporulation abundant, conidial masses dull green (29D3); reverse ash gray (1B2); soluble pigment absent.

Colony diameter on CYA after 7d (mm). 5 °C no growth, 15 °C 9–11, 20 °C 12–13, 30 °C 23–24, 35 °C 16–19, 37 °C 4–7, 40 °C no growth.

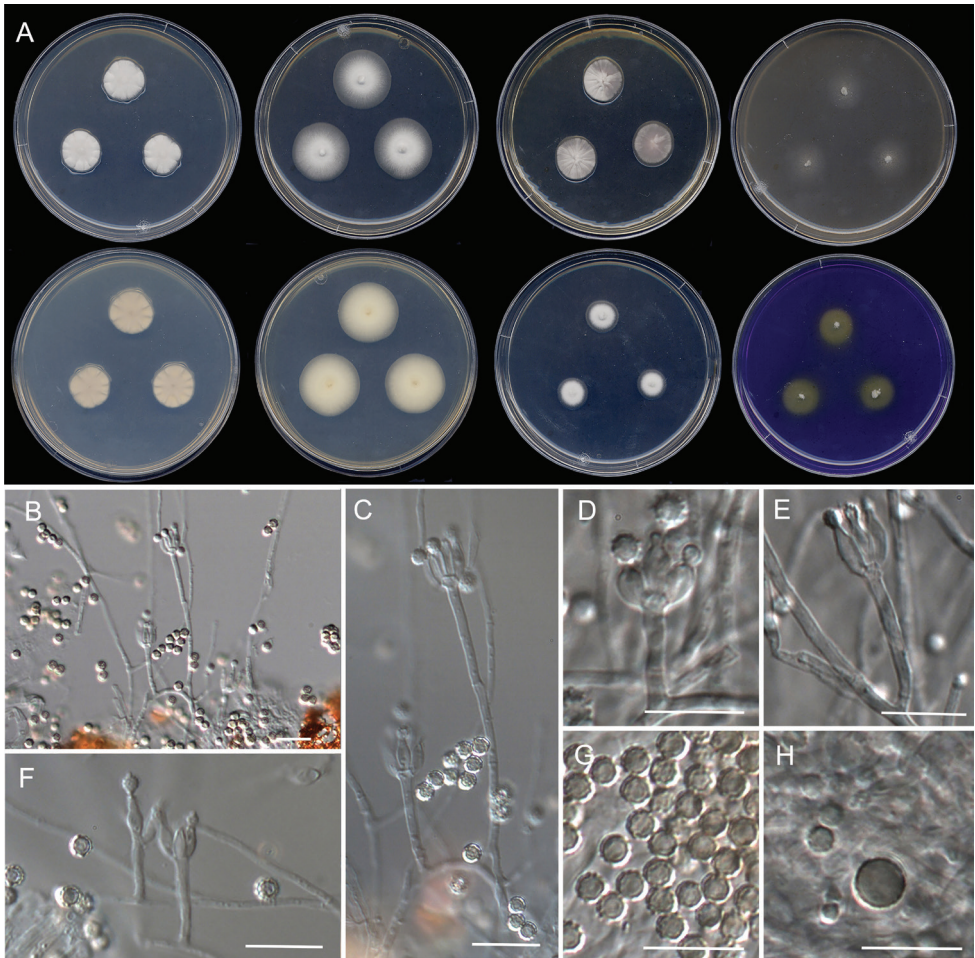


Figure 11. Morphological characters of *Penicillium heteromorphum* (FMR 18043). **A** colonies from left to right (top row) CYA, MEA, YES, and OA; (bottom row) CYA reverse, MEA reverse, DG18, and CREA **B, C, F** conidiophores on OA. **D, E** conidiophores on Czapek's Agar **G–H** conidia. Scale Bars: 25 µm (**B**), 10 µm (**C–H**).

Specimen examined. Spain, Catalonia, Berguedà, Gósol, from stream sediments, Nov. 2019, *J. Gené* (CBS 148239, FMR 18043).

Distribution. China and Spain.

Notes. *Penicillium heteromorphum* was first described from a soil sample collected in Shennongjia, China. FMR 18043 is thus the second isolate of this species. The protologue of *P. heteromorphum*, which was based on CYA and Czapek's agar, noted that it does not grow at 37 °C, has strictly monoverticillate conidiophores with stipes up to 60 µm long, and produce conidia that are globose to subglobose, smooth or nearly, which show two well-differentiated measures on Czapek's agar (ones of 2–2.5 (–3) µm diam, and the largest of 4–10 µm) (Kong and Qi 1988). By contrast, despite the

high sequence similarity to the ex-type strain, our isolate differs phenotypically in its ability to grow at 37 °C, and in the production of shorter conidiophores and rough-walled conidia in all media studied; some larger conidia (up to 5 µm diam.) were only observed on Czapek's agar. Nevertheless, features we observed in the sediment isolate *P. heteromorphum* match those of the species of series *Restricta*, which briefly consisted in growing restricted to moderately fast, producing generally short monoverticillate conidiophores with smooth stipes, globose to subglobose or (broadly) ellipsoidal, smooth or roughened conidia and they commonly grow at 37 °C (Houbraken et al. 2020). Based on the production of two types of conidia, Kong and Qi (1988) compared *P. heteromorphum* with *P. dimorphosporum*. However, although both species belongs in section *Exilicaulis*, the current taxonomy of the genus places *P. dimorphosporum* in the genetically distant series *Erubescens* (Visage et al. 2016b, Houbraken et al. 2020).

***Penicillium irregulare* Torres-García, Gené and Dania García, sp. nov.**

Mycobank No: 840558

Figure 12

Etymology. Referring to the variable branching pattern of the conidiophores of the species.

Type. SPAIN, Comunidad de Madrid, Miraflores de la Sierra, Miraflores River, from sediments, Jun. 2019, *J.F. Cano* (**holotype** CBS H-24783, cultures ex-type CBS 148240 = FMR 17859).

Subgeneric classification. Subgenus *Penicillium*, section *Canescentia*, series *Canescentia*.

Description. *Mycelium* superficial and immersed, composed of septate, smooth-walled, hyaline hyphae, 2–3.5 µm wide. **Conidiophores** biverticillate, in minor proportion monoverticillate, terverticillate or divaricate; **stipes** smooth-walled, 13–152 × 1.5–2 µm; **metulae** divergent, 2–3 per stipe/branch, unequal in length, vesiculate, 7–10 × 1.5–2.5 µm (vesicle up to 4 µm wide), occasionally a solitary phialide borne on same level as metulae; **phialides** 5–8 per metula, ampulliform, 6–7.5 × 1.5–2.5 µm; **conidia** smooth- to finely rough-walled, globose to subglobose, somewhat ellipsoidal, 1.5–3 × 1.5–2 µm.

Culture characteristics (7 d at 25 °C). Colonies on CYA, 36–38 mm diam, slightly elevated, radially sulcate, velvety, grayish orange (6B3) at center and white (1A1) towards periphery, margins entire, sporulation abundant, conidial masses grayish green (25B3); reverse brownish yellow (5C8) at center and vivid yellow towards periphery (3A8); exudate and soluble pigment absent. On MEA, 33–34 mm diam, elevated, floccose, light yellow (4A4) at center and white (1A1) towards periphery, margins fimbriate, sporulation abundant, conidial masses grayish green (25C3); reverse yellowish orange (4A7); exudate and soluble pigment absent. On YES, 43–44 mm diam, raised, concentrically sulcate and pale yellow (4A3) at center, radially sulcate and white (1A1) towards periphery, velvety, margins entire, sporulation absent to sparse, conidial masses

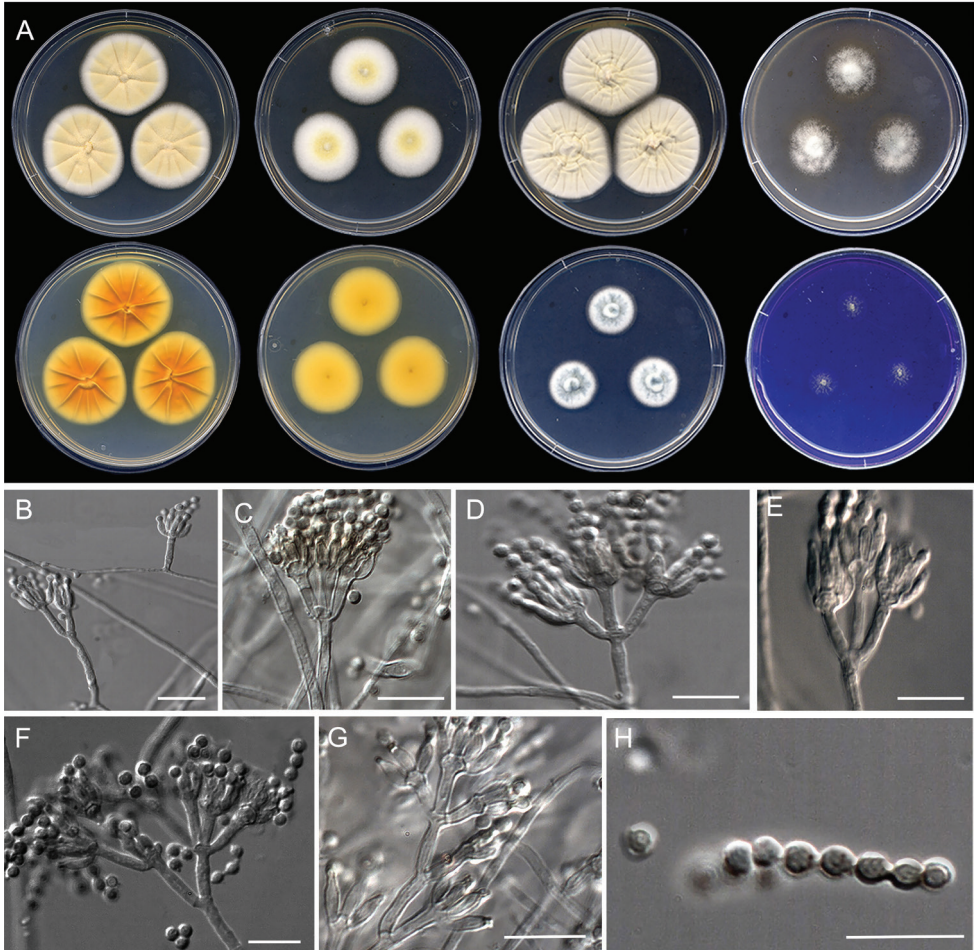


Figure 12. Morphological characters of *Penicillium irregulare* sp. nov. (ex-type FMR 17859). **A** colonies from left to right (top row) CYA, MEA, YES, and OA; (bottom row) CYA reverse, MEA reverse, DG18, and CREA **B–G** conidiophores on MEA **H** conidia. Scale Bars: 10 μ m (**B–H**).

grayish green (25D2); reverse brownish yellow (5C8) and white (1A1) at periphery; exudate and soluble pigment absent. On OA, 25–27 mm, slightly elevated at center, cottony and fasciculate, dull green (25E4) at center, gray (1D1) and white (1A1) towards periphery, margins entire, sporulation abundant, conidial masses dull green (30E3); reverse yellowish brown (5F4), golden brown (5D7) towards periphery; soluble pigment absent. On DG18, 14–15 mm, elevated, velvety, white (1A1) with grayish turquoise (24E4) areas, margins slightly fimbriate, sporulation abundant, conidial masses grayish turquoise (24B3–C5); reverse yellowish green (30B8) at center to pale green (30A3) and white (1A1) at periphery; soluble pigment absent. On CREA, 12–13 mm, flat, floccose, yellowish green (29B7), margins regular, sporulation sparse, conidial masses grayish green (27B3–C3); reverse dark gray (1F1); soluble pigment and acid production absent.

Colony diameter on CYA after 7 d (mm). 5 °C no growth, 15 °C 19–20, 20 °C 25–27, 30 °C 31–33, 35 °C 11–12, 37 °C 5–10, 40 °C no growth.

Distribution. Spain.

Notes. *Penicillium irregulare* is related to *P. arizonense*, *P. yarmokense* and *P. canescens*, all belonging to series *Canescentia* (Fig. 4). Species of this series are characterized by the production of biverticillate conidiophores, that occasionally produce additional branching stages (divaricate), with smooth- or rough-walled stipes (Houbraken et al. 2020; Visage et al. 2021). *Penicillium irregulare* can be differentiated from its closest relative *P. arizonense* by the production of shorter stipes (13–152 µm vs 50–400 µm) and metulae (7–10 µm vs. 8–16 µm), and colony reverse yellowish to orange, in contrast to brown shades, even red brown to violet brown on YES agar in *P. arizonense* (Grijseels et al. 2016). In addition, *P. irregulare* was able to grow at 37°C on CYA, but restrictedly (5–10 mm diam. 7 d), while *P. arizonense* does not grow at this temperature.

***Penicillium sicoris* Torres-Garcia, Gené and Dania García, sp. nov.**

Mycobank No: 840559

Figure 13

Etymology. Referring to the Segre River where the fungus was found.

Type. SPAIN, Catalonia, La Noguera, Camarassa, Segre river, from sediments, Dec. 2019, *D. Torres & J. Gené* (**holotype** CBS H-24784, cultures ex-type CBS 148241 = FMR 18076).

Subgeneric classification. Subgenus *Penicillium*, section *Paradoxa*, series *Atramentosa*.

Description. *Mycelium* superficial and immersed, composed of septate, smooth-walled, hyaline hyphae, 3–5 µm wide. **Conidiophores** biverticillate or terverticillate, occasionally irregularly branched with phialides growing directly from branches and divaricate; **stipes** smooth-walled, 25–215 × 3–4.5 µm; **metulae** divergent, 2–3 per branch, vesiculate, 7–20 × 2.5–4 µm (vesicle up to 5.5 µm wide); **phialides** 1–6 per metula, ampulliform, 4–7.5 × 2.5–4 µm; **conidia** smooth-walled, usually globose to subglobose, some broadly ellipsoidal, 2–4.5 × 2–3.5 µm.

Culture characteristics (7 d at 25 °C). Colonies on CYA, 32–34 mm diam., raised at center, radially sulcate, velvety, brownish violet (11D8) at center, pale orange (5A3) and white (1A1) towards periphery, margins entire, sporulation abundant, conidial masses grayish green (28B3); reverse light orange (6A5) to orange (6B7) at center and grayish yellow (4B4) towards periphery; soluble pigment absent. On MEA, 28–30 mm diam., flat, velvety, grayish green (30D6) at center, bluish green (25C8), and white (1A1) at periphery, margins entire, sporulation abundant, conidial masses grayish turquoise (24C3–C4); reverse pea green (29D5), yellowish white (4A2); soluble pigment absent. On YES, 39–43 mm diam., raised at center, radially sulcate, velvety, orange gray (5B2) at center and white (1A1) towards periphery, margins entire, sporulation sparse, conidial masses grayish green (28C3); reverse grayish yellow (4B4) and pale yellow (4A3) at

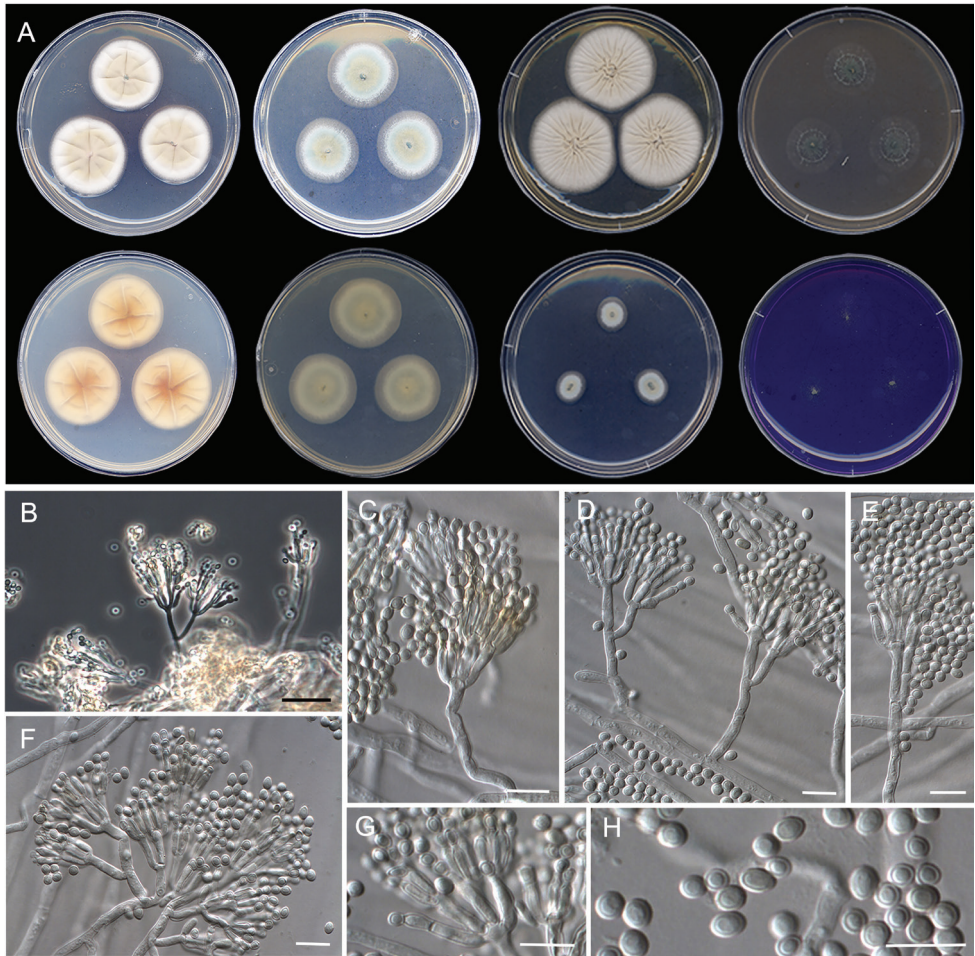


Figure 13. Morphological characters of *Penicillium sicoris* sp. nov. (ex-type FMR 18076). **A** colonies from left to right (top row) CYA, MEA, YES, and OA; (bottom row) CYA reverse, MEA reverse, DG18, and CREA **B–G** conidiophores on MEA **H** conidia. Scale Bars: 25 µm (**B**), 10 µm (**C–H**).

periphery; soluble pigment absent. On OA, 23–24 mm diam., slightly elevated at center, floccose, grayish green (26E6), opaline green (25C6) and brownish gray (5C2) towards periphery, margins slightly fimbriate, sporulation abundant, conidial masses dull green (27D3); reverse pea green (29D5) at center and brownish gray (5C2) towards periphery; soluble pigment absent. On DG18, 13–16 mm diam., slightly raised at center, velvety, olive (3D3) at center, grayish turquoise (24B3) and white (1A1) towards periphery, margins entire, sporulation abundant, conidial masses grayish turquoise (24B3); reverse, grayish green (1C4) and white (1A1) at periphery; soluble pigment absent. On CREA, 21–27 mm diam., slightly elevated at center, velutinous, apple green (29C7), margins regular, sporulation abundant, conidial masses grayish green (26B3–C3); reverse colorless; soluble pigment absent, acid production absent.

Colony diameter on CYA after 7d (mm). 5 °C 3–4, 15 °C 25–26, 20 °C 30–31, 30 °C 29–31, 35 °C no growth, 37 °C no growth, 40 °C no growth.

Distribution. Spain.

Notes. *Penicillium sicoris* is closely related to *P. mexicanum* in series *Atramentosa* (Fig. 3). Phenotypically, species of this series share a moderately fast colony growth and brown reverse on CYA and YES, and good growth on CREA without acid production (Houbraken et al. 2020). However, our species differs in having an orange to grayish yellow reverse on CYA. In addition, *P. sicoris* also differs from its counterpart in several micromorphological features: i.e., its conidiophores are bi- or terverticillate, whereas in *P. mexicanum* they are ter- or quaterverticillate, stipes are shorter (25–215 vs. 65–370 µm), phialides shorter (4–7.5 vs. 7–10 µm) and metulae longer (7–20 vs. 8.5–15.5 µm) than those of *P. mexicanum*, and its conidia are predominantly globose to subglobose, whereas in *P. mexicanum* they are broadly ellipsoidal to ellipsoidal (Visagie et al. 2014c). Moreover, *P. mexicanum* has a more restrictive growth on CREA than *P. sicoris* (5–8 vs. 21–27 mm diam. after 7 d).

***Penicillium submersum* Torres-Garcia, Gené and Dania García, sp. nov.**

MycoBank No: 840560

Figure 14

Etymology. Referring to the submerged sediment sample where the fungus was isolated.

Type. SPAIN, Catalonia, Montsant Natural Park, Siurana's Swamp, from sediments, Feb. 2018, *E. Carvalho* & *J. Gené* (**holotype** CBS H-24785, cultures ex-type CBS 148242 = FMR 17140).

Subgeneric classification. Subgenus *Penicillium*, section *Robsamsonia*, series *Urticicola*.

Description. *Mycelium* superficial and immersed composed of septate, smooth-walled, hyaline hyphae, 2–2.5 µm wide. **Conidiophores** mostly terverticillate, in minor proportion biverticillate and quarterverticillate; **stipes** smooth-walled, 29–142 × 1.5–2.5 µm; **metulae** divergent, mostly 2, occasionally 3 per stipe/branch, 5.5–7.5 × 1.5–4 µm; **phialides** 2–5 per metula, ampulliform, 4–5.5 × 1.5–2.5 µm; **conidia** smooth-walled, ellipsoidal, 3–3.5 × 2–2.5 µm.

Culture characteristics (7 d at 25 °C). Colonies on CYA, 34–37 mm diam., elevated, with some radially furrow, floccose, light yellow (4A5) and yellowish white (4A2) towards periphery, margins entire, sporulation sparse, conidial masses grayish green (28C4); reverse golden brown (5D7) and orange (5A6) at periphery; soluble pigment absent. On MEA, 28–29 mm diam., slightly elevated, floccose, white (1A1) to light yellow (4A5) at periphery, margins entire, sporulation sparse, conidial masses grayish green (27C3); reverse light yellow (4A5); soluble pigment absent. On YES, 33–36 mm diam., slightly elevated at center, radially sulcate, velvety, light brown (6D4) and white (1A1) towards periphery, margins slightly lobate, sporulation sparse, conidial

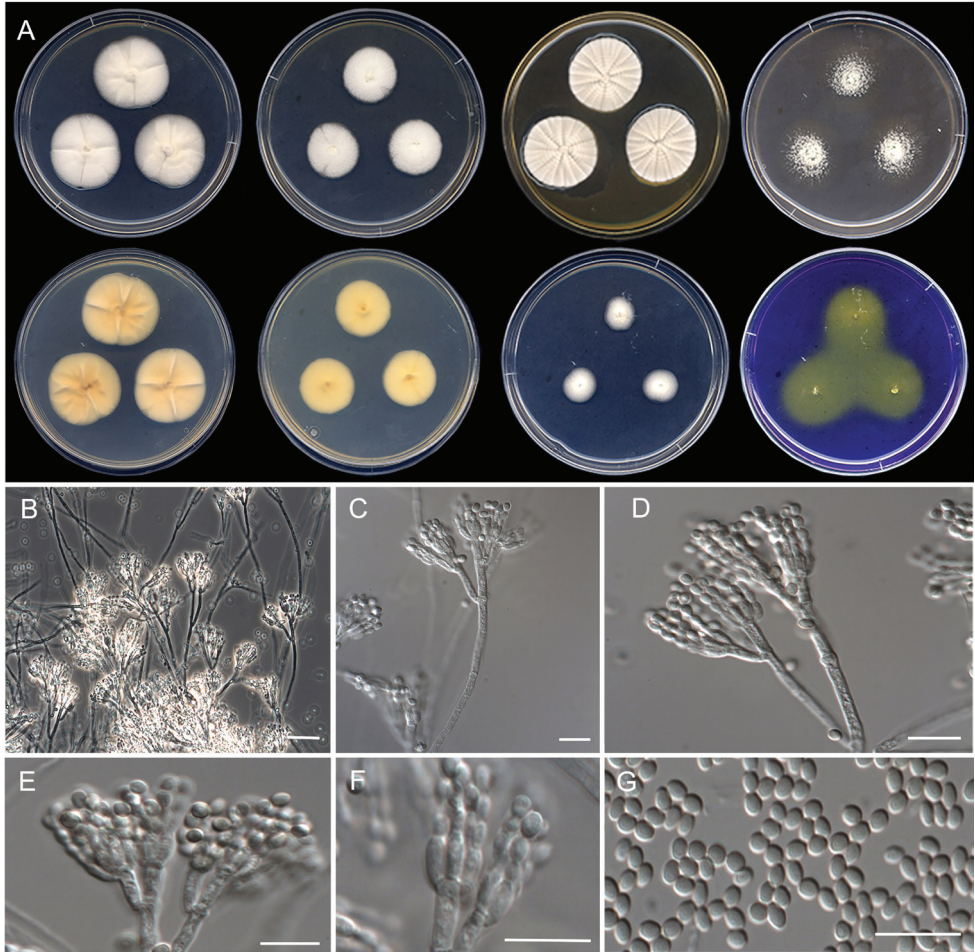


Figure 14. Morphological characters of *Penicillium submersum* sp. nov. (ex-type FMR 17140). **A** colonies from left to right (top row) CYA, MEA, YES, and OA; (bottom row) CYA reverse, MEA reverse, DG18, and CREA **B–F** conidiophores on MEA **G** conidia. Scale Bars: 25 μm (**B**), 10 μm (**C–G**).

masses grayish green (28C3); reverse grayish orange (5B5); soluble pigment absent. On OA, 18–20 mm diam., elevated at center, fasciculate, yellowish white (4A2) and pale gray towards periphery, margins low and entire, sporulation abundant, conidial masses grayish green (28B3); reverse grayish yellow (4C5); soluble pigment absent. On DG18, 11–13 mm diam., elevated, floccose, white (1A1) at center, pale yellow (4A3) and grayish yellow (4C3) towards periphery, margins entire, sporulation abundant, conidial masses grayish green (27C3); reverse light yellow (4A5) and yellowish white (2A2) at periphery; soluble pigment absent. On CREA, 15–19 mm diam., flattened, floccose, white (1A1) and pale yellow (3A3), margins low and irregular, sporulation sparse, conidial masses grayish green (28B3–C3); reverse white (1A1) and pale yellow (3A3); soluble pigment absent, acid production strong.

Colony diameter on CYA after 7d (mm). 5 °C no growth, 15 °C 20–21, 20 °C 25–26, 30 °C 28–30, 35 °C 17–16, 37 °C 9–11, 40 °C no growth.

Distribution. Spain.

Notes. Species in section *Robsamsonia* were characterized by restricted to moderately fast growth rate on CYA at 25 °C (15–32 mm diam in 7 d) and lack or slow of growth on CYA at 30 °C (up to 19 mm diam) (Houbraken et al. 2016; Houbraken et al. 2020). However, the novel species showed faster growth rates on CYA at both temperatures (i.e., 34–37 mm and 28–30 mm diam., respectively). *Penicillium submersum* shares morphological features with the other two species (*P. griseofulvum* and *P. dipodomycola*) of the series *Urticicola* where it is classified (Fig. 2), which consisted in having bi-, ter, or quarterverticillate, divergent, smooth-walled conidiophores and short phialides (up to 7 µm) (Houbraken et al. 2020). However, *P. submersum* shows the shortest phialides within the group (4–5.5 vs. 5–7 µm). In addition, our species has strong acid production on CREA, in contrast to the lack of acid production of *P. griseofulvum* and *P. dipodomycola* in the same medium (Houbraken et al. 2016, 2020); and colony reverse on CYA and YES in *P. submersum* is golden brown to orange and grayish orange, respectively, while in *P. griseofulvum* and *P. dipodomycola* it is beige brown to dark brown in both culture media (Houbraken et al. 2020). Furthermore, *P. griseofulvum* differs from *P. submersum* in its gray colony color, especially on CYA, which is in shades of yellow in our species.

***Penicillium tardochrysogenum* Frisvad, Houbraken & Samson. Persoonia 29: 93. 2012.**

Figure 15

Subgeneric classification. Subgenus *Penicillium*, section *Chrysogena*, series *Chrysogena*.

Description. *Mycelium* superficial and immersed composed of septate, smooth-walled, hyaline hyphae, 2.5–5.5 µm wide. *Conidiophores* biverticillate, terverticillate or quaterverticillate; *stipes* smooth-walled, 40–200 × 2.5–4 µm; *metulae* appressed to slightly divergent, 2–4 per branch or stipe, vesiculate, 6–12.5 × 2–4 µm (vesicle up to 4.5 µm wide); *phialides* 3–6 per metulae, ampulliform, 5.5–7.5 × 1.5–2.5 µm; *conidia* smooth-walled, globose to subglobose, 2.5–3 × 2.5–3 µm.

Culture characteristics (7 d at 25 °C). Colonies on CYA reaching 41–43 mm diam., slightly raised at center, floccose, radially sulcate, yellowish white (1A2) at center to orange white (6A2) and white (1A1) towards periphery, margins slightly lobate, sporulation sparse, conidial masses grayish green (28B3); reverse champagne (4B4) at center to red-haired (6C4) towards periphery; soluble pigment absent. On MEA, 38–39 mm diam., flattened, velvety, grayish green (26D2-E4), white (1A1) towards periphery, margins low and slightly fimbriate, sporulation abundant, conidial masses dull green (25D4); reverse colorless; soluble pigment absent. On YES, 56–57 mm diam., slightly raised at center, floccose, radially sulcate, yellowish white (4A2) at center to champagne (4B4) towards periphery, margins entire, sporulation sparse, conidial masses grayish green (27B3);

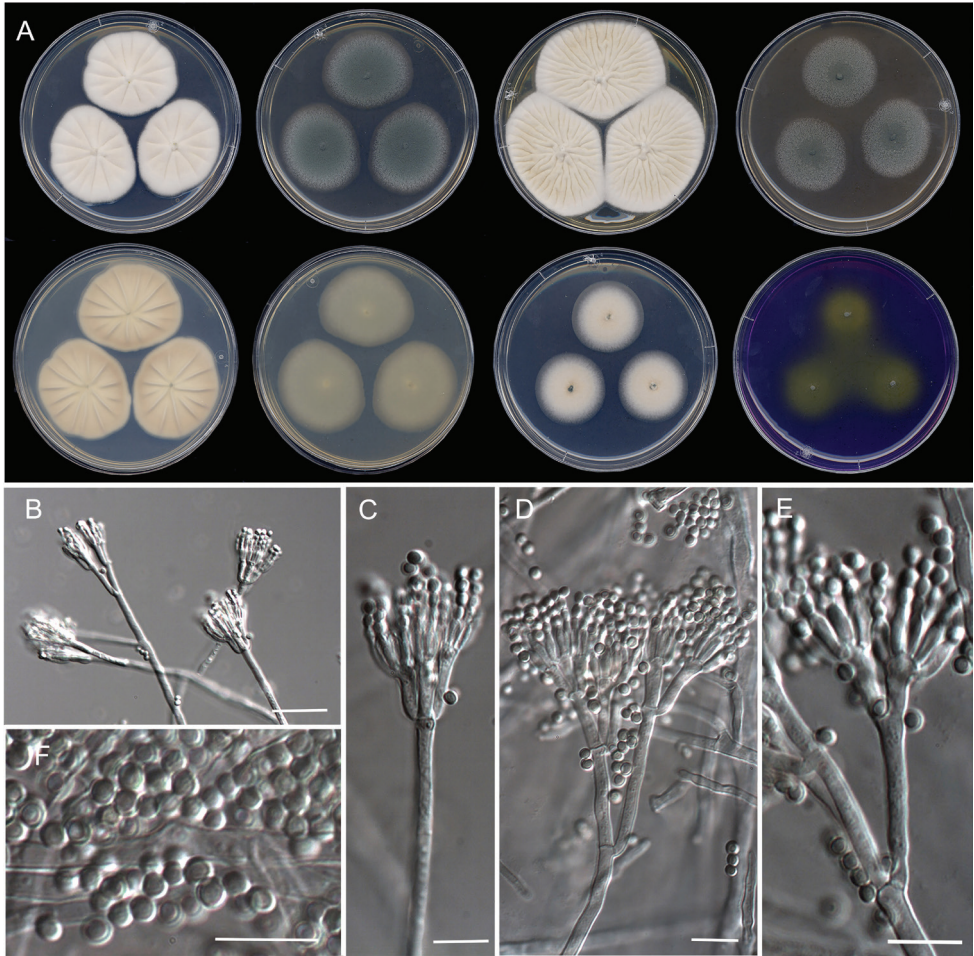


Figure 15. Morphological characters of *Penicillium tardochrysoygenum* (FMR 17137). **A** colonies from left to right (top row) CYA, MEA, YES, and OA; (bottom row) CYA reverse, MEA reverse, DG18, and CREA **B–E** conidiophores on MEA **F** conidia. Scale Bars: 25 µm (**B**), 10 µm (**C–F**).

reverse amber yellow (4B6) at center to maize (yellow) (4A5) towards periphery; soluble pigment absent. On OA, 35–37 mm diam., flattened, velvety, dark green (28F8) at center to greenish gray (28D4) and white (1A1) towards periphery, margins low and entire, sporulation abundant, conidial masses dull green (25D3); reverse honey yellow (4D6) at center and sand yellow (4B3) towards periphery; soluble pigment absent. On DG18, 30–32 mm diam., flattened, floccose, dark green (27F8) at center to pale orange (5A3) and white (1A1) towards periphery, margins low and entire, sporulation abundant, conidial masses grayish green (28C3) at the center; reverse wax yellow (3B5) at center to white (1A1) towards periphery; soluble pigment absent. On CREA, 24–25 mm diam., flattened, floccose, jade green (27E5) at center to yellowish green (30B8) towards periphery, margins slightly fimbriate, sporulation sparse, conidial masses grayish green (27C3–C4); reverse yellowish white (30B8), soluble pigment absent and acid production moderately strong.

Colony diameter on CYA after 7d (mm). 5 °C 3–4, 15 °C 23–24, 20 °C 27–28, 30 °C 31–33, 35 °C 16–19, 37 °C 8–9, 40 °C no growth.

Specimen examined. Spain, Catalonia, Montsant Natural Park, Siurana's Swamp, from sediments, Feb 2018, *E. Carvalho & J. Gené* (FMR 17137).

Distribution. Antarctica and Spain.

Notes. Although *P. tardochrysoenum* was introduced based only on the type specimen collected in the Antarctica, the species was later described as endemic of that continent since it was isolated at high densities on rocks from several Islands and Continental Antarctica (Houbraken et al. 2012; Alves et al. 2019). The Spanish isolate from freshwater sediments represents the first report of this species in temperate regions. Of note, however, is that recently the species has also been reported from historical manuscripts preserved in Iraq (Jasim et al. 2019), but only the ITS barcode was used for confirming the identity of isolates, a well-known gene marker unable to distinguish between closely related penicillia (Houbraken et al. 2012; Visagie et al. 2014a). *Penicillium tardochrysoenum* belongs to series *Chrysogena* and is closely related to *P. allii-sativi*, *P. chrysogenum*, *P. rubens* and *P. vanluykii* (Fig. 1), but it was distinguished from these species and other members of the series by more restricted and floccose colonies on MEA, the lack of sporulation on YES and the production of finely roughened conidia (Houbraken et al. 2012). Despite the high sequence similarity of the markers analyzed with the ex-type strain of *P. tardochrysoenum*, our isolate showed some phenotypic variation regarding the protologue; i.e., faster growth rate after 7 d on MEA (38–39 vs. 18–24 mm), sporulation (sparse) on YES, smooth-walled conidia, and shorter stipes (40–200 × 2.5–4 vs. 150–400 × 2–3 µm) and metulae (6–12.5 × 2–4 vs. 10–13(–18) × 2.5–3.5 µm). These differences suggest that more specimens should be examined for a more accurate morphological characterization of this fungus.

***Penicillium vaccaeorum* Quintanilla, Mycopathol. 80: 74. 1982.**

Mycobank No: 109999

Figure 16

=*Penicillium lacussarmientei* Ramírez, Mycopathol. 96: 29. 1986.

Type. SPAIN, Valladolid, San Miguel del Arroyo, from sandy soil under pine tree; J.A. Quintanilla (*holotype* CBS H-148.83, cultures ex-type CBS 148.83, DTO 9E2, CECT 2753).

Subgeneric classification. Subgenus *Aspergilloides*, section *Citrina*, series *Roseopurpurea*

Description. *Mycelium* superficial and immersed composed of septate, smooth-walled, hyaline hyphae of 1.5–2.5 µm wide. *Conidiophores* monoverticillate, rarely biverticillate and divaricate; *stipes* smooth-walled, vesiculate, 22.5–103 × 1.5–2.5 µm (vesicle up to 4.5 µm); *metulae* divergent 2–3, unequal in length, 7–37 × 1.5–3 µm; *phialides* 2–5 per stipe/metula, ampulliform, 6–8.5 × 2–2.5 µm; *conidia* smooth- or finely roughened, globose, 2–2.5 × 2–2.5 µm.

Culture characteristics (7 d at 25 °C). Colonies on CYA, 20–22 mm diam., slightly raised, velvety, radially sulcate, dull red (8C3) at center to light yellow (4A5) and white (1A1) towards periphery, margins slightly undulate, sporulation sparse, conidial masses grayish green (28B3); reverse brownish orange (5C6); with reddish soluble pigment. On MEA, 24–27 mm diam., slightly elevated, velvety, light yellow (4A5) and pale orange (5A2) at periphery, margins low and entire, sporulation sparse, conidial masses grayish green (27C4); reverse golden yellow (5B7) and reddish-yellow (4A6) at periphery; soluble pigment absent. On YES, 30–32 mm diam., slightly raised at center, velvety, radially sulcate, pale yellow (3A3) to white (1A1) and brownish orange (5C3) towards periphery, margins slightly undulate, sporulation abundant, conidial masses grayish green (28B3); reverse brownish yellow (5C8); soluble pigment absent. On OA, 18–20 mm diam., flattened, velvety, dark green (28F4) to light gray (25D1) and white (1A1) towards periphery, margins low and entire, sporulation abundant, conidial masses dull green (25D3); reverse brown (6E4) and yellowish gray (4B2) at periphery; soluble pigment absent. On DG18, 12–13 mm, slightly raised at center, velvety, radially sulcate, white (1A1) and yellowish white (1A2) towards periphery, margins regular, sporulation sparse, conidial masses grayish green (27C3); reverse light yellow (4A5) and white (1A1) at periphery; soluble pigment absent. On CREA, 9–11 mm diam., flattened, floccose, yellowish green (29B7) and white (1A1) towards periphery, margins entire, sporulation sparse, conidial masses grayish green (28B3); reverse dark gray (1F1); soluble pigment and production of acid absent.

Colony diameter on CYA after 7d (mm). On CYA: 5 °C no growth, 15 °C 13–14, 20 °C 16–17, 30 °C 18–20, 35 °C 6–11, 37 °C no growth, 40 °C no growth.

Specimens examined. Spain, Catalonia, Fogars de Montclús, La Costa de l'Infern, from stream sediments, Oct 2018, *D. Torres* (FMR 17531); Fogars de Montclús, La Costa de l'Infern, from stream sediments, Oct 2018, *D. Torres* (FMR 17534); Aitona, Segre River, from sediments, Dec 2020, *D. Torres* & *J. Gené* (FMR 18100); La Granja d'Escarp, Segre River, from sediments, Dec 2020, *D. Torres* & *J. Gené* (FMR 18123); Balearic Islands, Mallorca, Serra de Tramontana, from stream sediments, Dec 2018, *J. F. Cano* (FMR 17616); Basque Country, from stream sediments, Aug 2019, *J. Gené* (FMR 17967).

Distribution. Argentina, Canada, Chile, Spain, The Netherlands and Turkey.

Notes. *Penicillium vaccaeorum* and *P. lacussarmientei*, two species described from sandy soils in Spain and Chile (Quintanilla 1982; Ramírez 1986), respectively, were considered synonyms of *P. roseopurpureum* by Frisvad et al. (1990), noting that both species were fast growing variants of *P. roseopurpureum*. Later on, based on that criterion and the lack of morphological differences, Houbraken et al. (2011) considered the two former species synonyms of *P. sanguifluum* despite some sequence variation where *P. vaccaeorum* and *P. lacussarmientei* clustered together in a clade sister to that of *P. sanguifluum*. Our phylogeny correlates with Houbraken et al. (2011) who found the same topology. Having the opportunity to examine specimens from both monophyletic sister clades (Fig. 8), we observed consistent phenotypic features to distinguish them. For instance, isolates of *P. vaccaeorum* had longer stipes (up to 103 µm; up to 120 µm in the protologue of the species) (Quintanilla 1982), they were able to grow on CYA at 35 °C (6–11 mm diam. after 7 d), had good sporulation and faster growth on YES agar (30–32 mm diam. 7 d) and more restricted on DG18 (12–13 mm diam. 7 d). In contrast, isolates of

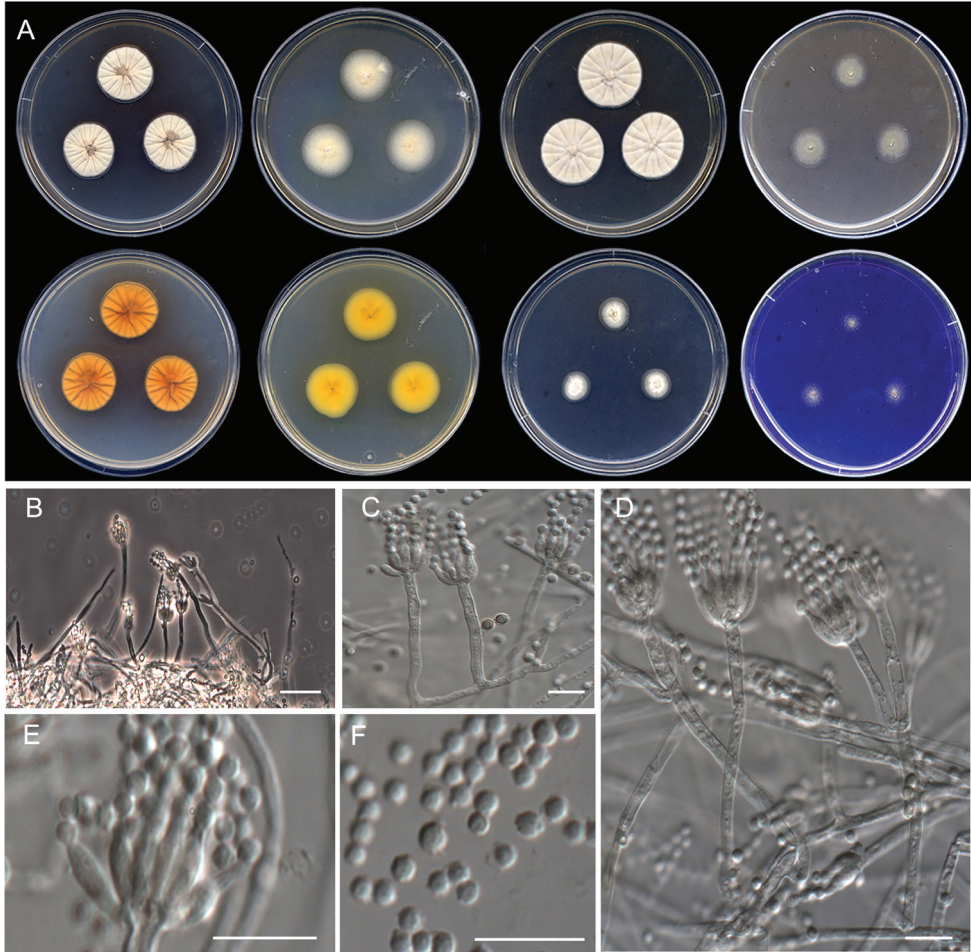


Figure 16. Morphological characters of *Penicillium vaccaeorum* (FMR 17967). **A** colonies from left to right (top row) CYA, MEA, YES, and OA; (bottom row) CYA reverse, MEA reverse, DG18, and CREA **B–E** conidiophores on MEA **F** conidia. Scale Bars: 25 μm (**B**), 10 μm (**C–F**).

the *P. sanguifluum* clade showed considerably shorter conidiophores (15–50 μm long), they were unable to grow above 30 °C, and the colonies on YES and DG18 showed sparsely or absent sporulation and attained 18–28 mm and 16–22 mm diam., respectively (Houbraken et al. 2011). Hence, genetic and phenotypic differences support the reinstatement of *P. vaccaeorum* as an accepted species, with *P. lacussarmientei* considered synonym. This species together with *P. sanguifluum* and *P. roseopurpureum* are classified in series *Roseopurpurea*, which differs from almost all series of the section *Citrina* by species’ monoverticillate conidiophores. The only other series in the section with monoverticillate conidiophores is *Gallaica*, represented exclusively by *P. gallaicum*, which differs from the former series mainly by the production of sclerotia (Houbraken et al. 2020).

According to the revised data, *P. vaccaeorum* occurs worldwide, and is commonly isolated from sandy soils of beaches and forests, and even associated with ants (Table 1).

Discussion

Due to nomenclatural revisions of *Penicillium*, and efforts to release extensive reference sequences for both ex-types and other reference strains (Houbraken and Samson 2011; Visagie et al. 2014a; Houbraken et al. 2020), the number of *Penicillium* species newly described in the last decade has significantly increased, particularly with the examination of fungi recovered from poorly studied substrates or unexplored areas (sensu Hawksworth and Lücking 2017; Wijayawardene et al. 2020). Although *Penicillium* species are commonly isolated from aquatic environments (Niewolak 1975; Tóthová 1999; Amaral-Zettler et al. 2002), studies exploring their diversity are scarce. For instance, Heo et al. (2019) recovered *P. brasilianum*, *P. crustosum*, *P. expansum*, *P. oxalicum* and *P. piscarium* from freshwater environments in Korea. Only recently, *Penicillium* diversity has begun to be investigated in marine sediments (Gonçalves et al. 2013; Kirichuk et al. 2017; Ogaki et al. 2020a), and some novel species have even been described from this substrate, such as *P. piltunense*, *P. ochotense* and *P. attenuatum* (Kirichuk et al. 2017), although they are currently considered conspecific with *P. antarcticum* (Visagie et al. 2021).

Several studies reveal that the fungal biomass and, subsequently, ascomycetes inhabiting freshwater sediments are fundamental to the decomposition of deposited organically bound C and N, using carbohydrates, phenolic compounds and carboxylic acids as carbon sources (Huang et al. 2010; Zhang et al. 2013; Zhang et al. 2014). The penicillia might also contribute greatly to this activity, although further studies are needed to define the spectrum of species and their role in this particular substrate.

In our contribution to the diversity of *Penicillium* from freshwater sediments, we identified several interesting species, such as *P. heteromorphum* and *P. tardochrysogenum* only so far known from China and Antarctica, respectively (Kong and Qi 1988; Alves et al. 2019). Our finding reveals a wider distribution of these taxa, being first reports in freshwater sediment samples, as in the case of the resurrected species *P. vaccaeorum* and its counterpart *P. sanguifluum*. These two latter species (classified in section *Citrina*) seem to be common penicillia inhabiting soil (Houbraken et al. 2011). Furthermore, we recovered several isolates representative of new species described above as *P. ausonianum*, *P. guarroi*, *P. irregulare*, *P. sicoris* and *P. submersum*. Of note is that of the fifteen *Penicillium* isolates investigated (Table 1), twelve were obtained from PDA supplemented with 0.2% cycloheximide, a culture technique previously used to recover keratinophilic or extremotolerant fungi such as black yeasts from various substrates (Ulfig et al. 1997; Salgado et al. 2004; Madrid et al. 2016). Isolates obtained using this culture medium, and therefore resistant to a relatively high concentration of cycloheximide, corresponded to *P. ausonianum*, *P. irregulare*, *P. submersum*, *P. tardochrysogenum*, as well as all those identified as *P. vaccaeorum* and *P. sanguifluum*. Cycloheximide tolerance in *Penicillium* has been previously studied by Seifert and Giuseppin (2000), even recently two novel species, *P. krskae* and *P. silybi*, have been described as resistant to cycloheximide (Labuda et al. 2021). Other fungi with the ability to grow at high doses of that antimicrobial agent can cause human infections, such as numerous dermatophytes, black yeasts, or members in the *Ophiostomatales* (de Hoog et al. 2020). However, the meaning of the cycloheximide

resistance in penicillia would deserve further studies, for instance at genomic level. On the other hand, the isolates of *P. guarroi*, *P. heteromorphum* and *P. sicoris* were obtained from DRBC. It is well-known that this culture medium restricts fast-growing moulds due mainly to the Rose Bengal effect, allowing them to recover fungi with slower growth rates, a feature shown by the mentioned species in comparison with other *Penicillium* species that have been previously recovered from aquatic environments (Gonçalves et al. 2019; Heo et al. 2019). The efficacy of the DRBC for the detection of filamentous fungi and yeasts in aquatic environments was proven in a study investigating the yield across different media, in which it was found to be the best in quantity and diversity of fungi detection in different water samples tested (Pereira et al. 2010). According to our experience, it is important to use different media in order to investigate and recover the greatest diversity of species as possible from environmental samples.

Most of the new species described here were mainly recovered from samples collected in rivers and streams of the north-western Mediterranean region, an area recognized as one of the most species-rich regions in Southern Europe (Máiz-Tomé et al. 2017; Rundel et al. 2018). This fact was particularly highlighted in the study of Guevara-Suarez et al. (2020) on species diversity of coprophilous penicillium-like fungi, from which the highest number of species identified and novel taxa described were recovered from samples collected in Mediterranean localities. Therefore, regarding fluvial sediments as an accumulative substrate in biodiversity of the environment, it is not surprising that freshwater sediments from the Mediterranean region comprise a great reservoir of novel fungal lineages in general.

Acknowledgements

This study was supported by the Spanish Ministerio de Economía y Competitividad, grant CGL2017–88094-P.

References

- Abdelwahab MF, Fouad MA, Kamel MS, Özkaya FC, Kalscheuer R, Müller WEG, Lin W, Liu Z, Ebrahim W, Daletos G, Proksch P (2018) Tanzawaic acid derivatives from freshwater sediment-derived fungus *Penicillium* sp. *Fitoterapia* 128: 258–264. <https://doi.org/10.1016/j.fitote.2018.05.019>
- Abe S (1956) Studies on the classification of the Penicillia. *The Journal of General and Applied Microbiology* 2: 1–194. <https://doi.org/10.2323/jgam.2.1>
- Aime MC, Miller AN, Aoki T, Bensch K, Cai L, Crous PW, Hawksworth DL, Hyde KD, Kirk PM, Lücking R, May TW, Malosso E, Redhead SA, Rossman AY, Stadler M, Thines M, Yurkov AM, Zhang N, Schoch CL (2021) How to publish a new fungal species, or name, version 3.0. *IMA Fungus*, 12: e11. <https://doi.org/10.1186/s43008-021-00063-1>
- Alves IM, Gonçalves VN, Oliveira FS, Schaefer CE, Rosa CA, Rosa LH (2019) The diversity, distribution, and pathogenic potential of cultivable fungi present in rocks from the

- South Shetlands archipelago, Maritime Antarctica. *Extremophiles* 23: 327–336. <https://doi.org/10.1007/s00792-019-01086-8>
- Amaral-Zettler LA, Gómez F, Zettler E, Keenan BG, Amils R, Sogin ML (2002) Microbiology: eukaryotic diversity in Spain's River of Fire. *Nature* 417: 137–137. <https://doi.org/10.1038/417137a>
- Barbosa RN, Bezerra JD, Souza-Motta CM, Frisvad JC, Samson RA, Oliveira NT, Houbraken J (2018) New *Penicillium* and *Talaromyces* species from honey, pollen and nests of stingless bees. *Antonie van Leeuwenhoek* 111: 1883–1912. <https://doi.org/10.1007/s10482-018-1081-1>
- Behera BK, Chakraborty HJ, Patra B, Rout AK, Dehury B, Das BK, Sarkar DJ, Parida PK, Raman RK, Rao AR, Rai A, Mohapatra T (2020) Metagenomic analysis reveals bacterial and fungal diversity and their bioremediation potential from sediments of river Ganga and Yamuna in India. *Frontiers in Microbiology* 11: e556136. <https://doi.org/10.3389/fmicb.2020.556136>
- Cecchi G, Vagge G, Cutroneo L, Greco G, Piazza SD, Faga M, Zotti M, Capello M (2019) Fungi as potential tool for polluted port sediment remediation. *Environmental Science and Pollution Research* 26: 35602–35609. <https://doi.org/10.1007/s11356-019-04844-5>
- Chen AJ, Sun B D, Houbraken J, Frisvad JC, Yilmaz N, Zhou YG (2016) New *Talaromyces* species from indoor environments in China. *Studies in Mycology* 84: 119–144. <https://doi.org/10.1016/j.simyco.2016.11.003>
- Darriba D, Taboada GL, Doallo R, Posada D (2012) jModelTest 2: more models, new heuristics and parallel computing. *Nature Methods* 9: 772–772. <https://doi.org/10.1038/nmeth.2109>
- De Hoog GS, Guarro J, Gené J, Ahmed S, Al-Hatmi AMS, Figueras MJ, Vitale RG (2020) Atlas of Clinical Fungi, 4th edn. Foundation Atlas of Clinical Fungi: Hilversum, The Netherlands, 1599 pp.
- Diao YZ, Chen Q, Jiang XZ, Houbraken J, Barbosa RN, Cai L, Wu WP (2019) *Penicillium* section *Lanata-Divaricata* from acidic soil. *Cladistics* 35: 514–549. <https://doi.org/10.1111/cla.12365>
- Edgar RC (2004) MUSCLE: multiple sequence alignment with high accuracy and high throughput. *Nucleic Acids Research* 32: 1792–1797. <https://doi.org/10.1093/nar/gkh340>
- Farris JS, Källersjö M, Kluge AG, Bult C (1994) Testing significance of incongruence. *Cladistics* 10: 315–319. <https://doi.org/10.1111/j.1096-0031.1994.tb00181.x>
- Frisvad JC (1981) Physiological criteria and mycotoxin production as aids in identification of common asymmetric *Penicillia*. *Applied and Environmental Microbiology* 41: 568–579. <https://doi.org/10.1128/aem.41.3.568579.1981>
- Frisvad JC, Samson RA, Stolk AC (1990) Disposition of recently described species of *Penicillium*. *Persoonia* 14: 209–232.
- Frisvad JC, Samson RA (2004) Polyphasic taxonomy of *Penicillium* subgenus *Penicillium*. A guide to identification of food and air-borne terverticillate *Penicillia* and their mycotoxins. *Studies in Mycology* 49: 1–174.
- Glass NL, Donaldson GC (1995) Development of primer sets designed for use with the PCR to amplify conserved genes from filamentous ascomycetes. *Applied and Environmental Microbiology* 61: 1323–1330. <https://doi.org/10.1128/aem.61.4.1323-1330.1995>

- Gonçalves MFM, Santos L, Silva BMV, Abreu AC, Vicente TF, Esteves AC, Alves A (2019) Biodiversity of *Penicillium* species from marine environments in Portugal and description of *Penicillium lusitanum* sp. nov., a novel species isolated from sea water. *International Journal of Systematic and Evolutionary Microbiology* 69: 3014–3021. <https://doi.org/10.1099/ijsem.0.003535>
- Gonçalves VN, Campos LS, Melo IS, Pellizari VH, Rosa CA, Rosa LH (2013) *Penicillium solitum*: a mesophilic, psychrotolerant fungus present in marine sediments from Antarctica. *Polar Biology* 36: 1823–1831. <https://doi.org/10.1007/s00300-013-1403-8>
- Grijseels S, Nielsen JC, Randelovic M, Nielsen J, Nielsen KF, Workman M, Frisvad JC (2016) *Penicillium arizonense*, a new, genome sequenced fungal species, reveals a high chemical diversity in secreted metabolites. *Scientific Reports – Nature* 6: 1–13. <https://doi.org/10.1038/srep35112>
- Grossart HP, Van den Wyngaert S, Kagami M, Wurzbacher C, Cunliffe M, Rojas-Jimenez K (2019) Fungi in aquatic ecosystems. *Nature Reviews Microbiology* 17: 339–354. <https://doi.org/10.1038/s41579-019-0175-8>
- Guevara-Suárez M, García D, Cano-Lira JF, Guarro J, Gené J (2020) Species diversity in *Penicillium* and *Talaromyces* from herbivore dung, and the proposal of two new genera of penicillium-like fungi in *Aspergillaceae*. *Fungal Systematics and Evolution* 5: 39–75. <https://doi.org/10.3114/fuse.2020.05.03>
- Guijarro B, Larena I, Melgarejo P, De Cal A (2017) Adaptive conditions and safety of the application of *Penicillium frequentans* as a biocontrol agent on stone fruit. *International Journal of Food Microbiology* 254: 25–35. <https://doi.org/10.1016/j.ijfoodmicro.2017.05.004>
- Guindon S, Gascuel O (2003) A simple, fast and accurate method to estimate large phylogenies by maximum-likelihood. *System* 52: 696–704. <https://doi.org/10.1080/10635150390235520>
- Haelewaters D, De Kesel A, Pfister DH (2018) Integrative taxonomy reveals hidden species within a common fungal parasite of ladybirds. *Scientific Reports* 8(1):1–16. <https://doi.org/10.1038/s41598-018-34319-5>
- Hageskal G, Knutsen AK, Gaustad P, de Hoog GS, Skaar I (2006) Diversity and significance of mold species in Norwegian drinking water. *Applied Environmental Microbiology* 72: 7586–7593. <https://doi.org/10.1128/AEM.01628-06>
- Hawksworth DL, Lücking R (2017) Fungal diversity revisited: 2.2 to 3.8 million species. In: Heitman J, Howlett B, Crous P, Stukenbrock E, James T, Gow N (Eds) *The Fungal Kingdom*. ASM Press, Washington, 79–95. <https://doi.org/10.1128/microbiolspec.FUNK-0052-2016>
- Heo I, Hong K, Yang H, Lee HB, Choi YJ, Hong SB (2019) Diversity of *Aspergillus*, *Penicillium*, and *Talaromyces* species isolated from freshwater environments in Korea. *Mycobiology* 47: 12–19. <https://doi.org/10.1080/12298093.2019.1572262>
- Hespanhol L, Vallio CS, Costa LM, Saragiotto BT (2019) Understanding and interpreting confidence and credible intervals around effect estimates. *Brazilian Journal of Physical Therapy* 23: 290–301. <https://doi.org/10.1016/j.bjpt.2018.12.006>
- Hillis DM, Bull JJ (1993) An empirical test of bootstrapping as a method for assessing confidence in phylogenetic analysis. *Systematic Biology* 42: 182–192. <https://doi.org/10.1093/sysbio/42.2.182>

- Hocking AD, Pitt JI (1980) Dichloran-glycerol medium for enumeration of xerophilic fungi from low-moisture foods. *Applied Environmental Microbiology* 39: 488–492. <https://doi.org/10.1128/aem.39.3.488-492.1980>
- Hong SB, Cho HS, Shin HD, Frisvad JC, Samson RA (2006) Novel *Neosartorya* species isolated from soil in Korea. *International Journal of Systematic and Evolutionary Microbiology* 56: 477–486. <https://doi.org/10.1099/ijms.0.63980-0>
- Houbraken J, Frisvad JC, Samson RA (2011) Taxonomy of *Penicillium* section *Citrina*. *Studies in Mycology* 70: 53–138. <https://doi.org/10.3114/sim.2011.70.02>
- Houbraken J, Samson RA (2011) Phylogeny of *Penicillium* and the segregation of *Trichocomaceae* into three families. *Studies in Mycology* 70: 1–51. <https://doi.org/10.3114/sim.2011.70.01>
- Houbraken J, Frisvad JC, Seifert KA, Overy DP, Tuthill DM, Valdez JG, Samson RA (2012) New penicillin-producing *Penicillium* species and an overview of section *Chrysogena*. *Persoonia* 29: 78–100. <https://doi.org/10.3767/003158512X660571>
- Houbraken J, de Vries RP, Samson RA (2014) Modern taxonomy of biotechnologically important *Aspergillus* and *Penicillium* species. *Applied and Environmental Microbiology* 86: 199–249. <https://doi.org/10.1016/B978-0-12-800262-9.00004-4>
- Houbraken J, Wang L, Lee HB, Frisvad JC (2016) New sections in *Penicillium* containing novel species producing patulin, pyripyropens or other bioactive compounds. *Persoonia* 36: 299–314. <https://doi.org/10.3767/003158516X692040>
- Houbraken J, Kocsubé S, Visagie CM, Yilmaz N, Wang XC, Meijer M, Kraak B, Hubka V, Bensch K, Samson RA, Frisvad JC (2020) Classification of *Aspergillus*, *Penicillium*, *Talaromyces* and related genera (*Eurotiales*): an overview of families, genera, subgenera, sections, series and species. *Studies in Mycology* 95: 5–169. <https://doi.org/10.1016/j.simyco.2020.05.002>
- Huang TL, Chai BB, Qiu ES, Zhou WH (2010) Microbial effects on phosphorus release from sediments on the multi-phase interface of water-sediment-biofacies. *Journal of Basic Science and Engineering* 18: 61–70.
- Jasim AA, Mohammed BT, Lahuf AA (2019) Molecular and enzymatic properties of fungi isolated from historical manuscripts preserved at the Al-Hussein Holy Shrine. *Biochemical and Cellular Archives* 19: 4295–4305.
- Jones EBG, Pang KL (2012) Tropical aquatic fungi. *Biodiversity and Conservation* 21: 2403–2423. <https://doi.org/10.1007/s10531-011-0198-6>
- Kelley J, Kinsey GC, Paterson RRM, Pitchers R (2001) Identification and control of fungi in distribution systems. AWWA Research Foundation. Denver, USA, 150pp.
- Khomich M, Davey ML, Kauserud H, Rasconi S, Andersen T (2017) Fungal communities in Scandinavian lakes along a longitudinal gradient. *Fungal Ecology* 27: 36–46. <https://doi.org/10.1016/j.funeco.2017.01.008>
- Kirichuk NN, Pivkin MV, Matveeva TV (2017) Three new *Penicillium* species from marine subaqueous soils. *Mycological Progress* 16: 15–26. <https://doi.org/10.1007/s11557-016-1247-z>
- Kong HZ, Qi ZT (1988) Three new species of *Penicillium*. *Mycosystema* 1: 107–114.
- Kornerup A, Wanscher JH (1978) *Methuen Handbook of Colour*, 3rd edn.; Methuen: London, UK, 256 pp.

- Labuda R, Bacher M, Rosenau T, Gasparotto E, Gratzl H, Doppler M, Sulyok M, Kubátova A, Berger H, Cank K, Raja HA, Oberlies NH, Schüller C, Strauss J (2021) Polyphasic approach utilized for the identification of two new toxigenic members of *Penicillium* section *Exilicaulis*, *P. krskae* and *P. silybi* spp. nov. *Journal of Fungi*, 7: e557. <https://doi.org/10.3390/jof7070557>
- Liang LJ, Jeewon R, Dhandevi P, Durairajan SSK, Li H, Lin FC, Wang HK (2021) A novel species of *Penicillium* with inhibitory effects against *Pyricularia oryzae* and fungal pathogens inducing *Citrus* diseases. *Frontiers in Cellular and Infection Microbiology* 10: e604504. <https://doi.org/10.3389/fcimb.2020.604504>
- Liu YJ, Whelen S, Hall BD (1999) Phylogenetic relationships among ascomycetes: evidence from an RNA polymerase II subunit. *Molecular Biology and Evolution* 16: 1799–1808. <https://doi.org/10.1093/oxfordjournals.molbev.a026092>
- Liu J, Wang J, Gao G, Bartlam MG, Wang Y (2015) Distribution and diversity of fungi in freshwater sediments on a river catchment scale. *Frontiers in Microbiology*. 6: e329. <https://doi.org/10.3389/fmicb.2015.00329>
- Madrid H, Hernández-Restrepo M, Gené J, Cano J, Guarro J, Silva V (2016) New and interesting Chaetothyrialean fungi from Spain. *Mycological Progress* 15: 1179–1201. <https://doi.org/10.1007/s11557-016-1239-z>
- Maharachchikumbura SSN, Chen Y, Ariyawansa HA, Hyde KD, Haelewaters D, Perera RH, Samarakoon MC, Wanasinghe DN, Bustamante DE, Liu J-K, Lawrence DP, Cheewangkoon R, Stadler, M. (2021) Integrative approaches for species delimitation in Ascomycota. *Fungal Diversity*, 109: 155–179. <https://doi.org/10.1007/s13225-021-00486-6>
- Máiz-Tomé L, Darwall W, Numa C, Barrios V, Smith KG (2017) Freshwater key biodiversity areas in the north-western Mediterranean sub-region. IUCN, Gland, Switzerland, Cambridge, UK and Malaga, Spain 64: 1–48. <https://doi.org/10.2305/IUCN.CH.2017.SSC-OP.64.en>
- Miller MA, Pfeifferm W, Schwartz T (2012) The CIPRES science gateway: Enabling high-impact science for phylogenetics researchers with limited resources. In *Proceedings of the 1st Conference of the extreme science and engineering discovery environment: Bridging from the extreme to the campus and beyond*, Chicago, IL, USA, 16 July 2012; Association for Computing Machinery, New York, USA, 39: 1–8. <https://doi.org/10.1145/2335755.2335836>
- Niewolak S (1975) The occurrence of microorganisms in the water of some lakes in the district of Wegorzewo. *Acta Hydrobiologica* 17: 371–390.
- Ogaki MB, Coelho LC, Vieira R, Neto AA (2020a) Cultivable fungi present in deep-sea sediments of Antarctica: taxonomy, diversity, and bioprospecting of bioactive compounds. *Extremophiles* 24: 227–238. <https://doi.org/10.1007/s00792-019-01148-x>
- Ogaki MB, Vieira R, Muniz MC, Zani CL (2020b) Diversity, ecology, and bioprospecting of culturable fungi in lakes impacted by anthropogenic activities in Maritime Antarctica. *Extremophiles* 24: 637–655. <https://doi.org/10.1007/s00792-020-01183-z>
- Park MS, Oh SY, Fong JJ, Houbraken J, Lim YW (2019) The diversity and ecological roles of *Penicillium* in intertidal zones. *Scientific Reports* 9: 1–11. <https://doi.org/10.1038/s41598-019-49966-5>
- Pangging M, Nguyen TT, Lee HB (2019) New records of four species belonging to *Eurotiales* from soil and freshwater in Korea. *Mycobiology* 47: 154–164. <https://doi.org/10.1080/12298093.2018.1554777>

- Pascoal C, Cássio F (2004) Contribution of fungi and bacteria to leaf litter decomposition in a polluted river. *Applied Environmental Microbiology* 70: 5266–5273. <https://doi.org/10.1128/AEM.70.9.5266-5273.2004>
- Pascoal C, Marvanová L, Cássio F (2005) Aquatic hyphomycete diversity in streams of Northwest Portugal. *Fungal Diversity* 19: 109–128.
- Pereira VJ, Fernandes D, Carvalho G, Benoliel MJ (2010) Assessment of the presence and dynamics of fungi in drinking water sources using cultural and molecular methods. *Water Research* 44: 4850–4859. <https://doi.org/10.1016/j.watres.2010.07.018>
- Perrone G, Susca A (2017) *Penicillium* species and their associated mycotoxins. In: *Mycotoxigenic Fungi. Methods in Molecular Biology* Moretti A., Susca A. (Eds). Humana Press: New York, NY, USA, Volume 1542, 107–119. https://doi.org/10.1007/978-1-4939-6707-0_5
- Peterson SW (2008) Phylogenetic analysis of *Aspergillus* species using DNA sequences from four loci. *Mycologia* 100: 205–226. <https://doi.org/10.3852/mycologia.100.2.205>
- Pitt JI (1979) The genus *Penicillium* and its teleomorphic states *Eupenicillium* and *Talaromyces*. Academic Press Inc. Ltd.: London, UK, 634 pp.
- Pitt JI, Hocking AD (2009) *Fungi and food spoilage*. 3rd edn.; Springer US: New York, NY, USA, 388 pp. https://doi.org/10.1007/978-0-387-92207-2_2
- Quintanilla JA (1982) Three new species of *Penicillium* isolated from soil. *Mycopathologia* 80: 73–82. <https://doi.org/10.1007/BF00641181>
- Ramírez C (1986) A new species of *Penicillium* from the Chilean Tierra del Fuego. *Mycopathologia* 96: 29–32. <https://doi.org/10.1007/BF00467682>
- Rodríguez-Andrade E, Stchigel AM, Cano-Lira JF (2021) New xerophilic species of *Penicillium* from Soil. *Journal of Fungi* 7: e126. <https://doi.org/10.3390/jof7020126>
- Ronquist F, Teslenko M, Van Der Mark P, Ayres DL, Darling A, Höhna S, Larget B, Liu L, Suchard, MA, Huelsenbeck JP (2012) MrBayes 3.2: efficient Bayesian phylogenetic inference and model choice across a large model space. *System* 61: 539–542. <https://doi.org/10.1093/sysbio/sys029>
- Rundel PW, Arroyo MTK, Cowling RM, Keeley JE, Lamont BB, Pausas JG, Vargas P (2018) Fire and plant diversification in Mediterranean-climate regions. *Frontiers in Plant Science* 9: e851. <https://doi.org/10.3389/fpls.2018.00851>
- Salgado CG, da Silva JP, Picanço-Diniz JA, da Silva MB, da Costa PF, Teixeira C, Salgado UI (2004) Isolation of *Fonsecaea pedrosoi* from thorns of *Mimosa pudica*, a probable natural source of chromoblastomycosis. *Revista do Instituto de Medicina Tropical de São Paulo* 46: 33–36. <https://doi.org/10.1590/S0036-46652004000100006>
- Samson RA, Houbraken J, Thrane U, Frisvad JC, Andersen B (2010) *CBS Laboratory Manual Series 2: Food and indoor fungi*. The Netherlands: CBS-KNAW Fungal Biodiversity Centre Utrecht, 269 pp.
- Samson R, Rajput V, Shah M, Yadav R, Sarode P, Dastager SG, Dharne MS, Khairnar K (2020) Deciphering taxonomic and functional diversity of fungi as potential bioindicators within confluence stretch of Ganges and Yamuna rivers, impacted by anthropogenic activities. *Chemosphere* 252: e126507. <https://doi.org/10.1016/j.chemosphere.2020.126507>
- Seifert KA, Giuseppin S (2000). Cycloheximide tolerance as a taxonomic character in *Penicillium*. In: *Integration of Modern Taxonomic Methods for Penicillium and Aspergillus Classification*. Samson RA, Pitt JI (Eds), Harword Publishers; Amsterdam, The Netherlands, 259–263

- Sonjak S, Frisvad JC, Gunde-Cimerman N (2006) *Penicillium* mycobiota in Arctic subglacial ice. *Microbial Ecology* 52: 207–216. <https://doi.org/10.1007/s00248-006-9086-0>
- Stamatakis A (2014) RAxML version 8: A tool for phylogenetic analysis and post-analysis of large phylogenies. *Bioinformatics* 30: 1312–1313. <https://doi.org/10.1093/bioinformatics/btu033>
- Sutcliffe B, Chariton AA, Harford AJ, Hose GC, Greenfield P, Midgley DJ, Paulsen IT (2018) Diverse fungal lineages in subtropical ponds are altered by sediment-bound copper. *Fungal Ecology* 34: 28–42. <https://doi.org/10.1016/j.funeco.2018.03.003>
- Tamura K, Stecher G, Peterson D, Filipinski A, Kumar S (2013) MEGA6: molecular evolutionary genetics analysis version 6.0. *Molecular Biology and Evolution* 30: 2725–2729. <https://doi.org/10.1093/molbev/mst197>
- Taylor JW, Jacobson DJ, Kroken S, Kasuga T, Geiser DM, Hibbeti DS, Fisher MC (2000) Phylogenetic species recognition and species concepts in fungi. *Fungal Genetics and Biology* 31: 21–32. <https://doi.org/10.1006/fgbi.2000.1228>
- Thambugala KM, Daranagama DA, Phillips AJL, Kannangara SD, Promputtha I (2020) Fungi vs. Fungi in biocontrol: an overview of fungal antagonists applied against fungal plant pathogens. *Frontiers in Cellular and Infection Microbiology* 10: e604923. <https://doi.org/10.3389/fcimb.2020.604923>
- Thompson JD, Higgins DG, Gibson TJ (1994) CLUSTAL W: improving the sensitivity of progressive multiple sequence alignment through sequence weighting, position-specific gap penalties and weight matrix choice. *Nucleic Acids Research* 22: 4673–4680. <https://doi.org/10.1093/nar/22.22.4673>
- Tóthová L (1999) Occurrence of mitosporic fungi in the Slovak section of the Danube river. *Biologia* 54: 379–385.
- Ulfing K, Guarro J, Cano J, Gené J, Vidal P, Figueras MJ (1997) General assessment of the occurrence of keratinolytic fungi in river and marine beach sediments of Catalanian waters (Spain). *Water Air Soil Pollution* 94: 275–287. <https://doi.org/10.1007/BF02406063>
- Vaidya G, Lohman DJ, Meier R (2011) SequenceMatrix: concatenation software for the fast assembly of multi-gene datasets with character set and codon information. *Cladistics* 27: 171–180. <https://doi.org/10.1111/j.1096-0031.2010.00329.x>
- Visagie CM, Houbraeken J, Frisvad JC, Hong SB, Klaassen CHW, Perrone G, Seifert KA, Varga J, Yaguchi T, Samson RA (2014a) Identification and nomenclature of the genus *Penicillium*. *Studies in Mycology* 78: 343–371. <https://doi.org/10.1016/j.simyco.2014.09.001>
- Visagie CM, Seifert KA, Houbraeken J, Samson RA, Jacobs K (2014b) Diversity of *Penicillium* section *Citrina* within the fynbos biome of South Africa, including a new species from a *Protea repens* infructescence. *Mycologia* 106: 537–552. <https://doi.org/10.3852/13-256>
- Visagie CM, Hirooka Y, Tanney JB, Whitfield E, Mwange K, Meijer M, Asmend AS, Seifert KA, Samson RA (2014c) *Aspergillus*, *Penicillium* and *Talaromyces* isolated from house dust samples collected around the world. *Studies in Mycology* 78: 63–139. <https://doi.org/10.1016/j.simyco.2014.07.002>
- Visagie CM, Renaud JB, Burgess KMN, Malloch DW, Clark D, Ketch L, Urb M, Louis-Seize G, Assabgui R, Sumarah MW, Seifert KA (2016a) Fifteen new species of *Penicillium*. *Persoonia* 36: 247–280. <https://doi.org/10.3767/003158516X691627>

- Visagie CM, Seifert KA, Houbraken J, Samson RA, Jacobs K. (2016b). A phylogenetic revision of *Penicillium* sect. *Exilicaulis*, including nine new species from fynbos in South Africa. *IMA fungus* 7: 75–117. <https://doi.org/10.5598/ima fungus.2016.07.01.06>
- Visagie CM, Frisvad JC, Houbraken J, Visagie A, Samson RA, Jacobs K (2021) A re-evaluation of *Penicillium* section *Canescentia*, including the description of five new species. *Persoonia* 46: 163–187. <https://doi.org/10.3767/persoonia.2021.46.06>
- Werner KE, Kasai M, Francesconi A, Mu FC, Chanock SJ, Walsh TJ (1998) Rapid extraction of genomic DNA from medically important yeasts and filamentous fungi by high-speed cell disruption. *Journal of Clinical Microbiology* 36: 1625–1629. <https://doi.org/10.1128/JCM.36.6.1625-1629.1998>
- White TJ, Bruns T, Lee S, Taylor J (1990) Amplification and direct sequencing of fungal ribosomal RNA genes for phylogenetics. In: Innis MA, Gelfand DH, Sninsky JJ, White TJ (Eds). *PCR Protocols: A guide to methods and applications*. Academic Press, San Diego, CA, USA, 315–322. <https://doi.org/10.1016/B978-0-12-372180-8.50042-1>
- Wijayawardene NN, Hyde KD, Al-Ani LKT, Tedersoo L, Haelewaters D, Rajeshkumar KC, Zhao RL, Aptroot A, Leontyev DV, Saxena RK, Tokarev YS, Dai DQ, Letcher PM, Stephenson SL, Ertz D, Lumbsch HT, Kukwa M, Issi IV, Madrid H, Phillips AJL, Selbmann L, Pfliegler WP, Horváth E, Bensch K, Kirk PM, Kolaříková K, Raja HA, Radek R, Papp V, Dima B, Ma J, Malosso E, Takamatsu S, Rambold G, Gannibal PB, Triebel D, Gautam AK, Avasthi S, Suetrong S, Timdal E, Fryar SC, Delgado G, Réblová M, Doilom M, Dolatabadi S, Pawłowska J, Humber RA, Kodsueb R, Sánchez-Castro I, Goto BT, Silva DKA, de Souza FA, Oehl F, da Silva GA, Silva IR, Błaszczowski J, Jobim K, Maia LC, Barbosa FR, Fiuza PO, Divakar PK, Shenoy BD, Castañeda-Ruiz RF, Somrithipol S, Lateef AA, Karunarathna SC, Tibpromma S, Mortimer PE, Wanasinghe DN, Phookamsak R, Xu J, Wang Y, Tian F, Alvarado P, Li DW, Kušan I, Matočec N, Maharachchikumbura SSN, Papizadeh M, Heredia G, Wartchow F, Bakhshi M, Boehm E, Youssef N, Hustad VP, Lawrey JD, Santiago ALCMA, Bezerra JDP, Souza-Motta CM, Firmino AL, Tian Q, Houbraken J, Hongsanan S, Tanaka K, Dissanayake AJ, Monteiro JS, Grossart HP, Suija A, Weerakoon G, Etayo J, Tsurukau A, Vázquez V, Mungai P, Damm U, Li QR, Zhang H, Boonmee S, Lu YZ, Becerra AG, Kendrick B, Brearley FQ, Motiejūnaitė J, Sharma B, Khare R, Gaikwad S, Wijesundara DSA, Tang LZ, He MQ, Flakus A, Rodriguez-Flakus P, Zhurbenko MP, McKenzie EHC, Stadler M, Bhat DJ, Liu JK, Raza M, Jeewon R, Nassonova ES, Prieto M, Jayalal RGU, Erdoğan M, Yurkov A, Schnittler M, Shchepin ON, Novozhilov YK, Silva-Filho AGS, Liu P, Cavender JC, Kang Y, Mohammad S, Zhang LF, Xu RF, Li YM, Dayarathne MC, Ekanayaka AH, Wen TC, Deng CY, Pereira OL, Navathe S, Hawksworth DL, Fan XL, Dissanayake LS, Kuhnert E, Grossart HP, Thines M (2020) Outline of Fungi and fungus-like taxa. *Mycosphere* 11: 1060–1456. <https://doi.org/10.5943/mycosphere/11/1/8>
- Yang X, Liu J, Mei J, Jiang R, Tu S, Deng H, Liu J, Yang S, Li J (2021) Origins, structures, and bioactivities of secondary metabolites from marine-derived *Penicillium* fungi. *Mini-Reviews in Medicinal Chemistry* 21(15):1–20. <https://doi.org/10.2174/1389557521666210217093517>
- Zhang H, Huang T, Chen S, Guo L, Liu T, Yang X (2014) Microbial community functional diversity and enzymatic activity in the sediments of drinking water reservoirs, Northwest

China. *Desalination and Water Treatment* 52: 1608–1614. <https://doi.org/10.1080/19443994.2013.827383>

Zhang H, Huang T, Liu T (2013) Sediment enzyme activities and microbial community diversity in an oligotrophic drinking water reservoir, eastern China. *PLoS One* 8: e78571. <https://doi.org/10.1371/journal.pone.0078571>

Supplementary material I

Figures S1–S9

Authors: D Torres-Garcia, J Gené, D García

Data type: phylogenetic trees

Explanation note: Additional phylogenetic trees of the *Penicillium* series corresponding to the individual analyses of the different molecular markers with additional reference strains representing the species closely related to penicillia described here.

Copyright notice: This dataset is made available under the Open Database License (<http://opendatacommons.org/licenses/odbl/1.0/>). The Open Database License (ODbL) is a license agreement intended to allow users to freely share, modify, and use this Dataset while maintaining this same freedom for others, provided that the original source and author(s) are credited.

Link: <https://doi.org/10.3897/mycokeys.86.73861.suppl1>

Thyridium revised: Synonymisation of *Phialemoniopsis* under *Thyridium* and establishment of a new order, Thyridiales

Ryosuke Sugita^{1,2}, Kazuaki Tanaka¹

1 Faculty of Agriculture and Life Science, Hirosaki University, 3 Bunkyo-cho, Hirosaki, Aomori 036-8561, Japan **2** The United Graduate School of Agricultural Sciences, Iwate University, 18-8 Ueda 3 chome, Morioka, Iwate 020-8550, Japan

Corresponding author: Kazuaki Tanaka (k-tanaka@hirosaki-u.ac.jp)

Academic editor: Huzefa Raja | Received 7 December 2021 | Accepted 11 January 2022 | Published 1 February 2022

Citation: Sugita R, Tanaka K (2022) *Thyridium* revised: Synonymisation of *Phialemoniopsis* under *Thyridium* and establishment of a new order, Thyridiales. MycoKeys 86: 147–176. <https://doi.org/10.3897/mycokeys.86.78989>

Abstract

The genus *Thyridium*, previously known as a saprobic or hemibiotrophic ascomycete on various plants, was revised taxonomically and phylogenetically. Sequences of the following six regions, that is, the nuclear ribosomal internal transcribed spacer (ITS) region, the large subunit (LSU) of rDNA, the second largest RNA polymerase II subunit (*rpb2*) gene, translation elongation factor 1-alpha (*tef1*) gene, the actin (*act*) gene, and the beta-tubulin (*tub2*) gene, were generated for molecular phylogenetic analyses of species of this genus. *Phialemoniopsis*, a genus encompassing medically important species, is synonymised with *Thyridium* based on molecular evidence and morphological similarities in their asexual characters. The generic concept for *Thyridium* is expanded to include species possessing both coelomycetous and hyphomycetous complex asexual morphs. In addition to type species of *Thyridium*, *T. vestitum*, nine species were accepted in *Thyridium* upon morphological comparison and molecular phylogenetic analyses in this study. All seven species of *Phialemoniopsis* were treated as members of the genus *Thyridium* and new combinations were proposed. A bambusicolous fungus, *Pleospora punctulata*, was transferred to *Thyridium*, and an epitype is designated for this species. A new species, *T. flavostromatum*, was described from *Phyllostachys pubescens*. The family Phialemoniopsidaceae, proposed as a familial placement for *Phialemoniopsis*, was regarded as a synonym of Thyridiaceae. A new order, Thyridiales, was established to accommodate Thyridiaceae; it forms a well-supported, monophyletic clade in Sordariomycetes.

Keywords

Ascomycota, Phialemoniopsidaceae, phylogeny, Sordariomycetes, taxonomy, Thyridiaceae

Introduction

Thyridium was originally established to accommodate species with cylindrical, uniseriate, 8-spored asci and muriform, dark-coloured, ascospores (Nitschke 1867). Species of this genus occur on various plants as saprobic or hemibiotrophic fungi (Eriksson and Yue 1989; Taylor et al. 1997; Checa et al. 2013). Currently, *Thyridium* includes 33 species and is placed in Thyridiaceae (family *incertae sedis*, Sordariomycetes; Yue and Eriksson 1987; Index Fungorum, <http://www.indexfungorum.org>, 2021). The type species *T. vestitum* has been verified to produce both coelomycetous and hyphomycetous asexual morphs, which have phialidic conidiogenous cells with collarette and ellipsoidal to allantoid hyaline conidia (Leuchtman and Müller 1986).

Molecular information on *Thyridium* species is available only for two non-type strains (CBS 113027, CBS 125582) of the type species *T. vestitum* (Lutzoni et al. 2004; Spatafora et al. 2006; Vu et al. 2019); however, the phylogenetic relationships among species of this genus are unclear. A recent study on the phylogeny of Sordariomycetes has shown that *T. vestitum* is closely related to two *Phialemoniopsis* spp. (*P. endophytica* and *P. ocularis*), but their phylogenetic and taxonomic relationships have not been clarified (Dong et al. 2021; Hyde et al. 2021).

The genus *Phialemoniopsis* was placed in Phialemoniopsidaceae (Diaporthomycetidae family *incertae sedis*, Sordariomycetes; Hyde et al. 2021). Species of this genus are widely distributed in various environments and substrates, including industrial water, plant materials, raw sewage, and soil (Gams and McGinnis 1983; Halleen et al. 2007; Su et al. 2016). Several species have been reported from parts of the human body, such as blood, eye, toenail, skin, and sinus (Perdomo et al. 2013; Tsang et al. 2014), and some of them have also been isolated from patients with keratomycosis and phaeohyphomycosis (Perdomo et al. 2013; Desoubeaux et al. 2014). All species in this genus are known to be asexual.

In our ongoing taxonomic study of sordariomycetous fungi in Japan, several new specimens of *Thyridium*-like sexual morphs were collected. Single ascospore isolates from these specimens formed typical *Phialemoniopsis*-like asexual morphs in culture, suggesting that both genera are closely related. This study aims to reveal the taxonomic and phylogenetic relationships between *Thyridium* and *Phialemoniopsis*, and to clarify their ordinal position in Sordariomycetes.

Material and method

Isolation and morphological observation

All materials were obtained from Japan. Morphological characteristics were observed in preparations mounted in distilled water by differential interference and phase contrast microscopy (Olympus BX53) using images captured with an Olympus digital

camera (DP21). All specimens were deposited in the herbarium at Hirosaki University (HHUF), Hirosaki, Japan. Single spore isolations were performed from all specimens. Colony characteristics were recorded from growth on potato dextrose agar (PDA), malt extract agar (MEA), and oatmeal agar (OA) from Becton, Dickinson and Company (MD, USA), after a week at 25 °C in the dark. Colony colours were recorded according to Rayner (1970). To observe the asexual morphs in culture, 5 mm squares of mycelial agar were placed on water agar containing sterilised plant substrates such as rice straws and banana leaves. Then these plates were incubated at 25 °C for 2 weeks in the dark. When the substrates were colonised, the plates were incubated at 25 °C under black light blue illumination for 1–2 weeks to observe sporulation.

Phylogenetic analyses

DNA was extracted from four isolates using the ISOPLANT II kit (Nippon Gene, Tokyo, Japan) following the manufacturer's instructions. The following loci were amplified and sequenced: the internal transcribed spacer (ITS) region with primers ITS1 and ITS4 (White et al. 1990), the large subunit nuclear ribosomal DNA (LSU) with primers LR0R (Rehner and Samuels 1994) and LR5 or LR7 (Vilgalys and Hester 1990), the second largest RNA polymerase II subunit (*rpb2*) gene with primers fRPB2-5F and fRPB2-7cR (Liu et al. 1999), the translation elongation factor 1-alpha (*tef1*) gene with primers 983F and 2218R (Rehner and Buckley 2005), the actin (*act*) gene with primers Act-1 and Act-5ra (Voigt and Wöstemeyer 2000) and the beta-tubulin (*tub2*) gene with primers TUB-F and TUB-R (Cruse et al. 2002). PCR products were purified using the FastGene Gel/PCR Extraction Kit (Nippon Gene, Tokyo, Japan) following the manufacturer's instructions and sequenced at SolGent (South Korea). Newly generated sequences were deposited in GenBank (Table 1).

Primary analysis of LSU-*rpb2-tef1* sequences from 88 strains of Sordariomycetes (Table 1) was conducted to clarify the ordinal/familial placement of *Thyridium* (or *Phialemoniopsis*) species. *Barrmaelia rhamnicola* and *Entosordaria perfidiosa* (Xylariomycetidae) were used as outgroups. As a secondary analysis, single gene trees of ITS, *act* and *tub2*, and a combined tree of these three loci were generated to assess the species boundaries of 17 strains within *Thyridium/Phialemoniopsis* (Table 2). All sequence alignments (LSU, ITS, *rpb2*, *tef1*, *act* and *tub2*) were produced using the server version of MAFFT (<http://www.ebi.ac.uk/Tools/msa/mafft>), checked and refined using MEGA v. 7.0 (Kumar et al. 2016).

Phylogenetic analyses were conducted using maximum-likelihood (ML) and Bayesian methods. The optimum substitution models for each dataset were estimated using Kakusan4 software (Tanabe 2011) based on the Akaike information criterion (AIC; Akaike 1974) for ML analysis and the Bayesian information criterion (BIC; Schwarz 1978) for Bayesian analysis. ML analyses were performed using the TreeFinder Mar 2011 program (<http://www.treefinder.de>) based on the models selected with the AICc4 parameter (used sequence length as sample size). ML bootstrap support

Table 1. Isolates and GenBank accessions of sequences used in the phylogenetic analyses of Sordariomycetes (Fig. 1).

Taxon	Isolate ^a	Status ^b	GenBank accession numbers ^a			Ref. ^c
			LSU	<i>rpb2</i>	<i>tef1</i>	
<i>Acrodictys aquatica</i>	MFLUCC 18-0356	HT	MG835712	–	–	47
<i>Acrodictys bambusicola</i>	HSAUP myr9510		KX033564	–	–	44
<i>Annulatascus velatisporus</i>	A70 18		AY316354	–	–	3
<i>Annulusmagnus triseptatus</i>	CBS 128831		GQ996540	JQ429258	–	25, 29
<i>Ascitendus austriacus</i>	CBS 131685		GQ996539	JQ429257	–	25, 29
<i>Atractospora reticulata</i>	CBS 127884	HT	KT991660	KT991649	–	41
<i>Atractospora thailandensis</i>	KUMCC 16-0067	HT	MF374362	MF370951	MF370962	45
<i>Barbatosphaeria arboricola</i>	CBS 127689	HT	KM492862	KM492901	–	38
<i>Barbatosphaeria barbirostris</i>	CBS 121149		EF577059	KM492903	–	18, 38
<i>Barbatosphaeria varioseptata</i>	CBS 137797	HT	KM492869	KM492907	–	38
<i>Barrmaelia rhannicola</i>	CBS 142772	ET	MF488990	MF488999	MF489009	52
<i>Bombardia bombardia</i>	AFTOL-ID 967		DQ470970	DQ470923	DQ471095	14
<i>Calosphaeria pulchella</i>	CBS 115999	IT	AY761075	GU180661	FJ238421	8, 27
<i>Camarops microspora</i>	CBS 649.92		AY083821	DQ470937	–	13, 14
<i>Camarotella costaricensis</i>	MM-149		KX430484	KX451954	KX451982	43
<i>Cancellidium cinereum</i>	MFLUCC 18-0424	HT	MT370363	MT370486	MT370488	57
<i>Cancellidium griseonigrum</i>	MFLUCC 17-2117	HT	MT370364	MT370487	–	57
<i>Ceratolenta caudata</i>	CBS 125234	HT	JX066704	JX066699	–	33
	PRM 899855		JX066705	–	–	33
<i>Chaetosphaeria ciliata</i>	ICMP 18253		GU180637	GU180659	–	27
<i>Chaetosphaeria curvispora</i>	ICMP 18255		GU180636	GU180655	–	27
<i>Cryptadelphina groenendalensis</i>	SH12		EU528007	–	–	20
	SMH3767		EU528001	–	–	20
<i>Diaporthe phaseolorum</i>	NRRL 13736		U47830	–	–	1
<i>Distoseptispora obpyriformis</i>	MFLUCC 17-1694	HT	MG979764	MG988415	MG988422	48
<i>Distoseptispora rostrata</i>	MFLUCC 16-096	HT	MG979766	MG988417	MG988424	48
<i>Endoxyla operculata</i>	UAMH 11085		JX460992	KY931927	–	34, 49
<i>Entosordaria perfidiosa</i>	CBS 142773	ET	MF488993	MF489003	MF489012	52
<i>Fluminicola aquatica</i>	MFLUCC 15-0962	HT	MF374366	–	MF370960	45
<i>Fluminicola saprotrophitica</i>	MFLUCC 15-0976	HT	MF374367	MF370954	MF370956	45
<i>Gnomonia gnomon</i>	CBS 199.53		AF408361	DQ470922	DQ471094	2, 14
<i>Jobbellisia fraterna</i>	SMH2863		AY346285	–	–	4
<i>Jobbellisia luteola</i>	SMH2753		AY346286	–	–	4
<i>Lanspora coronata</i>	AFTOL-ID 736		U46889	DQ470899	–	14
<i>Lasiochaeria ovina</i>	SMH4605		AY436413	AY600284	DQ836908	6, 7, 16
<i>Lentomitella cirrhosa</i>	ICMP 15131	ET	AY761085	KM492911	–	11, 38
<i>Lentomitella crinigera</i>	CBS 138678		KY931811	–	–	49
<i>Linocarpon livistonae</i>	HKUM 6520		DQ810205	DQ810248	–	10
<i>Magnaporthe salvinii</i>	M 21		JF414887	–	JF710406	28
<i>Magnaportheiopsis agrostidis</i>	CBS 142740	HT	KT364754	–	KT364756	37
<i>Melanconis stilbostoma</i>	CBS 109778		AF408374	EU219299	EU221886	2
<i>Myrmecridium montsegurinum</i>	JF 13180	HT	KT991664	KT991654	–	41
<i>Myrmecridium schulzeri</i>	CBS 100.54		EU041826	–	–	17
<i>Myrmecridium thailandicum</i>	CBS 136551	HT	KF777222	–	–	30
<i>Neolinocarpon ensiense</i>	HKUCC 2983		DQ810221	DQ810244	–	10
<i>Neolinocarpon globosicarpum</i>	HKUCC 1959		DQ810224	DQ810245	–	10
<i>Ophiostoma piliferum</i>	CBS 158.74		DQ470955	DQ470905	DQ471074	14
<i>Ophiostoma stenoceras</i>	CBS 139.51		DQ836904	DQ836891	DQ836912	16
<i>Papulosa amerospora</i>	AFTOL-ID 748		DQ470950	DQ470901	DQ471069	14
<i>Pararamichloridium caricicola</i>	CBS 145069	HT	MK047488	–	–	46
<i>Pararamichloridium livistonae</i>	CBS 143166	HT	MG386084	–	–	54
<i>Pararamichloridium verrucosum</i>	CBS 128.86	HT	MH873621	–	–	56
<i>Phaeoacremonium fraxinopennsylvanica</i>	M.R. 3064		HQ878595	HQ878609	–	26

Taxon	Isolate ^a	Status ^b	GenBank accession numbers ^a			Ref. ^c
			LSU	<i>rpb2</i>	<i>tef1</i>	
<i>Phaeoacremonium novae-zealandiae</i>	CBS 110156	HT	AY761081	–	–	8
<i>Phomatospora bellaminuta</i>	AFTOL-ID 766		FJ176857	FJ238345	–	23
<i>Phomatospora biseriata</i>	MFLUCC 14-0832A		KX549448	–	–	51
<i>Phyllachora graminis</i>	TH-544		KX430508	–	–	43
<i>Pleurostoma ootheca</i>	CBS 115329	IT	AY761079	HQ878606	FJ238420	8, 23, 26
<i>Pseudostanjehughesia aquitropica</i>	MFLUCC 16-0569	HT	MF077559	–	MF135655	53
<i>Pseudostanjehughesia lignicola</i>	MFLUCC 15-0352	HT	MK849787	MN124534	MN194047	55
<i>Pyricularia borealis</i>	CBS 461.65		DQ341511	–	–	24
<i>Pyricularia bothriochloae</i>	CBS 136427	HT	KF777238	–	–	30
<i>Rhizophoria delicatula</i>	CBS 132724		FJ617561	JX066702	–	22, 33
<i>Rhizophoria pyriformis</i>	CBS 139024		MG600397	MG600401	–	50
<i>Rubellisphaeria abscondita</i>	CBS 132078	HT	KT991666	KT991657	–	41
<i>Sordaria fimicola</i>	CBS 723.96		AY780079	DQ368647	–	9, 19
<i>Spadicoides bina</i>	CBS 137794		KY931824	KY931851	–	49
<i>Sporidesmium minigelatinosa</i>	NN 47497		DQ408567	DQ435090	–	12
<i>Sporidesmium parvum</i>	HKUCC 10836		DQ408558	–	–	12
<i>Thyridium cornearis</i>	CBS 131711	HT	KJ573450	–	LC382144	36
<i>Thyridium curvatum</i>	CBS 490.82	HT	AB189156	–	LC382142	15
<i>Thyridium endophyticum</i>	ACCC 38980	HT	KT799560	–	–	42
<i>Thyridium flavostromatum</i>	KT 3891 = MAFF 247509	HT	LC655963	LC655967	LC655971	This study
<i>Thyridium hongkongense</i>	HKU39	HT	KJ573447	–	–	36
<i>Thyridium limonesiae</i>	CBS 146752	HT	MW050976	–	–	58
<i>Thyridium oculorum</i>	CBS 110031	HT	KJ573449	–	LC382145	36
<i>Thyridium pluriloculosum</i>	CBS 131712	HT	HE599271	–	LC382141	32
	KT 3803 = MAFF 247508		LC655964	LC655968	LC655972	This study
<i>Thyridium punctulatum</i>	KT 1015 = MAFF 239669		LC655965	LC655969	LC655973	This study
	KT 3905 = MAFF 247510	ET	LC655966	LC655970	LC655974	This study
<i>Thyridium vestitum</i>	CBS 113027		AY544671	DQ470890	DQ471058 ^d	5, 14
	CBS 125582		MH875182	–	–	56
<i>Tirisporella beccariana</i>	BCC 36737		JQ655450	–	–	39
<i>Tirisporella bisetulosus</i>	BCC 00018		EF622230	–	–	21
<i>Wongia griffinii</i>	BRIP 60377		KU850470	–	KU850466	40
<i>Woswasia atropurpurea</i>	CBS 133167	HT	JX233658	JX233659	–	31
<i>Xylochrysis lucida</i>	CBS 135996	HT	KF539911	KF539913	–	35
<i>Xylolentia brunneola</i>	PRA-13611	HT	MG600398	MG600402	–	50

^a Strains and sequences generated in this study are shown in **bold**.

^b ET = epitype; HT = holotype; IT = isotype

^c 1: Viljoen et al. 1999; 2: Castlebury et al. 2002; 3: Raja et al. 2003; 4: Huhndorf et al. 2004; 5: Lutzoni et al. 2004; 6: Miller and Huhndorf 2004a; 7: Miller and Huhndorf 2004b; 8: Réblová et al. 2004; 9: Miller and Huhndorf 2005; 10: Bahl 2006; 11: Réblová 2006; 12: Shenoy et al. 2006; 13: Smith et al. 2006; 14: Spatafora et al. 2006; 15: Yaguchi et al. 2006; 16: Zhang et al. 2006; 17: Arzanlou et al. 2007; 18: Réblová 2007; 19: Tang et al. 2007; 20: Huhndorf et al. 2008; 21: Pinruan et al. 2008; 22: Réblová 2009; 23: Schoch et al. 2009; 24: Thongkantha et al. 2009; 25: Réblová et al. 2010; 26: Réblová 2011; 27: Réblová et al. 2011; 28: Zhang et al. 2011; 29: Réblová et al. 2012; 30: Crous et al. 2013; 31: Jaklitsch et al. 2013; 32: Perdomo et al. 2013; 33: Réblová 2013; 34: Untereiner et al. 2013; 35: Réblová et al. 2014; 36: Tsang et al. 2014; 37: Crous et al. 2015b; 38: Réblová et al. 2015; 39: Suetrong et al. 2015; 40: Khemmuk et al. 2016; 41: Réblová et al. 2016; 42: Su et al. 2016; 43: Mardones et al. 2017; 44: Xia et al. 2017; 45: Zhang et al. 2017; 46: Crous et al. 2018; 47: Hyde et al. 2018; 48: Luo et al. 2018; 49: Réblová et al. 2018; 50: Réblová and Štěpánek 2018; 51: Senanayake et al. 2018; 52: Voglmayr et al. 2018; 53: Yang et al. 2018; 54: Crous et al. 2019; 55: Luo et al. 2019; 56: Vu et al. 2019; 57: Hyde et al. 2021; 58: Martinez et al. 2021.

^d This *tef1* sequence (DQ471058) of *Thyridium vestitum* was excluded from this analysis. A Blast search using this sequence suggested that it is close to *Phialemonium obovatum* (Cephalothecales) rather than *Thyridium/Phialemoniopsis* (Thyridiales).

(ML BS) values were obtained using 1000 bootstrap replicates. Bayesian analyses were performed using MrBayes v. 3.2.6 (Ronquist et al. 2012), with substitution models selected based on the BIC₄ parameter (used sequence length as sample size). Two simultaneous and independent Metropolis-coupled Markov chain Monte Carlo (MCMC) runs were performed for 9,000,000 generations for primary analysis and 1,000,000 generations for secondary analyses (except for the ITS dataset for 1,500,000 generations) with the tree sampled every 1,000 generations. Convergence of the MCMC procedure was assessed from the effective sample size scores (all > 100) using MrBayes and Tracer v. 1.6 (Rambaut et al. 2014). First 25% of the trees were discarded as burn-in, and the remainder were used to calculate the 50% majority-rule trees and to determine the posterior probabilities (PPs) for individual branches. These alignments were submitted to TreeBASE under study number S28934.

Result

Phylogeny

For primary analysis, ML and Bayesian phylogenetic trees were generated using an aligned sequence dataset comprising of LSU (1,205 base pairs), *rpb2* (1,059 bp) and *tef1* (954 bp). Of the 3,218 characters included in the alignment, 1,478 were variable and 1,686 were conserved. This combined dataset provided higher confidence values for ordinal and familial classification than those of individual gene trees, with 25 orders and three families (order unknown) being reconstructed in Sordariomycetes (Fig. 1). ML analysis of the combined dataset was conducted based on the selected substitution model for each partition (GTR+G for LSU, J2+G for the first and third codon positions of *rpb2*, J1+G for the second codon positions of *rpb2*, F81+G for the first codon positions of *tef1*, JC69+G for the second codon positions of *tef1*, and J2+G for the third codon position of *tef1*). The ML tree with the highest log likelihood (−43687.562) is shown in Fig. 1. Topology recovered by Bayesian analysis was almost identical to that of the ML tree. All species previously described as *Phialemoniopsis* (marked with blue circle in Fig. 1), one species of “*Linocarpon*”, two species of “*Neolinocarpon*” and four strains newly obtained in this study formed a monophyletic clade with the type species of *Thyridium* (*T. vestitum*). Their monophyly was completely supported (100% ML BS/1.0 Bayesian PP; Fig.1). The family Thyridiaceae was found to be related to Annulatascales and Myrmecridiales but did not cluster with any existing order in Sordariomycetes.

For secondary analysis, ML and Bayesian phylogenetic trees were generated using sequences of ITS (483 bp), *act* (646 bp), *tub2* (375 bp), and a combined dataset of these three regions (1,504 bp). The selected substitution models for each region were as follows: J2ef+G for ITS, F81+H for the first and second codon positions of *act*, J2+G for the third codon position of *act*, K80+H for the first codon positions

Table 2. Isolates and GenBank accessions of sequences used in the phylogenetic analyses of *Thyridium* species (Fig. 2).

Taxon	Isolate ^a	Substrate/Host	Status ^b	GenBank accession numbers ^a			Ref. ^c
				ITS	<i>act</i>	<i>tub2</i>	
<i>Thyridium cornearis</i>	CBS 131711	human corneal fluid	HT	KJ573445	HE599252	HE599301	1, 2
	UTHSC 06-1465	shin aspirate		HE599285	HE599253	HE599302	2
<i>Thyridium curvatum</i>	CBS 490.82	skin lesion	HT	AB278180	HE599258	HE599307	2
<i>Thyridium endophyticum</i>	UTHSC R-3447	human eye		HE599291	HE599259	HE599308	2
<i>Thyridium endophyticum</i>	ACCC 38979	lower stem of <i>Luffa cylindrica</i> (endophyte)		KT799556	KT799553	KT799562	4
	ACCC 38980	lower stem of <i>Luffa cylindrica</i> (endophyte)	HT	KT799557	KT799554	KT799563	4
<i>Thyridium flavostromatum</i>	KT 3891 = MAFF 247509	dead twigs of <i>Phyllostachys pubescens</i>	HT	LC655959	LC655979	LC655975	This study
<i>Thyridium hongkongense</i>	HKU39	the right forearm nodule biopsy of a human	HT	KJ573442	KJ573452	KJ573457	3
<i>Thyridium limonesiae</i>	CBS 146752	Skin nodule	HT	MW050977	MW349126	MW048608	6
<i>Thyridium oculorum</i>	CBS 110031	human keratitis	HT	KJ573444	HE599247	HE599296	2, 3
	UTHSC 05-2527	peritoneal dialysis catheter		HE599281	HE599249	HE599298	2
<i>Thyridium pluriloculosum</i>	CBS 131712	human toe nail	HT	HE599286	HE599254	HE599303	2
	KT 3803 = MAFF 247508	dead wood of <i>Betula maximowicziana</i>	HT	LC655960	LC655980	LC655976	This study
	UTHSC 09-3589	synovial fluid		HE599287	HE599255	HE599304	2
<i>Thyridium punctulatum</i>	KT 1015 = MAFF 239669	dead culms of <i>Phyllostachys pubescens</i>		LC655961	LC655981	LC655977	This study
	KT 3905 = MAFF 247510	dead twigs of <i>Phyllostachys nigra</i> var. <i>nigra</i>	ET	LC655962	LC655982	LC655978	This study
<i>Thyridium vestitum</i>	CBS 125582			MH863721	–	–	5

^a Strains and sequences generated in this study are shown in **bold**.

^b ET = epitype; HT = holotype

^c 1: Tang et al. 2007; 2: Perdomo et al. 2013; 3: Tsang et al. 2014; 4: Su et al. 2016; 5: Vu et al. 2019; 6: Martinez et al. 2021.

of *tub2*, JC69+H for the second codon position of *tub2* and TN93+H for the third codon position of *tub2*. The ML trees with the highest log likelihood (–1172.0198 in ITS, –1196.6012 in *act*, –859.37115 in *tub2* and –3315.7254 in ITS-*act-tub2*) are shown in Fig. 2. Our results confirmed close phylogenetic relationships between *Thyridium* and *Phialemoniopsis* (Fig. 2A–D). Except for *act* (Fig. 2B) and *tub2* (Fig. 2C), where sequence data of *T. vestitum* were unavailable, the existence of ten distinct species was suggested (Fig. 2A, D). The following three lineages were found in our four strains (Fig. 2A–D): 1) a bambusicolous lineage (KT 3891) close to *T. curvatum* and *T. limonesiae*, 2) a fungus on *Betula maximowicziana* (KT 3803) nested with *T. pluriloculosum*, which was previously reported from clinical sources (Perdomo et al. 2013), and 3) another bambusicolous lineage represented by two strains (KT 1015 and KT 3905).

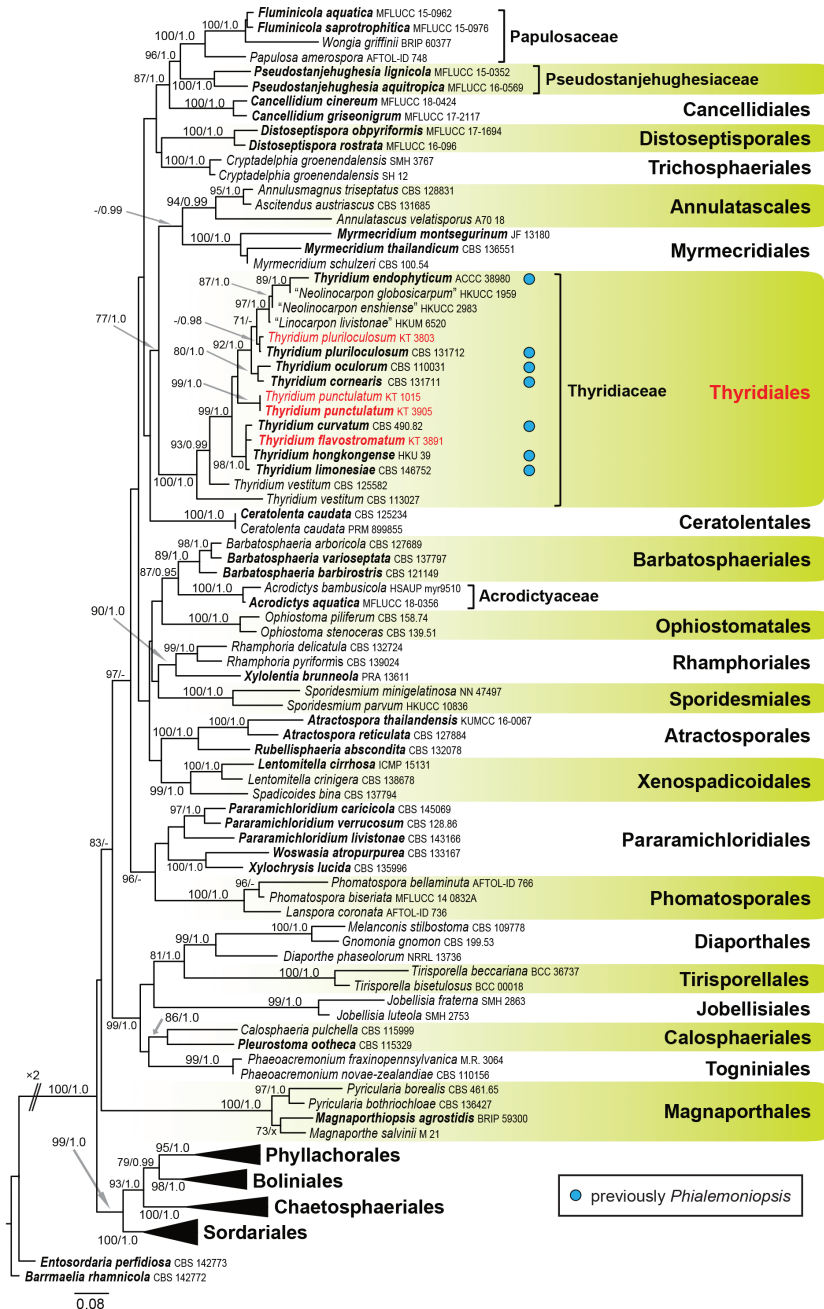


Figure 1. Maximum-likelihood tree of Sordariomycetes based on combined LSU, *rpb2* and *tef1* sequence. ML bootstrap proportion (BP) greater than 70% and Bayesian posterior probabilities (PP) above 0.95 are presented at the nodes as ML BP/Bayesian PP and a node not present in the Bayesian analysis is shown with ‘x’. A hyphen (‘-’) indicates values lower than 70% BP or 0.95 PP. Ex-holotype, isotype, paratype and epitype strains are shown in bold and the newly obtained sequences are shown in red. Strains previously described as *Phialemoniopsis* species are marked with a blue circle. The scale bar represents nucleotide substitutions per site.

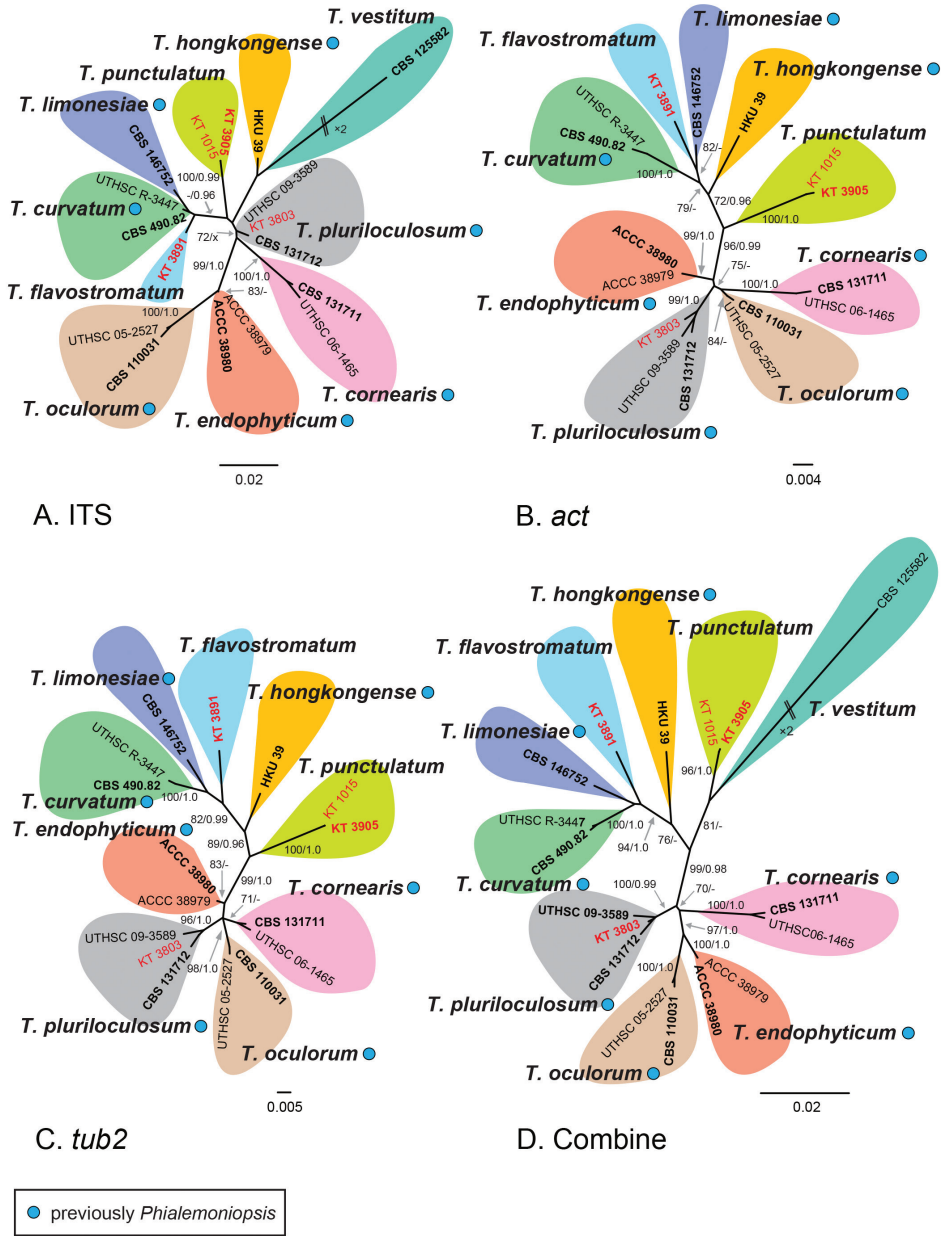


Figure 2. Maximum-likelihood tree of *Thyridium* species based on each ITS (A), *act* (B), *tub2* (C) and combined sequences (ITS-*act*-*tub2*; D). ML bootstrap proportion (BP) greater than 70% and Bayesian posterior probabilities (PP) above 0.95 are presented at the nodes as ML BP/Bayesian PP. A hyphen ('-') indicates values lower than 70% BP or 0.95 PP and a node not present in the Bayesian analysis is shown with 'x'. Ex-holotype and epitype strains are shown in bold and the newly obtained sequences are shown in red. Strains previously as *Phialemoniopsis* species are marked with a blue circle. The scale bars represent nucleotide substitutions per site.

Taxonomy

A new order, Thyridiales, is introduced to accommodate Thyridiaceae because its lineage is phylogenetically and morphologically distinct from any known orders in Sordariomycetes. We concluded *Thyridium* and *Phialemoniopsis* to be congeneric based on their morphological similarities and phylogenetic relatedness. An expanded generic circumscription of *Thyridium* that integrates the generic concept of *Phialemoniopsis* is provided below. One new species and eight new combinations of *Thyridium* are proposed.

Thyridiales R. Sugita & Kaz. Tanaka, ord. nov.

Mycobank No: 841916

Type family. Thyridiaceae J.Z. Yue & O.E. Erikss., Syst. Ascom. 6(2): 233 (1987).

Sexual morph. Stromata scattered to grouped. Ascomata perithecial, subglobose to ampulliform. Ostiolar neck cylindrical, periphysate. Paraphyses numerous, unbranched, cylindrical, hyaline. Asci unitunicate, cylindrical, with an apical annulus, pedicellate. Ascospores obovoid to ellipsoid, muriform, hyaline to brown.

Asexual morph. Coelomycetous asexual morph: Conidiomata pycnidial, globose to subglobose. Conidiogenous cells phialidic. Conidia ellipsoidal to obovoid, aseptate, hyaline. Hyphomycetous synasexual morph: Colonies effuse or sporodochial. Conidiophores micronematous, mononematous, simple or branched, hyaline, thin-walled. Conidiogenous cells phialidic. Conidia ellipsoidal to allantoid, aseptate, hyaline.

Notes. Thyridiaceae has been treated as *incertae sedis* in Sordariomycetes (Yue and Eriksson 1987). Members of Thyridiaceae differ from Myrmecridiales by having pycnidial conidiomata, becoming cup-shaped in the coelomycetous state and micronematous conidiophores with monophialidic conidiogenous cells in the hyphomycetous state. Myrmecridiales have brown thick-walled conidiophores with polyblastic conidiogenous cells (Crous et al. 2015a). Annulatascales have relatively massive refractive, well-developed, conspicuous apical annulus in asci (Wong et al. 1999; Campbell and Shearer 2004; Dong et al. 2021). In contrast, those of members of Thyridiaceae are compact and inconspicuous. Therefore, a new order, Thyridiales, is introduced for this lineage.

Thyridiaceae J.Z. Yue & O.E. Erikss., Syst. Ascom. 6(2): 233 (1987).

Phialemoniopsidaceae K.D. Hyde & Hongsanan, [as Phialemoniopsaceae] Fungal Divers. 107: 95 (2021).

Type genus. *Thyridium* Nitschke, Pyrenomyc. Germ. 1: 110 (1867).

Notes. Phialemoniopsidaceae is considered a synonym of Thyridiaceae because *Phialemoniopsis*, the type genus of Phialemoniopsidaceae, was revealed congeneric with *Thyridium* and is placed in the synonymy of the latter genus in this study. The type

genera of both families, that is, *Thyridium* and *Phialemoniopsis*, share many morphological features in their asexual states, as noted below.

***Thyridium* Nitschke, Pyrenomyc. Germ. 1: 110 (1867).**

Melanospora subgen. *Bivonella* Sacc., Syll. fung. (Abellini) 2: 464 (1883).

Bivonella (Sacc.) Sacc., Syll. fung. (Abellini) 9: 989 (1891).

Pleurocytospora Petr., Annl. mycol. 21: 256 (1923).

Sinosphaeria J.Z. Yue & O.E. Erikss., Syst. Ascom. 6: 231 (1987).

Phialemoniopsis Perdomo, Dania García, Gené, Cano & Guarro, Mycologia 105: 408 (2013).

Type species. *Thyridium vestitum* (Fr.) Fuckel, Jb. Nassau. Ver. Naturk. 23–24: 195 (1870) [1869–70].

Sexual morph. Stromata scattered to grouped, subepidermal to erumpent, yellowish to dark brown, red in KOH or not changing. Ascomata perithecial, subglobose to ampulliform, single to grouped, immersed in stromata to erumpent through host surface. Ascomatal wall composed of several layers of polygonal, dark brown cells. Ostiolar neck cylindrical, short or long, separated or convergent in upper stromata, periphysate. Paraphyses numerous, septate, unbranched, cylindrical, hyaline. Asci unitunicate, cylindrical, broadly rounded at the apex, with a pronounced non-amyloid apical annulus, pedicellate. Ascospores obovoid or ellipsoid, smooth, pale brown to brown, with several transverse and 0–3 longitudinal or oblique septa.

Asexual morph. Coelomycetous and/or hyphomycetous morphs formed. Coelomycetous asexual morph: Conidiomata pycnidial, single to grouped, superficial or immersed in stromata, globose to subglobose, composed of polygonal to prismatic cells, often becoming cup-shaped when mature, surrounded by setose hyphae. Conidiomatal wall composed of several layers of polygonal, dark brown cells. Ostiolar neck cylindrical, central, periphysate. Setose hyphae erect, usually unbranched, septate, cylindrical, with slightly pointed or blunt tips, hyaline to pale brown, smooth-walled. Conidiophores hyaline, thin-walled, simple or irregularly branched, with branches bearing a small group of phialides terminally. Phialides swollen at the base, tapering at the tip, hyaline. Conidia obovoid to oblong, with a slightly apiculate base, hyaline, smooth-walled, in slimy masses. Hyphomycetous synasexual morph: Colonies effuse or sporodochial. Conidiophores micronematous, mononematous, hyaline, thin-walled, simple or irregularly branched, with branches bearing a small group of phialides terminally. Phialides swollen at the base, tapering at the tip, hyaline. Adelophialides absent or rarely present. Conidia ellipsoidal to allantoid, with a slightly apiculate base, hyaline, smooth-walled, in slimy head. Chlamydospores absent or rarely present, hyaline to pale brown, thick- and rough-walled.

Notes. The newly obtained *Thyridium* collections formed synasexual morphs, coelomycetous and hyphomycetous, in culture that were similar to those of *Phialemoniopsis*, having coelomycetous and/or hyphomycetous conidial states in culture (Perdomo

et al. 2013). In this study, *Phialemoniopsis* is treated as a synonym of *Thyridium* because of their morphological similarities in asexual morphs and phylogenetic relatedness. The genus *Pleurocytospora* has been proposed as a synonym of *Thyridium* by culture studies (Leuchtmann and Müller 1986). We agree that the morphological features of *Pleurocytospora*, such as phialidic conidiogenous cells and hyaline, ellipsoidal conidia formed from both coelomycetous and hyphomycetous states (Leuchtmann and Müller 1986), are almost identical to those of the generic concept of *Thyridium* emended here.

We accept both *Bivonella* and *Sinosphaeria* as synonyms of *Thyridium*, as proposed in previous studies (Eriksson and Yue 1989; Checa et al. 2013). *Sinosphaeria* (typified by *S. bambusicola* = *Thyridium chrysomallum*; Yue and Eriksson 1987) was established as a new genus without knowing the existence of *Bivonella* (typified by *B. lycopersici*; Saccardo 1891). Both genera are characterised by yellowish stromata. The validity of these genera being synonymised under *Thyridium* is confirmed by the presence of *T. flavostromatum*, which has yellowish stromata, in the strongly supported *Thyridium* clade (Fig. 1).

***Thyridium flavostromatum* R. Sugita & Kaz. Tanaka, sp. nov.**

MycoBank No: 841917

Figs 3, 6A

Holotype. JAPAN, Yamaguchi, Nagato, Misumikami, near Kusaritoge, on dead twigs of *Phyllostachys pubescens*, 26 March 2018, K. Tanaka, K. Arayama and R. Sugita, KT 3891 (HHUF 30647, holotype designated here), living culture MAFF 247509.

Etymology. The name refers to yellowish stromata.

Sexual morph. Stromata scattered to grouped, subepidermal, becoming erumpent to superficial, 0.7–1.4 mm long, 0.4–0.7 mm wide, yellowish to dark brown, red in 2% KOH. Ascum perithecial, subglobose to ampulliform, mostly 2–6 grouped, 190–240 µm high, 200–220 µm diam., immersed in stromata to erumpent through host surface. Ascum wall 15–23 µm thick, composed of 5–8 layers of polygonal, 2.5–7 × 1.5–3.5 µm, dark brown cells. Ostiolar neck central, cylindrical, 80–140 µm long, 55–90 µm wide, periphysate. Paraphyses numerous, septate, unbranched, cylindrical, 50–105 µm long. Asci unitunicate, cylindrical, 62.5–90 × 6.5–10 µm (av. 78.7 × 7.8 µm, n = 30), broadly rounded at the apex, with a pronounced non-amyloid apical annulus, short-stalked (5–17.5 µm long), with 8 ascospores. Ascospores obovoid to ellipsoid, smooth, hyaline to pale brown, with 3 transverse and 0–2 vertical septa, 9.5–14 × 5–7.5 µm (av. 11.3 × 5.8 µm, n = 50), l/w 1.4–2.5 (av. 2.0, n = 50).

Asexual morph (nature). Not observed.

Asexual morph (culture). Hyphomycetous asexual morph formed. Conidiophores micronematous, mononematous, hyaline, thin-walled, simple or irregularly branched, with branches bearing a group of 2–3 phialides terminally. Phialides swollen at the base, tapering at the tip, hyaline, 3–6 × 1–1.5 µm. Adelophialides rarely present. Conidia ellipsoidal to allantoid, with a slightly apiculate base, hyaline, smooth-walled, 2–7 × 1–2.5 µm (av. 4.1 × 1.6 µm, n = 50). Chlamydospores rarely present, solitary, 3.5–6.5 µm diam., hyaline to pale brown, thick- and rough-walled.

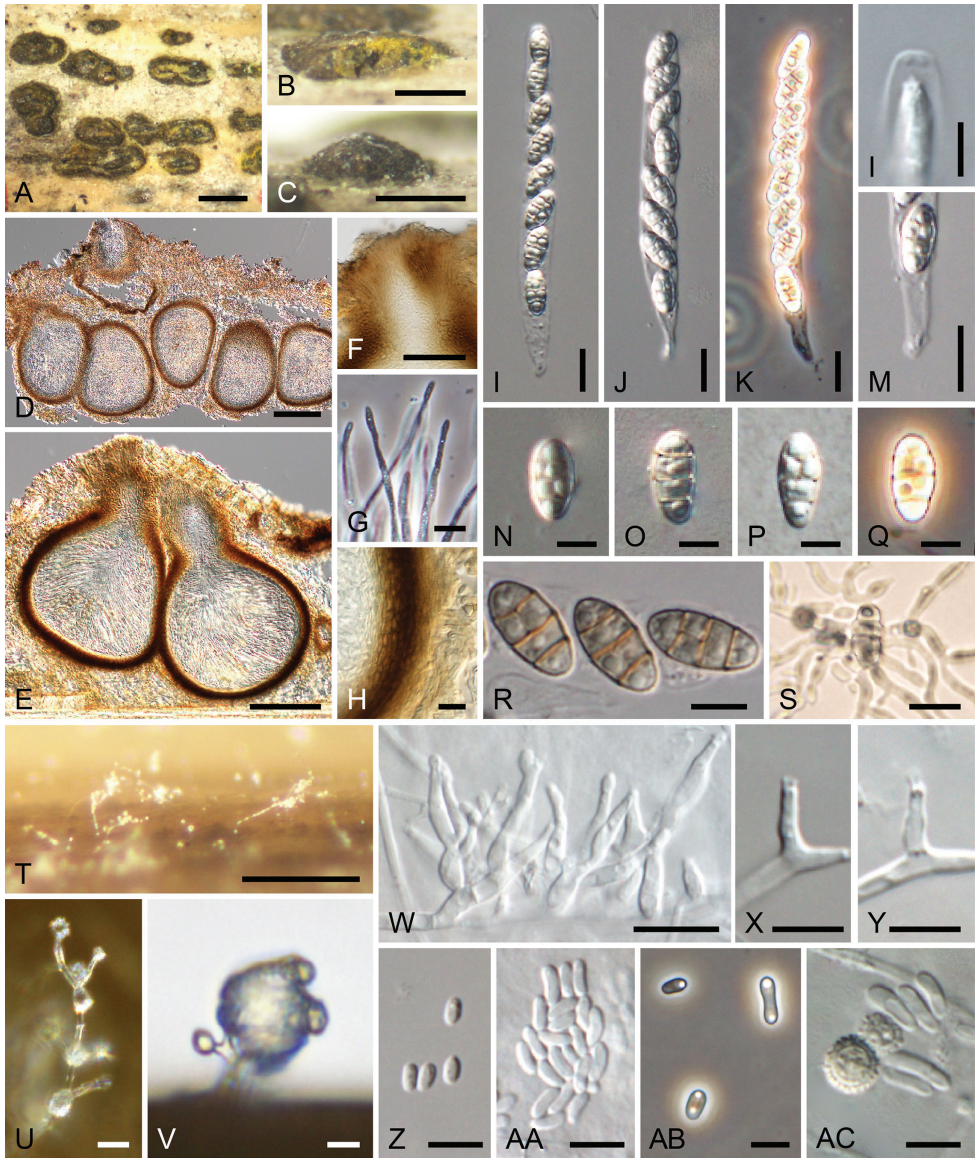


Figure 3. *Thyridium flavostromatum* (A–S KT 3891 = HHUF 30647 T–AC culture KT 3891 = MAFF 247509) A–S sexual morph A–C appearance of stromata on substrate D, E ascomata in longitudinal section (D in 2% KOH) F ostiolar neck of ascoma G paraphyses H ascomatal wall I–K asci L apex of the ascus M stipe of the ascus N–R ascospores S germinating ascospore T–AC hyphomycetous asexual morph T sporulation in culture U phialides V slimy conidial heads W conidiophores X phialide Y adelophialide Z–AB conidia AC chlamydospores and conidia. Scale bars: 1 mm (A); 500 µm (B, C); 100 µm (D, E); 50 µm (F); 10 µm (G–K, M, S, U, V); 5 µm (L, N–R, W–AC); 250 µm (T).

Culture characteristics. Colonies on MEA at 25 °C attained 28–29 mm diam. after a week in the dark, whitish. On OA attained 35–37 mm diam., whitish. On PDA attained 28–31 mm diam., whitish to buff (45; Rayner 1970) (Fig. 6A).

Notes. Phylogenetic analyses based on ITS, *act*, and *tub2* sequences suggested that *T. flavostromatum* was closely related to *T. curvatum*, *T. hongkongense* and *T. limonesiae* (Fig. 2), of which only *T. hongkongense* has unknown conidial state. Although *T. curvatum* forms sporodochial conidiomata (Perdomo et al. 2013), those are not found in *T. flavostromatum*. Conidia of *T. limonesiae* ($2.3\text{--}4.9 \times 1.4\text{--}2 \mu\text{m}$; Martinez et al. 2021) are smaller than those of *T. flavostromatum* ($2\text{--}7 \times 1\text{--}2.5 \mu\text{m}$). *Thyridium flavostromatum* is similar to *T. lasiacidis* on *Lasiacis ligulata* (Samuels and Rogerson 1989) in 1) having yellowish stromata becoming red in KOH, and 2) ellipsoidal ascospores with three transverse septa, with or without one longitudinal septum in 1–2 median cells. However, *T. lasiacidis* differs from *T. flavostromatum* by ascomata with a longer ostiolar neck (90–170 μm long) and dark brown ascospores with terminal pale brown cells (Samuels and Rogerson 1989).

***Thyridium pluriloculosum* (Perdomo, Dania García, Gené, Cano & Guarro) R. Sugita & Kaz. Tanaka, comb. nov.**

Mycobank No: 841918

Figs 4, 6B

Basionym. *Phialemoniopsis pluriloculosa* Perdomo, Dania García, Gené, Cano & Guarro, Mycologia 105: 412 (2013).

Holotype. USA, Nevada, human toe nail, D.A. Sutton, CBS H-20782, living culture CBS 131712 = UTHSC 04–7 = FMR 11070 (not seen).

Sexual morph. Stromata scattered to grouped, pulvinate, circular to elliptical in outline, elevated beyond bark surface forming pustules, 0.6–0.7 mm high, 0.9–1.0 mm diam., dark brown to black. Ascomata perithecial, subglobose to ampulliform, 4–8 grouped, 700–780 μm high, 220–280 μm diam., immersed in stromata. Ascomatal wall 17–25 μm thick, composed of 7–10 layers of polygonal, $4\text{--}6.5 \times 2\text{--}4 \mu\text{m}$, dark brown cells. Ostiolar neck central, cylindrical, 400–430 μm long, 100–110 μm wide, periphysate. Paraphyses septate, unbranched, cylindrical, 92.5–110 μm long, 3.5–5.5 μm wide. Asci unitunicate, cylindrical, $110\text{--}175 \times 9\text{--}12.5 \mu\text{m}$ (av. $145.6 \times 10.3 \mu\text{m}$, $n = 15$), broadly rounded at the apex, with a pronounced non-amyloid apical annulus, pedicellate (12.5–27.5 μm long), with 8 ascospores. Ascospores fusiform to ellipsoid, smooth, brown, with 3 transverse and 0–2 oblique or vertical septa, $13.5\text{--}18 \times 6\text{--}8 \mu\text{m}$ (av. $15.5 \times 7.3 \mu\text{m}$, $n = 50$), l/w 1.7–2.6 (av. 2.1, $n = 50$).

Asexual morph (nature). Conidiomata pycnidial, globose to subglobose, grouped, 220–300 μm high, 90–150 μm diam., immersed in stromata. Conidiomatal wall 8–18 μm thick, composed of 3–5 layers of polygonal, $3\text{--}4.5 \times 2.5\text{--}4 \mu\text{m}$, dark brown cells. Ostiolar neck central, cylindrical, 80–110 μm long, 90–110 μm wide, composed of polygonal cells, periphysate. Conidiophores hyaline, thin-walled, with branches bearing a group of 2–5 phialides terminally. Phialides tapering toward the tip, hyaline, $11\text{--}16 \times 1\text{--}2 \mu\text{m}$. Conidia ellipsoidal, with a slightly apiculate base, hyaline, smooth-walled, $3\text{--}4.5 \times 1\text{--}2 \mu\text{m}$ (av. $3.7 \times 1.5 \mu\text{m}$, $n = 50$). Chlamydo spores not observed.

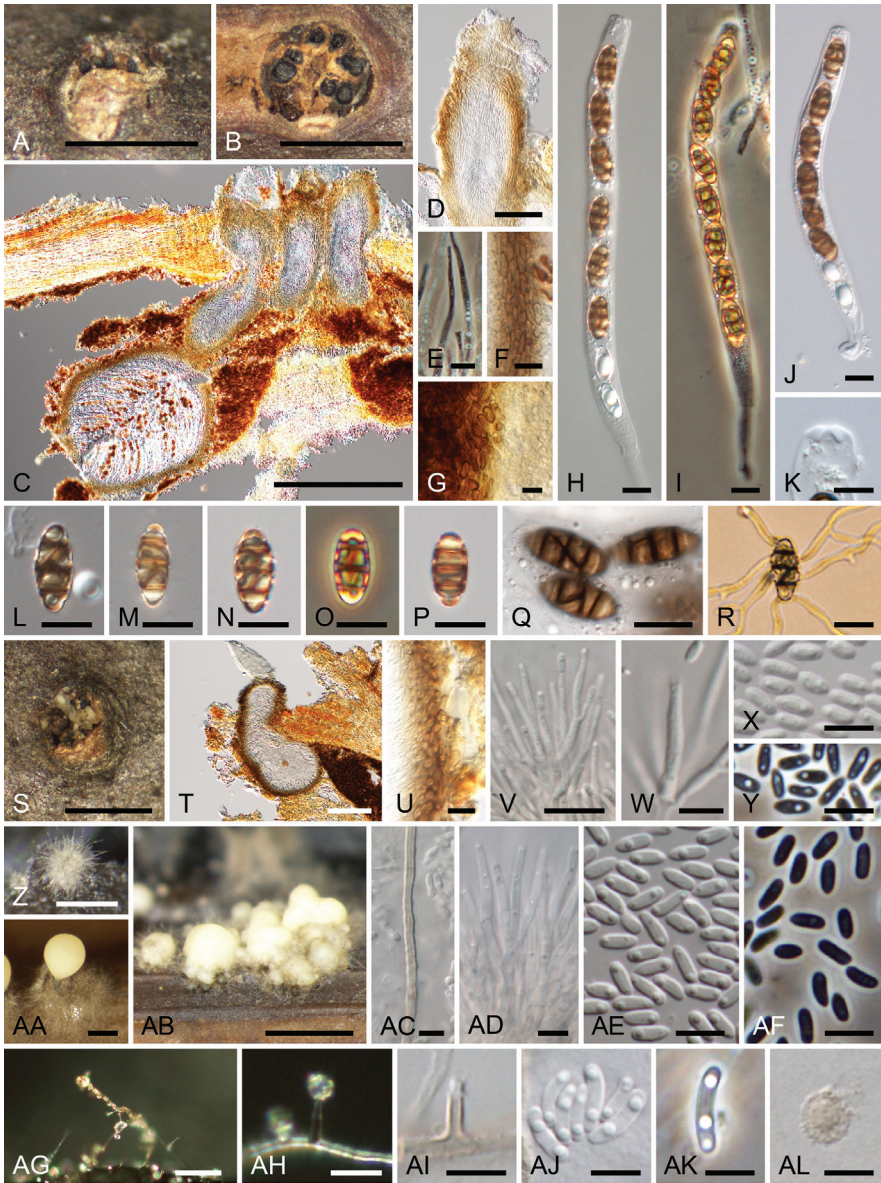


Figure 4. *Thyridium pluriloculosum* (A–Y KT 3803 = HHUF 30648 Z–AL culture KT 3803 = MAFF 247508) A–R sexual morph A, B appearance of stromata on substrate (B transverse sections) C ascomata in longitudinal section D ostiolar neck of ascoma E paraphyses F ascomatal wall G pseudostromatic tissue H–J asci K apex of ascus L–Q ascospores R germinating ascospore S–AF coelomycetous asexual morph (S–Y nature Z–AF culture) S appearance of conidiomata on substrate T conidiomata in longitudinal section U conidiomatal wall V conidiophores W phialide X, Y conidia Z–AB conidiomata in culture (AB multiloculate conidiomata) AC setose hypha of conidiomata AD conidiophores with groups of phialides AE, AF conidia AG–AL hyphomycetous synasexual morph AG, AH sporulation in culture AI phialide AJ, AK conidia AL chlamydospores. Scale bars: 1 mm (A, B, S, AB); 500 µm (C, Z, AA); 100 µm (D, T); 20 µm (AG, AH); 10 µm (E–J, L–R, U, V); 5 µm (K, W–Y, AC–AF, AI–AL).

Asexual morph (culture). Coelomycetous asexual morph: Conidiomata pycnidial, scattered, single to grouped, superficial, globose to subglobose, 180–380 μm high, mostly 80–580 μm diam., up to 1170 μm diam. when grouped, often becoming cup-shaped when mature, surrounded by setose hyphae. Conidiomatal wall composed of polygonal to prismatic, 3–4.5 \times 2.5–4 μm , dark brown cells. Setose hyphae erect, usually unbranched, septate, up to 360 μm long, 2–3 μm wide, pale brown. Conidiophores hyaline, thin-walled, simple or irregularly branched, with branches bearing a group of 2–5 phialides terminally. Phialides tapering toward the tip, hyaline, 10–25 \times 1–2.5 μm . Conidia ellipsoidal, with a slightly apiculate base, hyaline, smooth-walled, in slimy masses, 3–4.5 \times 1–2 μm (av. 3.8 \times 1.4 μm , $n = 50$). Hyphomycetous synasexual morph: Conidiophores micronematous, mononematous, hyaline, simple or rarely branched. Phialides slightly tapering toward the tip, 4–11 \times 1–2.5 μm , hyaline. Adelophialide absent. Conidia allantoid, hyaline, smooth-walled, in slimy heads, 3–9 \times 1–2.5 μm (av. 6.2 \times 1.7 μm , $n = 50$). Chlamydo spores rarely present, solitary, 3.5–6.5 μm diam., hyaline to pale brown, thick- and rough-walled.

Culture characteristics. Colonies on MEA at 25 $^{\circ}\text{C}$ attained 31–33 mm diam. after a week in the dark, whitish. On OA attained 32–36 mm diam., whitish to grey olivaceous (107). On PDA attained 32–33 mm diam., whitish to buff (45) (Fig. 6B).

Specimen examined. JAPAN, Aomori, Hirakawa, Hirofune, Shigabo Forest Park, on dead twigs of *Betula maximowicziana*, 10 October 2017, K. Tanaka, KT 3803 (HHUF 30648), living culture MAFF 247508.

Notes. The conidia from aerial hyphae of strain KT 3803 were larger (3–9 \times 1–2.5 μm) in culture than those of the original description of *Thyridium pluriloculosum* (3–5 \times 1–2.5 μm ; Perdomo et al. 2013). However, we identified this new collection on *Betula maximowicziana* as *T. pluriloculosum*, based on the high sequence homology of three loci with ex-type culture of this species (CBS 131712; 99.6% in ITS, 99.2% in *act*, and 99.5% in *tub2*). The sexual-aseexual relationship of *T. pluriloculosum* was verified in this study. Although this species has been reported from clinical sources as an asexual morph (Perdomo et al. 2013), the recently collected material represents a sexual morph on plant material.

In *Thyridium*, *T. betulae* has also been recorded on *Betula* sp. in France (Roumeuguère 1891). Although sequences of *T. betulae* are unavailable for molecular comparison, it is clearly different from *T. pluriloculosum* in having ascospores with 5–7 transverse and one longitudinal septum.

***Thyridium punctulatum* (I. Hino & Katum.) R. Sugita & Kaz. Tanaka, comb. nov.**

MycoBank No: 841919

Figs 5, 6C

Basionym. *Pleospora punctulata* I. Hino & Katum., *Icones Fungorum Bamb. Jpn.*: 181 (1961).

Holotype. JAPAN, Shizuoka, Fuji Bamboo Garden, on dead twigs of *Phyllostachys nigra* var. *henonis*, 1 April 1958, K. Katumoto, YAM 21851.

Epitype. JAPAN, Yamaguchi, Hagi, Akiragi, near Chikurindoro-park, on dead twigs of *Phyllostachys nigra* var. *nigra*, 26 March 2018, K. Tanaka, K. Arayama and R. Sugita, KT 3905 (HHUF 30649 epitype designated here; MBT 10004137), ex-epitype culture MAFF 247510.

Sexual morph. Stromata scattered to grouped, subepidermal, becoming erumpent to superficial, 0.5–1.2 mm long, 0.2–0.4 mm wide, dark brown. Ascomata perithecial, subglobose to conical, single to 2–3 grouped, 130–190 µm high, 140–230 µm diam., immersed in stromata to erumpent through host surface. Ascomatal wall 7–15 µm thick, composed of 3–5 layers of polygonal, 3–6.5 × 1–4.5 µm, dark brown cells. Ostiolar neck central, cylindrical, 37–85 µm long, 37–63 µm wide, periphysate. Paraphyses numerous, septate, unbranched, cylindrical, hyaline, 77–103 µm long. Asci unitunicate, cylindrical, 67.5–105 × 7.5–11.5 µm (av. 82.9 × 9.4 µm, n = 60), broadly rounded at the apex, with a pronounced non-amyloid apical annulus, short-stalked (3.5–11.5 µm long), with 8 ascospores. Ascospores ellipsoid to oblong, smooth, pale brown, with 3 transverse and 1–2 vertical septa, 10–15 × 5–9 µm (av. 12.8 × 7.0 µm, n = 60), l/w 1.4–2.4 (av. 1.8, n = 60).

Asexual morph (nature). Not observed.

Asexual morph (culture). Coelomycetous asexual morph: Conidiomata pycnidial, single to grouped, superficial, globose to subglobose, 100–250 µm high, 170–620 µm diam., composed of polygonal to prismatic, 3.5–7.5 × 2.5–4 µm cells, often becoming cup-shaped when mature, surrounded by setose hyphae. Setose hyphae erect, usually unbranched, septate, up to 225 µm long, 1.5–2.5 µm wide, pale brown. Conidiophores hyaline, thin-walled, simple or irregularly branched, with branches bearing a group of 2–5 phialides terminally. Phialides swollen at the base, tapering at the tip, 7–20 × 1–3 µm, hyaline. Conidia ellipsoidal to obovoid, with a slightly apiculate base, hyaline, smooth-walled, in slimy masses, 2–3.5 × 1–2 µm (av. 2.9 × 1.4 µm, n = 50). Hyphomycetous synasexual morph: Conidiophores micronematous, mononematous, hyaline, thin-walled, simple or irregularly branched, with branches bearing a group of 2–3 phialides terminally. Phialides swollen at the base, tapering at the tip, hyaline, 3–9 × 1–2 µm. Adelophialide absent. Conidia ellipsoidal to allantoid, hyaline, smooth-walled, in slimy heads, 2.5–8 × 1–3 µm (av. 4.3 × 1.6 µm, n = 87). Chlamydospores rarely present, solitary or chained, 4–5.5 µm diam., hyaline to pale brown.

Culture characteristics. Colonies on MEA at 25 °C attained 31–32 mm diam. after a week in the dark, granulose, whitish. On OA attained 38–39 mm diam., granulose, whitish. On PDA attained 35–36 mm diam., whitish to buff (45) (Fig. 6C).

Other specimen examined. JAPAN, Iwate, Morioka, Ueda, Campus of Iwate University, on dead culms of *Phyllostachys pubescens*, 17 February 2003, K. Tanaka and Y. Harada, KT 1015 (HHUF 29350), living culture JCM 13159 = MAFF 239669.

Notes. This species has been described from *Phyllostachys nigra* var. *henonis*, as a species of *Pleospora* (Dothideomycetes; Hino 1961). Our phylogenetic analysis (Fig. 1) shows that this species is a member of the genus *Thyridium* (Sordariomycetes). The morphological features of this species are consistent with those of the genus *Thyridium*, including immersed to erumpent, single to grouped, perithecial ascomata with a cylindrical ostiolar neck, unitunicate asci and muriform, pigmented ascospores (Eriksson and Yue 1989). Therefore, we propose a new combination, *T. punctulatum*, for *Pleospora punctulata*.

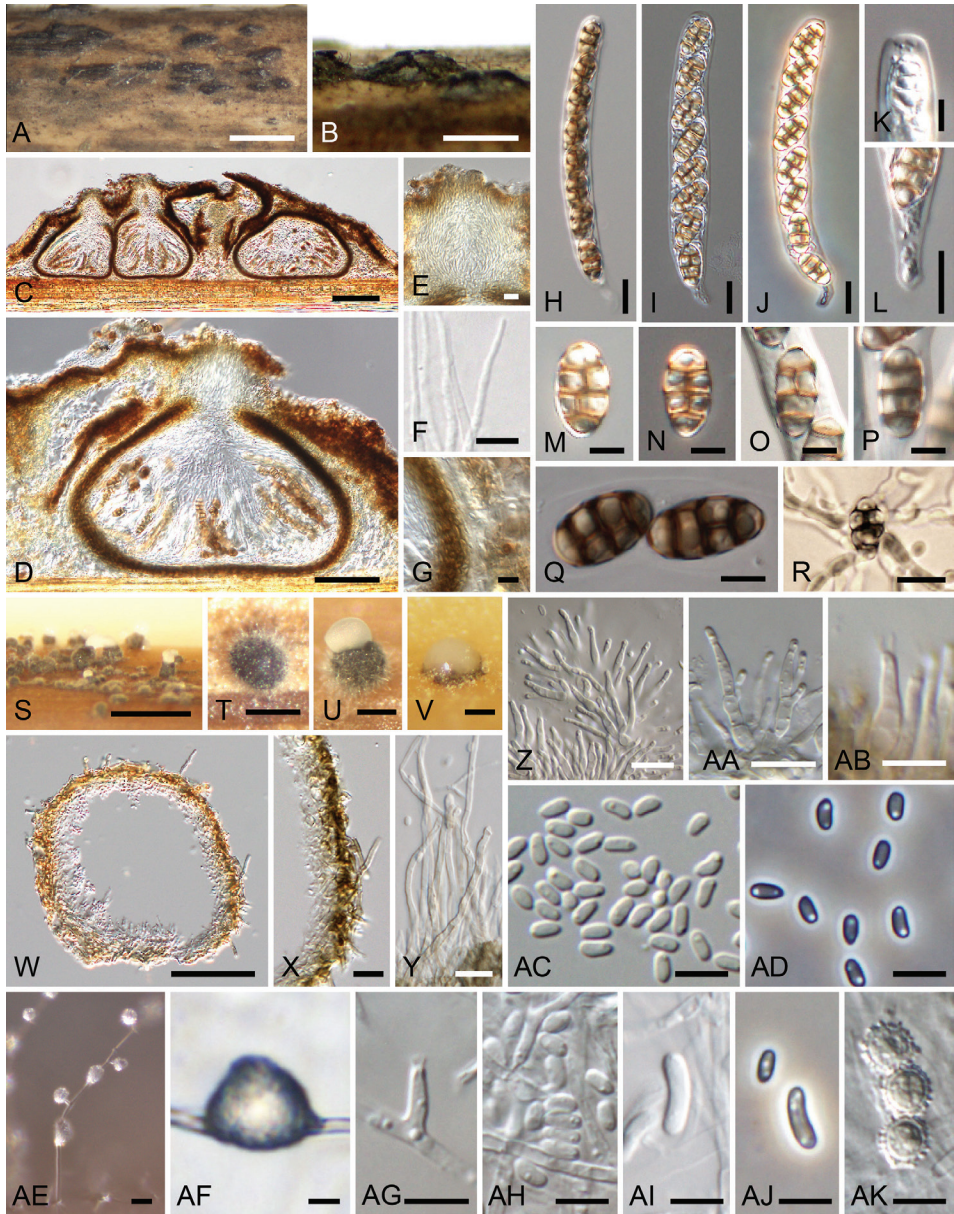


Figure 5. *Thyridium punctulatum* (A–N, Q, R KT 3905 = HHUF 30649 O, P YAM 21851 S, T, W–AB culture KT 1015 = JCM 13159 = MAFF 239669 U, V, AC–AK culture KT 3905 = MAFF 247510) A–R sexual morph A, B appearance of stromata on substrate C, D ascomata in longitudinal section E ostiolar neck of ascoma F paraphyses G ascomal wall H–J asci K apex of ascus L stipe of ascus M–Q ascospores R germinating ascospore S–AD coelomycetous asexual morph S–V conidiomata in culture W conidioma in longitudinal section X conidiomatal wall Y setose hyphae of conidiomata Z, AA conidiophores AB phialides AC, AD conidia AE–AK hyphomycetous synasexual morph AE conidiophore AF slimy head AG phialide AH–AJ conidia AK chlamydospores. Scale bars: 1 mm (A, S); 500 μ m (B); 100 μ m (C, W); 50 μ m (D); 10 μ m (E–J, L, R, X–AA, AE, AF); 5 μ m (K, M–Q, AB–AD, AG–AK); 200 μ m (T–V).

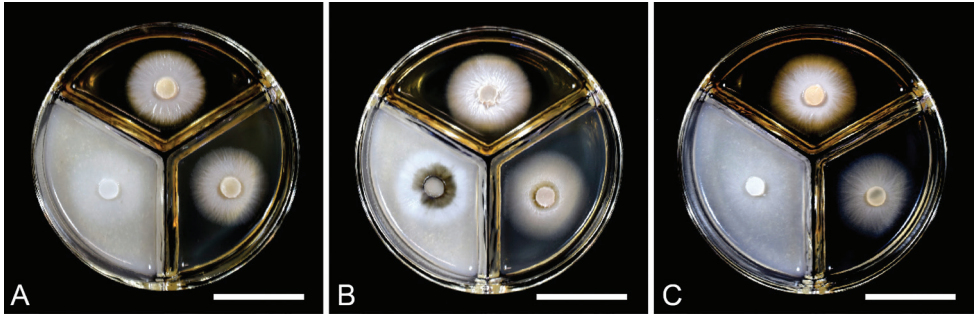


Figure 6. Colony characters of *Thyridium* species used in this study on MEA (bottom right), OA (bottom left) and PDA (upper) within 1 week at 25 °C in the dark **A** *T. flavostromatum* (culture KT 3891 = MAFF 247509) **B** *T. pluriloculosum* (culture KT 3803 = MAFF 247508) **C** *T. punctulatum* (culture KT 3905 = MAFF 247510). Scale bars: 3 cm (**A–C**).

***Thyridium cornearis* (Perdomo, Dania García, Gené, Cano & Guarro) R. Sugita & Kaz. Tanaka, comb. nov.**

Mycobank No: 841920

Basionym. *Phialemoniopsis cornearis* Perdomo, Dania García, Gené, Cano & Guarro, *Mycologia* 105: 408 (2013).

***Thyridium curvatum* (W. Gams & W.B. Cooke) R. Sugita & Kaz. Tanaka, comb. nov.**

Mycobank No: 841921

Phialemoniopsis curvata (W. Gams & W.B. Cooke) Perdomo, Dania García, Gené, Cano & Guarro, *Mycologia* 105: 410 (2013).

Basionym. *Phialemonium curvatum* W. Gams & W.B. Cooke, *Mycologia* 75: 980 (1983).

***Thyridium endophyticum* (Lei Su & Y.C. Niu) R. Sugita & Kaz. Tanaka, comb. nov.**

Mycobank No: 841922

Basionym. *Phialemoniopsis endophytica* Lei Su & Y.C. Niu, *Mycol. Progr.* 15: 3 (2016).

***Thyridium hongkongense* (Tsang, Chan, Ip, Ngan, Chen, Lau, Woo) R. Sugita & Kaz. Tanaka, comb. nov.**

Mycobank No: 841923

Basionym. *Phialemoniopsis hongkongensis* Tsang, Chan, Ip, Ngan, Chen, Lau, Woo, *J. Clin. Microbiol.* 52: 3284 (2014).

***Thyridium limonesiae* (A. Riat, L.W. Hou & Crous) R. Sugita & Kaz. Tanaka, comb. nov.**

MycoBank No: 841927

Basionym. *Phialemoniopsis limonesiae* A. Riat, L.W. Hou & Crous, *Emerging Microbes & Infections* 10: 403 (2021).

***Thyridium oculorum* (Gené & Guarro) R. Sugita & Kaz. Tanaka, comb. nov.**

MycoBank No: 841924

Phialemoniopsis ocularis (Gené & Guarro) Perdomo, Dania García, Gené, Cano & Guarro, *Mycologia* 105: 411 (2013).

Basionym. *Sarcopodium oculorum* Gené & Guarro, *J. Clin. Microbiol.* 40: 3074 (2002).

Discussion

We show that the asexual genus *Phialemoniopsis* (established by Perdomo et al. 2013) is a synonym of the sexual genus *Thyridium* (established by Nitschke 1867). We found a new species of *Thyridium* (*T. flavostromatum*), transferred *Pleospora punctulata* into *Thyridium*, and proposed seven new combinations in *Thyridium* for strains previously treated in *Phialemoniopsis*. We provided a revised generic circumscription of *Thyridium* based on both sexual and asexual characteristics and revealed the phylogenetic relationships of species within this genus.

The genus *Thyridium* has been defined mainly on the basis of sexual characters (Nitschke 1867; Eriksson and Yue 1989). Currently, 33 species are recorded in this genus (<http://www.indexfungorum.org>, 2021). Asexual morphs are unknown in most species of *Thyridium*, with the exceptions of *T. flavum* and *T. vestitum*, in which asexual morphs have been recorded based on sexual-aseexual association on the same specimen (Petch 1917) and on the basis of culture study (Leuchtmann and Müller 1986, this study), respectively. In contrast, the genus *Phialemoniopsis* has been defined based only on asexual characters (Perdomo et al. 2013). Its ordinal affiliation within Sordariomycetes has not been resolved, but recent phylogenetic analyses of this class suggest that *Phialemoniopsis* is close to *Thyridium* (Hyde et al. 2021). In our phylogenetic analysis, all species previously described as *Phialemoniopsis* (marked with blue circle; Fig. 1) were clustered in a single clade, including the type species of *Thyridium* (*T. vestitum*), as well as two new strains proposed here (*T. flavostromatum* and *T. punctulatum*). Both genera have similar asexual morphs, which have conidiophores bearing small groups of phialides, hyaline phialidic conidiogenous cells, and ellipsoidal or allantoid, hyaline conidia in both coelomycetous and hyphomycetous states (Petch 1917; Leuchtmann and Müller 1986; Perdomo et al. 2013). Morphological and molecular phylogenetic evidence clearly shows that *Phialemoniopsis* is congeneric with *Thyridium*.

Synonymising *Phialemoniopsis* under *Thyridium* expanded information about the asexual morphs of *Thyridium*. In this genus, only *T. vestitum* has been demonstrated to have asexual morphs by culture studies (Leuchtmann and Müller 1986). It has both coelomycetous and hyphomycetous complex asexual morphs, which have phialidic conidiogenous cells with collarette and ellipsoidal to allantoid hyaline conidia (Leuchtmann and Müller 1986). Members of *Phialemoniopsis* also have coelomycetous and/or hyphomycetous conidial states (Perdomo et al. 2013; Tsang et al. 2014; Su et al. 2016; Martinez et al. 2021). The close relationship of *Phialemoniopsis* and *Thyridium* suggests that such complex asexual morphs may be common within *Thyridium* species.

In *Thyridium*, *T. endophyticum* and *T. curvatum* have been isolated from both plants and animals (Gam and McGinnis 1983; Halleen et al. 2007; Perdomo et al. 2013; Su et al. 2016; Ito et al. 2017). There are several examples of fungal species, including human pathogens, detected from various substrates. For example, *Phaeoacremonium minimum* is a pathogen on grapevines, where it forms both sexual and asexual morphs (Crous et al. 1996; Pascoe et al. 2004), but it has also been reported as a causative agent of subcutaneous phaeohyphomycosis in humans as asexual morph (Choi et al. 2011). Other species of *Thyridium* may also have cryptic life cycles and can colonise each host substrate at different reproductive stages. An example of this prediction can be found in *T. pluriloculosum*. This species was originally found in human nails as an asexual fungus (Perdomo et al. 2013), and its sexual state was rediscovered on twigs of *Betula maximowicziana* in our study.

Epitypification of the type species of *Thyridium* (*T. vestitum*) will be a necessary issue in the future. We used sequences from two non-type strains (CBS 113027, CBS 125582) of this species for phylogenetic analyses but they did not form a monophyletic clade (Fig. 1). Sequence differences between these two strains were found at 34 positions with four gaps in the LSU. These results indicate that the strains obtained from *Acer pseudoplatanus* (CBS 113027) and no host information (CBS 125582) in Austria are not conspecific. A fresh collection of *T. vestitum* on original host plant from the type locality (*Ribes rubrum*, Sweden; Fries 1823) and its phylogenetic analysis are required to fix generic circumscription of *Thyridium*.

Thyridiales established here may encompass other genera and families with morphologies distinct from the genus *Thyridium* (Thyridiaceae). Some species of “*Linocarpon*” and “*Neolinocarpon*” are nested within the Thyridiales (Fig. 1). *Linocarpon* and *Neolinocarpon* sensu stricto belong to Linocarpaceae (Chaetosphaerales) and are morphologically distinct from *Thyridium* in having filiform, straight or curved, unicellular, hyaline, or pale-yellowish ascospores (Huhndorf and Miller 2011; Konta et al. 2017). The “*Linocarpon*” and “*Neolinocarpon*” species phylogenetically unrelated to *Linocarpon* and *Neolinocarpon* sensu stricto may be new lineages in Thyridiaceae or belong to its own new undescribed family. However, we cannot clarify the phylogenetic/taxonomic relatedness of these atypical *Linocarpon*-like species because none of them are ex-types and their morphological information are unavailable. Further molecular phylogenetic study of these fungi based on protein-coding sequences and finding additional specimens/isolates of “*Linocarpon*” and “*Neolinocarpon*” species related to *Thyridium* will be necessary to clarify their taxonomic affiliation and better understand the concept of Thyridiales.

Acknowledgments

We gratefully acknowledge Y. Harada and K. Arayama for their help with the collection of fungal specimens. We thank the curator of YAM, S. Ito, who permitted us to examine type collection. This work was partially supported by grants from the Japan Society for the Promotion of Science (JSPS 19K06802).

References

- Akaike H (1974) A new look at the statistical model identification. *IEEE Transactions on Automatic Control* 19: 716–723. <https://doi.org/10.1109/TAC.1974.1100705>
- Arzanlou M, Groenewald JZ, Gams W, Braun U, Shin H-D, Crous PW (2007) Phylogenetic and morphotaxonomic revision of *Ramichloridium* and allied genera. *Studies in Mycology* 58: 57–93. <https://doi.org/10.3114/sim.2007.58.03>
- Bahl J (2006) Molecular evolution of three morphologically similar families in the Xylariomycetidae (Apiosporaceae, Clypeosphaeriaceae, Hyponectriaceae). PhD thesis, The University of Hong Kong. Pokfulam, Hong Kong. <http://hdl.handle.net/10722/51007>
- Campbell J, Shearer CA (2004) *Annulusmagnus* and *Ascitendus*, two new genera in the Annulatascaceae. *Mycologia* 96: 822–833. <https://doi.org/10.1080/15572536.2005.11832929>
- Castlebury LA, Rossman AY, Jaklitsch WJ, Vasilyeva LN (2002) A preliminary overview of the Diaporthales based on large subunit nuclear ribosomal DNA sequences. *Mycologia* 94: 1017–1031. <https://doi.org/10.1080/15572536.2003.11833157>
- Checa J, Blanco MN, Moreno G (2013) Contributions to the family Thyridiaceae. New data on *Sphaeria mutabilis*. *Mycotaxon* 125: 149–164. <https://doi.org/10.5248/125.149>
- Choi J, Lee Y, Chung HS, Koo JS, Yong D, Kim YS, Lee K, Chong Y (2011) Subcutaneous Phaeohyphomycosis caused by *Phaeoacremonium* species in a kidney transplant patient: the first case in Korea. *The Korean Journal of Laboratory Medicine* 31: 201–204. <https://doi.org/10.3343/kjlm.2011.31.3.201>
- Crous PW, Gams W, Wingfield MJ, Wyk PSV (1996) *Phaeoacremonium* gen. nov. associated with wilt and decline diseases of woody hosts and human infections. *Mycologia* 88: 786–796. <https://doi.org/10.1080/00275514.1996.12026716>
- Crous PW, Luangsa-Ard JJ, Wingfield MJ, Carnegie AJ, Hernández-Restrepo M, Lombard L, Roux J, Barreto RW, Baseia IG, Cano-Lira JF, Martín MP, Morozova OV, Stchigel AM, Summerell BA, Brandrud TE, Dima B, García D, Giraldo A, Guarro J, Gusmão LFP, Kham-suntorn P, Noordeloos ME, Nuankaew S, Pinruan U, Rodríguez-Andrade E, Souza-Motta CM, Thangavel R, van Iperen AL, Abreu VP, Accioly T, Alves JL, Andrade JP, Bahram M, Baral H-O, Barbier E, Barnes CW, Bendixsen E, Bernard E, Bezerra JDP, Bezerra JL, Bizio E, Blair JE, Bulyonkova TM, Cabral TS, Caiafa MV, Cantillo T, Colmán AA, Conceição LB, Cruz S, Cunha AOB, Darveaux BA, da Silva AL, da Silva GA, da Silva GM, da Silva RMF, de Oliveira RJV, Oliveira RL, De Souza JT, Dueñas M, Evans HC, Epifani F, Felipe MTC, Fernández-López J, Ferreira BW, Figueiredo CN, Filippova NV, Flores JA, Gené J, Ghorbani G, Gibertoni TB, Glushakova AM, Healy R, Huhndorf SM, Iturrieta-González

- I, Javan-Nikkhah M, Juciano RF, Jurjević Ž, Kachalkin AV, Keochanpheng K, Krisai-Greilhuber I, Li Y-C, Lima AA, Machado AR, Madrid H, Magalhães OMC, Marbach PAS, Melanda GCS, Miller AN, Mongkolsamrit S, Nascimento RP, Oliveira TGL, Ordoñez ME, Orzes R, Palma MA, Pearce CJ, Pereira OL, Perrone G, Peterson SW, Pham THG, Piontelli E, Pordel A, Quijada L, Raja HA, Rosas de Paz E, Ryvar den L, Saitta A, Salcedo SS, Sandoval-Denis M, Santos TAB, Seifert KA, Silva BDB, Smith ME, Soares AM, Sommai S, Sousa JO, Suetrong S, Susca A, Tedersoo L, Telleria MT, Thanakitpipattana D, Valenzuela-Lopez N, Visagie CM, Zapata M, Groenewald JZ (2018) Fungal Planet description sheets: 785–867. *Persoonia* 41: 238–417. <https://doi.org/10.3767/persoonia.2018.41.12>
- Crous PW, Schumacher RK, Akulov A, Thangavel R, Hernández-Restrepo M, Carnegie AJ, Cheewangkoon R, Wingfield MJ, Summerell BA, Quaedvlieg W, Coutinho TA, Roux J, Wood AR, Giraldo A, Groenewald JZ (2019) New and Interesting Fungi. 2. *Fungal Systematics and Evolution* 3: 57–134. <https://doi.org/10.3114/fuse.2019.03.06>
- Crous PW, Wingfield MJ, Guarro J, Cheewangkoon R, van der Bank M, Swart WJ, Stchigel AM, Cano-Lira JF, Roux J, Madrid H, Damm U, Wood AR, Shuttleworth LA, Hodges CS, Munster M, de Jesús Yáñez-Morales M, Zúñiga-Estrada L, Cruywagen EM, de Hoog GS, Silvera C, Najafzadeh J, Davison EM, Davison PJN, Barrett MD, Barrett RL, Manamgoda DS, Minnis AM, Kleczewski NM, Flory SL, Castlebury LA, Clay K, Hyde KD, Maússe-Sitoe SND, Chen S, Lechat C, Hairaud M, Lesage-Meessen L, Pawłowska J, Wilk M, Śliwińska-Wyrzychowska A, Mętrak M, Wrzosek M, Pavlic-Zupanc D, Maleme HM, Slippers B, Mac Cormack MP, Archuby DI, Grünwald NJ, Telleria MT, Dueñas M, Martín MP, Marincowitz S, de Beer ZW, Perez CA, Gené J, Marin-Felix Y, Groenewald JZ (2013) Fungal Planet description sheets: 154–213. *Persoonia* 31: 188–296. <https://doi.org/10.3767/003158513X675925>
- Crous PW, Wingfield MJ, Guarro J, Hernández-Restrepo M, Sutton DA, Acharya K, Barber PA, Boekhout T, Dimitrov RA, Dueñas M, Dutta AK, Gené J, Gouliamova DE, Groenewald M, Lombard L, Morozova OV, Sarkar J, Smith MT, Stchigel AM, Wiederhold NP, Alexandrova AV, Antelmi I, Armengol J, Barnes I, Cano-Lira JF, Castañeda Ruiz RF, Contu M, Courtecuisse PR, da Silveira AL, Decock CA, de Goes A, Edathodu J, Ercole E, Firmino AC, Fourie A, Fournier J, Furtado EL, Geering ADW, Gershenson J, Giraldo A, Gramaje D, Hammerbacher A, He X-L, Haryadi D, Khemmuk W, Kovalenko AE, Krawczynski R, Laich F, Lechat C, Lopes UP, Madrid H, Malysheva EF, Marin-Felix Y, Martín MP, Mostert L, Nigro F, Pereira OL, Picillo B, Pinho DB, Popov ES, Rodas Peláez CA, Rooney-Latham S, Sandoval-Denis M, Shivas RG, Silva V, Stoilova-Disheva MM, Telleria MT, Ullah C, Unsicker SB, van der Merwe NA, Vizzini A, Wagner H-G, Wong PTW, Wood AR, Groenewald JZ (2015a) Fungal Planet description sheets: 320–370. *Persoonia* 34: 167–266. <http://dx.doi.org/10.3767/003158515X688433>
- Crous PW, Wingfield MJ, Le Roux JJ, Richardson DM, Strasberg D, Shivas RG, Alvarado P, Edwards J, Moreno G, Sharma R, Sonawane MS, Tan YP, Altés A, Barasubiye T, Barnes CW, Blanchette RA, Boertmann D, Bogo A, Carlavilla JR, Cheewangkoon R, Daniel R, de Beer ZW, de Jesús Yáñez-Morales M, Duong TA, Fernández-Vicente J, Geering ADW, Guest DI, Held BW, Heykoop M, Hubka V, Ismail AM, Kajale SC, Khemmuk W, Kolařík M, Kurli R, Lebeuf R, Lévesque CA, Lombard L, Magista D, Manjón JL, Marincowitz

- S, Mohedano JM, Nováková A, Oberlies NH, Otto EC, Paguigan ND, Pascoe IG, Pérez-Butrón JL, Perrone G, Rahi P, Raja HA, Rintoul T, Sanhueza RMV, Scarlett K, Shouche YS, Shuttleworth LA, Taylor PWJ, Thorn RG, Vawdrey LL, Vidal RS, Voitk A, Wong PTW, Wood AR, Zamora JC, Groenewald JZ (2015b) Fungal Planet description sheets: 371–399. *Persoonia* 35: 264–327. <http://dx.doi.org/10.3767/003158515X690269>
- Cruse M, Telerant R, Gallagher T, Lee T, Taylor JW (2002) Cryptic species in *Stachybotrys chartarum*. *Mycologia* 94: 814–822. <https://doi.org/10.1080/15572536.2003.11833175>
- Desoubeaux G, García D, Bailly E, Augereau O, Bacle G, De Muret A, Bernard L, Cano-Lira JF, Garcia-Hermoso D, Chandener J (2014) Subcutaneous phaeohyphomycosis due to *Phialemoniopsis ocularis* successfully treated by voriconazole. *Medical Mycology Case Reports* 5: 4–8. <https://doi.org/10.1016/j.mmcr.2014.04.001>
- Dong W, Hyde KD, Jeewon R, Doilom M, Yu XD, Wang GN, Liu NG, Hu DM, Nalumpang S, Zhang H (2021) Towards a natural classification of annulatasceae-like taxa II: introducing five new genera and eighteen new species from freshwater. *Mycosphere* 12: 1–88. <https://doi.org/10.5943/mycosphere/12/1/1>
- Eriksson OE, Yue J-Z (1989) An amended description and disposition of the genus *Thyridium*. *Systema Ascomycetum* 8: 9–16.
- Fries EM (1823) *Systema Mycologicum* 2: 276–620.
- Gams W, McGinnis MR (1983) *Phialemonium*, a new anamorph genus intermediate between *Phialophora* and *Acremonium*. *Mycologia* 75: 977–987. <https://doi.org/10.1080/00275514.1983.12023783>
- Halleen F, Mostert L, Crous PW (2007) Pathogenicity testing of lesser-known vascular fungi of grapevines. *Australasian Plant Pathology* 36: 277–285. <https://doi.org/10.1071/AP07019>
- Hino I (1961) *Icones fungorum bambusicolorum japonicorum*. The Fuji Bamboo Garden, Gotenba.
- Huhndorf SM, Greif M, Mugambi GK, Miller AN (2008) Two new genera in the Magnaporthaceae, a new addition to *Ceratosphaeria* and two new species of *Lentomitella*. *Mycologia* 100: 940–955. <https://doi.org/10.3852/08-037>
- Huhndorf SM, Miller AN (2011) A molecular re-appraisal of taxa in the Sordariomycetidae and a new species of *Rimaconus* from New Zealand. *Studies in Mycology* 68: 203–210. <https://doi.org/10.3114/sim.2011.68.09>
- Huhndorf SM, Miller AN, Fernández FA (2004) Molecular systematics of the Sordariales: the order and the family Lasiosphaeriaceae redefined. *Mycologia* 96: 368–387. <https://doi.org/10.1080/15572536.2005.11832982>
- Hyde KD, Bao DF, Hongsanan S, Chethana KWT, Yang J, Suwannarach N (2021) Evolution of freshwater Diaporthomycetidae (Sordariomycetes) provides evidence for five new orders and six new families. *Fungal Diversity* 107: 71–105. <https://doi.org/10.1007/s13225-021-00469-7>
- Hyde KD, Chaiwan N, Norphanphoun C, Boonmee S, Camporesi E, Chethana KWT, Dayarathne MC, de Silva NI, Dissanayake AJ, Ekanayaka AH, Hongsanan S, Huang SK, Jayasiri SC, Jayawardena R, Jiang HB, Karunarathna A, Lin CG, Liu JK, Liu NG, Lu YZ, Luo ZL, Maharachchimbura SSN, Manawasinghe IS, Pem D, Perera RH, Phukhamsakda C, Samarakoon MC, Senwannana C, Shang QJ, Tennakoon DS, Thambugala KM, Tibpromma S, Wanasinghe DN, Xiao YP, Yang J, Zeng XY, Zhang JF, Zhang SN, Bulgakov TS, Bhat

- DJ, Cheewangkoon R, Goh TK, Jones EBG, Kang JC, Jeewon R, Liu ZY, Lumyong S, Kuo CH, McKenzie EHC, Wen TC, Yan JY, Zhao Q (2018) Mycosphere notes 169–224. *Mycosphere* 9: 271–430. <https://doi.org/10.5943/mycosphere/9/2/8>
- Ito A, Yamada N, Kimura R, Tanaka N, Kurai J, Anzawa K, Mochizuki T, Yamamoto O (2017) Concurrent double fungal infections of the skin caused by *Phialemoniopsis endophytica* and *Exophiala jeanselmei* in a patient with microscopic polyangiitis. *Acta Dermato-Venereologica* 97: 1142–1144. <https://doi.org/10.2340/00015555-2734>
- Jaklitsch WM, Réblová M, Voglmayr H (2013) Molecular systematics of *Woswasia atropurpurea* gen. et sp. nov. (Sordariomycetidae), a fungicolous ascomycete with globose ascospores and holoblastic conidiogenesis. *Mycologia* 105: 476–485. <https://doi.org/10.3852/12-244>
- Khemmuk W, Geering ADW, Shivas RG (2016) *Wongia* gen. nov. (Papulosaceae, Sordariomycetes), a new generic name for two root-infecting fungi from Australia. *IMA Fungus* 7: 247–252. <https://doi.org/10.5598/imafungus.2016.07.02.04>
- Konta S, Hongsanan S, Liu JK, Eungwanichayapant PD, Jeewon R, Hyde KD, Maharachchikumbura SSN, Boonmee S (2017) *Leptosporella* (Leptosporaceae fam. nov.) and *Linocarpon* and *Neolinocarpon* (Linocarpaceae fam. nov.) are accommodated in Chaetosphaeriales. *Mycosphere* 8: 1943–1974. <https://doi.org/10.5943/mycosphere/8/10/16>
- Kumar S, Stecher G, Tamura K (2016) MEGA7: Molecular evolutionary genetics analysis version 7.0 for bigger datasets. *Molecular Biology and Evolution* 33: 1870–1874. <https://doi.org/10.1093/molbev/msw054>
- Leuchtmann A, Müller E (1986) Über *Thyridium vestitum* und sein anamorph (Ascomycetes). *Botanica Helvetica* 96: 283–287. <https://doi.org/10.5169/seals-67205>
- Liu YJ, Whelen S, Hall BD (1999) Phylogenetic relationships among ascomycetes: Evidence from an RNA polymerase II subunit. *Molecular Biology and Evolution* 16: 1799–1808. <https://doi.org/10.1093/bioinformatics/btq224>
- Luo ZL, Hyde KD, Liu JK, Bhat DJ, Bao DF, Li WL, Su HY (2018) Lignicolous freshwater fungi from China II: Novel *Distoseptispora* (Distoseptisporaceae) species from northwestern Yunnan Province and a suggested unified method for studying lignicolous freshwater fungi. *Mycosphere* 9: 444–461. <https://doi.org/10.5943/mycosphere/9/3/2>
- Luo ZL, Hyde KD, Liu JK, Maharachchikumbura SSN, Jeewon R, Bao DF, Bhat DJ, Lin CG, Li WL, Yang J, Liu NG, Lu Y-Z, Jayawardena RS, Li JF, Su HY (2019) Freshwater Sordariomycetes. *Fungal Diversity* 99: 451–660. <https://doi.org/10.1007/s13225-019-00438-1>
- Lutzoni F, Kauff F, Cox CJ, McLaughlin D, Celio G, Dentinger B, Padamsee M, Hibbett D, James TY, Baloch E, Grube M, Reeb V, Hofstetter V, Schoch C, Arnold AE, Miadlikowska J, Spatafora J, Johnson D, Hambleton S, Crockett M, Shoemaker R, Sung GH, Lücking R, Lumbsch T, O'Donnell K, Binder M, Diederich P, Ertz D, Gueidan C, Hansen K, Harris RC, Hosaka K, Lim Y-W, Matheny B, Nishida H, Pfister D, Rogers J, Rossman A, Schmitt I, Sipman H, Stone J, Sugiyama J, Yahr R, Vilgalys R (2004) Assembling the fungal tree of life: progress, classification, and evolution of subcellular traits. *American Journal of Botany* 91: 1446–1480. <https://doi.org/10.3732/ajb.91.10.1446>
- Mardones M, Trampe-Jaschik T, Oster S, Elliott M, Urbina H, Schmitt I, Piepenbring M (2017) Phylogeny of the order Phyllachorales (Ascomycota, Sordariomycetes): among and within order relationships based on five molecular loci. *Persoonia* 39: 74–90. <https://doi.org/10.3767/persoonia.2017.39.04>

- Martinez DA, Alberto C, Riat A, Schuhler C, Valladares P, Ninet B, Kraak B, Crous PW, Hou LW, Trelu LT (2021) *Phialemoniopsis limonesiae* sp. nov. causing cutaneous phaeohyphomycosis in an immunosuppressed woman. *Emerging Microbes & Infections* 10: 400–406. <https://doi.org/10.1080/22221751.2021.1892458>
- Miller AN, Huhndorf SM (2004a) A natural classification of *Lasiosphaeria* based on nuclear LSU rDNA sequences. *Mycological Research* 108: 26–34. <https://doi.org/10.1017/S0953756203008864>
- Miller AN, Huhndorf SM (2004b) Using phylogenetic species recognition to delimit species boundaries within *Lasiosphaeria*. *Mycologia* 96: 1106–1127. <https://doi.org/10.1080/15572536.2005.11832909>
- Miller AN, Huhndorf SM (2005) Multi-gene phylogenies indicate ascomal wall morphology is a better predictor of phylogenetic relationships than ascospore morphology in the Sordariales (Ascomycota, Fungi). *Molecular Phylogenetics and Evolution* 35: 60–75. <https://doi.org/10.1016/j.ympev.2005.01.007>
- Nitschke T (1867) Pyrenomycetes Germanici. *Die Kernpilze Deutschlands*. 1: 1–160. Eduard Trewendt, Breslau. <https://hdl.handle.net/2027/coo.31924000644199>
- Pascoe IG, Edwards J, Cunnington JH, Cottral EH (2004) Detection of the *Togninia* teleomorph of *Phaeoacremonium aleophilum* in Australia. *Phytopathologia Mediterranea* 43: 51–58. <https://doi.org/10.1400/14571>
- Perdomo H, García D, Gené J, Cano J (2013) *Phialemoniopsis*, a new genus of Sordariomycetes, and new species of *Phialemonium* and *Lecythophora*. *Mycologia* 105: 398–421. <https://doi.org/10.3852/12-137>
- Petch T (1917) Additions to Ceylon fungi. *Annals of the Royal Botanic Gardens Peradeniya* 6: 195–256. <https://www.biodiversitylibrary.org/page/52423816>
- Pinruan U, Sakayaroj J, Hyde KD, Jones EBG (2008) *Thailandiomyces bisetulosus* gen. et sp. nov. (Diaporthales, Sordariomycetidae, Sordariomycetes) and its anamorph *Craspedodidymum*, is described based on nuclear SSU and LSU rDNA sequences. *Fungal Diversity* 29: 89–98.
- Raja HA, Campbell J, Shearer CA (2003) Freshwater ascomycetes: *Cyanoannulus peterseii*, a new genus and species from submerged wood. *Mycotaxon* 88: 1–17. <http://www.cybertruffle.org.uk/cyberliber/>
- Rambaut A, Suchard MA, Drummond AJ (2014) Tracer 1.6. <http://beast.bio.ed.ac.uk/Tracer>
- Rayner RW (1970) A mycological colour chart. CMI and British Mycological Society, Kew, Surrey.
- Réblová M (2006) Molecular systematics of *Ceratostomella* sensu lato and morphologically similar fungi. *Mycologia* 98: 68–93. <https://doi.org/10.1080/15572536.2006.11832714>
- Réblová M (2007) *Barbatosphaeria* gen. et comb. nov., a new genus for *Calosphaeria barbirostris*. *Mycologia* 99: 723–732. <https://doi.org/10.1080/15572536.2007.11832536>
- Réblová M (2009) Teleomorph of *Rhodoveronea* (Sordariomycetidae) discovered and re-evaluation of *Pleurophragmium*. *Fungal Diversity* 36: 129–139.
- Réblová M (2011) New insights into the systematics and phylogeny of the genus *Jattaea* and similar fungi of the Calosphaerales. *Fungal Diversity* 49: 167–198. <https://doi.org/10.1007/s13225-011-0099-8>
- Réblová M (2013) Two taxonomic novelties in the Sordariomycetidae: *Ceratolenta caudata* gen. et sp. nov. and *Platytrachelan abietis* gen. et comb. nov. for *Ceratospaeria abietis*. *Mycologia* 105: 462–475. <https://doi.org/10.3852/12-199>

- Réblová M, Fournier J, Hyde KD (2010) *Achroceratosphaeria*, a new ascomycete genus in the Sordariomycetes, and re-evaluation of *Ceratosphaeria incolorata*. Fungal Diversity 43: 75–84. <https://doi.org/10.1007/s13225-010-0032-6>
- Réblová M, Fournier J, Štěpánek V (2016) Two new lineages of aquatic ascomycetes: *Atractospora* gen. nov. and *Rubellisphaeria* gen. et sp. nov., and a sexual morph of *Myrmecridium montse-gurinum* sp. nov. Mycological Progress 15: 21. <https://doi.org/10.1007/s11557-016-1166-z>
- Réblová M, Gams W, Seifert KA (2011) *Monilochaetes* and allied genera of the Glomerellales, and a reconsideration of families in the Microascales. Studies in Mycology 68: 163–191. <https://doi.org/10.3114/sim.2011.68.07>
- Réblová M, Miller AN, Réblová K, Štěpánek V (2018) Phylogenetic classification and generic delineation of *Calyptosphaeria* gen. nov., *Lentomitella*, *Spadicoides* and *Torrentispora* (Sordariomycetes). Studies in Mycology 89: 1–62. <https://doi.org/10.1016/j.simyco.2017.11.004>
- Réblová M, Mostert L, Gams W, Crous PW (2004) New genera in the Calosphaeriales: *Togniniella* and its anamorph *Phaeocrella*, and *Calosphaeriophora* as anamorph of *Calosphaeria*. Studies in Mycology 50: 533–550.
- Réblová M, Réblová K, Štěpánek V (2015) Molecular systematics of *Barbatosphaeria* (Sordariomycetes): multigene phylogeny and secondary ITS structure. Persoonia 35: 21–38. <http://dx.doi.org/10.3767/003158515X687434>
- Réblová M, Seifert KA, Fournier J, Štěpánek V (2012) Phylogenetic classification of *Pleurothecium* and *Pleurotheciella* gen. nov. and its *dactylaria*-like anamorph (Sordariomycetes) based on nuclear ribosomal and protein-coding genes. Mycologia 104: 1299–1314. <https://doi.org/10.3852/12-035>
- Réblová M, Štěpánek V (2018) Introducing the Rhamphoriaceae, fam. nov. (Sordariomycetes), two new genera, and new life histories for taxa with *Phaeoisaria*- and *Idriella*-like anamorphs. Mycologia 110: 750–770. <https://doi.org/10.1080/00275514.2018.1475164>
- Réblová M, Štěpánek V, Schumacher RK (2014) *Xylochrysis lucida* gen. et sp. nov., a new lignicolous ascomycete (Sordariomycetidae) with holoblastic conidiogenesis. Mycologia 106: 564–572. <https://doi.org/10.3852/13-266>
- Rehner SA, Buckley E (2005) A *Beauveria* phylogeny inferred from nuclear ITS and EF1- α sequences: evidence for cryptic diversification and links to *Cordyceps* teleomorphs. Mycologia 97: 84–98. <https://doi.org/10.1080/15572536.2006.11832842>
- Rehner SA, Samuels GJ (1994) Taxonomy and phylogeny of *Gliocladium* analysed from nuclear large subunit ribosomal DNA sequences. Mycological Research 98: 625–634. [https://doi.org/10.1016/S0953-7562\(09\)80409-7](https://doi.org/10.1016/S0953-7562(09)80409-7)
- Ronquist F, Teslenko M, van der Mark P, Ayres DL, Drling A, Höhna S, Larget B, Liu L, Suchard MA, Huelsenbech JP (2012) MrBayes 3.2: efficient Bayesian phylogenetic inference and model choice across a large model space. Systematic Biology 61: 539–542. <https://doi.org/10.1093/sysbio/sys029>
- Roumeguère C (1891) Fungi exsiccati praecipue Gallici. Centurie LIX. Revue Mycologique Toulouse. 13: 163–173. <https://www.biodiversitylibrary.org/page/11828914>
- Saccardo PA (1891) Supplementum Universale, Pars I. Agaricaceae-Laboulbeniaceae. Sylloge Fungorum 9: 1–1141. <https://www.biodiversitylibrary.org/page/4300290>
- Samuels GJ, Rogerson CT (1989) *Endocreas lasiacidis* and *Sinosphaeria lasiacidis*, new tropical ascomycetes. Studies in Mycology. 31: 145–149. <http://www.cybertruffle.org.uk/cyberliber/>

- Schoch CL, Sung G-H, López-Giráldez F, Townsend JP, Miadlikowska J, Hofstetter V, Robertse B, Matheny PB, Kauff F, Wang Z, Gueidan C, Andrie RM, Trippe K, Ciufetti LM, Wynns A, Fraker E, Hodkinson BP, Bonito G, Groenewald JZ, Arzanlou M, de Hoog GS, Crous PW, Hewitt D, Pfister DH, Peterson K, Gryzenhout M, Wingfield MJ, Aptroot A, Suh S-O, Blackwell M, Hillis DM, Griffith GW, Castlebury LA, Rossman AY, Lumbsch TH, Lücking R, Büdel B, Rauhut A, Diederich P, Ertz D, Geiser DM, Hosaka K, Inderbitzin P, Kohlmeyer J, Volkmann-Kohlmeyer B, Mostert L, O'Donnell K, Sipman H, Rogers JD, Shoemaker RA, Sugiyama J, Summerbell RC, Untereiner W, Johnston PR, Stenroos S, Zuccaro A, Dyer PS, Crittenden PD, Cole MS, Hansen K, Trappe JM, Yahr R, Lutzoni F, Spatafora JW (2009) The Ascomycota Tree of Life: A Phylum-wide Phylogeny Clarifies the Origin and Evolution of Fundamental Reproductive and Ecological Traits. *Systematic Biology* 58: 224–239. <https://doi.org/10.1093/sysbio/syp020>
- Schwarz G (1978) Estimating the dimension of a model. *The Annals of Statistics* 6: 461–464. <https://doi.org/10.1214/aos/1176344136>
- Senanayake IC, Al-Sadi AM, Bhat JD, Camporesi E, Dissanayake AJ, Lumyong S, Maharachchikumbura SSN, Hyde KD (2018) Phomatosporales ord. nov. and Phomatosporaceae fam. nov., to accommodate *Lanspora*, *Phomatospora* and *Tenuimurus*, gen. nov. *Mycosphere* 7: 628–641. <https://doi.org/10.5943/mycosphere/7/5/8>
- Shenoy BD, Jeewon R, Wu WP, Bhat DJ, Hyde KD (2006) Ribosomal and RPB2 DNA sequence analyses suggest that *Sporidesmium* and morphologically similar genera are polyphyletic. *Mycological Research* 110: 916–928. <https://doi.org/10.1016/j.mycres.2006.06.004>
- Smith GJD, Liew ECY, Hyde KD (2006) The Xylariales: a monophyletic order containing 7 families. *Fungal Diversity* 13: 185–218.
- Spatafora JW, Sung GH, Johnson D, Hesse C, O'Rourke B, Serdani M, Spotts R, Lutzoni F, Hofstetter V, Miadlikowska J, Reeb V, Gueidan C, Fraker E, Lumbsch T, Lücking R, Schmitt I, Hosaka K, Aptroot A, Roux C, Miller AN, Geiser DM, Hafellner J, Hestmark G, Arnold AE, Büdel B, Rauhut A, Hewitt D, Untereiner WA, Cole MS, Scheidegger C, Schultz M, Sipman H, Schoch CL (2006) A five-gene phylogeny of Pezizomycotina. *Mycologia* 98: 1018–1028. <https://doi.org/10.1080/15572536.2006.11832630>
- Suetrong S, Klaysuban A, Sakayaroj J, Preedanon S, Ruang-Areerate P, Phongpaichit S, Pang K-L, Jones EBG (2015) Tirisporellaceae, a new family in the order Diaporthales (Sordariomycetes, Ascomycota). *Cryptogamie, Mycologie* 36: 319–330. <https://doi.org/10.7872/crym/v36.iss3.2015.319>
- Su L, Deng H, Niu Y-C (2016) *Phialemoniopsis endophytica* sp. nov., a new species of endophytic fungi from *Luffa cylindrica* in Henan, China. *Mycological Progress* 15: e48. <https://doi.org/10.1007/s11557-016-1189-5>
- Tanabe AS (2011) Kakusan4 and Aminosan: two programs for comparing nonpartitioned, proportional and separate models for combined molecular phylogenetic analyses of multi-locus sequence data. *Molecular Ecology Resources* 11: 914–921. <https://doi.org/10.1111/j.1755-0998.2011.03021.x>
- Tang AMC, Jeewon R, Hyde KD (2007) Phylogenetic utility of protein (RPB2, b-tubulin) and ribosomal (LSU, SSU) gene sequences in the systematics of Sordariomycetes (Ascomycota, Fungi). *Antonie van Leeuwenhoek* 91: 327–349. <https://doi.org/10.1007/s10482-006-9120-8>

- Taylor JE, Hyde KD, Jones EBG (1997) Fungi from palms. XXXV. *Thyridium chrysomallum* associated with *Archontophoenix alexandrae* (Palmae) cultivated in Hong Kong. *Sydowia* 49: 94–100. https://www.zobodat.at/pdf/Sydowia_49_0094-0100.pdf
- Thongkantha S, Jeewon R, Vijaykrishna D, Lumyong S, McKenzie EHC, Hyde KD (2009) Molecular phylogeny of Magnaporthaceae (Sordariomycetes) with a new species *Ophioceras chiangdaoense* from *Dracaena loureiroi* in Thailand. *Fungal Diversity* 34: 157–173.
- Tsang C-C, Chan JFW, Ip PPC, Ngan AHY, Chen JHK, Lau SKP, Woo PCY (2014) Subcutaneous phaeohyphomycotic nodule due to *Phialemoniopsis hongkongensis* sp. nov. *Journal of Clinical Microbiology* 52: 3280–3289. <https://doi.org/10.1128/JCM.01592-14>
- Untereiner WA, Bogale M, Carter A, Hanson SÅ, Læssøe T, Štěpánek V, Réblová M (2013) Molecular phylogeny of Boliniales (Sordariomycetes) with an assessment of the systematics of *Apiorhynchostoma*, *Endoxyla* and *Pseudovalsaria*. *Mycologia* 105: 564–588. <https://doi.org/10.3852/12-326>
- Vilgalys R, Hester M (1990) Rapid genetic identification and mapping of enzymatically amplified ribosomal DNA from several *Cryptococcus* species. *Journal of Bacteriology* 172: 4238–4246. <https://doi.org/10.1128/jb.172.8.4238-4246.1990>
- Viljoen CD, Wingfield BD, Wingfield MJ (1999) Relatedness of *Custingophora olivaceae* to *Gondwanamyces* spp. from *Protea* spp. *Mycological Research* 103: 497–500. <https://doi.org/10.1017/S0953756298007424>
- Voglmayr H, Friebes G, Gardiennet A, Jaklitsch WM (2018) *Barrmaelia* and *Entosordaria* in Barrmaeliaceae (fam. nov., Xylariales) and critical notes on *Anthostomella*-like genera based on multigene phylogenies. *Mycological Progress* 17: 155–177. <http://dx.doi.org/10.1007/s11557-017-1329-6>
- Voigt K, Wöstemeyer J (2000) Reliable amplification of actin genes facilitates deep-level phylogeny. *Microbiological Research* 155: 179–195. [https://doi.org/10.1016/S0944-5013\(00\)80031-2](https://doi.org/10.1016/S0944-5013(00)80031-2)
- Vu D, Groenewald M, de Vries M, Gehrman T, Stielow B, Eberhardt U, Al-Hatmi A, Groenewald JZ, Cardinali G, Houbraken J, Boekhout T, Crous PW, Robert V, Verkley GJM (2019) Large-scale generation and analysis of filamentous fungal DNA barcodes boosts coverage for kingdom fungi and reveals thresholds for fungal species and higher taxon delimitation. *Studies in Mycology* 92: 135–154. <https://doi.org/10.1016/j.simyco.2018.05.001>
- White TJ, Bruns T, Lee S, Taylor J (1990) Amplification and direct sequencing of fungal ribosomal RNA genes for phylogenetics. In: Innis MA, Gelfand DH, Sninsky JJ, White TJ (Eds) *PCR Protocols: a guide to methods and amplifications*. Academic Press, San Diego, 315–322. <https://doi.org/10.1016/B978-0-12-372180-8.50042-1>
- Wong S-W, Hyde KD, Jones EBG, Moss ST (1999) Ultrastructural studies on the aquatic ascomycetes *Annulatascus velatisporus* and *A. triseptatus* sp. nov. *Mycological Research* 103: 561–571. <https://doi.org/10.1017/S0953756298007473>
- Xia JW, Ma YR, Li Z, Zhang XG (2017) *Acrodictys*-like wood decay fungi from southern China, with two new families Acrodictyceae and Junewangiaceae. *Scientific Reports* 7: 7888. <https://doi.org/10.1038/s41598-017-08318-x>
- Yaguchi T, Sano A, Yarita K, Suh MK, Nishimura K, Udagawa S (2006) A new species of *Cephalotheca* isolated from a Korean patient. *Mycotaxon* 96: 309–322. <http://www.cybertruffle.org.uk/cyberliber/>

- Yang J, Maharachchikumbura SSN, Liu J-K, Hyde KD, Jones EBG, Al-Sadi AM, Liu Z-Y (2018) *Pseudostanjehughesia aquitropica* gen. et sp. nov. and *Sporidesmium* sensu lato species from freshwater habitats. *Mycological Progress* 17: 591–616. <https://doi.org/10.1007/s11557-017-1339-4>
- Yue J-Z, Eriksson OE (1987) *Sinosphaeria bambusicola* gen. et sp. nov., (Thyridiaceae fam. nov.). *Systema Ascomycetum* 6: 229–236.
- Zhang H, Dong W, Hyde KD, Maharachchikumbura SSN, Hongsanan S, Bhat DJ, Al-Sadi AM, Zhang D (2017) Towards a natural classification of Annulatascaceae-like taxa: introducing *Atractosporales* ord. nov. and six new families. *Fungal Diversity* 85: 75–110. <https://doi.org/10.1007/s13225-017-0387-z>
- Zhang N, Castlebury LA, Miller AN, Huhndorf SM, Schoch CL, Seifert KA, Rossman AY, Rogers JD, Kohlmeyer J, Volkmann-Kohlmeyer B, Sung G-H (2006) An overview of the systematics of the Sordariomycetes based on a four-gene phylogeny. *Mycologia* 98: 1076–1087. <https://doi.org/10.1080/15572536.2006.11832635>
- Zhang N, Zhao S, Shen Q (2011) A six-gene phylogeny reveals the evolution of mode of infection in the rice blast fungus and allied species. *Mycologia* 103: 1267–1276. <https://doi.org/10.3852/11-022>

The curse of the uncultured fungus

Kessy Abarenkov¹, Erik Kristiansson², Martin Ryberg³, Sandra Nogal-Prata⁴,
Daniela Gómez-Martínez⁵, Katrin Stüer-Patowsky⁶, Tobias Jansson⁵,
Sergei Pölme¹, Masoomeh Ghobad-Nejhad⁷, Natàlia Corcoll⁸,
Ruud Scharn⁹, Marisol Sánchez-García¹⁰, Maryia Khomich¹¹,
Christian Wurzbacher⁶, R. Henrik Nilsson⁸

1 Natural History Museum, University of Tartu, Vanemuise 46, Tartu 51014, Estonia **2** Department of Mathematical Sciences, Chalmers University of Technology and University of Gothenburg, Göteborg, Sweden **3** Department of Organismal Biology, Uppsala University, Uppsala, Sweden **4** Department of Mycology, Real Jardín Botánico-CSIC, Madrid, Spain **5** University of Gothenburg, Department of Biological and Environmental Sciences, Box 461, 405 30 Göteborg, Sweden **6** Technical University of Munich, Chair of Urban Water Systems Engineering, Am Coulombwall 3, 85748 Garching, Germany **7** Iranian Research Organization for Science and Technology, Department of Biotechnology, PO Box 3353-5111, Tehran 3353136846, Iran **8** University of Gothenburg, Gothenburg Global Biodiversity Centre, Department of Biological and Environmental Sciences, Box 461, 405 30 Göteborg, Sweden **9** University of Gothenburg, Department of Earth Sciences, Box 460, 405 30 Göteborg, Sweden **10** Swedish University of Agricultural Sciences, Department of Forest Mycology and Plant Pathology, Uppsala, Sweden **11** University of Bergen, Department of Clinical Science, Box 7804, 5020 Bergen, Norway

Corresponding author: R. Henrik Nilsson (henrik.nilsson@bioenv.gu.se)

Academic editor: Thorsten Lumbsch | Received 2 October 2021 | Accepted 24 November 2021 | Published 2 February 2022

Citation: Abarenkov K, Kristiansson E, Ryberg M, Nogal-Prata S, Gómez-Martínez D, Stüer-Patowsky K, Jansson T, Pölme S, Ghobad-Nejhad M, Corcoll N, Scharn R, Sánchez-García M, Khomich M, Wurzbacher C, Nilsson RH (2022) The curse of the uncultured fungus. *MycoKeys* 86: 177–194. <https://doi.org/10.3897/mycokeys.86.76053>

Abstract

The international DNA sequence databases abound in fungal sequences not annotated beyond the kingdom level, typically bearing names such as “uncultured fungus”. These sequences beget low-resolution mycological results and invite further deposition of similarly poorly annotated entries. What do these sequences represent? This study uses a 767,918-sequence corpus of public full-length fungal ITS sequences to estimate what proportion of the 95,055 “uncultured fungus” sequences that represent truly unidentifiable fungal taxa – and what proportion of them that would have been straightforward to annotate to some more meaningful taxonomic level at the time of sequence deposition. Our results suggest that more than 70% of these sequences would have been trivial to

identify to at least the order/family level at the time of sequence deposition, hinting that factors other than poor availability of relevant reference sequences explain the low-resolution names. We speculate that researchers' perceived lack of time and lack of insight into the ramifications of this problem are the main explanations for the low-resolution names. We were surprised to find that more than a fifth of these sequences seem to have been deposited by mycologists rather than researchers unfamiliar with the consequences of poorly annotated fungal sequences in molecular repositories. The proportion of these needlessly poorly annotated sequences does not decline over time, suggesting that this problem must not be left unchecked.

Keywords

Data interoperability, data mining, DNA barcoding, scientific practice, species identification, taxonomic annotation

Introduction

DNA sequencing enables researchers to explore environmental habitats such as soil, wood and water for fungal diversity. A common choice of genetic marker for such pursuits is the nuclear ribosomal internal transcribed spacer (ITS) region, the formal fungal barcode (Schoch et al. 2012). Assessment of the taxonomic affiliation of newly-generated ITS sequences is typically accomplished through similarity-based searches in databases, such as the International Nucleotide Sequence Database Collaboration (INSDC; Arita et al. 2021) and UNITE (Nilsson et al. 2019). A number of factors combine to impede such assessments. For instance, sequences may be subject to distortive technical complications, such as low read quality or chimeric unions (Zinger et al. 2019). Interpretation of match statistics across a genetic marker that features both very conserved and very variable parts – such as the ITS region – can furthermore present a challenge and it seems unlikely to come up with well-defined similarity thresholds to demarcate the species and other ranks in a unified way across the entire fungal kingdom (Abarenkov et al. 2016). However, the foremost challenge is probably of taxonomic nature: reference ITS sequence data are available for a modest 25% of the ~150,000 formally described species of fungi, less than 2% of the estimated 2.3–6 million extant species of fungi (<http://www.speciesfungorum.org>; Hawksworth and Lücking 2017; Baldrian et al. 2021). Thus, the public sequence databases clearly suffer from a significant taxon sampling problem when it comes to their coverage of fungal biodiversity.

Roughly 42% (326,062) of the 767,918 full-length Sanger-derived fungal ITS sequences in the INSDC (November 2020) lack a full species name and 29% (95,055) of these are not annotated beyond the kingdom level (e.g. “uncultured fungus” from the environmental (ENV) sample division and “fungal sp.” from the plants and fungal (PLN) division; Sayers et al. 2021). Some proportion of these sequences are truly unidentifiable at present and stem from the many “dark lineages” or less well explored parts of otherwise well-studied groups of the fungal tree of life (Tedersoo et

al. 2020; Lücking et al. 2021). Others, however, represent sequences for which some more meaningful taxonomic annotation would have been only a sequence similarity search in, for example, BLAST (Altschul et al. 1997) away at the time of sequence deposition. These sequences can be thought of as false negatives: it is well-known (or straightforward to find out) what taxon they represent, yet their annotation does not convey that information. This lack of meaningful taxonomic annotations hurts the study of fungi. The sheer number of false negatives in BLAST match lists introduces uncertainty in what should have been straightforward taxonomic decisions, often with the result that researchers adopt these uninformative names for their newly-generated sequences in what has been dubbed the “percolation” or “snowballing” effect (Gilks et al. 2002). This leads to mycology-orientated articles with low taxonomic resolution, something that mycology clearly could do without. In addition, many researchers are reluctant to include sequences without taxonomic annotation in their studies, thus missing out on potentially valuable information in phylogenetics, ecology, biogeography, and other aspects (Ryberg et al. 2008; Bonito et al. 2010; Nilsson et al. 2011; Fryssouli et al. 2020).

Many of the present authors are curators of specific taxonomic groups in the UNITE database. In that role, we revisit our favourite fungal groups and multiple sequence alignments after each incremental update with new INSDC sequences. Unfortunately, we regularly find that previously tidy and well-annotated species hypotheses have been watered down by tens to hundreds of sequences of the “uncultured fungus” kind (Figure 1). Spending valuable curation time on handling this needless and avoidable problem is a breeding ground for frustration. Does this problem extend beyond the relatively limited number of primarily basidiomycete species hypotheses that the present authors monitor out of personal interest? If it does, mycology is at the receiving end of a seemingly never-ending stream of unnecessarily uninformative taxonomic annotations, much to its detriment. We set out to establish the background and context of the “uncultured fungus” problem through three main questions: (i) for what proportion of the 95,055 fungal ITS sequences that lack taxonomic annotation beyond the kingdom level is that lack justified due to the absence of relevant reference sequences with richer taxonomic annotations at the time of sequence deposition?; (ii) were the unjustified “uncultured fungus” sequences generated by mycologists (who perhaps should know better) or do they stem from other scientific disciplines?; and (iii) is the proportion of needlessly imprecise annotations going down over time? We pursued these questions considering all 767,918 more or less full-length, Sanger-derived fungal ITS sequences that were assigned to a UNITE species hypothesis as of November 2020. Our results suggest that “uncultured fungus” and “fungal sp.” are labels that are routinely attached to newly-generated sequences regardless of whether a more informative annotation would have been available or not. A surprisingly high proportion of these sequences stem from mycologists – researchers one would think would know that mycology does not stand to benefit from such actions.

All sequences belonging to the SH are shown

Sequence ID	UNITE taxon name	INSD taxon name	Source	Interacting Taxa	Area	RefSeq
FJ237060	Vishniacozyma	Fungi (uncultured fungus)	Fungal mycelium (ingrowth bag)		Austria	
ABA76529 clone Ep8...	Vishniacozyma	Fungi (uncultured fungus)	Ericoid mycorrhiza	Vaccinium	Sweden	
FJ236200	Vishniacozyma	Fungi (fungi sp. B59)	Soil fungal DNA		Antarctica	
EF687931	Vishniacozyma	Cryptococcus (Cryptococcus sp. Vega039)	Plant leaf	Coffea arabica	Mexico	
EF504558	Vishniacozyma	Fungi (uncultured endophytic fungus)	Zea mays tissue sample	Zea mays	United States	
AF444645	Vishniacozyma victoriae	Cryptococcus victoriae (Cryptococcus victoriae)			Unspecified	
AF444469	Vishniacozyma victoriae	Vishniacozyma victoriae (Vishniacozyma victoriae)	CBS 8685T		Antarctica	✓
AF444447	Vishniacozyma victoriae	Vishniacozyma victoriae (Vishniacozyma victoriae)			Unspecified	
FN298568	Vishniacozyma	Cryptococcus (Cryptococcus aff. victoriae AY-68)			Russian Federation	
AM901845	Vishniacozyma	Basidiomycota (uncultured Basidiomycota)	Dust fungal DNA		Finland	
AM901703	Vishniacozyma	Cryptococcus (Cryptococcus sp. BFT08)			Japan	
AB520394	Vishniacozyma	Fungi (uncultured fungus)	Soil fungal DNA		Japan	
AB520393	Vishniacozyma	Fungi (uncultured fungus)	Soil fungal DNA		Japan	
AB520391	Vishniacozyma	Fungi (uncultured fungus)	Soil fungal DNA		Japan	
AB520390	Vishniacozyma	Fungi (uncultured fungus)	Soil fungal DNA		Japan	
AB520389	Vishniacozyma	Fungi (uncultured fungus)	Soil fungal DNA		Japan	
AB520387	Vishniacozyma	Fungi (uncultured fungus)	Soil fungal DNA		Japan	
AB520386	Vishniacozyma	Fungi (uncultured fungus)	Soil fungal DNA		Japan	
AB520385	Vishniacozyma	Fungi (uncultured fungus)	Soil fungal DNA		Japan	
AB520384	Vishniacozyma	Fungi (uncultured fungus)	Soil fungal DNA		Japan	
AB520383	Vishniacozyma	Fungi (uncultured fungus)	Soil fungal DNA		Japan	
AB520382	Vishniacozyma	Fungi (uncultured fungus)	Soil fungal DNA		Japan	
AB520381	Vishniacozyma	Fungi (uncultured fungus)	Soil fungal DNA		Japan	
AB520379	Vishniacozyma	Fungi (uncultured fungus)	Soil fungal DNA		Japan	
AB520378	Vishniacozyma	Fungi (uncultured fungus)	Soil fungal DNA		Japan	
AB520376	Vishniacozyma	Fungi (uncultured fungus)	Soil fungal DNA		Japan	
AB520375	Vishniacozyma	Fungi (uncultured fungus)	Soil fungal DNA		Japan	
AB520374	Vishniacozyma	Fungi (uncultured fungus)	Soil fungal DNA		Japan	
AB520373	Vishniacozyma	Fungi (uncultured fungus)	Soil fungal DNA		Japan	
AB520371	Vishniacozyma	Fungi (uncultured fungus)	Soil fungal DNA		Japan	
AB520370	Vishniacozyma	Fungi (uncultured fungus)	Soil fungal DNA		Japan	
AB520369	Vishniacozyma	Fungi (uncultured fungus)	Soil fungal DNA		Japan	
AB520368	Vishniacozyma	Fungi (uncultured fungus)	Soil fungal DNA		Japan	
AB520366	Vishniacozyma	Fungi (uncultured fungus)	Soil fungal DNA		Japan	
AB520364	Vishniacozyma	Fungi (uncultured fungus)	Soil fungal DNA		Japan	
AB520363	Vishniacozyma	Fungi (uncultured fungus)	Soil fungal DNA		Japan	
AB520361	Vishniacozyma	Fungi (uncultured fungus)	Soil fungal DNA		Japan	
AB520360	Vishniacozyma	Fungi (uncultured fungus)	Soil fungal DNA		Japan	

Figure 1. A screenshot from species hypothesis SH1159264.08FU (*Vishniacozyma victoriae*; <https://dx.doi.org/10.15156/BIO/SH1159264.08FU>) in UNITE. Identifying a *Vishniacozyma victoriae* ITS sequence to at least the genus level is trivial, yet the screenshot hints at the swathes of kingdom level-annotated *Vishniacozyma victoriae* sequences regularly deposited in the INSDC. SequenceID – INSDC accession number. UNITE taxon name – taxonomic annotation in UNITE. INSD taxon name – original taxonomic annotation in INSDC. RefSeq – indicates a type-derived sequence. More than thirty studies have deposited kingdom-level annotations in this species hypothesis. The ones shown primarily stem from Nishizawa et al. (2010).

Materials and methods

Defining the reference corpus

We targeted all 767,918 full-length, Sanger-derived fungal ITS sequences (annotated as such) in the INSDC (November 2020) as mirrored in the UNITE species hypotheses release 8. For each such sequence, UNITE extracts and stores relevant metadata from the GenBank flat file format (<https://www.ncbi.nlm.nih.gov/Sitemap/samplerecord.html>). Sequence quality control is part of the species hypotheses generation and seeks to exclude clear cases of, for example, chimeras and low read quality sequences through tools, such as USEARCH (Edgar 2010) and ITSx (Bengtsson-Palme et al. 2013). All sequences are first clustered at 80% similarity in USEARCH to obtain compound clusters. These clusters typically revolve around the family/subfamily/genus level. Each compound cluster is then clustered into species hypotheses (SHs) at distance thresholds 0.0% through to 3.0% in steps of 0.5%. These can be thought of as entities roughly at the species level.

UNITE uses the NCBI Taxonomy classification (Schoch et al. 2020) as the taxonomic backbone, supplemented with modifications from Index Fungorum (<http://www.indexfungorum.org>), MycoBank (Robert et al. 2013), Tedersoo et al. (2018) and

the UNITE user base. UNITE uses the taxonomic annotations of the sequences in each SH to determine the taxonomic affiliation of the SH. The algorithm underpinning this determination ignores low-resolution annotations as long as they are not contradictory: an SH that contains five sequences annotated as *Amanita muscaria* and one annotated as “Basidiomycota sp.” will be scored to represent *Amanita muscaria*. However, a (compromised) two-sequence SH containing *Amanita muscaria* and *Cantharellus cibarius* will be assigned to the most resolved level where their classifications are compatible, in this case the class *Agaricomycetes*. In this way, each sequence and species hypothesis in UNITE are assigned to the most resolved position possible in the fungal tree of life given the available information. For this study, we targeted all 95,055 sequences originally released in INSDC without any more refined taxonomic annotation than the kingdom level (such as “uncultured fungus” and “fungal sp.”), irrespective of whether UNITE – or a UNITE user – subsequently had been able to assign a more refined name to it.

Mimicking BLAST searches

The fact that UNITE stores the INSDC initial release date for each sequence allowed us to build a map of what sequences were available in INSDC at any time. We wanted to capture what we feel are the two most common scenarios of INSDC sequence deposition, namely: (i) a user deposits sequences for immediate release and (ii) a user deposits sequences for release, pending acceptance of the underlying manuscript. Thus, for each sequence A that was only annotated at the kingdom level, we considered all sequences that were released at least seven days before A as being available for BLAST searches by the authors of A. This leaves room for the authors of A to have done a final double check of the taxonomic affiliation of their soon-to-be-released sequences, including A, prior to setting them free.

We sought to recreate what such a BLAST search would have looked like to the authors of A with respect to closely matching ($\geq 97\%$ similarity) sequences (the topmost, high-scoring sequences in a BLAST hit list), as well as sequences that produced reasonable ($\geq 80\%$ similarity), but not top-scoring, matches to A. This captures our experience of BLAST – most users, it seems to us, do not bother looking beyond the first ~ 20 BLAST matches for clues to the taxonomic affiliation of a query sequence. For this “closely matching sequences” dataset, we examined the 3.0% species hypothesis of each kingdom-level sequence for the presence of sequences at least 7 days older than the kingdom-level sequence. Any such sequences were examined for their INSDC taxonomic annotation from kingdom to the species level. This allowed us to build a view of what the author of the kingdom-level sequence would have seen, had they done a BLAST search prior to the release of the kingdom-level sequence. For the “reasonable, but not top-scoring, matches” dataset, we, instead, considered the ($\geq 80\%$ similarity) compound cluster where each kingdom-level sequence was found. This allowed us to model the scenario where the kingdom-level sequence authors progressed further down in the BLAST hit list for taxonomic clues, plus the scenario where there were no close BLAST matches to begin with.

Metadata assessment and statistical analyses

We examined the GenBank FEATURES field for information on the country of collection of each sequence to get a feeling for whether kingdom-level sequences and the sequences annotated beyond the kingdom level stemmed from dramatically different sampling areas. Some two percent (2,049) of the sequences annotated only at the kingdom level (e.g. “uncultured fungus”) were found to initially lack an explicit country of collection, yet stem from a published or otherwise available (e.g. a pre-print) study (as opposed to being a “Direct submission” or an “Unpublished” INSDC submission). Similarly, some 7% (48,540) of the sequences with at least a phylum-level annotation (e.g. “Ascomycota sp.” and “*Rhizoplaca* sp.”) were found to lack an explicit country of collection, but to stem from a published or otherwise available study. These sequences offer some hope of restoration of the missing country of collection through recourse to the presumed underlying publication; sequences merely listed as “Direct submission” or “Unpublished” do not, in our experience (e.g. Abarenkov et al. 2016). Based on published information and online queries in, for example, preprint repositories, we thus made an effort to restore the country of collection for all 2,049 kingdom-level sequences whose GenBank REFERENCE field specified a tangible publication (published, preprint or in press). We repeated this task for a random 2,049 of the 48,540 sequences annotated to at least the phylum level. Ideally, we would have targeted all 48,540 phylum-level sequences, but this substantial task was deemed beyond the capacity of the present set of authors (cf. Durkin et al. 2020). Insofar as the underlying publications could be tracked down and the country of collection could be derived from the paper (or through contacting its authors), the country of collection was added to UNITE and used in this study.

When the GenBank REFERENCE field specified a scientific journal, we used the journal name as a proxy for whether the author(s) of each sequence were mycologists or not. We made the admittedly crude assumptions that a mycologist is someone who publishes in a mycological journal; that only mycologists publish papers in mycological journals; and to only consider the 29 journals listed under “Mycology” in Web of Science (November 2020; Suppl. material 1) as mycological journals. All other journals and sequence authors were scored as non-mycological.

The year of deposition of each sequence was assessed to examine whether the proportion of kingdom-level INSDC depositions fluctuated over time (2001–2020).

Results

Taxonomic resolution

Regarding our attempt to mimic BLAST users who only consider matches with very high match scores, we found that a full 68,929 (73%) of the 95,055 sequences annotated only at the kingdom level (Fungi) were false negatives (Figure 2). A name

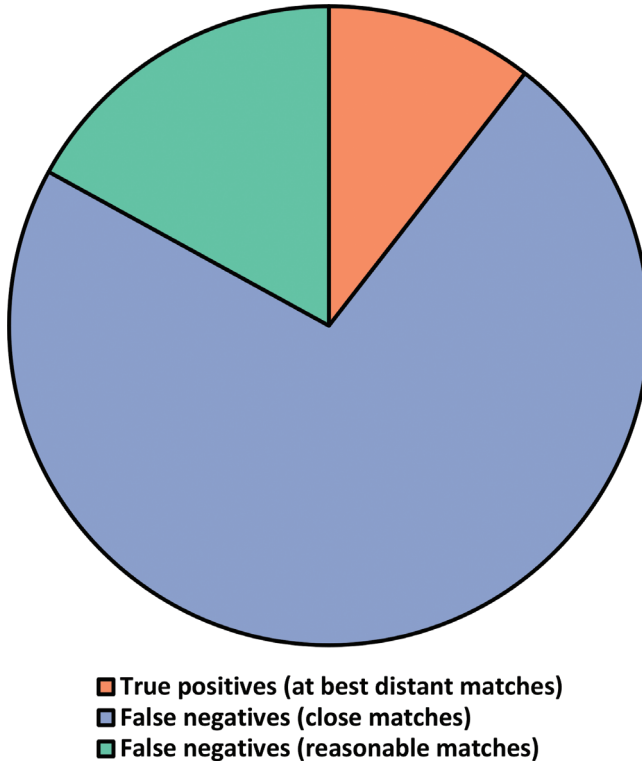


Figure 2. Pie chart representing all the 95,055 kingdom-level ITS sequences and the proportion of these that were true-positives (had no or only very distant taxonomically more well-annotated BLAST matches at the time of sequence deposition/release; red, 10%), false-negatives (had only reasonable matches; green, 17%) and false-negatives (had close matches; blue, 73%). The chart suggests that nearly all kingdom-level fungal ITS sequences in INSDC could have been given a more taxonomically-resolved name at the time of sequence deposition/release.

at the class, order, family, genus, and species level was available in the corresponding UNITE species hypothesis (and would have been available amongst the top-scoring BLAST matches) for 71%, 70%, 67%, 64% and 60% of the sequences, respectively. The BLAST hit list would have contained an average of 74% sequences annotated to at least the phylum level; 69% to the class level; 67% to the order level; 62% to the family level; 54% to the genus level and 38% to the species level. The median number of sequences in a non-singleton species hypothesis was 77 at the time of deposition of the query sequence at hand.

If we include the “reasonable, but not top-scoring, matches” from the corresponding compound cluster (i.e. sequences that would have appeared further down in the BLAST hit list) in these statistics, we found that 85,093 (90%) of the 95,055 sequences annotated only at the kingdom level were false negatives (Figure 2). A name at the class, order and family level was available for 88%, 88% and 87% of the sequences,

respectively. The BLAST hit list would have contained an average of 75% sequences annotated to at least the phylum level; 70% to the class level and 68% to the order level. The average non-singleton compound cluster contained 386 sequences at the time of deposition of the query sequence at hand.

Metadata

Initially, 2,049 (2.2%) of the publication-associated kingdom-level sequences were found to lack information on country of collection. The corresponding number was 7% (48,540) for the publication-associated sequences with at least a phylum-level annotation. We were able to restore the country of collection for 1,983 (96.8%) of these kingdom-level sequences and 1,812 (89.3%) of these phylum-level sequences. The newly-obtained countries of collection were deposited in UNITE for each sequence to facilitate further mycological enterprises by UNITE users. Figure 3 shows the 15 most common countries of collection for the sequences annotated to at least the phylum level, overlaid with the corresponding results from the kingdom-level dataset. The two 15-country sets share 10 (67%) countries, primarily from parts of the world that are relatively well-studied from a mycological point of view. Several countries known as

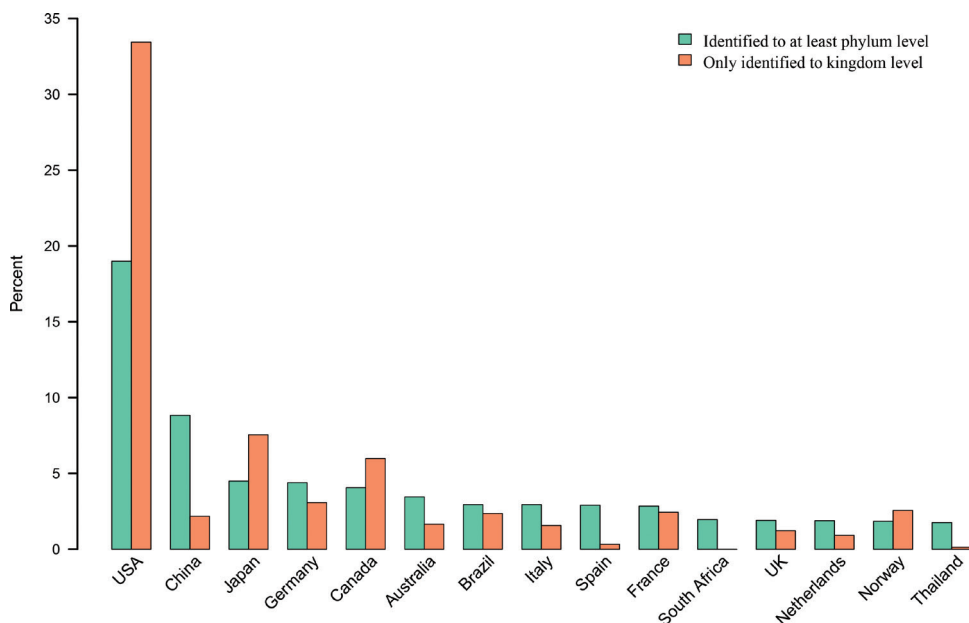


Figure 3. The top 15 most common countries of collection for the publication-associated sequences annotated at or beyond the phylum level (green) expressed as the proportion of the sequences stemming from each country out of all phylum-level-and-beyond sequences. The corresponding country for publication-associated sequences annotated only at the kingdom level (orange) is similarly expressed as the proportion of sequences stemming from that country out of all kingdom-level sequences. The figure is ordered in decreasing order by the country of collection for the phylum-level sequences.

veritable hotspots for fungal diversity – for example, Thailand and Brazil (Hyde et al. 2018; Menolli and Sánchez-García 2020) – report dramatically lower proportions of kingdom-level sequences than do some countries with a more well-studied mycobiota. The figure suggests that factors other than lack of reference sequences are behind the prevalence of kingdom-level sequences.

For the “closely matching sequences” scenario, we found that 22% (21,205) of the full INSDC set of kingdom-level sequences, for which a more resolved name would have been only a BLAST search away, were generated by mycologists (following our admittedly crude definition of a mycologist). When, instead, considering the fully identified sequences, 182,402 (27.1%) were deposited by mycologists. The proportion of false-negative INSDC depositions does not decline over time (Figure 4).

Discussion

Overall results

The present paper examines the corpus of reasonably full-length public fungal ITS sequences not annotated to any meaningful taxonomic level. We found that our initial, UNITE curation-based hunches were largely right: reasons other than lack of established taxonomy and available reference sequences lie behind the lack of resolved



Figure 4. The proportion of false-negative sequences (had reasonable matches; green) and false-negative sequences (had close matches; blue) out of all kingdom-level sequences over time (2001-2020). The figure suggests that the act of taking sequence annotation very lightly is not in an abating trend. The data for 2020 extend through early November 2020 and are thus partial.

taxonomic annotations for the overwhelming majority of these sequences. A full 12% of the 767,918 sequences in our dataset were annotated only to kingdom level – and in at least 73% of these cases seemingly without clear justification. In fact, for 64% of these sequences, an annotation to at least the genus level seems to have been possible and only a BLAST search away at the time of sequence deposition/release. The tendency of researchers not to name fungal sequences beyond the kingdom level, even when this would have been perfectly possible, does not seem to go down over time (Figure 4). One cannot help but ponder a future scenario where BLAST searches become increasingly tedious and time-consuming to interpret – and, in fact, may not be meaningful at all in some cases. This is acting out in a time when the opposite should be the case – BLAST searches become increasingly informative and easy to interpret – owing to rapid taxonomic progress in mycology through initiatives such as Yuan et al. (2020) and Tedersoo et al. (2020).

It would somehow have been nice to conclude that mycology is the victim of the decisions of non-mycologist researchers: only non-mycologists are behind the countless “uncultured fungus” depositions. Our results are not in line with this though; mycologists seem to be behind more than one fifth of these sequences. We find this remarkable, considering that mycology is often touted as an overlooked and easily dismissed discipline (Pautasso 2013). As such, mycology should surpass, rather than dodge, expectations. It does not really seem to be happening though. We feel that mycologists are not in a robust position to accuse others of taking fungi too lightly, if mycologists themselves take fungi too lightly. The act of claiming that mycology needs more money, without backing that claim by robust and reproducible data, may well prove to be counterproductive (Durkin et al. 2020).

Our results make it painfully clear that human nature, rather than lack of taxonomic information and resolution, is the cause of the lion’s share of the kingdom-level annotations. Indeed, more than 70% of the kingdom-level sequences belong to lineages for which an established Latin name – and at least one reference sequence annotated accordingly – were readily available at the time of sequence deposition. This begs the question why those sequence authors did not go looking for that information to begin with. One can think of many answers: lack of mycological or bioinformatics expertise, lack of money/time, a research focus other than taxonomy, wanting journal policies on metadata richness and availability and, indeed, lack of a perceived good reason to take the time to do it in the first place. All those reasons can be countered one way or the other. For instance, any environmental sequencing effort likely to unravel fungi – although they may not target fungi or taxonomic aspects specifically – should always include a mycologist as well as a bioinformatician to maximise resolution in the analysis, but also the data deposition step. Grant applications should be written in such a way to provide sufficient time and resources for reproducible down-the-road data handling and not just the field and sequencing expenses. Similarly, journal policies on data availability should ideally be extended – and enforced – to also include aspects of data annotation and re-usability, perhaps to the extent that any pending INSDC entries to be released upon publication of the study must be submitted to the

journal for review alongside the other manuscript files. Above all, individual research efforts should be seen not only as a way to increase the length of one's CV and to meet promises to funding agencies, but also as a contribution to the ever-growing corpus of scientific – mycological – knowledge. In fact, we speculate that this last issue is the main reason behind the findings of the present study. Researchers do not perceive their sequence data as atomised contributions to science and, thus, fail to take the steps that would have enabled meaningful use of those sequences beyond the study at hand.

The present results dispel the assertion that only mycologists are in a position to add to our growing knowledge of the fungal kingdom. This, in turn, suggests that mycologists should make it as easy as possible for anyone to make use of, but also add to, the corpus of mycological data. After all, DNA sequences form a key component of contemporary mycology (Crous et al. 2021; Lücking et al. 2021). Thus, significant mycological expertise should not be needed to arrive at reasonable conclusions – such as a genus-level annotation – from BLAST hit lists. As mycologists, we need to take the time to annotate our sequences accordingly. Annotating newly-generated sequences to some reasonable taxonomic level – say the genus or order level in the case of environmental sequences – is, however, a process that takes time. As the list of sequences runs into the hundreds and sometimes more, we could be talking days. However, what many mycologists do not seem to realise is that there is always room for more co-authors on a scientific paper. That room is clearly not maximised right now – we found an average of 4.9 co-authors per study in the 58,898 studies behind our full 767,918-sequence dataset. The non-trivial number of kingdom-level annotations testifies to the many aspiring or junior researchers who could have received training in robust sequence annotation and then been asked to annotate the newly-generated sequences to some more meaningful level (e.g. class, order or genus) prior to deposition in exchange for a non-prominent co-authorship – but who never got the chance (Ryberg et al. 2016). We find this hard to swallow.

Observations on sequence annotation

It is painful to come across sequences that are annotated as “uncultured fungus” or “fungal sp.” in INSDC, but that are deeply nested (and sometimes even well annotated) in well-supported clades in phylogenetic trees of, for example, *Fusarium*, Helotiales, and *Lactarius* in the associated publications. The present study argues that taxonomic annotations of the “uncultured fungus” kind should be reserved for cases where taxonomic annotation beyond the kingdom level was attempted, but came up short. Then users would know that each such sequence carries a non-trivial potential for taxonomic discovery – you could even argue that such sequences would be amongst the most interesting and exciting of all fungal sequences. Right now, however, the “uncultured fungus” label is used as a catch-all device whose routine use serves to mask the presence of truly unidentifiable fungi. Many researchers seem to shun unidentified sequences also in situations where these sequences clearly should have been considered (Nilsson et al. 2011). Improved taxonomic annotation is a way out of this dilemma.

Phylogenetic analysis is probably the most robust way to assess the taxonomic affiliation of sequences and hence to annotate sequences. However, we acknowledge that not all studies use phylogenetic approaches to begin with and that phylogenetic analysis may not be applicable in all situations. Fortunately, similarity-based searches, such as BLAST in INSDC, will take you a long way. By ticking the GenBank-BLAST box “Exclude: Uncultured/environmental sample sequences”, a more taxonomy-oriented picture is likely to emerge. We feel that a sequence that produces a long list of, say, robust *Fusarium* matches – when both BLAST coverage and similarity are considered closely (Nilsson et al. 2012) – should be annotated as “uncultured *Fusarium*” or perhaps “uncultured Nectriaceae”. Most taxonomic contradictions in BLAST hit lists can be resolved by further restricting the searches to the largely type-derived NCBI RefSeq Targeted Loci ITS Project (GenBank identifier PRJNA177353; Schoch et al. 2014). Judging by the results of the present study, these simple steps would have taken the edge off the majority of the sequences currently bearing only a kingdom-level annotation.

We would like to stress that annotating sequences is always a balance between under- and over-annotation. There is no shortage of incorrectly annotated fungal sequences in the public repositories (Hofstetter et al. 2019) and we certainly do not want this study to give rise to even more. Thus, we would be happy to see any of the names “uncultured *Fusarium*”, “uncultured Nectriaceae”, “uncultured Hypocreales”, “uncultured Sordariomycetes” and “uncultured Ascomycota”, depending on what the data at hand showed. This is one of the reasons why we feel that taxonomic expertise should be involved also in sequencing efforts that do not pursue taxonomic questions explicitly. While it borders on the impossible to algorithmise threshold values for when a sequence can be safely annotated to some specific level, rough guidelines are available. Based on the ITS2 subregion, Tedersoo et al. (2014) “typically” used the global similarity thresholds 90, 85, 80, and 75% identity for assigning operational taxonomic units to the genus, family, order, and class level, respectively. We take the caveat “typically” to refer to taxonomic expertise, because it makes little sense to insist that these threshold values will always hold true. They offer guidance, but in the face of uncertainty, we argue that it is preferable to annotate a sequence at the parental lineage, such as “uncultured Nectriaceae”, as opposed to a more tentative “uncultured *Fusarium*”.

Tedersoo et al. (2014) do not specify when a sequence should be annotated at the species level; indeed, sequences were not annotated at the species level in that study. We agree with this move and we personally do not annotate newly-generated environmental sequences to the species level other than in very rare and particularly unequivocal cases. After all, there are many examples of clearly distinct species that have identical ITS sequences (Abarenkov et al. 2016) and, in the absence of other evidence, it is simply not always possible to derive a robust species-level identification based on ITS data. At a more general level, this study advocates taxonomic annotations at the level warranted by the data as interpreted by a knowledgeable mycologist. That level is typically not that of species, but as this study shows, it is also not that of kingdom.

Potential shortcomings of the present study

The present study should be viewed as a rough estimation of the reasons why we keep seeing INSDC submissions of the “uncultured fungus” kind. Many aspects of the present study are clearly hard to algorithmise. For instance, in our mimicking of BLAST searches, we used default BLAST settings and a single version of BLAST. However, the BLAST output may have looked somewhat different to a user with non-default parameter values or another version of BLAST. It is, furthermore, difficult to model human behaviour when it comes to processing and interpreting BLAST hit lists. One can also think of cases where the sequence authors did, in fact, do BLAST searches, but were presented with contradictory information: “Ascomycota sp.” and “Basidiomycota sp.”. In our experience, it is often easy to single out and resolve many mis-annotated sequences, based on the annotations of the other relevant BLAST hits – a single *Lactarius* (*Basidiomycota*) annotation in a large group of *Fusarium* (*Ascomycota*), for instance – but we can certainly see why some users would feel uncomfortable doing this. The magnitude of this problem appears limited, as 0.5% of the SHs and 1.8% of the compound clusters contained annotation conflicts at the phylum level. Complications such as these, nevertheless, suggest that our estimate that more than 70% of the kingdom-level annotations are false negatives may be off by several percentage units. That said, many of our parameter settings – such as the permissive single-linkage clustering underlying the SH generation – were deliberately set to be very forgiving. We, therefore, argue that at least the order of magnitude of our estimate is reasonable. Our estimate is, furthermore, in line with our admittedly basidiomycete-centric experience of UNITE sequence curation.

The scoring of sequence authors as mycologists or non-mycologists, based on the journal of the underlying publication, is clearly a move that will prove to be wrong in many cases. We are well aware – and welcome – that also non-mycologists publish their findings in mycological journals. Conversely, mycologists often – and rightfully – seek to publish their findings beyond mycological journals. Finally, Web of Science is not an ideal arbiter of what is mycology and what is not, given that there are many mycological journals that do not yet have a formal impact factor. Thus, while we agree that these shortcomings haunt our estimate that 22.3% of the kingdom-level sequences were submitted by mycologists, it is not immediately clear whether our estimate is biased towards, or away from, mycologists. Our estimate is clearly so high that it would be counter-intuitive to argue that only non-mycologists are behind it.

Conclusions

The study of fungi is being reshaped by the many novel and hitherto nameless fungal lineages unearthed by environmental sequencing efforts (Lücking et al. 2021). However, the study of fungi is simultaneously being watered down by the needless yet continual deposition of sequences of low-resolution taxonomic annotations for taxa,

for which a more appropriate annotation would have been only seconds away should the underlying authors have taken the time to look. The curse of the uncultured fungus is that these two cases, at least at a cursory glance, are hard to tell apart. We urge all members of the scientific – and particularly the mycological – community to reconsider their stance on batch, haphazard sequence annotation. It is a game without clear winners, but where the scientific community – and particularly mycology – certainly comes out on the losing end. This is not in anybody's interest. Mycology is under enough strain already without having to grapple with the consequences of negligence and the urge to save time for oneself, even if at the expense of others.

Acknowledgements

The work of KA was supported by the Estonian Research Council grant (PRG1170). KSP and CW gratefully acknowledge funding from the German Research Foundation (DFG: WU890/2–1). NC gratefully acknowledges funding from the Swedish Research Council Formas (project HerbEvol grant No. 2015–1464). SNP gratefully acknowledges funding from the Spanish Ministry of Economy and Competitiveness (CGL2015–67459–P and BES–2016–077793). MG gratefully acknowledges funding from the International Association for Plant Taxonomy (IAPT: 2021).

References

- Abarenkov K, Adams RI, Laszlo I, Agan A, Ambrosio E, Antonelli A, Bahram M, Bengtsson-Palme J, Bok G, Cangren P, Coimbra V, Coleine C, Gustafsson C, He J, Hofmann T, Kristiansson E, Larsson E, Larsson T, Liu Y, Martinsson S, Meyer W, Panova M, Pombubpa N, Ritter C, Ryberg M, Svantesson S, Scharn R, Svensson O, Töpel M, Unterseher M, Visagie C, Wurzbacher C, Taylor AFS, Kõljalg U, Schriml L, Nilsson RH (2016) Annotating public fungal ITS sequences from the built environment according to the MIxS-Built Environment standard – a report from a May 23–24, 2016 workshop (Gothenburg, Sweden). *MycoKeys* 16: 1–15. <https://doi.org/10.3897/mycokeys.16.10000>
- Altschul SF, Madden TL, Schäffer AA, Zhang J, Zhang Z, Miller W, Lipman DJ (1997) Gapped BLAST and PSI-BLAST: a new generation of protein database search programs. *Nucleic Acids Research* 25(17): 3389–3402. <https://doi.org/10.1093/nar/25.17.3389>
- Arita M, Karsch-Mizrachi I, Cochrane G (2021) The international nucleotide sequence database collaboration. *Nucleic Acids Research* 49(D1): D121–D124. <https://doi.org/10.1093/nar/gkaa967>
- Baldrian P, Větrovský T, Lepinay C, Kohout P (2021) High-throughput sequencing view on the magnitude of global fungal diversity. *Fungal Diversity*. <https://doi.org/10.1007/s13225-021-00472-y>
- Bengtsson-Palme J, Ryberg M, Hartmann M, Branco S, Wang Z, Godhe A, DeWit P, Sanchez-Garcia M, Ebersberger I, de Sousa F, Amend AS, Jumpponen A, Unterseher M, Kristiansson

- E, Abarenkov K, Bertrand YJK, Sanli K, Eriksson KM, Vik U, Veldre V, Nilsson RH (2013) Improved software detection and extraction of ITS1 and ITS 2 from ribosomal ITS sequences of fungi and other eukaryotes for analysis of environmental sequencing data. *Methods in Ecology and Evolution* 4(10): 914–919. <https://doi.org/10.1111/2041-210X.12073>
- Bonito GM, Gryganskyi AP, Trappe JM, Vilgalys R (2010) A global meta-analysis of Tuber ITS rDNA sequences: species diversity, host associations and long-distance dispersal. *Molecular Ecology* 19(22): 4994–5008. <https://doi.org/10.1111/j.1365-294X.2010.04855.x>
- Crous PW, Lombard L, Sandoval-Denis M, Seifert KA, Schroers H-J, Chaverri P, Gené J, Guarro J, Hirooka Y, Bensch K, Kema GHJ, Lamprecht SC, Cai L, Rossman AY, Stadler M, Summerbell RC, Taylor JW, Ploch S, Visagie CM, Yilmaz N, Frisvad JC, Abdel-Azeem AM, Abdollahzadeh J, Abdolrasouli A, Akulov A, Alberts JF, Araújo JPM, Ariyawansa HA, Bakhshi M, Bendiksby M, Ben Hadj Amor A, Bezerra JDP, Boekhout T, Câmara MPS, Carbia M, Cardinali G, Castañeda-Ruiz RF, Celis A, Chaturvedi V, Collemare J, Croll D, Damm U, Decock CA, de Vries RP, Ezekiel CN, Fan XL, Fernández NB, Gaya E, González CD, Gramaje D, Groenewald JZ, Grube M, Guevara-Suarez M, Gupta VK, Guarnaccia V, Haddaji A, Hagen F, Hansen K, Hashimoto A, Haelewaters D, Hernández-Restrepo M, Houbraken J, Hubka V, Hyde KD, Iturriaga T, Jeewon R, Johnston PR, Jurjević Ž., Karalti İ, Korsten L, Kuramae EE, Kušan I, Labuda R, Lawrence DP, Lee HB, Lechat CLL, Li HY, Litovka YA, Maharachchikumbura SSN, Marin-Felix Y, Matio Kemkuignou B, Matočec N, McTaggart AR, Mlčoch P, Mugnai L, Nakashima C, Nilsson RH, Noumeur SR, Pavlov IN, Peralta MP, Phillips AJL, Pitt JI, Polizzi G, Quaedvlieg W, Rajeshkumar KC, Restrepo S, Rhaïem A, Robert J, Robert V, Rodrigues AM, Salgado-Salazar C, Samson RA, Santos ACS, Shivas RG, Souza-Motta CM, Sun GY, Swart WJ, Szoke S, Tan YP, Taylor JE, Taylor PWJ, Tiago PV, Váczy KZ, van de Wiele N, van der Merwe NA, Verkley GJM, Vieira WAS, Vizzini A, Weir BS, Wijayawardene NN, Xia JW, Yañez-Morales MJ, Yurkov A, Zamora JC, Zare R, Zhang CL, Thines M (2021) *Fusarium*: more than a node or a foot-shaped basal cell. *Studies in Mycology* 98: e100116. <https://doi.org/10.1016/j.simyco.2021.100116>
- Durkin L, Jansson T, Sanchez M, Khomich M, Ryberg M, Kristiansson E, Nilsson RH (2020) When mycologists describe new species, not all relevant information is provided (clearly enough). *Mycology* 72: 109–128. <https://doi.org/10.3897/mycokeys.72.56691>
- Edgar RC (2010) Search and clustering orders of magnitude faster than BLAST. *Bioinformatics* 26(19): 2460–2461. <https://doi.org/10.1093/bioinformatics/btq461>
- Fryssouli V, Zervakis GI, Polemis E, Typas MA (2020) A global meta-analysis of ITS rDNA sequences from material belonging to the genus *Ganoderma* (Basidiomycota, Polyporales) including new data from selected taxa. *Mycology* 75: 71–143. <https://doi.org/10.3897/mycokeys.75.59872>
- Gilks WR, Audit B, De Angelis D, Tsoka S, Ouzounis CA (2002) Modeling the percolation of annotation errors in a database of protein sequences. *Bioinformatics* 18(12): 1641–1649. <https://doi.org/10.1093/bioinformatics/18.12.1641>
- Hawksworth DL, Lücking R (2017) Fungal diversity revisited: 2.2 to 3.8 million species. The fungal kingdom. *Microbiology Spectrum* 5(4): 79–95. <https://doi.org/10.1128/microbiolspec.FUNK-0052-2016>

- Hofstetter V, Buyck B, Eyssartier G, Schnee S, Gindro K (2019) The unbearable lightness of sequenced-based identification. *Fungal Diversity* 96: 243–284. <https://doi.org/10.1007/s13225-019-00428-3>
- Hyde DK, Norphanphoun C, Chen J, Dissanayake AJ, Doilom M, Hongsanan S, Jayawardena RS, Jeewon R, Perera RH, Thongbai B, Wanasinghe DN, Wisitrasameewong K, Tibpromma S, Stadler M (2018) Thailand's amazing diversity: up to 96% of fungi in northern Thailand may be novel. *Fungal Diversity* 93: 215–239. <https://doi.org/10.1007/s13225-018-0415-7>
- Lücking R, Aime MC, Robbertse B, Miller AN, Aoki T, Ariyawansa HA, Cardinali G, Crous PW, Druzhinina IS, Geiser DS, Hawksworth DL, Hyde KD, Irinyi L, Jeewon R, Johnston PR, Kirk PM, Malosso M, May TW, Meyer W, Nilsson RH, Öpik M, Robert V, Stadler M, Thines M, Vu D, Yurkov AM, Zhang N, Schoch CL (2021) Fungal taxonomy and sequence-based nomenclature. *Nature Microbiology* 6: 540–548 <https://doi.org/10.1038/s41564-021-00888-x>
- Menolli N, Sánchez-García M (2020) Brazilian fungal diversity represented by DNA markers generated over 20 years. *Brazilian Journal of Microbiology* 51: 729–749. <https://doi.org/10.1007/s42770-019-00206-y>
- Nilsson RH, Ryberg M, Sjökvist E, Abarenkov K (2011) Rethinking taxon sampling in the light of environmental sequencing. *Cladistics* 27(2): 197–203. <https://doi.org/10.1111/j.1096-0031.2010.00336.x>
- Nilsson RH, Tedersoo L, Abarenkov K, Ryberg M, Kristiansson E, Hartmann M, Schoch CL, Nylander JAA, Bergsten J, Porter TM, Jumpponen A, Vaishampayan P, Ovaskainen O, Hallenberg N, Bengtsson-Palme J, Eriksson KM, Larsson K-H, Larsson E, Kõljalg U (2012) Five simple guidelines for establishing basic authenticity and reliability of newly generated fungal ITS sequences. *MycoKeys* 4: 37–63. <https://doi.org/10.3897/mycokeys.4.3606>
- Nilsson RH, Larsson KH, Taylor AFS, Bengtsson-Palme J, Jeppesen TS, Schigel D, Kennedy P, Picard K, Glöckner FO, Tedersoo L, Saar I, Kõljalg U, Abarenkov K (2019) The UNITE database for molecular identification of fungi: handling dark taxa and parallel taxonomic classifications. *Nucleic Acids Research* 47(D1): D259–D264. <https://doi.org/10.1093/nar/gky1022>
- Nishizawa T, Komatsuzaki M, Sato Y, Kaneko N, Ohta H (2010) Molecular characterization of fungal communities in non-tilled, cover-cropped upland rice field soils. *Microbes and Environments* 25(3): 204–210. <https://doi.org/10.1264/jms2.ME10108>
- Pautasso M (2013) Fungal under-representation is (indeed) diminishing in the life sciences. *Fungal Ecology* 6(5): 460–463. <https://doi.org/10.1016/j.funeco.2013.03.001>
- Robert V, Vu D, Amor ABH, van de Wiele N, Brouwer C, Jabas B, Szoke S, Dridi A, Triki M, ben Daoud S, Chouchen O, Vaas L, de Cock A, Stalpers JA, Stalpers D, Verkley GJM, Groenewald M, dos Santos FB, Stegehuis G, Li W, Wu L, Zhang R, Ma J, Zhou M, Pérez Gorjón S, Eurwilaichitr L, Ingsriswang S, Hansen K, Schoch C, Robbertse B, Irinyi L, Meyer W, Cardinali G, Hawksworth DL, Taylor JW, Crous PW (2013) MycoBank gearing up for new horizons. *IMA Fungus* 4: 371–379. <https://doi.org/10.5598/ima fungus.2013.04.02.16>
- Ryberg M, Nilsson RH, Kristiansson E, Töpel M, Jacobsson S, Larsson E (2008) Mining metadata from unidentified ITS sequences in GenBank: a case study in *Inocybe* (Basidiomycota). *BMC Evolutionary Biology* 8(1): 1–14. <https://doi.org/10.1186/1471-2148-8-50>

- Ryberg M, Kristiansson E, Wurzbacher C, Nilsson RH (2016) New Ph.D. students in the empirical sciences should be recruited into ongoing scientific studies right from the start. *Journal of Brief Ideas*. <https://doi.org/10.5281/zenodo.48179>
- Sayers EW, Cavanaugh M, Clark K, Pruitt KD, Schoch CL, Sherry ST, Karsch-Mizrachi I (2021) GenBank. *Nucleic Acids Research* 49(D1): D92–D96. <https://doi.org/10.1093/nar/gkaa1023>
- Schoch CL, Seifert KA, Huhndorf A, Robert V, Spouge JL, Levesque CA, Chen W, Fungal Barcoding Consortium (2012) Nuclear ribosomal internal transcribed spacer (ITS) region as a universal DNA barcode marker for Fungi. *Proceedings of the National Academy of Sciences USA* 109(16): 6241–6246. <https://doi.org/10.1073/pnas.1117018109>
- Schoch CL, Robbertse B, Robert V, Vu D, Cardinali G, Irinyi L, Meyer W, Nilsson RH, Hughes K, Miller AN, Kirk PM, Abarenkov K, Aime MC, Ariyawansa HA, Bidartondo M, Boekhout T, Buyck B, Cai Q, Chen J, Crespo A, Crous PW, Damm U, De Beer ZW, Dentinger BTM, Divakar PK, Dueñas M, Feau N, Fliegerova K, García MA, Ge Z-W, Griffith GW, Groenewald JZ, Groenewald M, Grube M, Gryzenhout M, Gueidan C, Guo L, Hambleton S, Hamelin R, Hansen K, Hofstetter V, Hong S-B, Houbraken J, Hyde KD, Inderbitzin P, Johnston PR, Karunarathna SC, Kõljalg U, Kovács GM, Kraichak E, Krizsan K, Kurtzman CP, Larsson K-H, Leavitt S, Letcher PM, Liimatainen K, Liu J-K, Lodge DJ, Luangsa-ard JJ, Lumbsch HT, Maharachchikumbura SSN, Manamgoda D, Martín MP, Minnis AM, Moncalvo J-M, Mulè G, Nakasone KK, Niskanen T, Olariaga I, Papp T, Petkovits T, Pino-Bodas R, Powell MJ, Raja HA, Redecker D, Sarmiento-Ramirez JM, Seifert KA, Shrestha B, Stenroos S, Stielow B, Suh S-O, Tanaka K, Tedersoo L, Telleria MT, Udayanga D, Untereiner WA, Uribeondo JD, Subbarao KV, Vágvölgyi C, Visagie C, Voigt K, Walker DM, Weir BS, Weiß M, Wijayawardene NN, Wingfield MJ, Xu JP, Yang ZL, Zhang N, Zhuang W-Y, Federhen S (2014) Finding needles in haystacks: linking scientific names, reference specimens and molecular data for Fungi. *Database (Oxford)* 2014: bau061. <https://doi.org/10.1093/database/bau061>
- Schoch CL, Ciufo S, Domrachev M, Hotton CL, Kannan S, Khovanskaya R, Leipe D, Mcveigh R, O'Neill K, Robbertse B, Sharma S, Soussov V, Sullivan JP, Sun L, Turner S, Karsch-Mizrachi I (2020) NCBI Taxonomy: a comprehensive update on curation, resources and tools. *Database* 2020: baaa062. <https://doi.org/10.1093/database/baaa062>
- Tedersoo L, Sánchez-Ramírez S, Koljalg U, Bahram M, Döring M, Schigel D, May T, Ryberg M, Abarenkov K (2018) High-level classification of the Fungi and a tool for evolutionary ecological analyses. *Fungal Diversity* 90: 135–159. <https://doi.org/10.1007/s13225-018-0401-0>
- Tedersoo L, Anslan S, Bahram M, Kõljalg U, Abarenkov K (2020) Identifying the 'unidentified' fungi: a global-scale long-read third-generation sequencing approach. *Fungal Diversity* 103: 273–293. <https://doi.org/10.1007/s13225-020-00456-4>
- Yuan H-S, Lu X, Dai Y-C, Hyde KD, Kan Y-H, Kušan I, He S-H, Liu N-G, Sarma VV, Zhao C-L, Cui B-K, Yousaf N, Sun G, Liu S-Y, Wu F, Lin C-G, Dayarathne MC, Gibbertoni TB, Conceição LB, Garibay-Orijel R, Villegas-Ríos M, Salas-Lizana R, Wei T-Z, Qiu J-Z, Yu Z-F, Phookamsak R, Zeng M, Paloi S, Bao D-F, Abeywickrama PD, Wei D-P, Yang J, Manawasinghe IS, Harishchandra D, Brahmanage RS, de Silva NI, Tennakoon DS, Karunarathna A, Gafforov Y, Pem D, Zhang S-N, de Azevedo Santiago ALCM, Bezerra JDP, Dima B, Acharya K, Alvarez-Manjarrez J, Bahkali AH, Bhatt VK, Brandrud TE,

- Bulgakov TS, Camporesi E, Cao T, Chen Y-X, Chen Y-Y, Devadatha B, Elgorban AM, Fan L-F, Du X, Gao L, Gonçalves CM, Gusmão LFP, Huanraluek N, Jadan M, Jayawardena RS, Khalid AN, Langer E, Lima DX, de Lima-Júnior NC, de Lira CRS, Liu J-K, Liu S, Lumyong S, Luo Z-L, Matočec N, Niranjana M, Oliveira-Filho JRC, Papp V, Pérez-Pazos E, Phillips AJL, Qiu P-L, Ren Y, Ruiz RFC, Semwal KC, Soop K, de Souza CAF, Souza-Motta CM, Sun L-H, Xie M-L, Yao Y-J, Zhao Q, Zhou L-W (2020) Fungal diversity notes 1277–1386: taxonomic and phylogenetic contributions to fungal taxa. *Fungal Diversity* 104: 1–266. <https://doi.org/10.1007/s13225-020-00461-7>
- Zinger L, Bonin A, Alsos IG, Bálint M, Bik H, Boyer F, Chariton AA, Creer S, Coissac E, Deagle BE, De Barba M, Dickie IA, Dumbrell AJ, Ficetola GF, Fierer N, Fumagalli L, Gilbert MTP, Jarman S, Jumpponen A, Kausrud H, Orlando L, Pansu J, Pawłowski L, Tedersoo L, Thomsen PF, Willerslev E, Taberlet P (2019) DNA metabarcoding—Need for robust experimental designs to draw sound ecological conclusions. *Molecular Ecology* 28(8): 1857–1862. <https://doi.org/10.1111/mec.15060>

Supplementary material I

A list of the 29 journals under the Web of Science heading “Mycology” as of November 2020

Authors: Kessy Abarenkov, Erik Kristiansson, Martin Ryberg, Sandra Nogal-Prata, Daniela Gómez-Martínez, Katrin Stüer-Patowsky, Tobias Jansson, Sergei Pölme, Masoomeh Ghobad-Nejhad, Natália Corcoll, Ruud Scharn, Marisol Sánchez-García, Maryia Khomich, Christian Wurzbacher, R. Henrik Nilsson

Data type: Text

Copyright notice: This dataset is made available under the Open Database License (<http://opendatacommons.org/licenses/odbl/1.0/>). The Open Database License (ODbL) is a license agreement intended to allow users to freely share, modify, and use this Dataset while maintaining this same freedom for others, provided that the original source and author(s) are credited.

Link: <https://doi.org/10.3897/mycokeys.86.76053.suppl1>

A long-read amplicon approach to scaling up the metabarcoding of lichen herbarium specimens

Cécile Gueidan¹, Lan Li¹

¹ Australian National Herbarium, National Research Collections Australia, NCMI, CSIRO, Canberra, ACT, 2601, Australia

Corresponding author: Cécile Gueidan (cecile.gueidan@csiro.au)

Academic editor: Imke Schmitt | Received 1 November 2021 | Accepted 24 January 2022 | Published 2 February 2022

Citation: Gueidan C, Li L (2022) A long-read amplicon approach to scaling up the metabarcoding of lichen herbarium specimens. MycoKeys 86: 195–212. <https://doi.org/10.3897/mycokeys.86.77431>

Abstract

Reference sequence databases are critical to the accurate detection and identification of fungi in the environment. As repositories of large numbers of well-curated specimens, herbaria and fungal culture collections have the material resources to generate sequence data for large number of taxa, and could therefore allow filling taxonomic gaps often present in reference sequence databases. Financial resources to do that are however often lacking, so that recent efforts have focused on decreasing sequencing cost by increasing the number of multiplexed samples per sequencing run while maintaining high sequence quality. Following a previous study that aimed at decreasing sequencing cost for lichen specimens by generating fungal ITS barcodes for 96 specimens using PacBio amplicon sequencing, we present a method that further decreases lichen specimen metabarcoding costs. A total of 384 mixed DNA extracts obtained from lichen herbarium specimens, mostly from the four genera *Buellia*, *Catillaria*, *Endocarpon* and *Parmotrema*, were used to generate new fungal ITS sequences using a Sequel I sequencing platform and the PacBio M13 barcoded primers. The average success rate across all taxa was high (86.5%), with particularly high rates for the crustose saxicolous taxa (*Buellia*, *Catillaria* and others; 93.3%) and the terricolous squamulose taxa (*Endocarpon* and others; 96.5%). On the other hand, the success rate for the foliose genus *Parmotrema* was lower (60.4%). With this taxon sampling, greater specimen age did not appear to impact sequencing success. In fact, the 1966–1980 collection date category showed the highest success rate (97.3%). Compared to the previous study, the abundance-based sequence denoising method showed some limitations, but the cost of generating ITS barcodes was further decreased thanks to the higher multiplexing level. In addition to contributing new ITS barcodes for specimens of four interesting lichen genera, this study further highlights the potential and challenges of using new sequencing technologies on collection specimens to generate DNA sequences for reference databases.

Keywords

Collection specimens, ITS barcode, lichenised fungi, PacBio amplicon sequencing

Introduction

Reference nucleotide sequence databases aim at providing access to curated and high-quality nucleotide sequences representing a broad taxonomic range of living organisms. They are critical to the accurate detection and identification of organisms from environmental samples and, for organisms lacking diagnostic characters, they are a useful tool to confirm morphology-based identifications. In fungi, the internal transcribed spacer region (ITS) has historically been used for species-level molecular identification (Gardes and Bruns 1993; Kõljalg et al. 2005; Abarenkov et al. 2010) and this gene region was later chosen as the fungal universal barcode (Schoch et al. 2012). Well-curated and high-quality fungal ITS sequences are now available from several databases, including RefSeq (Schoch et al. 2014; O’Leary et al. 2015), UNITE (Kõljalg et al. 2013; Nilsson et al. 2018) and ISHAM-ITS (Irinnyi et al. 2015). However, the taxonomic coverage for fungi represented in these sequence databases remains incomplete (Orok et al. 2012; Kõljalg et al. 2013; Crous et al. 2014; Nilsson et al. 2018). As well-curated resources of dried or living material of large numbers of fungal species, herbaria and culture collections can contribute to fill some of the taxonomic gaps in these sequence databases (Yahr et al. 2016; Gueidan et al. 2019), and guarantee high taxonomic standards, in particular by prioritising the sequencing of generic and species types (Crous et al. 2014).

Taking advantage of the development of next generation sequencing (NGS) methods, large numbers of fungal ITS sequences have been generated these last ten years. Fungal metabarcoding studies that detect and identify fungi in environmental samples based on inferred operational taxonomic units have mostly generated partial ITS sequences, either ITS1 or ITS2 (Nilsson et al. 2010; Mello et al. 2011; Blaaliid et al. 2013). This stems from their preferential use of Illumina sequencing technology which, although allowing affordable high-quality mass molecular barcoding, restricts the maximum read length to 300 bp. Other fungal metabarcoding studies have used long-read technologies, either Roche 454 pyrosequencing (Buée et al. 2009; Lumini et al. 2010; Blaaliid et al. 2012; Geml et al. 2014), Pacific Biosciences SMRT sequencing (Chen et al. 2015; Cline and Zak 2015; James et al. 2016; Schlaeppli et al. 2016; Walder et al. 2017; Heeger et al. 2018; Terdersoo and Anslan 2019; Castaño et al. 2020), or Oxford Nanopore MinION sequencing (Hu et al. 2019; Loit et al. 2019) to generate ITS sequences or other molecular barcodes. For lichenised fungi, early long-read metabarcoding studies used Roche 454 pyrosequencing technology (Hodkinson and Lendemer 2013; Lücking et al. 2014; Mark et al. 2016). After the decline of this technology, Pacific Biosciences SMRT sequencing was shown to be a viable option to generate full length high-quality sequences from lichen herbarium specimens (Gueidan et al. 2019).

Although used for whole genome sequencing of lichen metagenomes (Tzovaras et al. 2020), to our knowledge, PacBio SMRT sequencing has only been used for metabarcoding purposes in one study involving lichenised fungi (Gueidan et al. 2019). In this previous study, ITS sequences of 96 lichen specimens were amplified using a

two-step PCR approach, with modified ITS primers and PacBio barcoded universal primers. PCR products were then sequenced using the PacBio RS II platform and assembled and denoised using Long Amplicon Analysis (LAA; Bowman et al. 2014). High quality ITS sequences were generated for 88.5% of the samples, with a cost per sample of AU\$37. The mixed DNA samples resulting from the DNA extractions of these 96 lichen herbarium specimens also allowed the sequencing of other associated fungi. Here, the same method is used to generate ITS sequences from 384 lichen herbarium specimens, with the main goal of further decreasing the cost per sample. A new set of barcoded universal primers (M13 barcoding system, Larrea et al. 2018) developed by PacBio (Menlo Park, CA, USA) was tested in this study, as well as the then new PacBio Sequel I sequencing platform. Finally, sequence assembly and denoising were performed with a different pipeline, which included SMRT Tools (PacBio, Menlo Park, CA, USA) and DADA2 (Callahan et al. 2016).

The main goals of this study were to 1) assess the current cost and efficiency of a PacBio metabarcoding method applied to lichen herbarium specimens following changes in laboratory and bioinformatic pipelines, and 2) generate high-quality ITS sequences to contribute to reference sequence databases, as well as to molecular taxonomic studies of several lichen groups.

Material and methods

Taxon sampling and DNA extractions

For this study, 384 lichen specimens were selected because of their importance to several ongoing taxonomic works on Australian lichens at the Australian National Herbarium (see Suppl. material 1: Table S1). Four main genera were represented (Fig. 1A–D): *Catillaria* (14 specimens from Australia and France), *Buellia* (99 specimens from Australia), *Endocarpon* (167 specimens, including 157 from Australia) and *Parmotrema* (96 specimens from Australia). Additionally, a few other specimens were sampled: *Sporastatia* (4 specimens), and *Halecania* (1 specimen) and 3 unidentified specimens (one crustose saxicolous species and two squamulose terricolous species). The majority of the specimens were identified to the species or genus levels. The specimens were collected between 1966 and 2018, and are kept at CANB, UNSW, NSW, MARSSJ, ABL, BM, HO and in the private herbaria of P. McCarthy, M. Bertrand, B. McCune, and D. Stone. The material of crustose specimens (eg, *Catillaria*, *Buellia*) was detached from the substrate with a clean single-edge razor blade and a weigh paper was used to collect and transfer it to tubes containing a banded ceramic sphere and garnets (2 mL Lysing Matrix A, MP Biomedicals, Seven Hills, NSW, Australia). For squamulose and foliose species (e.g., *Endocarpon*, *Parmotrema*), lobes or squamules were detached from the substrate using clean tweezers and transferred directly to Lysing Matrix A tubes.

The samples were ground with a Precellys Evolution (Bertin Instruments, Montigny-le-Bretonneux, France) in 2–3 cycles of 30 sec at 6,000 rpm. To avoid cross-con-

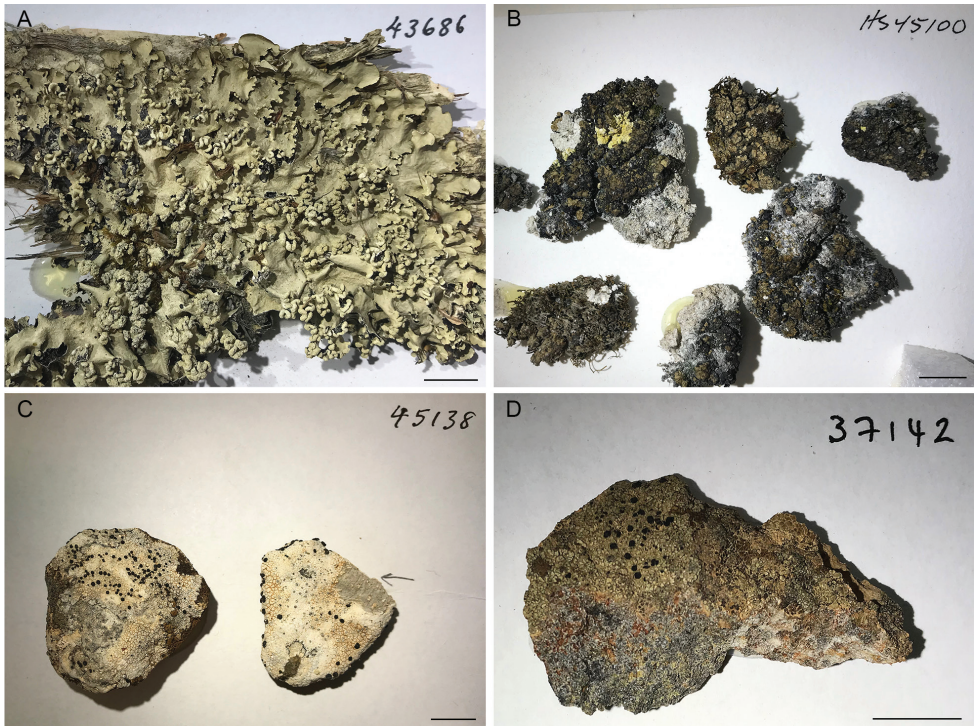


Figure 1. Examples of lichen herbarium specimens used for this study **A** *Parmotrema perlatum*, specimen J.A. Elix 43686 (CANB790817) **B** *Endocarpon pusillum*, specimen H. Streiman 45100 (CBG9011273) **C** *Buellia albula*, specimen J.A. Elix 45138 (CANB810791) **D** *Catillaria* sp., specimen J.A. Elix 37142 (CANB872684). Scale bar: 1 cm. Photos C. Gueidan.

taminations, the tubes were briefly centrifuged before the caps were removed. Genomic DNA was extracted using the Invisorb DNA Plant HTS 96 kit (Stratec Molecular, Berlin, Germany) adhering to the manufacturer's instructions, except for the few following modifications. The lysis buffer and proteinase K were added to each tube of ground material, which were then manually homogenised and incubated at 65 °C for 1 hour. The tubes were centrifuged at 11,000 rpm for 2 min and the supernatants were transferred onto the 96-well prefilter plate using a width-adjustable multichannel pipette. The RNase A (40 µl/well of a 10 mg/ml solution) was added after the prefiltration step and the tubes were incubated at room temperature for 15–20 min before adding the binding buffer. The last centrifugation step was changed to 10 min at 2,000 rpm (instead of 5 min at 4,000 rpm) to avoid breaking the elution plates. The DNA was eluted in 100 µl of elution buffer and 1/10 dilutions of the DNA samples were prepared.

Amplification, normalisation and pooling

Indexed PCR products were generated using a 2-step PCR approach as described in the PacBio Barcoded Universal Primers protocol (<https://www.pacb.com/wp-content/>

uploads/2015/09/Procedure-and-Checklist-Preparing-SMRTbell-Libraries-PacB-Bar-coded-Universal-Primers.pdf), but with few modifications. The fungal ITS barcode (internal transcribed spacer 1, 5.8S ribosomal RNA subunit and internal transcribed spacer 2) was the target region. With a first PCR, our target region was amplified using the primers ITS1F (Gardes and Bruns 1993) and ITS4 (White et al. 1990), both modified by adding a 5' block and a tail representing the PacBio M13 primer sequence (Larrea et al. 2018): /5AmMC6/GTA AAA CGA CGG CCA GTC TTG GTC ATT TAG AGG AAG TAA for ITS1F-M13 and /5AmMC6/CAG GAA ACA GCT ATG ACT CCT CCG CTT ATT GAT ATG C for ITS4-M13. In a 25 µl reaction, 5 µl of MyFi buffer (Bioline, London, UK), 1 µl of MyFi polymerase, 2.5 µl of 3 µM of each primer, 13 µl of water and 1 µl of DNA template were added. For each plate, the amplification was done twice, once using the raw DNA extracts and once using a 1/10 dilution of the raw DNA extracts. The 96 PCR reactions were performed in strip tubes with individual caps to avoid cross-contaminations. The PCR program was 5 min at 95 °C, then 20–25 (and occasionally 35) cycles of 30 sec at 95 °C, 30 sec at 53 °C and 1:30 min at 72 °C, followed by a final elongation step for 7 min at 72 °C. Selected PCR products were run onto an agarose gel using the nucleic acid stain GelRed (Biotium, Fremont, CA, USA). If the gel did not show primer dimer bands, no PCR product cleaning was undergone at this stage.

A second amplification was then performed using part of a set of 64 barcoded M13 primers (32 forward and 32 reverse) provided by PacBio (Menlo Park, CA, USA). The barcode sequences were 16 bp long (see Suppl. material 1: Table S2 for their names and sequences). For the second amplification, the PCR products resulting from the raw extracts and the ones resulting from the 1/10 dilutions were first pooled together in order to minimize the number of negative samples. In a 25 µl reaction, 5 µl of MyFi buffer, 1 µl of MyFi polymerase, 2.5 µl of each barcoded primer pairs (3 µM), 13 µl of water and 1 µl of the pooled product of the first round of PCRs were added. The PCR program was 5 min at 95 °C, then 25 cycles of 30 sec at 95 °C, 30 sec at 65 °C and 1:30 min at 72 °C, followed by a final elongation step for 5 min at 72 °C. All PCR products were checked on a gel as previously described and cleaned using AMPureXP beads (Beckman Coulter, Brea, CA, USA). First, the beads were prewashed as recommended for SMRTbell™ library preparation by the Ramaciotti Centre for Genomics (https://www.ramaciotti.unsw.edu.au/sites/default/files/2019-04/RAMAC_Long_Linked_Read_guidelines_2019.pdf). The cleaning was then done by adding 0.8X volume of beads to each PCR product, followed by two washes with 200 µl of 70% ethanol. Dry beads were then resuspended in 25 µl of the EB elution buffer (Qiagen, Hilden, Germany). The concentrations were measured with a Nanodrop 8000 spectrophotometer (Thermo Scientific, Waltham, MA, USA) and 10 ng/µl working solutions were manually prepared. One µl of each of the 384 samples was then pooled into a single tube.

Library preparation, sequencing and primary analysis

The pooled sample was sent to the Ramaciotti Centre for Genomics (UNSW Sydney, Australia) for single molecular real-time (SMRT) sequencing. The library preparation

was done using the SMRTbell Template Prep Kit v. 1.0 (Pacific Biosciences, Menlo Park, CA, USA). The sample was sequenced in one SMRT cell and with a ten-hour movie, using the Sequel Binding Kit v. 3.0 and the Sequel Sequencing Plate v. 3.0 (Pacific Biosciences). The subread bam file provided by Ramaciotti was generated using SMRT Link v. 6.0 (Pacific Biosciences). This subread bam file was then demultiplexed using the “lima” command in SMRT Tools v. 7.0.1 (Pacific Biosciences), and the circular consensus sequences (CCSs) generated using the “ccs” command (0.9999 minimum predicted accuracy and 3 minimum passes).

Secondary analysis and sequence identification

Generated CCSs were denoised using DADA2 v. 1.14 (Callahan et al. 2016), a software that infers sequence variants from high-throughput amplicon sequencing datasets. A custom R script, written by the bioinformatics team at the BRF (ANU, Canberra, Australia) and available upon request, allowed the batch processing of each CCS fastq file through the DADA2 pipeline. First, the primers were removed and the reads reoriented. Read quality profiles and length distribution histograms were then generated for each file. The reads were filtered (maxEE = 1, minQ = 3 and minLen = 300) and dereplicated. The error model was then estimated from the data (BAND-SIZE = 32) and the data further filtered for errors. After a last check for chimeras, fasta files of sequence variants were generated. For sequence identification, a blastn query (BLASTN 2.9.0+) was performed on these files against the NCBI nt database using a max_target_seqs of 3.

The blastn output was parsed into a single text file using a custom script and the results checked manually. Sequencing was considered successful if one of the generated sequence variants matched the same genus as the target taxa. For the unsuccessful samples, the fastq ccs files were converted to fasta using the fastqtofasta command in fastx 0.0.14, and an additional blastn query (BLASTN 2.12.0+) was performed on the ccs files using the same parameter as above. The blastn results were checked manually and sequencing was considered successful if one of the ccs matched the same genus as the target taxa. Demultiplexed fastq files were deposited in the Sequence Read Archive on NCBI (BioProject ID PRJNA796455).

Results

Amplification and sequencing

The two-step amplification approach generated PCR products with concentrations ranging from 11 to 1,573 ng/μl (Suppl. material 1: Table S1). The average concentration was 90 ng/μl and only 51 of the 384 samples were under 50 ng/μl (Suppl. material 1: Table S1). A total of 1.16 μg of PCR products was submitted to Ramaciotti in a pooled sample. The sample met the quality control requirements and showed DNA fragments ranging from 581 to 1,447 bp, with two clear peaks at 694 and 998 bp,

which are within the expected size range for the ITS barcode. The SMART cell generated 217,195 polymerase reads, with a mean length of 52,801 bp. This corresponded to 12,955,790 subreads with a mean length of 841 bp, and an average of 60 passes per ccs.

Sequence analysis and sequence identity

Using SMRT Tools, CCSs were recovered for 372 of the 384 samples, with only 12 samples for which no reads were generated (Suppl. material 1: Table S1). For each positive sample, between 22 and 1,368 CCSs were generated. After sequence denoising using the DADA2 amplicon pipeline, 1 to 21 sequence variants were found per sample. A blast analysis was conducted on all sequence variants and the results were compared to the morphology-based genus and/or species identification. Following this denoising step, a sequence of the target taxa was generated for 262 of the 384 initial samples. For 70 samples, no sequence variant matching the target taxon was generated by DADA2, but one or more sequences of the target taxon could be recovered from the CCS files. Therefore, in total, 332 of the 384 initial samples were considered as successful (86.5%). For 40 samples, sequence of the target taxon could not be found neither amongst the sequence variants generated by DADA2, nor among the CCSs. The majority of the samples that failed to generate sequences from the target species were from specimens of the genus *Parmotrema* (33 samples out of 40, or 82.5%).

When divided into three main morphological groups of taxa (Fig. 2), *Buellia*, *Catillaria* and other saxicolous crustose taxa had a sequencing success rate of 93.3% (111 positive samples out of 119). *Endocarpon* and other terricolous squamulose taxa had a sequencing success rate of 96.5% (163 positive samples out of 169 sample). Finally, the foliose genus *Parmotrema* had a sequencing success rate of only 60.4% (58 positive samples out of 96). When divided in five categories of time of collection (1966–1980, 1981–1990, 1991–2000, 2001–2010 and 2011–2020), the proportion of unsuccessful samples does not increase with the age of specimens: all but one category had more than 90% success rate (Fig. 3). In fact, the highest success rate was for the oldest class of specimens, 1966–1980, with 97.2%. The lower success rate for the 2001–2010 class (64.5%) was due to the lower success rate of specimens of *Parmotrema*, most of which were collected between 2005 and 2010.

Discussion

Building upon a previous work (Gueidan et al. 2019), the goal of this study was to generate high-quality ITS sequences for 384 lichen herbarium specimens and assess the current efficiency and cost of a modified PacBio metabarcoding method that had previously been applied to lichen herbarium specimens.

Generation of ITS barcodes for 384 lichen herbarium specimens

ITS sequences were successfully generated for 332 of the 384 herbarium specimens included in this study. Most of the specimens included belonged to the four genera

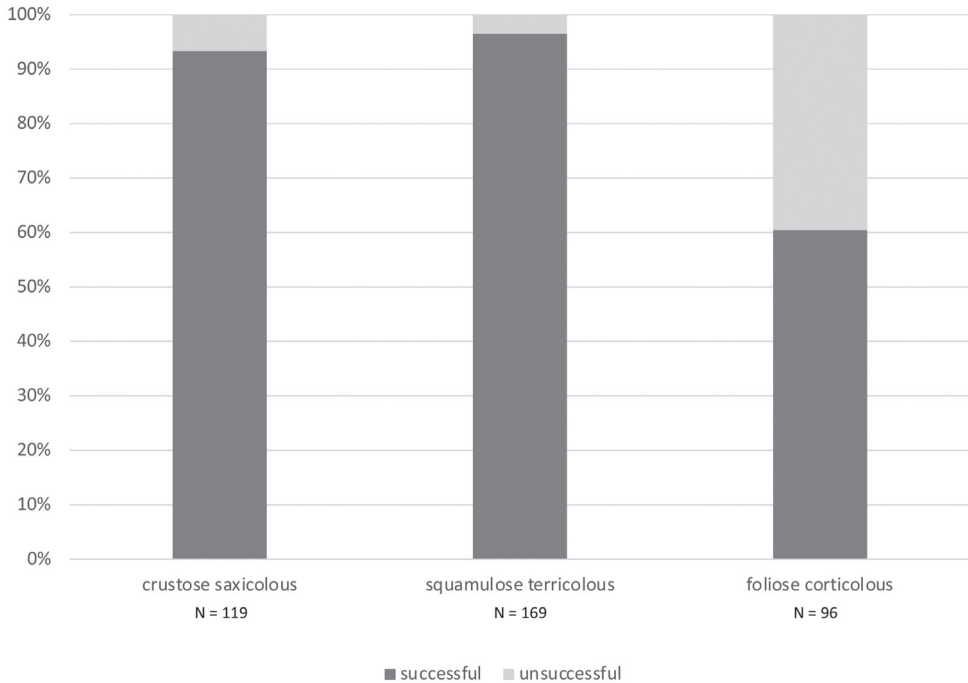


Figure 2. Sequencing success for different morphological groups of taxa included in this study. Specimens were grouped into three main morphological categories: **1** *Buellia*, *Catillaria* and other crustose saxicolous taxa **2** *Endocarpon* and other squamulose terricolous taxa **3** the foliose corticolous genus *Parmotrema*. In the graph, stalked columns show successful samples (sequence generated for the target species) in dark grey and unsuccessful samples (no sequence generated or generated sequences not from the target species) in light grey. The total number of samples (N) is indicated below each corresponding column.

Buellia, *Catillaria*, *Endocarpon* and *Parmotrema*. The success rate for the sequencing of the target ITS barcode was high (an average of 86.5% across all taxa) and similar to the one reported in Gueidan et al. (2019), which was of 88.5%. The sequencing success rate for the genus *Parmotrema* was, however, particularly low (60.4%), especially in comparison to *Buellia*, *Catillaria* and other crustose taxa (93.3%) and *Endocarpon* and other squamulose taxa (96.5%). Although a PCR product was obtained for all the *Parmotrema* samples, generated ITS sequences did often not belong to the target species, but to other fungi. This is likely due to inefficient amplification of the ITS barcode from the target *Parmotrema* species using the ITS1F-ITS4 primer pair. Although this primer pair is commonly used to amplify ITS of lichenised fungi (e.g., James et al. 2006; Kelly et al. 2011; Mark et al. 2016), it seems to have been used in combination with one other primer pair, ITS1-LM (Myllys et al. 1999) and ITS2-KL (Lohtander et al. 1998), in previous studies on the genus *Parmotrema* (Divakar et al. 2005; Del Prado et al. 2011). This indicates a possible amplification issue with the ITS1F-ITS4 primer pair for these species. Further sequencing will be carried out in the future for this genus using the alternative primer pair ITS1-LM/ITS2-KL, to attempt recovering ITS barcodes for additional *Parmotrema* species.

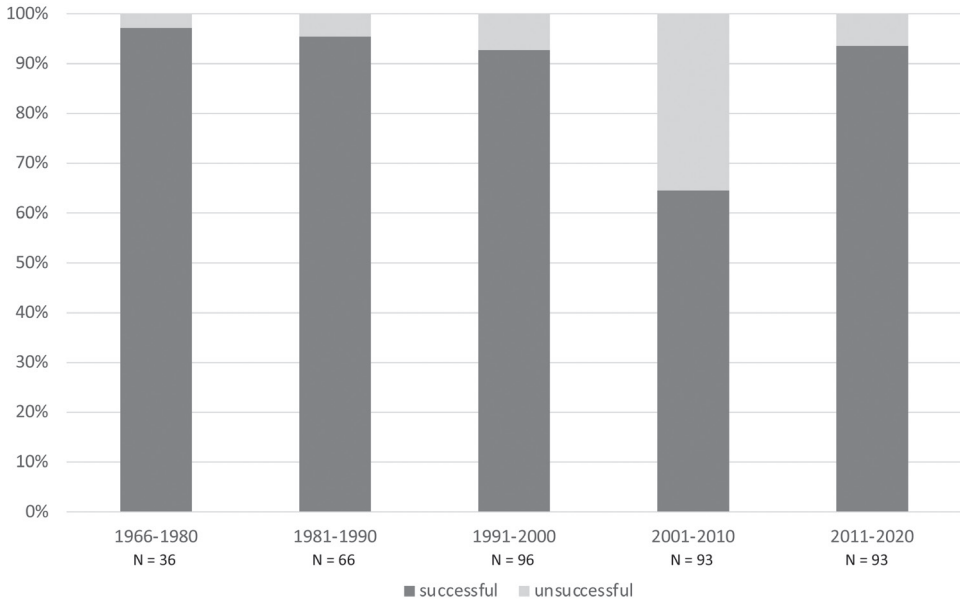


Figure 3. Sequencing success for different ages of specimens included in this study. Specimens were grouped in five categories: 1966–1980, 1981–1990, 1991–2000, 2001–2010, 2011–2020. In the graph, stalked columns show successful samples (sequence generated for the target species) in dark grey and unsuccessful samples (no sequence generated or generated sequences not from the target species) in light grey. The total number of samples (N) is indicated below each corresponding column.

The genomic DNA of some groups of lichens, most often from crustose corticolous tropical families (e.g., Staiger et al. 2006 for the Graphidaceae; Weerakoon et al. 2012 and Gueidan et al. 2016 for the Pyrenulaceae), is notoriously difficult to obtain from dried specimens. However, for most lichens, ITS sequences can usually easily be obtained from extracts of a large range of lichen herbarium specimens, including some relatively old ones. The oldest ones were a 75-year-old specimen of *Aspicilia aschabadensis* (Sohrabi et al. 2010), a 100-year-old specimen of *Staurolemma omphalarioides* (Bendiksby et al. 2014), and a 151-year-old specimen of *Caloplaca conversa* (Redchenko et al. 2012). A sequence of the small subunit of the mitochondrial ribosomal RNA gene (mtSSU) was also obtained from a 127-year-old specimen of *Peltigera collina* (Kistenich et al. 2019). In the latter study, which used Ion Torrent sequencing to generate mtSSU sequences from historical lichen specimens collected from 1885 onwards, specimen age had a significant influence on sequencing success, with older specimens less likely to yield good quality sequences (Kistenich et al. 2019). In our study, ages of lichen herbarium specimens ranged from 2 to 54 years. Apart from the specimen age category which included most *Parmotrema* samples (2001–2010), for which a primer issue caused low sequencing success, all age categories had high sequencing success rates, ranging from 92.7% to 97.2% (Fig. 3). Therefore, at least for some of the represented groups (*Endocarpon*

and saxicolous *Buellia* and *Catillaria*), generating ITS sequences for specimens up to 50 years old was not an issue. These results highlight the importance and relevance of older herbarium specimens, including types, in molecular taxonomy.

Efficiency and cost of the applied method

PacBio long read sequencing is a powerful approach, which when applied to amplicons, can utilise circular sequencing to generate high quality consensus of shorter nucleotide fragments. In order to correct sequencing errors, subreads extracted from one polymerase read – therefore generated from a single amplicon molecule, are aligned and assembled into one circular consensus sequence (CCS). Following CCS generation, additional software and pipelines are available to further correct sequencing errors, a step often called denoising. Although several software are available for denoising Illumina amplicon data (e.g., unoise, Edgar 2016; deblur, Amir et al. 2017), very few are available for PacBio amplicon data. In a previous study (Gueidan et al. 2019), a denoising approach developed for allele phasing of PacBio amplicon data (LAA) was used to generate high quality ITS sequences from lichen herbarium specimens. Parallel Sanger sequencing for a subset of samples confirmed that this method worked well for generating high-quality sequences for target and associated fungal species (Gueidan et al. 2019). However, a more relevant approach for metabarcoding is available (DADA2, Callahan et al. 2016) and was tested here. DADA2 is a software package that allows to generate amplicon sequence variants from high-throughput amplicon sequencing data. Conveniently, it can use PacBio data and a protocol is available for the size-variable ITS marker.

Despite DADA2 generating target sequence variants for a large number of our samples, a significant number of samples (70) did not yield sequences from the target taxon despite having one to several CCSs that matched the target taxon. For error correction, DADA2 is trained on a pool of sequences and uses sequence abundance to discriminate between sequencing error and true sequence variation. In our case the sequence pools corresponded to each of the 384 samples and were rather small due to the high level of multiplexing (average of 229 CCSs per sample/pool). In addition, among the CCSs available for each pool, in particular for the samples for which DADA2 did not recover the target taxon, the target CCSs were in low abundance within a large pool of lichen-associated fungal sequences or contaminant sequences. Because DADA2 error correction is based on sequence abundance, sequence variants are only inferred for high-abundance sequences. It is therefore not fully applicable to the metabarcoding of lichen herbarium specimens, or at least not when sequences of associated fungi are abundant. In this case, denoising methods that are not based on sequence abundance may perform better.

In terms of sequencing efficiency, with an average sequencing success rate of 86.5%, the new M13 amplicon sequencing protocol from PacBio is comparable to the protocol used in Gueidan et al. (2019). More recently, a UMI-based protocol for both Nanopore and PacBio long-read sequencing, which further decreases chimera and error rates, has been developed (Karst et al. 2021) and would be worth testing as well in

the future. In terms of time, both plate DNA extractions and batch sequence editing allowed us to decrease the time necessary to obtain the final ITS barcode sequences. The method also allows eliminating the time-consuming cloning step for samples with co-amplified fungal products. In terms of cost, the present method allowed us to decrease the cost per sample from AU\$37 (Gueidan et al. 2019) to AU\$27 (this study). The cost reduction is less than what was anticipated in Gueidan et al. (2019), mostly due to the transition from the RSII sequencing platform to the Sequel sequencing platform, which is more expensive. It is also due to the initial cost of a plate of M13 PacBio universal barcoded primers, which was more expensive than the Barcoded Universal F/R Primers Plate-96 from PacBio used in Gueidan et al. (2019). The M13 PacBio universal barcoded primer plate, however, includes larger volumes and can be used for more reactions. Similarly, although more expensive, the Sequel platform generates a much larger data output than the RSII platform (5–11 Gb versus 500 Mb, respectively). Sequel II, the next generation of SMRT sequencing platform, generates an even larger output (about 80 Gb), while the RSII platform is currently being discontinued in most sequencing services. These changes to the SMRT sequencing platforms and protocols imply that, at present, for lichen specimen metabarcoding, only pooled samples of large numbers of specimens (>500) or larger number of markers will make this technology cost-efficient.

Conclusion

With an average sequencing success of 86.5%, this long-read amplicon sequencing method is confirmed as a potential alternative to Sanger sequencing for the generation of full-length and high-quality DNA barcodes from mixed DNA samples extracted from lichen specimens. It performed particularly well for crustose saxicolous (93.3% success) and squamulose terricolous (96.5% success) taxa. In terms of cost (AU\$27/sample), although still more expensive than Sanger sequencing, it allows recovering high-quality sequences even when other lichen-associated fungi amplify as well, eliminating the need for using gel separation or cloning. At high multiplexing level (more than 500 samples/run), this high-throughput method is therefore an attractive option for the generation of DNA barcodes from large number of herbarium specimens.

Acknowledgements

The authors would like to thank Judith Curnow (CANB, Canberra) for her help with specimen databasing and curation, and the BM and NSW herbaria as well as the following collectors and herbaria for providing specimens used in this study: A. Aptroot (ABL), M. Bertrand, J.A. Elix (CANB), G. Kantvilas (HO), M. Mallen-Cooper (UNSW), P.M. McCarthy, B. McCune, R.W. Purdie (CANB), C. Roux (MARSSJ) and D. Stone. They would also like to acknowledge the contribution of Cameron

Jack (ANU, Canberra) and Nunzio Knerr (CANB, Canberra) to various bioinformatic scripts. They also thank Tonia Russell (Ramaciotti, UNSW, Sydney) and Cheryl Heiner (PacBio, USA) for their advice with sample preparation and sequencing.

References

- Abarenkov K, Nilsson RH, Larsson KH, Alexander IJ, Eberhardt U, Erland S, Høiland K, Kjølner R, Larsson E, Pennanen T, Sen R, Taylor AFS, Tedersoo L, Ursing BM, Vrålstad T, Liimatainen K, Peintner U, Kõljalg U (2010) The UNITE database for molecular identification of fungi - recent updates and future perspectives. *New Phytologist* 186: 281–285. <https://doi.org/10.1111/j.1469-8137.2009.03160.x>
- Amir A, McDonald D, Navas-Molina JA, Kopylova E, Morton JT, Zech Xu Z, Kightley EP, Thompson LR, Hyde ER, Gonzalez A, Knight R (2017) Deblur rapidly resolves single-nucleotide community sequence patterns. *mSystems* 2: e00191-16. <https://doi.org/10.1128/mSystems.00191-16>
- Bendiksby M, Mazzoni S, Jørgensen MH, Halvorsen R, Holien H (2014) Combining genetic analyses of archived specimens with distribution modelling to explain the anomalous distribution of the rare lichen *Staurolemma omphalarioides*: long-distance dispersal or vicariance? *Journal of Biogeography* 41: 2020–2031. <https://doi.org/10.1111/jbi.12347>
- Blaalid R, Carlsen T, Kumar S, Halvorsen R, Ugland KI, Fontana G, Kauserud H (2012) Changes in the root-associated fungal communities along a primary succession gradient analysed by 454 pyrosequencing. *Molecular Ecology* 21: 1897–1908. <https://doi.org/10.1111/j.1365-294X.2011.05214.x>
- Blaalid R, Kumar S, Nilsson RH, Abarenkov K, Kirk PM, Kauserud H (2013) ITS1 versus ITS2 as DNA metabarcodes for fungi. *Molecular Ecology Resources* 13: 218–224. <https://doi.org/10.1111/1755-0998.12065>
- Bowman BN, Marks P, Hepler NL, Eng K, Harting J, Shiina T, Suzuki S, Ranade S (2014) Long amplicon analysis: highly accurate, full-length, phased, allele-resolved gene sequences from multiplexed SMRT sequencing data. *Pacific Biosciences* (poster <https://www.pacb.com/proceedings/long-amplicon-analysis-highly-accurate-full-length-phased-allele-resolved-gene-sequences-from-multiplexed-smrt-sequencing-data>).
- Buée M, Reich M, Murat C, Nilsson RH, Uroz S, Martin F (2009) 454 Pyrosequencing analyses of forest soils reveal an unexpectedly high fungal diversity. *New Phytologist* 184: 449–456. <https://doi.org/10.1111/j.1469-8137.2009.03003.x>
- Callahan BJ, McMurdie PJ, Rosen MJ, Han AW, Johnson AJA, Holmes SP (2016) DADA2: high-resolution sample inference from Illumina amplicon data. *Nature Methods* 13: 581–583. <https://doi.org/10.1038/nmeth.3869>
- Castaño C, Berlin A, Brandström Durling M, Ihrmark K, Lindahl BD, Stenlid J, Clemmensen KE, Olson Å (2020) Optimized metabarcoding with Pacific Biosciences enables semi-quantitative analysis of fungal communities. *New Phytologist* 228: 1149–1158. <https://doi.org/10.1111/nph.16731>

- Chen Y, Frazzitta AE, Litvintseva AP, Fang C, Mitchell TG, Springer DJ, Ding Y, Yuan G, Perfect JR (2015) Next generation multilocus sequence typing (NGMLST) and the analytical software program MLST-EZ enable efficient, cost-effective, high-throughput, multilocus sequence typing. *Fungal Genetics and Biology* 75: 64–71. <https://doi.org/10.1016/j.fgb.2015.01.005>
- Cline LC, Zak DR (2015) Initial colonization, community assembly and ecosystem function: fungal colonist traits and litter biochemistry mediate decay rate. *Molecular Ecology* 24: 5045–5058. <https://doi.org/10.1111/mec.13361>
- Crous PW, Giraldo A, Hawksworth DL, Robert V, Kirk PM, Guarro J, Robbertse B, Schoch CL, Damm U, Trakunyingcharoen T, Groenwald JZ (2014) The Genera of Fungi: fixing the application of type species of generic names. *IMA Fungus* 5: 141–160. <https://doi.org/10.5598/imafungus.2014.05.01.14>
- Del Prado R, Divakar PK, Crespo A (2011) Using genetic distances in addition to ITS molecular phylogeny to identify potential species in the *Parmotrema reticulatum* complex: a case study. *The Lichenologist* 43: 569–583. <https://doi.org/10.1017/S0024282911000582>
- Divakar PK, Blanco O, Hawksworth DL, Crespo A (2005) Molecular phylogenetic studies on the *Parmotrema reticulatum* (syn. *Rimelia reticulata*) complex, including the confirmation of *P. pseudoreticulatum* as a distinct species. *The Lichenologist* 37: 55–65. <https://doi.org/10.1017/S0024282904014586>
- Edgar RC (2016) UNOISE2: Improved error-correction for Illumina 16S and ITS amplicon reads. <http://dx.doi.org/10.1101/081257>
- Gardes M, Bruns TD (1993) ITS primers with enhanced specificity for basidiomycetes - application to the identification of mycorrhizae and rusts. *Molecular Ecology* 2: 113–118. <https://doi.org/10.1111/j.1365-294X.1993.tb00005.x>
- Geml J, Gravendeel B, van der Gaag KJ, Neilen M, Lammers Y, Raes N, Semenova TA, de Knijff P, Noordeloos ME (2014) The Contribution of DNA metabarcoding to fungal conservation: diversity assessment, habitat partitioning and mapping red-listed fungi in protected coastal *Salix repens* communities in the Netherlands. *PLoS ONE* 9: e99852. <https://doi.org/10.1371/journal.pone.0099852>
- Gueidan C, Aptroot A, Cáceres MES (2016) Molecular phylogeny of the tropical family Pyrenulaceae: contribution from dried specimens and FTA card samples. *Mycological Progress* 15: 1–21. <https://doi.org/10.1007/s11557-015-1154-8>
- Gueidan C, Elix JA, McCarthy PM, Roux C, Mallen-Cooper M, Kantvilas G (2019) PacBio amplicon sequencing for metabarcoding of mixed DNA samples from lichen herbarium specimens. *MycKeys* 53: 73–91. <https://doi.org/10.3897/mycokeys.53.34761>
- Heeger F, Bourne EC, Baschien C, Yurkov A, Bunk B, Spröer C, Overmann J, Mazzoni CJ, Monaghan MT (2018) Long-read DNA metabarcoding of ribosomal RNA in the analysis of fungi from aquatic environments. *Molecular Ecology Resources* 18: 1500–1514. <https://doi.org/10.1111/1755-0998.12937>
- Hodkinson BP, Lendemer JC (2013) Next-generation sequencing reveals sterile crustose lichen phylogeny. *Mycosphere* 4: 1028–1039. <https://doi.org/10.5943/mycosphere/4/6/1>
- Hu Y, Green G, Milgate A, Stone E, Rathjen J, Schwessinger B (2019) Pathogen detection and microbiome analysis of infected wheat using a portable DNA sequencer. *Phytobiomes Journal* 3: 92–101. <https://doi.org/10.1094/PBIOMES-01-19-0004-R>

- Irinyi L, Serena C, Garcia-Hermoso D, Arabatzis M, Desnos-Ollivier M, Vu D, Cardinali G, Arthur I, Normand A-C, Giraldo A, da Cunha KC, Sandoval-Denis M, Hendrickx M, Nishikaku AS, de Azevedo Melo AS, Merseguel KB, Khan A, Parente-Rocha JA, Sampaio P, da Silva Briones MR, e Ferreira RC, Muniz M de M, Castanon-Olivares LR, Estrada-Barcenas D, Cassagne C, Mary C, Duan SY, Kong F, Sun AY, Zeng X, Zhao Z, Gantois N, Botterel F, Robbertse B, Schoch CL, Gams W, Ellis D, Halliday C, Chen S, Sorrell TC, Piarroux R, Colombo AL, Pais C, de Hoog S, Zancopé-Oliveira RM, Taylor ML, Toriello C, de Almeida Soares CM, Delhaes L, Stubbe D, Dromer F, Ranque S, Guarro J, Cano-Lira JF, Robert V, Velegraki A, Meyer W (2015) International Society of Human and Animal Mycology (ISHAM)-ITS reference DNA barcoding database - the quality controlled standard tool for routine identification of human and animal pathogenic fungi. *Medical Mycology* 53: 313–337. <https://doi.org/10.1093/mmy/myv008>
- James TY, Kauff F, Schoch CL, Matheny PB, Hofstetter V, Cox CJ, Celio G, Gueidan C, Fraker E, Miadlikowska J, Lumbsch HT, Rauhut A, Reeb V, Arnold AE, Amtoft A, Stajich JE, Hosaka K, Sung GH, Johnson D, O'Rourke B, Crockett M, Binder M, Curtis JM, Slot JC, Wang Z, Wilson AW, Schüssler A, Longcore JE, O'Donnell K, Mozley-Standridge S, Porter D, Letcher PM, Powell MJ, Taylor JW, White MM, Griffith GW, Davies DR, Humber RA, Morton JB, Sugiyama J, Rossman AY, Rogers JD, Pfister DH, Hewitt D, Hansen K, Hambleton S, Shoemaker RA, Kohlmeyer J, Volkman-Kohlmeyer B, Spotts RA, Serdani M, Crous PW, Hughes KW, Matsuura K, Langer E, Langer G, Untereiner WA, Lücking R, Büdel B, Geiser DM, Aptroot A, Diederich P, Schmitt I, Schultz M, Yahr R, Hibbett DS, Lutzoni F, McLaughlin DJ, Spatafora JW, Vilgalys R (2006) Reconstructing the early evolution of Fungi using a six-gene phylogeny. *Nature* 443: 818–22. <https://doi.org/10.1038/nature05110>
- James TY, Marino JA, Perfecto I, Vandermeer J (2016) Identification of putative coffee rust mycoparasites via single-molecule DNA sequencing of infected pustules. *Applied Environmental Microbiology* 82: 631–639. <https://doi.org/10.1128/AEM.02639-15>
- Karst SM, Ziels RM, Kirkegaard RH, Sørensen EA, McDonald D, Zhu Q, Knight R, Albertsen M (2021) High-accuracy long-read amplicon sequences using unique molecular identifiers with Nanopore or PacBio sequencing. *Nature Methods* 18: 165–169. <https://doi.org/10.1038/s41592-020-01041-y>
- Kelly LJ, Hollingsworth PM, Coppins BJ, Ellis CJ, Harrold P, Tosh J, Yahr R (2011) DNA barcoding of lichenized fungi demonstrates high identification success in a floristic context. *New Phytologist* 191: 288–300. <https://doi.org/10.1111/j.1469-8137.2011.03677.x>
- Kistenich S, Halvorsen R, Schröder-Nielsen A, Thorbek L, Timdal E, Bendiksby M (2019) DNA sequencing historical lichen specimens. *Frontiers in Ecology and Evolution* 7: e5. <https://doi.org/10.3389/fevo.2019.00005>
- Kójalg U, Larsson K-H, Abarenkov K, Nilsson RH, Alexander IJ, Eberhardt U, Erland S, Høiland K, Kjøller R, Larsson E, Pennanen T, Sen R, Taylor AFS, Tedersoo L, Vrålstad T, Ursing BM (2005) UNITE: a database providing web-based methods for the molecular identification of ectomycorrhizal fungi. *New Phytologist* 166: 1063–1068. <https://doi.org/10.1111/j.1469-8137.2005.01376.x>
- Kójalg U, Nilsson RH, Abarenkov K, Tedersoo L, Taylor AF, Bahram M, Bates ST, Bruns TD, Bengtsson-Palme J, Callaghan TM, Douglas B, Drenkhan T, Eberhardt U, Dueñas

- M, Grebenc T, Griffith GW, Hartmann M, Kirk PM, Kohout P, Larsson E, Lindahl BD, Lücking R, Martín MP, Matheny PB, Nguyen NH, Niskanen T, Oja J, Peay KG, Peintner U, Peterson M, Pöldmaa K, Saag L, Saar I, Schüßler A, Scott JA, Senés C, Smith ME, Suija A, Taylor DL, Telleria MT, Weiss M, Larsson KH (2013) Towards a unified paradigm for sequence-based identification of fungi. *Molecular Ecology* 22: 5271–5277. <https://doi.org/10.1111/mec.12481>
- Larrea A, Yuan G, Wagner K, Butt B, Norvell B, Aro L, Gu J, Lleras R, Ranade S, Korlach J, Krueger B, Heiner C (2018) A simple segue from Sanger to high-throughput SMRT Sequencing with a M13 barcoding system. *Pacific Biosciences* (poster <https://www.pacb.com/wp-content/uploads/Aro-ASHG-2018-Targeted-Sequencing-M13-10-6-2018-FINAL.pdf>).
- Lohtander K, Myllys L, Sundin R, Källersjö M, Tehler A (1998) The species pair concept in the lichen *Dendrographa leucophaea* (Arthoniales): analyses based on ITS sequences. *Bryologist* 101: 404–411. <https://doi.org/10.2307/3244179>
- Loit K, Adamson K, Bahram M, Puusepp R, Anslan S, Kiiker R, Drenkhan R, Tedersoo L (2019) Relative performance of MinION (Oxford Nanopore Technologies) versus Sequel (Pacific Biosciences) third-generation sequencing instruments in identification of agricultural and forest fungal pathogens. *Applied Environmental Microbiology* 85: e01368–19. <https://doi.org/10.1128/AEM.01368-19>
- Lücking R, Lawrey JD, Gillevet PM, Sikaroodi M, Dal-Forno M, Berger SA (2014) Multiple ITS haplotypes in the genome of the lichenized basidiomycete *Cora inversa* (Hygrophoraceae): Fact or artifact? *Journal of Molecular Evolution* 78: 148–162. <https://doi.org/10.1007/s00239-013-9603-y>
- Lumini E, Orgiazzi A, Borriello R, Bonfante P, Bianciotto V (2010) Disclosing arbuscular mycorrhizal fungal biodiversity in soil through a land-use gradient using a pyrosequencing approach. *Environmental Microbiology* 12: 2165–2179. <https://doi.org/10.1111/j.1462-2920.2009.02099.x>
- Mark K, Cornejo C, Keller C, Flück D, Scheidegger C (2016) Barcoding lichen-forming fungi using 454 pyrosequencing is challenged by artifactual and biological sequence variation. *Genome* 59: 685–704. <https://doi.org/10.1139/gen-2015-0189>
- Mello A, Napoli C, Morin CME, Marceddu G, Bonfante P (2011) ITS-1 versus ITS-2 pyrosequencing: a comparison of fungal populations in truffle grounds. *Mycologia* 103: 1184–1193. <https://doi.org/10.3852/11-027>
- Myllys L, Lohtander K, Källersjö M, Tehler A (1999) Sequence insertions and ITS data provide congruent information on *Roccella canariensis* and *R. tuberculata* (Arthoniales, Euascomycetes) phylogeny. *Molecular Phylogenetics and Evolution* 12: 295–309. <https://doi.org/10.1006/mpev.1999.0620>
- Nilsson RH, Veldre V, Hartmann M, Unterseher M, Amend A, Bergsten J, Kristiansson E, Ryberg M, Jumpponen A, Abarenkov K (2010) An open-source package for automated extraction of ITS1 and ITS2 from fungal ITS sequences for use in high-throughput community assays and molecular ecology. *Fungal Ecology* 3: 284–287. <https://doi.org/10.1016/j.funeco.2010.05.002>
- Nilsson RH, Taylor AFS, Adams RI, Baschien C, Bengtsson-Palme J, Cangren P, Coleine C, Daniel H-M, Glassman SI, Hirooka Y, Irinyi L, Iršenaite R, Martin-Sanchez PM, Meyer

- W, Oh S-Y, Sampaio JP, Seifert KA, Sklenář F, Stubbe D, Suh S-O, Summerbell R, Svantesson S, Unterseher M, Visagie CM, Weiss M, Woudenberg JHC, Wurzbacher C, Van den Wyngaert S, Yilmaz N, Yurkov A, Kõljalg U, Abarenkov K (2018) Taxonomic annotation of public fungal ITS sequences from the built environment – a report from an April 10–11, 2017 workshop (Aberdeen, UK). *MycoKeys* 28: 65–82. <https://doi.org/10.3897/mycokeys.28.20887>
- O’Leary NA, Wright MW, Brister JR, Ciufu S, Haddad D, McVeigh R, Rajput B, Robbertse B, Smith-White B, Ako-Adjei D, Astashyn A, Badretdin A, Bao Y, Blinkova O, Brover V, Chetvernin V, Choi J, Cox E, Ermolaeva O, Farrell CM, Goldfarb T, Gupta T, Haft D, Hatcher E, Hlavina W, Joardar VS, Kodali VK, Li W, Maglott D, Masterson P, McGarvey KM, Murphy MR, O’Neill K, Pujar S, Rangwala SH, Rausch D, Riddick LD, Schoch C, Shkeda A, Storz SS, Sun H, Thibaud-Nissen F, Tolstoy I, Tully RE, Vatsan AR, Wallin C, Webb D, Wu W, Landrum MJ, Kimchi A, Tatusova T, DiCuccio M, Kitts P, Murphy TD, Pruitt KD (2015) Reference sequence (RefSeq) database at NCBI: current status, taxonomic expansion, and functional annotation. *Nucleic Acids Research* 44: 733–745. <https://doi.org/10.1093/nar/gkv1189>
- Orock EA, Leavitt SD, Fonge BA, St Clair LL, Lumbsch HT (2012) DNA-based identification of lichen-forming fungi: can publicly available sequence databases aid in lichen diversity inventories of Mount Cameroon (West Africa)? *The Lichenologist* 44: 833–839. <https://doi.org/10.1017/S0024282912000424>
- Redchenko O, Vondrák J, Košnar J (2012) The oldest sequenced fungal herbarium sample. *The Lichenologist* 44: 715–718. <https://doi.org/10.1017/S002428291200031X>
- Schlaeppli K, Bender SF, Mascher F, Russo G, Patrignani A, Camenzind T, Hempel S, Rillig MC, van der Heijden MGA (2016) High-resolution community profiling of arbuscular mycorrhizal fungi. *New Phytologist* 212: 780–791. <https://doi.org/10.1111/nph.14070>
- Schoch CL, Seifert KA, Huhndorf C, Robert V, Spouge JL, Levesque CA, Chen W, and Fungal Barcoding Consortium (2012) Nuclear ribosomal internal transcribed spacer (ITS) region as a universal DNA barcode marker for Fungi. *Proceedings of the National Academy of Sciences USA* 109: 6241–6246. <https://doi.org/10.1073/pnas.1117018109>
- Schoch CL, Robbertse B, Robert V, Vu D, Cardinali G, Irinyi L, Meyer W, Nilsson RH, Hughes K, Miller AN, Kirk PM, Abarenkov K, Aime MC, Ariyawansa HA, Bidartondo M, Boekhout T, Buyck B, Cai Q, Chen J, Crespo A, Crous PW, Damm U, De Beer ZW, Dentinger BTM, Divakar PK, Dueñas M, Feau N, Fliegerova K, García MA, Ge Z-W, Griffith GW, Groenewald JZ, Groenewald M, Grube M, Gryzenhout M, Gueidan C, Guo L, Hambleton S, Hamelin R, Hansen K, Hofstetter V, Hong S-B, Houbraken J, Hyde KD, Inderbitzin P, Johnston PR, Karunarathna SC, Kõljalg U, Kovács GM, Kraichak E, Krizsan K, Kurtzman CP, Larsson K-H, Leavitt S, Letcher PM, Liimatainen K, Liu J-K, Lodge DJ, Luangsa-Ard JJ, Lumbsch HT, Maharachchikumbura SSN, Manamgoda D, Martín MP, Minnis AM, Moncalvo J-M, Mulè G, Nakasone KK, Niskanen T, Olariaga I, Papp T, Petkovits T, Pino-Bodas R, Powell MJ, Raja HA, Redecker D, Sarmiento-Ramirez JM, Seifert KA, Shrestha B, Stenroos S, Stielow B, Suh S-O, Tanaka K, Tedersoo L, Telleria MT, Udayanga D, Untereiner WA, Uribeondo JD, Subbarao KV, Vágvölgyi C, Visagie C, Voigt K, Walker DM, Weir BS, Weiß M, Wijayawardene NN, Wingfield MJ, Xu JP, Yang ZL,

- Zhang N, Zhuang W-Y, Federhen S (2014) Finding needles in haystacks: linking scientific names, reference specimens and molecular data for Fungi. Database 2014: 1–21. <https://doi.org/10.1093/database/bau061>
- Sohrabi M, Myllys L, Stenroos S (2010) Successful DNA sequencing of a 75 year-old herbarium specimen of *Aspicilia aschabadensis* (J. Steiner) Mereschk. Lichenologist 42: 626–628. <https://doi.org/10.1017/S0024282910000344>
- Staiger B, Kalb K, Grube M (2006) Phylogeny and phenotypic variation in the lichen family Graphidaceae (Ostropomycetidae, Ascomycota). Mycological Research 110: 765–772. <https://doi.org/10.1017/S0024282910000344>
- Tedersoo L, Anslan S (2019) Towards PacBio-based pan-eukaryote metabarcoding using full-length ITS sequences. Environmental Microbiology Reports 11: 659–668. <https://doi.org/10.1111/1758-2229.12776>
- Tzovaras BG, Segers FHID, Bicker A, Dal Grande F, Otte J, Anvar SY, Hankeln T, Schmitt I, Ebersberger I (2020) What is in *Umbilicaria pustulata*? A metagenomic approach to reconstruct the holo-genome of a lichen. Genome Biology and Evolution 12: 309–324. <https://doi.org/10.1093/gbe/evaa049>
- Walder F, Schlaeppi K, Wittwer R, Held AY, Vogelgsang S, van der Heijden MGA (2017) Community profiling of *Fusarium* in combination with other plant-associated fungi in different crop species using SMRT sequencing. Frontiers in Plant Science 8: e2019. <https://doi.org/10.3389/fpls.2017.02019>
- Weerakoon G, Aptroot A, Lumbsch HT, Wolseley PA, Wijeyaratne SC, Gueidan C (2012) New molecular data on Pyrenulaceae from Sri Lanka reveal two well supported groups within this family. The Lichenologist 44: 639–647. <https://doi.org/10.1017/S0024282912000333>
- White TJ, Bruns T, Lee S, Taylor J (1990) Amplification and direct sequencing of fungal ribosomal RNA genes for phylogenetics. In: Innis MA, Gelfand DH, Sninsky JJ, White TJ (Eds) PCR Protocols, a Guide to Methods and Applications. Academic Press, San Diego, 315–322. <https://doi.org/10.1016/B978-0-12-372180-8.50042-1>
- Yahr R, Schoch C, Dentinger BTM (2016) Scaling up discovery of hidden diversity in fungi: impacts of barcoding approaches. Philosophical Transactions of the Royal Society B 371: e20150336. <https://doi.org/10.1098/rstb.2015.0336>

Supplementary material I

Table S1. List of specimens used for this study, including their voucher information, plate location, indexing, amplicon concentration and sequencing results, both as an output from SMRT tools (CCSs) and as an output from DADA2 (sequence variants). Table S2. List of the 64 barcode sequences used to index the samples. Used barcode pairs are listed in Table S1

Authors: Cécile Gueidan, Lan Li

Data type: Taxon sampling

Explanation note: List of specimens used for this study, including their voucher information, plate location, indexing, amplicon concentration and sequencing results, both as an output from SMRT tools (CCSs) and as an output from DADA2 (sequence variants). A summary of the blast results for the sequence variants is also listed for each sample. In the "recovered target" column, samples for which the target sequence was recovered from the CCS file but not the sequence variant file are indicated by a star.

Copyright notice: This dataset is made available under the Open Database License (<http://opendatacommons.org/licenses/odbl/1.0/>). The Open Database License (ODbL) is a license agreement intended to allow users to freely share, modify, and use this Dataset while maintaining this same freedom for others, provided that the original source and author(s) are credited.

Link: <https://doi.org/10.3897/mycokeys.86.77431.suppl1>